UNIVERSITI TEKNOLOGI MARA

JUNIOR SCIENCE COMMUNICATION

E-ISSN 2637-0689

FACULTY OF APPLIED SCIENCES

Vol. 2 (2019)

CCE 2018

Colloquium of Chemistry and Environment 2018

Faculty of Applied Sciences, Universiti Teknologi MARA, Shah Alam Malaysia.

Colloquium date 19 December 2018
Publication date 11 November 2019

Proceedings of Extended Abstracts

Editors

Guest Editors

Volume Editors

Published by Faculty of Applied Sciences, Universiti Teknologi MARA, Shah Alam

Faculty of Applied Sciences,
Universiti Teknologi MARA,
Shah Alam 40450, Shah Alam,
Selangor, Malaysia

eISSN 2637-0689

TABLE OF CONTENTS

JUNIOR SCIENCE COMMUNICATION | Volume 2 (2019)
https://jscfsg.uitm.edu.my/ | eISSN 2637-0689

Colloquium of Chemistry and Environment 2018

Faculty of Applied Sciences, Universiti Teknologi MARA, Shah Alam.

RADIOLOGICAL RISK ASSESSMENT OF RADIONUCLIDES IN BUILDING MATERIALS IN PENINSULAR MALAYSIA

Arif Izzuddin Bin Mohd Sahat, Sabarina Md Yunus*,
Faculty of Applied Sciences, Universiti Teknologi MARA, 40450 Shah Alam, Selangor, Malaysia.

*sabarina2020@uitm.edu.my

Abstract: The high concentration of radionuclides contain in building materials will cause negative result to human health. This study was done with the aims to determine the concentration of radionuclides as well as to determine the activity concentration of radionuclides and to estimate the radiological risk assessment of radionuclides in building materials. The samples concentration were analysed using the Energy dispersive x-ray fluorescence (EDXRF). For concentration of radionuclides in building materials sample, mean value obtained for uranium-238, thorium-232 and potassium-40 were 22.71 mg/kg, 14 mg/kg and 2.61 %, respectively. The concentration of uranium-238 in building materials sample from highest to lowest were; B > F > D > C > E > A > G, for thorium-232 were; D > C > E > F > B > A > G and for potassium-40 were; F > B > C > D > E > A > G. Meanwhile, for the activity concentration of radionuclides, the mean values obtained for uranium-238, thorium-232 and potassium-40 were 280.38, 56.92 and 809.94 Bq/kg. Each of samples gave an average of 103.15 nGy/h for absorbed dose rate, 0.15 mSv/y for annual effective dose, and the value of 0.53 for external hazard index. As a safety precaution, some remedial actions have to be taken to prevent occurrence of high doses to workers and general public. Therefore, mitigation procedure can be taken as public awareness.

Keywords: *Radionuclides, EDXRF, uranium, thorium, potassium.*

INTRODUCTION

This research will be focused on the study of the levels of radionuclides present in building materials. The high presence of radionuclides in building materials may be hazardous to human due to both internal and external radiation exposure. This study was done with the aims to determine the concentration of radionuclides as well as to determine the activity concentration of radionuclides and to estimate the radiological risk assessment of radionuclides in building materials Energy Dispersive X-ray Fluorescence technique (EDXRF) is used for measurement of radionuclides.

METHODOLOGY

XRF is normally used to determine the concentration of elements that appear to be solid, liquid, as well as powdered form (Frahm & Doonan, 2013). EDXRF is able to accumulate all of the elemental information in the sample at one time. Seven samples were grind using a grinder to make it homogenous and were transferred into a seven different container. Then, all samples were analysed using a EDXRF and data were recorded.

FINDINGS

Figure 1(a) shows the activity concentration of radionuclides in building materials samples. For uranium, the highest activity concentration of uranium obtained in B (rocks) sample and the lowest concentration was obtained in sample G (cement). Rocks are richer in uranium due to bound in the matrix making them easily separable, which is a prerequisite in the uranium forming process (Maithani & Srinivasan, 2011). For thorium, the highest value was obtained in sample D (soil) and the lowest concentration was obtained in sample G (cement). Thorium is found mostly in soil, surface and underground water, plants, and animals

(Höllriegl *et al*., 2007). The highest value was found in sample F (sand). Most potassium-40 was found dissolved in sea water, trace particle and considered as minerals (Strom *et al*., 2009). Sand grains are either mineral particles, rock fragments or biogenic in origin.

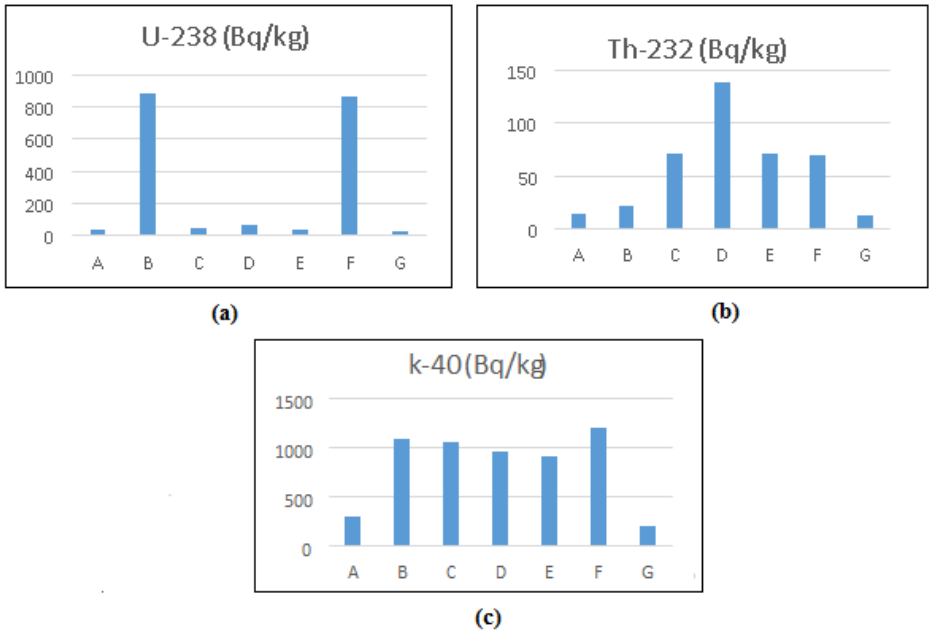

Figure 1 (a) Uranium-238, (b) Thorium-232 and (c) Potassium-40 for activity concentration of radionuclides in building material samples.

CONCLUSIONS

Potassium-40 has the highest value obtained in the samples since it is the largest source of natural radioactivity. Some value obtained from all the samples are above the limit indicates that sample collected from location contribute health hazard to public.

REFERENCES

i. Frahm, E. & Doonan, R.C.P. (2013). The technological versus methodological revolution of portable XRF in archaeology. *Journal of Archaeological Science*, *40*(2), 1425–1434.
ii. Höllriegl, V., Greiter, M., Giussani, A., Gerstmann, U., Michalke, B., Roth, P. & Oeh, U. (2007). Observation of changes in urinary excretion of thorium in humans following ingestion of a therapeutic oil. *Journal of Environmental Radioactivity*, *95*(2–3), 149–160.
iii. Maithani, P.B. & Srinivasan, S. (2011). Felsic Volcanic Rocks, a Potential Source of Uranium - An Indian Overview, *Energy Procedia*, *7*, 163–168.
iv. Strom, D.J., Lynch, T.P. & Weier, D.R. (2009). *Radiation Doses to Hanford Workers from Natural Potassium-40*. Retrieved September 5, 2019, from https://www.pnnl.gov/main/publications/external/technical_reports/PNNL-18240.pdf

JUNIOR SCIENCE COMMUNICATION
https://jscfsg.uitm.edu.my/
Volume 2 (2019)
eISSN 2637-0689

Colloquium of Chemistry and Environment 2018
Faculty of Applied Sciences, Universiti Teknologi MARA, Shah Alam.

IONIC LIQUID BASED POLYMER ELECTROLYTE

Arinnie Sahrin, Mohd. Azri Ab Rani*
Faculty of Applied Sciences, Universiti Teknologi MARA, 40450 Shah Alam, Selangor, Malaysia.
*azri@uitm.edu.my

Abstract: The using of ionic liquid as a solvent in electrochemical devices can lead to a leakage problem. This problem can be overcome by using a polymer electrolyte which is safer compared to liquid electrolyte. Thus, it can be used more widely in electrochemical devices as well as improves the ionic conductivity of the sample. The ILPE sample were prepared through casting technique using sodium fluorosulfonylamide, Na [FSA], NMethyl-N-propylpyrrolidinium Bis(fluorosulfonyl)imide, [C1C3pyrr] [FSA] ionic liquid, polyvinyl chloride polymer (PVC) and tetrahydrofuran (THF). It was found that, the higher the amount of ionic liquid in the polymer, the diffraction pattern of the samples become amorphous. In addition, the ionic conductivity increased as the amount of the ionic liquid in the polymer increased. This was supported by and Electrochemical Impedance Spectroscopy (EIS) analysis.

Keywords: *Ionic liquid polymer electrolyte (ILPE), ionic liquid (IL), polyvinyl chloride, [C_1C_3pyrr][FSA], Na [FSA], polymer electrolytes.*

INTRODUCTION

Ionic liquid polymer electrolyte (ILPE) is a thin film which consists of ionic liquid, salt and host polymer that has higher conductivity and safer as compared to liquid electrolyte. Ionic liquids (ILs) have great advantage in terms of safety for example it has low vapour pressure, low flammability, high thermal stability, high conductivity and wide electronic window. According to Aziz *et al.* (2018), a safer alternative to liquid electrolyte is by creating dry solid polymer electrolytes (SPEs) which have attracted a great attention. The using of ionic liquid as a solvent in electrochemical devices can lead to a leakage problem. Thus, through casting technique, the ILPE was made by using sodium fluorosulfonylamide, Na [FSA], N-Methyl-N-propylpyrrolidinium Bis(fluorosulfonyl)imide, [C1C3pyrr] [FSA] ionic liquid, polyvinyl chloride polymer (PVC) and tetrahydrofuran (THF) as a solvent. In this study, the ionic liquid polymer electrolyte was synthesized and characterized by using XRD and EIS.

METHODOLOGY

A 1.0 g PVC was dissolved in 40 mL THF. The mixture was stirred vigorously and fixed amount of Na [FSA] salt at 1.0 g was added into ILPE 1 until 5. Different ratio of [C1C3pyrr] [FSA] ionic liquid (20.0%, 33.3%, 42.9% and 50.0%) were then added to ILPE 2 to 5 and stirred for 24hrs. The solutions were then casted into petri dish and left in open air. The polymer blend films were peeled and vacuum at 333K for 24 hrs before further characterizes.

FINDINGS

X-ray Diffraction Analysis Blank sample and ILPE 1 exhibit semi-crystalline structure as the polymer does not contain ionic liquid while ILPE 2, 3, 4 and 5 exhibit an amorphous structure respectively when the ionic liquid was added into the polymer. The peak intensity of the samples was decreased as the addition of ionic liquid increased in the polymer. As the amount of ionic liquid increases, the diffraction patterns of the polymer become amorphous. Saroj and Singh (2012) stated that, the polymer film diffraction pattern

becomes amorphous as the amount of ionic liquid increases and the higher the amount of ionic liquid in the polymer, the lower the peak intensity (Radzir *et al.*, 2015). The addition of ionic liquid will break the crystallinity structure of the polymer thus increases the ionic transportation of the ionic liquid as well.

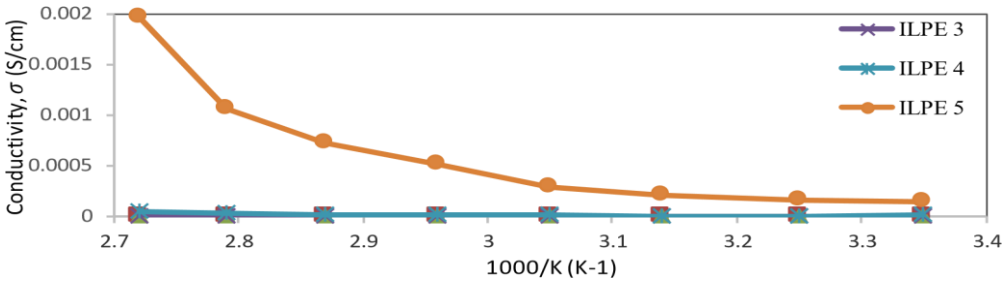

Figure 1 Arrhenius plot for ILPE 3, 4 and 5

Electrochemical Impedance Spectroscopy Analysis

The ionic conductivity increased as the amount of ionic liquid in the polymer increased. The addition of ionic liquid N-Methyl-N-propylpyrrolidinium Bis(fluorosulfonyl)imide into the polymer improves the mobility and flexibility of the polymer (Liew *et al.*, 2014). When the mobility and flexibility increases, it will improve the ionic transportation thus increasing the ionic conductivity of the polymer. The ionic conductivity for ILPE 3 at 95°C is 1.88 x 10^{-6} Scm^{-1} while the ionic conductivity for ILPE 5 is 1.96 x 10^{-3} Scm^{-1}.

CONCLUSIONS

The addition of ionic liquid has decreased the peak intensity of the polymer and as the amount of ionic liquid increases, the crystalline structure of the polymer breaks and become amorphous. Furthermore, the addition of ionic liquid into the polymer increases the ionic conductivity as it improves the mobility and flexibility of the polymer. Thus, the characterization of the ILPE was successfully done using EIS.

REFERENCES

i. Aziz, S.B., Woo, T.J., Kadir, M.F.Z. & Ahmed, H.M. (2018). A conceptual review on polymer electrolytes and ion transport models. *Journal of Science: Advanced Materials and Devices*, *3*(1), 1–17.

ii. Liew, C.-W., Ramesh, S. & Arof, A.K. (2014). Good prospect of ionic liquid based-poly(vinyl alcohol) polymer electrolytes for supercapacitors with excellent electrical, electrochemical and thermal properties. *International Journal of Hydrogen Energy*, *39*(6), 2953–2963.

iii. Radzir, N.N.M., Anuar, F.H., Hanifah, S.A., Ahmad, A. & Hassan, N.H. (2015). An investigation of polymer electrolyte based on poly(glycidylmethacrylate) doped with imidazolium ionic liquid. *Journal of Materials and Environmental Science*, *6*(5), 1436-1443.

iv. Saroj, A.L. & Singh, R.K. (2012). Thermal, dielectric and conductivity studies on PVA/Ionic liquid [EMIM][$EtSO_4$] based polymer electrolytes. *Journal of Physics and Chemistry of Solids*, *73*(2), 162–168.

JUNIOR SCIENCE COMMUNICATION
https://jscfsg.uitm.edu.my/
Volume 2 (2019)
eISSN 2637-0689

Colloquium of Chemistry and Environment 2018
Faculty of Applied Sciences, Universiti Teknologi MARA, Shah Alam.

EXTRACTION AND PHYSICAL CHARACTERIZATION OF SILICA FROM OIL PALM LEAVES (*Elaies guineensis*)

Awangku Muhammad Haziq Awang Kamaruddin, Wan Nazihah Wan Ibrahim*
Faculty of Applied Sciences, Universiti Teknologi MARA, 40450 Shah Alam, Selangor, Malaysia

*wannazihah@uitm.edu.my

Abstract: Palm oil productions are increasing drastically every year due to its high demand in global market and thus the oil palm trees tend to produce more biomass with no proper way to dispose it. This study was conducted to reduce the biomass produced by extracting the silica (SiO_2) content within the leaves of the oil palm (*Elaies guineensis*) through acid and thermal treatment and use the silica ash obtained to coat onto magnetite (Fe_3O_4) nanoparticles that was previously synthesized through co-precipitation of Fe^{2+} and Fe^{3+} ions in alkaline condition. The coating process was done through sol-gel method to obtain the $Fe_3O_4@SiO_2$ composite and all the products were then physically characterized using Fourier transform infrared spectroscopy (FTIR), scanning electron microscopy (SEM), x-ray diffraction (XRD) and nitrogen adsorption (BET). It was observed that the silica was successfully extracted and coated onto the magnetite based. The products were tested as an adsorbent for the removal of organophosphate pesticide (OPPs) compounds namely chlorpyrifos, diazinon and parathion methyl in aqueous sample (strawberries). From the results, it shows that both SiO_2 and $Fe_3O_4@SiO_2$ have the potential to be an excellent adsorbent for the removal of OPPs from aqueous sample and further optimization is required to obtain better results.

Keywords: *Silica, magnetite, magnetic silica, SiO_2, Fe_3O_4, $Fe_3O_4@SiO_2$*

INTRODUCTION

The palm oil production in Malaysia are increasing every year due to its demand in the global market. Harvesting the oil palm fruits would leave the oil palm frond and leaves to decompose naturally on the ground or burnt openly. Disposing large quantities of agricultural biomass using this kind of method in a long term are environmentally challenging and also unmanageable (Elias *et al*., 2018). Therefore, this project is significance to minimize the agricultural waste generated by the oil palm plantation in Malaysia by converting the oil palm biomass into a value-added product. One of the valuable products is the silica that present within the frond leaves part of oil palm which could be used to realize the industrial and used in biological fields.

METHODOLOGY

Silica was extracted by treating the oil palm leaves with HCl and then subjected into the furnace to produce white silica ash (SiO2) which then converted into sodium silicate (Na2SiO3) by mixing with NaOH solution. Magnetite (Fe3O4) nanoparticles was synthesized separately through co-precipitation of iron (II) sulphate and iron (III) chloride. NaOH was added as a precipitating agent. Then, the Na2SiO3 was used to coat onto Fe3O4 via sol-gel method to produce magnetic silica (Fe3O4@SiO2). All the products obtained were then characterized and tested as potential adsorbents for the removal of OPPs from aqueous samples by using magnetic solid phase extraction method (MSPE) for adsorption of OPPs onto Fe3O4@SiO2

sorbent and dispersive solid phase extraction method (DSPE) for SiO2 sorbent before analyzing both sorbents using HPLC-UV.

FINDINGS

FTIR (Figure 1(a)) was obtained to determine the functional groups presence in the materials. The result shows that SiO_2 exhibit the asymmetric and symmetric siloxane Si-O-Si stretch at 1049 cm^{-1} and 800.7 cm^{-1}, respectively (Sompech *et al*., 2016). The absorption peak at 548.8 cm^{-1} represents the Fe-O stretching of Fe_3O_4 (Panwar *et al*., 2015). Both Fe-O and Si-O-Si absorption peaks were observed at Fe_3O_4@SiO_2 but lower in intensity due to covering of SiO_2 onto Fe_3O_4. The SEM images (Figure 1(b)) of SiO_2 consist of agglomerated particles with irregular morphology and shape varies in sizes. Fe_3O_4 shows that most of the particles are roughly cubic and aggregate together (Alzaidi *et al*., 2016). Fe_3O_4@SiO_2 still retain the morphologies properties of SiO_2 except for a greater particle size and absence of cubic Fe_3O_4 indicating the coating process was successful.

From the XRD analysis (Figure (c)), SiO_2 exhibits a single broad peak at $2\theta = 22.978°$ indicating the amorphous state while Fe_3O_4 shows multiple peaks centering at various 2θ values representing the crystallographic cubic crystal structure of magnetite. Fe_3O_4@SiO_2 exhibits both crystalline and amorphous state, except for the shifted 2θ values due to lattice distortion causes by high temperature and higher peak intensities due to increase in degree of crystallinity of the composite.

The BET analysis shows that SiO2 have greater particle size compared to Fe3O4@SiO2 which might be due to the agglomeration of Fe3O4 in the core of the Fe3O4 andSiO2 thus increasing its pore size (Pasandideh *et al*., 2016).

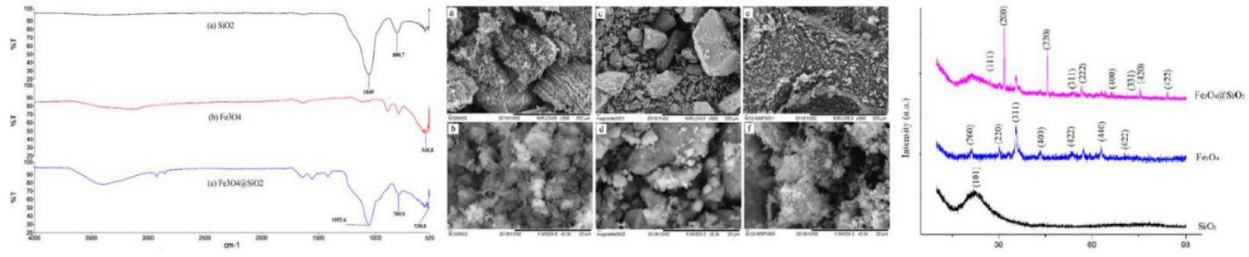

(a) (b) (c)

Figure 1 (a) FTIR spectra, (b) SEM images at magnification 500X (above), 5000X (below) and (c) XRD diffractograms of SiO2, Fe3O4 and Fe3O4@SiO2 respectively

Colloquium of Chemistry and Environment 2018
Faculty of Applied Sciences, Universiti Teknologi MARA, Shah Alam.

Table 1 Nitrogen adsorption analysis for SiO2 and Fe3O4@SiO2

	Analysis	SiO2	Fe3O4@SiO2
	a. Surface Area (m^2/g)		
	Single Point Surface Area	183.2656	62.9924
	BET Surface Area	193.3477	66.7914
	Langmuir Surface Area	267.5511	93.3625
	b. Pore Volume (cm^3/g)		
	Single Point Adsorption Total Pore Volume of Pores	0.497545	0.327157
	c. Pore Size (nm)		
	Adsorption Average Pore Diameter by BET	10.2933	19.5928

Testing for Potential Adsorbents

The testing was conducted without any calibration and optimization. The analysis was made solely based on the peak areas of the HPLC chromatograms. The result shows that the SiO2 gives better separation of OPPs compared to Fe3O4@SiO2 due to the higher surface area of SiO2 permits better adsorption of OPPs onto the sorbent.

CONCLUSION

The SiO2 was successfully extracted from oil palm leaves and coated with Fe3O4 to produce Fe3O4@SiO2 based on the characterizations. Both SiO2 and Fe3O4@SiO2 shows that the potential to become good adsorbents based on the chromatogram results. Further calibration and optimization are required to obtain better results.

REFERENCES

i. Alzaidi, J., Alzahrani, E. & El-Mouhty, N.R.A. (2016). Chemical Studies on the Preparation of Magnetic Nanoparticles Coated with Glycine and its Application for Removal of Heavy Metals. *Oriental Journal of Chemistry, 32*(3), 1503-1513.

ii. Elias, N., Chandren, S., Abdul Razak, F.I., Jamalis, J., Widodo, N. & Abdul Wahab, R. (2018). Characterization, optimization and stability studies on *Candida rugosa* lipase supported on nanocellulose reinforced chitosan prepared from oil palm biomass. *International Journal of Biological Macromolecules, 114*, 306-316.

iii. Panwar, V., Kumar, P., Bansal, A., Ray, S.S. & Jain, S.L. (2015). PEGylated magnetic nanoparticles (PEG@Fe_3O_4) as cost effective alternative for oxidative cyanation of tertiary amines *via* C-H activation. *Applied Catalysis A: General*, *498*, 25–31.

iv. Pasandideh, E.K., Kakavandi, B., Nasseri, S., Mahvi, A.H., Nabizadeh, R., Esrafili, A. & Kalantary, R.R. (2016). Silica-coated magnetite nanoparticles coreshell spheres (Fe_3O_4@SiO_2) for natural organic matter removal. *Journal of Environmental Health Science & Engineering, 14*(21), 1-13.

v. Sompech, S., Dasri, T. & Thaomola, S. (2016). Preparation and Characterization of Amorphous Silica and Calcium Oxide from Agricultural Wastes. *Oriental Journal of Chemistry, 32*(4), 1923-1928.

JUNIOR SCIENCE COMMUNICATION
https://jscfsg.uitm.edu.my/
Volume 2 (2019)
eISSN 2637-0689

Colloquium of Chemistry and Environment 2018
Faculty of Applied Sciences, Universiti Teknologi MARA, Shah Alam.

DETERMINATION OF PHENOLS IN SOIL BY HEADSPACE SOLID PHASE MICROEXTRACTION-GAS CHROMATOGRAPHY MASS SPECTROMETRY

Alyanie Nazirah Abdul Rahman@Awang, Khairulmazidah Mohamed, Reena Abd Rashid*
Faculty of Applied Sciences, Universiti Teknologi MARA, 40450 Shah Alam, Selangor

*reena1572@uitm.edu.my

Abstract: Phenol, or hydroxybenzene is a substance marked by US Environmental Protection Agency (US EPA) into The List of Priority Pollutants, and are classified as dangerous due to its health effects when exposed to acute toxicity levels. The presence of phenol is caused by anthropogenic activities for example wood burning, smoking, and incineration of rubbish and cars exhausts which will get embedded in soil. The objective of this study is to identify the primary phenols in soil samples using Headspace Solid Phase Micro Extraction-Gas Chromatography Mass Spectrometry (HS SPME-GCMS) and to quantify primary phenols found in soil samples collected in Malaysia, Holland, Canada and Sweden. In this study, four peat soil samples from Malaysia, Canada, Holland and Sweden were selected. Soil sample (10g) was dried at 105 ℃ overnight until three consistent weight readings were obtained to ensure absence of moisture. The samples were then suspended in water, potassium bicarbonate ($KHCO_3$) and acetic anhydride ($(CH_3CO)_2O$). The extraction of phenol was done using HS SPME by exposing the polydimethylsiloxane (PDMS) fibre with 100 μm thickness to the headspace for 15 minutes. All three samples from Malaysia, Canada, and Holland exhibited four phenols which were 2,4-dimethylphenol, 2,4-dichlorophenol, 2,4,6-trichlorophenol and 2,4,5-trichlorophenol. Sweden soil sample indicated no phenol. The four types of phenols were quantified by running a set of standards which were 2,4-dimethylphenol, 2,4-dichlorophenol, 2,4,6-trichlorophenol and 2,4,5-trichlorophenol from 0 ppm to 10 ppm. Calibration curves of the four phenol standards were plotted with R2 value >0.98. Phenol standards which are 2,4-dimethylphenol, 2,4-dichlorophenol, 2,4,6-trichlorophenol, 2,4,5-trichlorophenol quantified in soil sample was between 4-10 ppm. The LOD values calculated for the phenols were 0.23 ppm, 0.19 ppm, 1.15 ppm and 0.29 ppm each, respectively whereas the LOQ values for each phenol were 0.71 ppm, 0.56 ppm, 3.48 ppm and 0.87 ppm, respectively. The average % recovery for all four phenols are 54.43% with average %RSD value is 4.53%.

Keywords: *Phenol, HSSPME-GCMS, chlorophenol, soil.*

INTRODUCTION

Phenolic compounds are found to be harmful to human life and it can bioaccumulate in living organisms, thus the production of these compounds must be controlled (Michalowicz and Duda, 2006). Phenol contamination of groundwater that was used for drinking purposes in 1974 had caused tremendous health hazard (Delfino and Dube, 1976). Phenols like chlorophenols mainly come through industrialization such as manufacturing of polymeric resin, purification of oil and cooking plants. Chlorophenol are used as pesticide to control bacteria, fungi, insects and weeds. 2,4-Dichlorophenol reacts with formaldehyde to form methylenebis which is used as mothproofing agent, an antiseptic and a seed disinfectant. 2,4,6-Trichlorophenol is used as a bactericide and fungicide and 2,4,5-trichlorophenol has similar functions and can be changed into hexachlorophene or into thiobis. Both trichlorophenols isomers are used as germicides in soap (Carey, 2011). This study would compare the phenol level in soils with the toxicity levels for safety purposes.

Volume 2 (2019)
eISSN 2637-0689

METHODOLOGY

The soil used for the headspace SPME-GCMS was peat soil. Four different peat soils were purchased from the local nurseries in Malaysia, Holland, Canada and Sweden. The crucibles are pre-dried in the oven at 135℃ for 1 hour to remove any possible moisture. Each soil sample (10 g) was put into the crucible and dried for another 24 hours at 105℃. The drying process was repeated until three consistent weight readings were obtained. Then, each soil sample was directly transferred into the SPME vials for extraction process. A non-automatic SPME holder with a 100-μm PDMS fiber was used. An aliquot of 0.5 g of peat soil was placed in a headspace vial. After the addition of potassium bicarbonate, (0.2 g), acetic anhydride (0.2 ml), sodium chloride (0.2 g) and water (1 ml), the vial was sealed with a headspace aluminum cap. The sample was immersed in a SPME vial and put in 100 ℃ water bath, and allowed to equilibrate for 15 minutes. The fiber was exposed to the headspace for 15 minutes. Desorption time of fiber was set at exactly 3 minutes and all samples were analysed by GCMS.

FINDINGS

Four peat soil from different regions are analysed using GC-MS and HS- SPME extraction procedure and tabulated in Table 1. Using the standard calibration curves, the concentration of the four standard phenols which are 2,4-dimethylphenol, 2,4-dichlorophenol, 2,4,6-trichlorophenol and 2,4,5-trichlorophenol was obtained. As observed in Table 1, the concentration of chlorophenols present are higher compared to dimethylpehnols in the soil sample except soil sample from Sweden. Chlorophenols are significant in soil samples from industrialization area due to use of antiseptic, pesticides and seeds disinfectant on the land prior to construction activities(Michalowicz and Duda, 2006).

Table 1 Concentration of primary phenols in soil samples

Soil Sample	Detected phenols	Correlation Area	Concentration (ppm)
Malaysia	a) 2,4-dichlorophenol	61302749	3.38
	b) 2,4,6-trichlorophenol	137767624	7.89
	c) 2,4,5-trichlorophenol	625550507	7.95
Canada	a) 2,4,6-trichlorophenol	14157102	1.71
Holland	a) 2,4-dimethylphenol	60601772	2.78
	b) 2,4-dichlorophenol	62094911	3.40
	c) 2,4,6-trichlorophenol	141234361	8.06
	d) 2,4,5-trichlorophenol	546840655	7.08

Sweden	(no phenol peaks detected)	-	-

Table 2 LOD, LOQ, percent recovery and %RSD of four phenols in EPA 8270 Phenols Mix

Primary phenols	**LOD (ppm)**	**LOQ (ppm)**	**Percent recovery (%)**	**%RSD**
2,4-dimethylphenol	0.23	0.71	43.98	2.55
2,4-dichlorophenol	0.19	0.56	60.94	2.01
2,4.6-trichlorophenol	1.15	3.48	67.90	8.23
2,4,5-trichlorophenol	0.29	0.87	44.90	5.32

CONCLUSIONS

This assessment was conducted to determine and quantify phenols in four different soil regions in Holland, Malaysia, Sweden and Canada. Soil from Sweden indicated no presence of phenols. The % recovery, LOD and LOQ values were calculated to support the significance of the findings. The %RSD for all primary phenols are all <10%.

REFERENCES

i. Delfino, F., & Dube D. (1976). Persistent contamination of ground water by phenol. *J. Environ. Sci. Health., 43*, 345, 1976.
ii. Carey, F. A. (2011, November 16). Chlorophenol. Retrieved from https://www.britannica.com/science/chlorophenol
iii. Michalowicz, J. & Duda, W. (2006). Phenols - sources and toxicity. *Polish J. of Environ. Stud.,16*, 347-362

JUNIOR SCIENCE COMMUNICATION
https://jscfsg.uitm.edu.my/
Volume 2 (2019)
eISSN 2637-0689

Colloquium of Chemistry and Environment 2018
Faculty of Applied Sciences, Universiti Teknologi MARA, Shah Alam.

ANALYTICAL PERFORMANCE ASSESSMENT OF CHEMICAL OXYGEN DEMAND FOR LAKE OF SHAH ALAM, SELANGOR

Brandon Dee Jikat, Shariff Che Ibrahim*
Faculty of Applied Sciences, Universiti Teknologi MARA, 40450 Shah Alam, Selangor, Malaysia

* sha88@uitm.edu.my

Abstract: Analytical performance assessment of chemical oxygen demand (COD) for lake of Shah Alam, Selangor was observed. Analytical methods of performances determined includes; recovery, precision, limit of detection and limit quantification that is required to assure data receive in laboratory is reliable. This method was quite precise with the mean relative standard deviation (RSD) values found to be 4.44%. Then, LOD and LOQ obtained were in the range 6 mg/L – 8 mg/L and 20 mg/L – 24 mg/L, respectively. The mean recovery percentage for 3 different concentrations is 108%. This value indicates that the developed method is acceptable because it falls between the acceptable range of recovery which is 80% - 120%. Then, the assessment of COD for lake of Shah Alam, Selangor which are Taman Tasik Shah Alam and Tasik Seksyen 7 Shah Alam were evaluated. The highest concentration of COD value of 48.96 mg/L was recorded for both location and the lowest value of 35.9 mg/L was recorded in Taman Tasik Shah Alam. Hence, by using the water quality index (WQI) tool, both location falls into Class III. Apart from that, pH was also observed and found to be in the range of 6 - 7 for both lakes. Hence, it is indicated that the lakes in Shah Alam, Selangor water is slightly polluted and need extensive treatment.

Keywords: *Chemical oxygen demand, recovery, precision, limit of detection, limit of quantification*

INTRODUCTION

Lakes have important sources of existence of aquatic life. The pollutions of surface water such as toxic and eutrophication of lakes can endanger the aquatic life. Thus, it is importance to observed the quality of lake water to control the pollution. Thus, an assessment on lake water is needed. In order to have precise data receive in laboratory, analytical method of performance is required to assure data receive is reliable. This study provides the data of assessment on lake in Shah Alam, Selangor which is in Taman Tasik Shah Alam and Tasik Seksyen 7, Shah Alam. Apart from that, method of analytical methods performance was done to ensure the data received are precise.

METHODOLOGY

This method used closed reflux chemical oxygen demand by using method of APHA (2005). In chemical oxygen demand process, 2.5 mL of sample was added into the vessel of COD containing potassium dichromate ($K_2Cr_2O_7$) and sulfuric acid reagent (H_2SO_4 reagent). This solution was digested in COD reactor for 2 hours at 150 ^oC. Then, the digested solution was titrated with ferrous ammonium sulphate after a drop of ferroin indicator was added. Then concentration of COD was measured. For precision, spike of potassium hydrogen phthalate with addition of blank was prepared before undergoing chemical oxygen demand process. For recovery, spike and unspike sample were prepared where spike sample contain solution of potassium hydrogen phthalate and lake sample while for unspike solution contained lake sample only. Then, the sample underwent a process of chemical oxygen demand. The precision was done by repeating the procedures for 3 days while for recovery the procedure was repeated for 3 concentrations which were 50

mg/L, 70 mg/L and 100 mg/L. Then, the lakes water samples were analyzed for their pH values using pH meter and their chemical oxygen demand values.

FINDINGS

Precision

The mean relative standard deviation obtained for 3 days is 4.44 %. According to Gonzalez *et al.* (2007), maximum acceptable RSD percentage can be obtained in between 10 mg/L to 100 mg/L are in the range of 11.3% and 8% respectively. Apart from that, Ricardo *et al.* (2002) also stated that, RSD that is below 10% can be considered to be satisfactory.

Limit of Detection (LOD) and Limit of Quantification (LOQ)

Based on this result, LOD and LOQ were found to be 6.28 ppm and 20 ppm, respectively. It shows that LOQ was much higher than LOD. According to Armbruster *et al*. (2008), LOQ will be higher or equal with LOD. Hence, analyte cannot be lower than LOD because LOD provide an estimate concentration which distinguish from zero. Previous study by Almeida *et al.* (2012), based on determination of chemical oxygen demand by a flow injection method found that LOD and LOQ for this method were 0.94 mg/L and 2.78 mg/L respectively. This method was less sensitive for analyzing organic matter content compared to the previous study by using flow injection method.

Recovery

Based on the result, recovery for the 3 concentrations were 90% - 120%. According to APHA (2005), recovery that is acceptable are in the range of 80-120%. Therefore, this study has an accurate quantification of the recovery's solution.

Water quality parameter of lake at Shah Alam, Selangor

The highest concentration of COD value of 48.96 mg/L was recorded for both location and the lowest value of 35.9 mg/L was recorded in Taman Tasik Shah Alam. Hence, by using the water quality index (WQI) tool, both location falls into Class III. Apart from that, pH also was observed and found to be in the range of 6-7 for both lakes. Hence, it is indicated the lakes water in Shah Alam, Selangor is slightly polluted and need extensive treatment (Department of Environment, 2009).

CONCLUSIONS

In conclusion, data of analytical method on surface of lake water using closed reflux chemical oxygen demand showed very good performance for most of the studied analytes in terms of sensitivity, accuracy and precision. Based on the result of recovery, all concentrations were in the acceptable range of 80-120% which is 96%, 86% and 100% for 50 mg/L, 70 mg/L and 100 mg/L, respectively. Precision obtained from the analysis of seven known concentrations within three days are 4.08%, 4.85% and 4.41%. Thus, limit of detection (LOD) are 6.28 mg/L, 7.31 mg/L and 6.78 mg/L while for limit of quantification are 20, 23.3 and 21.6. Hence, the data received in the lab are reliable and precise. Water parameter index for both locations were observed. Based on the result, pH was in the range of desirable value which is 6.5-8.5 that indicate,

the existence of aquatic life in both places. Then, chemical oxygen demand for both places are considered as class III which needed extensive treatment for both locations.

REFERENCES

i. Almeida, C. A., González, P., Mallea, M., Martinez, L. D., & Gil, R. A. (2012). Determination of Chemical Oxygen Demand by A Flow Injection Method Based on Microwave Digestion and Chromium Speciation Coupled Toinductively Coupled Plasma Optical Emission Spectrometry. *Talanta*, *97*, 273-278.
ii. APHA. (2005). Standard Methods for The Examination of Water and Wastewater (21st Edition ed.). Washington, DC: American Public Health Association.
iii. Armbruster, D. A., & Pry, T. (2008). Limit of Blank, Limit of Detection and Limit of Quantitation. *Clin Biochem Rev*, *29*, 49-52.
iv. Department of Environment. (2009). Malaysian Environmental Quality Report (EQR). Retrieved Sep 5, 2019 from http://www.wepa-db.net/policies/law/malaysia/eq_surface.htm
v. Gonzalez, A. G., & Herrador, M. A. (2007). A Practical guide to analytical method validation, including measurement uncertainty and accuracy profiles. *Trends in Analytical Chemistry*, *26*, 227-238.
vi. Ricardo, L. p., Margarita, A., Juan, C., & Vicente, F. (2002). Determination of Minor and Trace Volatile Compounds in Wine Bysolid-Phase Extraction and Gas Chromatography with Mass Spectrometric Detection. *Journal of Chromatography A, 966*, 167–177.

JUNIOR SCIENCE COMMUNICATION
https://jscfsg.uitm.edu.my/
Volume 2 (2019)
eISSN 2637-0689

Colloquium of Chemistry and Environment 2018
Faculty of Applied Sciences, Universiti Teknologi MARA, Shah Alam.

PRODUCTION OF BIODIESEL FROM WASTE COOKING OIL USING BENTONITE CATALYSTS

Cherlice Allessandra Seminding, Noraini Hamzah*
Faculty of Applied Sciences, Universiti Teknologi MARA, 40450 Shah Alam, Selangor, Malaysia.
*pnoraini@uitm.edu.my

Abstract: Production of biodiesel, also known as fatty acid methyl ester (FAME), is costly as it uses edible oil as a feedstock. Therefore, in this study waste cooking was used due to its abundance and it is cheaper as compared to edible oil. The production of biodiesel from waste cooking oil was carried out via transesterification process using two types of bentonite catalyst, which are raw bentonite and NaOH/bentonite. The NaOH/bentonite catalyst was prepared by impregnation method using 0.1M NaOH and reflux at 60 ^{o}C for 12 hours. The XRD patterns for both raw bentonite and NaOH/bentonite were almost similar. However Na_2O, a new peak appeared at the NaOH/bentonite XRD pattern. BET isotherm linear plot shows that both catalyst have a Type IV, indicates that the catalyst is mesoporous material. It was observed that total basicity of NaOH/bentonite is much higher compared to raw bentonite. The optimum condition obtained for methanol/oil molar ratio and reaction temperature obtained were 15:1 and 55 ^{o}C with highest yield of FAME (72 %) under continuous stirring with 0.5wt.% (0.15g) NaOH/bentonite catalyst. This study shows that treated bentonite with NaOH could enhance the basicity of the catalyst that gave good catalytic property in transesterification of waste cooking oil.

Keywords: Waste cooking oil(WCO), Fatty Acid Methyl Ester (FAME),

INTRODUCTION

Diesel is a non-renewable energy source which commonly used as fuel for transportation such as car, motorcycle, buses and aeroplane. However, due to rapid population growth, the fossil fuel (diesel) depleted with time. Therefore, it is crucial to find a renewable source as a substituent for diesel. Biodiesel is renewable fuel which has similar properties as the conventional diesel. Biodegradability, low sulphur content, low toxicity and lower greenhouse gases emission are another benefit brought by biodiesel (Atabani *et al.,* 2013). Due to this, biodiesel might be the most suitable substituent for diesel. Many researchers have been searching for ways on how to produce biodiesel in a way that would benefit everybody who get involved in the biodiesel production process. There are many methods available to produce biodiesel. One of the method is transesterifcation whereby the glycerides present in fats or oils react with an alcohol in the presence of a basic catalyst to form esters and glycerol (Bhuiya *et al.,* 2016). However, the cost production of biodiesel is high as it uses edible oil as feedstock. To encounter this problem, waste cooking oil was used as a feedstock. Since catalyst also affect the amount of biodiesel produced, heterogenous catalyst was used instead of homogenous catalyst. Therefore, in this study, production of biodiesel was done through transesterification process using waste cooking oil as the feedstock, methanol as the solvent and bentonite based as the heterogenous basic catalyst.

Volume 2 (2019)
eISSN 2637-0689

METHODOLOGY

The WCO was collected from Dataran Cendekia, a food court in Universiti Teknologi MARA. Pre-treatment was done by centrifugation and heating for the removal of suspended particle and moisture. Fatty Acid Test was conducted prior to transesterification. Raw bentonite was taken directly from the bottle while NaOH/bentonite was prepared through impregnation method and reflux under 60°C for 12 hours. The transesterification of waste cooking oil (WCO) was done in 250 ml three-neck round bottomed flask using 15g of waste cooking oil, methanol/oil molar ratio which range from 15:1 to 19:1, under continuous stirring at 65°C for 2 hours. Upon completion, the mixture was placed in separating funnel and left for one night for a complete separation between the biodiesel and glycerol. Analysis of the synthesized biodiesel was done using GC-FID to determine the presence of FAME.

FINDINGS

Figure 1(a) shows the effect of methanol/oil molar ratio on the yield of biodiesel using raw bentonite and NaOH/bentonite catalyst. The results showed that increasing in methanol/oil molar ratio, raw bentonite shows a significant increase in biodiesel yield with a maximum yield of 70% biodiesel at 17:1 methanol/oil molar ratio. However, for NaOH/bentonite the biodiesel yields significantly decreased. Since at 15:1 molar ratio, NaOH/bentonite only produced 66% of biodiesel, it is expected that the NaOH/bentonite might produce higher yield of biodiesel at methanol/oil molar ratio lower than 15:1. This may due to the presence of NaOH particles in the bentonite pores. Wu *et al*., (2016), reported that bentonite can preserve the catalytically active methoxide species during the methanolysis by shifting the hydroxide/methoxide equilibrium towards the formation of the alkoxide, leading to increased amounts of FAME. This effect might increase the total basicity value of the NaOH/bentonite. The NaOH/bentonite catalyst become more basic where it contains more number of basic sites compared to raw bentonite (Lee *et al*., 2014). Thus, lower methanol/oil molar ratio was needed to convert the waste cooking oil into biodiesel completely. Since transesterification reaction is a reversible reaction, it crucial to determine the most optimum methanol/oil molar ratio. This is because a high methanol/oil molar ratio favored the formation of glycerol instead of biodiesel and only little biodiesel yields will be produced at low methanol/oil molar ratio (Ali *et al.,* 2016).

Figure 1(b) shows that as the reaction temperature increased, biodiesel yield also increases. However, no significant increment was observed at temperature above 55ºC for NaOH/bentonite catalyst. No significant changes above 60°C was observed for raw bentonite. Optimum reaction temperature was observed at 55°C for NaOH/bentonite catalyst. This finding fulfills the requirement where the reaction temperature should be lower than the boiling point of the methanol.

Colloquium of Chemistry and Environment 2018
Faculty of Applied Sciences, Universiti Teknologi MARA, Shah Alam.

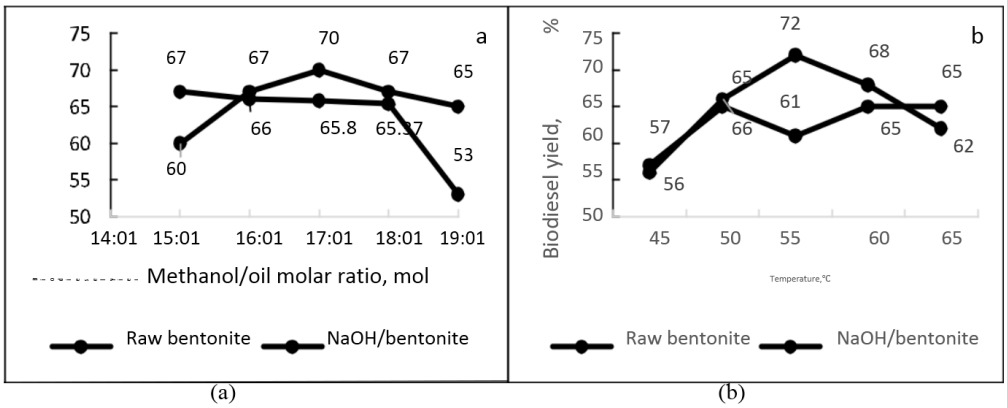

(a) (b)

Figure 1 Effect of a) methanol/oil molar ratio and b) reaction temperature on biodiesel yield using raw bentonite and NaOH/bentonite

CONCLUSION

The present study reveals that NaOH/bentonite gave better performance due to higher biodiesel yield compared to raw bentonite. Experimental has been done on waste cooking oil as a feedstock and the result showed that biodiesel yield for NaOH/bentonite catalyst (72.75%) was higher compared to raw bentonite catalyst (60.86%). The optimum condition for the maximum biodiesel yield was obtained at 15:1 methanol/oil molar ratio with 0.5wt.% catalyst (0.15g), with reaction temperature at 55ºC for 2 hours. Analysis on GC-FID shows that the major compound in the synthesized biodiesel were methyl palmitate and methyl stearate.

REFERENCES

i. Ali, B., Yusup, S., Quitain, A.T., Kamil, R.N.M., Sumigawa, Y., Ammar, M. & Kida, T. (2016). Pretreatment and Bentonite-based Catalyzed Conversion of Palm-rubber Seed Oil Blends to Biodiesel. *Procedia Engineering*, *148*, 501-507.

ii. Atabani, A.E., Silitonga, A.S., Ong, H.C., Mahlia, T.M.I., Masjuki, H.H., Badruddin, I.A. & Fayaz, H. (2013). Non-edible vegetable oils: A critical evaluation of oil extraction, fatty acid compositions, biodiesel production, characteristics, engine performance and emissions production. *Renewable and Sustainable Energy Reviews*, *18*, 211-245.

iii. Bhuiya, M.M.K., Rasul, M.G., Khan, M.M.K., Ashwath, N. & Azad, A.K. (2016). Prospects of 2nd generation biodiesel as a sustainable fuel—Part: 1 selection of feedstocks, oil extraction techniques and conversion technologies. *Renewable and Sustainable Energy Reviews*, *55*, 1109-1128.

iv. Lee, H.V., Juan, J.C., Abdullah, N.F., MF, R.N. & Taufiq-Yap, Y.H. (2014). Heterogeneous base catalysts for edible palm and non-edible Jatropha-based biodiesel production. *Chemistry Central Journal*, *8*(1), 30.

v. Wu, L., Wei, T.-Y., Tong, Z.-F., Zou, Y., Lin, Z.-J. & Sun, J.-H. (2016). Bentonite-enhanced biodiesel production by NaOH-catalyzed transesterification of soybean oil with methanol. *Fuel Processing Technology*, *144*, 334-340.

JUNIOR SCIENCE COMMUNICATION
https://jscfsg.uitm.edu.my/
Volume 2 (2019)
eISSN 2637-0689

Colloquium of Chemistry and Environment 2018
Faculty of Applied Sciences, Universiti Teknologi MARA, Shah Alam.

SYNTHESIS AND CHARACTERIZATION OF SBA-16 FROM COAL FLY ASH

Dayang Nurfaridahana Abg Mentaril, Mohammad Noor Jalil*
*Faculty of Applied Sciences, Universiti Teknologi MARA, 40450 Shah Alam Selangor, Malaysia.
* moham423@uitm.edu.my

Abstract: Silica was extracted from coal fly ash (CFA) adopting the alkali fusion method and the resulting supernatant was used to prepare SBA-16. For comparison, SBA-16 was synthesized by using tetraethylorthosilicate (TEOS) as the pure silica source. According to SEM analyses, the morphology of SBA-16 prepared from extracted supernatant showed small to large colloidal particles with some spherical features, while SBA-16 synthesized from TEOS revealed the combination of decahedral with spherical features. EDXA results established O, Na, C and Si as the major components in the extracted supernatant. The percentage yield of silica extracted from the CFA was found to be 53.55%.

Keywords: Coal Fly Ash, Mesoporous Silica, SBA-16, Tetraethylorthosilicate, Alkali Fusion Method, Silica Source

INTRODUCTION

Coal combustion in power plants produces a large amount of ash, as such CFA, and its disposal is causing serious environment problems (Chandrasekar & Ahn, 2008). Hence, methods of converting CFA into useful materials are vital. The interest in the field led to the preparation of SBA-16 utilizing CFA as the silica source. CFA has been investigated for its potential as a silica source for the manufacture of mesoporous silica. Besides, limited reports have addressed converting CFA into SBA-16. Thus, this research aims to extract silica from CFA and utilize the extracted supernatant for the synthesis of SBA16. Silicate extraction from CFA adopted the alkali fusion method, whilst the procedure to synthesis SBA-16 was conducted following the procedure reported by Cao *et al*. (2016).

METHODOLOGY

Chemicals and Raw Materials

The chemicals used were CFA, Pluronic F127 ($EO_{106}PO_{70}EO_{106}$), 2M HCl, 35 wt% HCl, n-butanol, deionized water, Tetraethylorthosilicate (TEOS), sodium hydroxide powder (NaOH), potassium chloride (KCl), and sodium metasilicate (Na_2SiO_3).

Silicate Extraction from CFA

Fine powder of CFA was mixed with NaOH powder at a 1:1.2 weight ratio and fused at 550 ˚C for 1 hour. The obtained fused mass was cooled to room temperature and ground. Thereafter, the fused mixture was mixed with deionized water at a 1:4 weight ratio and stirred for 24 hours. The resulting supernatant was used to synthesis SBA-16.

Synthesis of SBA-16

A 2 g of F127 and 5 g of KCl were dissolved in 150 g of 2M HCl and stirred for 2 hours at 38 ˚C. A 6 g of n-butanol was added to the mixture and stirred for 10 minutes. A 8.3 g of extracted supernatant was added

and 1 g of sodium metasilicate was added thereafter. The mixture was kept static for 24 hours before being transferred into reflux conditions at 100 ˚C for another 24 hours. The solid products were filtered and dried at 80 ˚C for 6 hours. At last, the SBA-16 material was calcined at 550 ˚C for the next 6 hours. For comparison, synthesis of SBA-16 using TEOS was also conducted using the same procedure. The SBA16 samples synthesized from fly ash supernatant and TEOS were designated as FASBA-16 and PSBA-16, respectively.

FINDINGS

Scanning Electron Microscopy (SEM)

Figure 1 showed the SEM micrograph for both PSBA-16 and FASBA-16. PSBA-16 exhibited a decahedral morphology together with sphere. The micellization was favored by the addition of KCl. Meanwhile, FASBA-16 revealed very small to large colloidal particles with a slight formation of spherical features. The sodium metasilicate appears to cause the particles to grow larger in size and randomly agglomerate together.

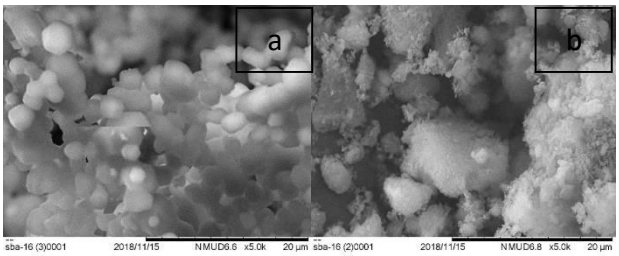

Figure 1 SEM micrograph of (a) PSBA-16 and (b) FASBA-16.

CONCLUSIONS

In conclusions, a supernatant solution was successfully extracted from the CFA with the percent yield of 53.55%. SBA-16 was successfully synthesized using CFA as the silica source. The structures and the features of PSBA-16 and FASBA-16 were confirmed by SEM micrographs. This study clearly demonstrated that the industrial by-product, CFA with a disposal problem can be successfully utilized to prepare mesoporous silica material via a relatively simple recycling process involving the alkali fusion method.

REFERENCES

i. Cao, Z., Du, P., Duan, A., Guo, R., Zhao, Z., Zhang, H.L., Zheng, P., Xu, C. & Chen, Z. (2016). Synthesis of mesoporous materials SBA-16 with different morphologies and their application in dibenzothiophene hydrodesulfurization. *Chemical Engineering Science*, *155*, 141–152.
ii. Chandrasekar, G. & Ahn, W.-S. (2008). Synthesis of cubic mesoporous silica and carbon using fly ash. *Journal of Non-Crystalline Solids*, *354*(33), 4027–4030.

JUNIOR SCIENCE COMMUNICATION
https://jscfsg.uitm.edu.my/
Volume 2 (2019)
eISSN 2637-0689

Colloquium of Chemistry and Environment 2018
Faculty of Applied Sciences, Universiti Teknologi MARA, Shah Alam.

ADSORPTION OF METHYLENE BLUE BY MESOPOROUS SILICA SANTA BARBARA AMORPHUS SBA-15

Farah Amira Shahrul Effendi, Hamizah Md Rasid*
Faculty of Applied Sciences, Universiti Teknologi MARA, 40450 Shah Alam Selangor, Malaysia.
* hamizah7708@uitm.edu.my

Abstract: The synthesis of SBA-15 was done using sol gel method by TEOS in acidic condition using 2 M hydrochloric acid solution and Pluronic P123 as a surfactant, then it was calcined at 500 °C. The characterization of SBA-15 was done to determine the chemical and physical properties using attenuated total reflectance - Fourier transform infrared spectroscopy (ATR-FTIR), field emission scanning electron microscopy (FESEM), X-ray diffraction (XRD) and Brunauer-Emmet-Teller (BET) analysis. It was found that the structured SBA-15 comprised a circle-like surface with a BET surface area of 961.78 m^2/g and total pore volumes of 1.11726 cm^3/g. Batch studies were conducted that give the optimum condition of 0.05 g of SBA-15 can adsorb 100 ppm of methylene blue in pH 9 condition with a contact time of 30 minutes. Several isotherm studies were conducted that conclude it is a Langmuir isotherm and pseudo-second-order.

Keywords: *SBA-15, methylene blue, and sol-gel method.*

INTRODUCTION

Porous materials are solids in which the framework comprise of empty pores (Bauer *et al.*, 2005). The pores allow an easy diffusion and adsorption of macromolecules for extensive applications (Fedeyko *et al.*, 2006). Porous materials have various morphologies which can be categorized based on their diameter sizes of the pore (d) which are microporous ($d < 2$ nm), mesoporous ($2 \leq d \leq 50$ nm) and macroporous ($d > 50$ nm) as allocated in the International Union of Pure and Applied Chemistry (IUPAC). Santa Barbara Amorphous (SBA-15) is a triblock organic copolymer templated silica with hexagonally well-ordered mesopores and nanoporous silica with pore size range of 4.6 nm to 30 nm which was successfully prepared at University of California in Santa Barbara in 1996. SBA-15 has large surface area, uniformity in pore size, easily-controlled surface and regeneration properties of adsorption (Sabri *et al*., 2015). SBA-15 was prepared by using sol-gel method using triblock copolymer Pluronic P123 ($EO_{20}PO_{70}EO_{20}$) with tetraethyl orthosilicate (TEOS) in acidic condition of 2 M of hydrochloric acid (HCl). Dye can cause the eutrophication of a water as the colouring materials present in the water disturbs the light penetration and cause adverse effect on aquatic system (Mittal *et al*., 2007). The efficient method to eliminate MB from aqueous effluents is through a process of adsorption. With positive result, the SBA-15 can remove other ionic pollutants in the wastewater where the world can recycle and rejuvenate a sustainable lifestyle.

METHODOLOGY

SBA-15 was synthesized using 4.0 g of amphiphilic triblock polymer of Pluronic P123 ($EO_{20}PO_{70}EO_{20}$) dissolved in 30.0 mL deionized water and 120.0 mL of 2 M hydrochloric acid (HCl). Then the solution was stirred for 20 hours at 35°C. Then, 8.5 g of tetraethyl orthosilicate (TEOS) was slowly added for 15 minutes under vigorous stirring. The mixture was left for 20 hours under aging condition. Then, it was placed in the oven for 24 hours with temperature of 90°C. The product was filtered and calcined for 6 hours at 500°C

Colloquium of Chemistry and Environment 2018
Faculty of Applied Sciences, Universiti Teknologi MARA, Shah Alam.

(Sayari *et al.*, 2004). The characterization of SBA15 was done using attenuated total reflectance-Fourier transform infrared spectroscopy (ATR-FTIR), field emission scanning electron microscopy (FESEM), X-ray diffraction (XRD) and Brunauer-Emmet-Teller (BET) analysis. Methylene blue (MB) stock solution was prepared for 1000 ppm and being diluted to 7 concentrations which were 20, 40, 60, 80, 100, 120 and 140 mg/L in 100 mL of deionized water. The batch studies were done to determine the effect of contact time (10, 20, 30, 40, and 50 minutes; fixed parameters: 80 ppm MB and pH 7), initial concentration time (60, 80, 100, 120 and 140 ppm; fixed parameters: 30 minutes and pH 7) and pH (3, 5, 7, 9 and 11; fixed parameters: 30 minutes and 80 ppm) using 0.05 g of SBA-15 and then shaken. The analysis was done by using UV-Vis Spectroscopy at wavelength of 660.24 nm and A PTFE (polytetrafluoroethylene) 0.22 µm membrane filter.

FINDINGS

The results obtained from this study shows that at pH 9 using 100 ppm of methylene blue with a contact time of 30 minutes gives the optimum condition in removing methylene blue efficiently at 87.37 %.

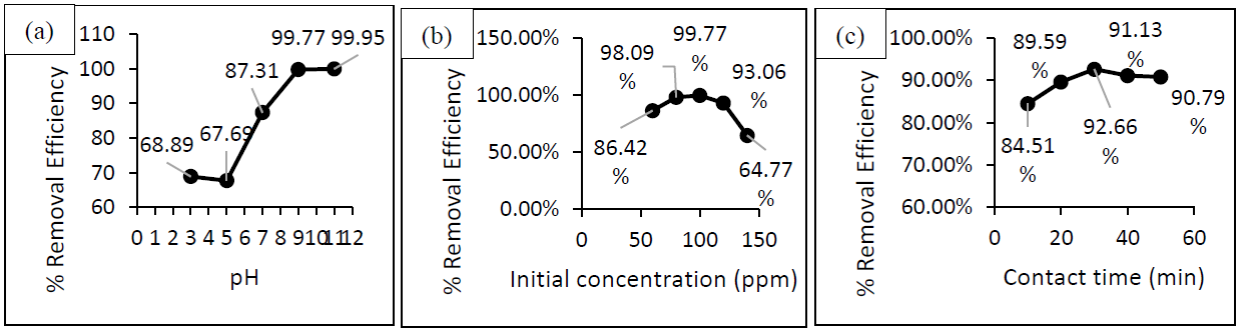

Figure 1 Removal efficiency (%) in various (a) pH (b) initial concentration and (c) contact time

As depicted in Figure 1(a), increase in pH gives a saturated proton which later compete with the methylene blue for adsorption process on the surface of SBA-15 which gives an optimum at pH 9. Whereas in Figure 1(b) where 0.05 g of SBA-15 can remove 100 ppm of MB efficiently as the surface area of SBA-15 is 961.78 m^2/g and has a total pore volume of 1.11726 cm^3/g from BET analysis. Meanwhile, in Figure 1(c) shows the optimum of 30 minutes in contact time as it is the sufficient time for the methylene blue to be in contact with SBA-15.

CONCLUSION

In conclusion, SBA-15 was successfully synthesized using a sol-gel method. The synthesis of SBA15 had revealed the absence of Pluronic P123 as a surfactant after calcination in the ATR-FTIR spectrum. The FESEM had shown the morphologies of SBA-15 as a circle-like in structure whereas, XRD diffractogram had shown the presence of amorphocity of SBA-15. Furthermore, the BET surface area of SBA-15 with the

volume of 1.11726 cm^3/g and surface area of 961.78 m^2/g were also obtained from the BET analysis. The optimum parameters in removing 87.37 % of 10 mL of 100 ppm methylene blue was achieved using 0.05 g of SBA-15 at pH 9 with contact time of 30 minutes.

REFERENCES

i. Bauer, J., Ulatowska-Jarża, A., Podbielska, H., Lechna-Marczyńska, M., Bindig, U., Muller, G. & Beuthan, J. (2005). Influence of heating temperature on structural properties of sol-gel materials. *Optica Applicata*, *35*(4), 791–797.
ii. Mittal, A., Malviya, A., Kaur, D., Mittal, J. & Kurup, L. (2007). Studies on the adsorption kinetics and isotherms for the removal and recovery of Methyl Orange from wastewaters using waste materials. *Journal of Hazardous Materials*, *148*(1-2), 229-240.
iii. Sabri, A.A., Albayati, T.M. & Alazawi, R.A. (2015). Synthesis of ordered mesoporous SBA-15 and its adsorption of methylene blue. *Korean Journal of Chemical Engineering*, *32(9),* 1835-1841.
iv. Sayari, A., Han, B.-H. & Yang, Y. (2004). Simple Synthesis Route to Monodispersed SBA-15 Silica Rods. *Journal of the American Chemical Society*, *126*(44), 14348-14349.

JUNIOR SCIENCE COMMUNICATION
https://jscfsg.uitm.edu.my/
Volume 2 (2019)
eISSN 2637-0689

Colloquium of Chemistry and Environment 2018
Faculty of Applied Sciences, Universiti Teknologi MARA, Shah Alam.

AGE DETERMINATION OF DOCUMENTS BY ATR-FTIR

Farah Nadira Aznoor Hisham, Ezlan Elias*
School of Chemistry and Environment, Faculty of Applied Sciences, Universiti Teknologi MARA, 40450 Shah Alam Selangor
*ezlan@uitm.edu.my

Abstract: A non-destructive ATR-FTIR technique was applied to estimate the age of documents of different ages based on paper analysis. The samples were artificially aged for a specific period before been analysed with ATR-FTIR to determine the chemical composition of each samples. Results showed that newspaper and magazine produced the identical IR spectra except for the presence of calcium carbonate in white paper. Magazine has a slightly different spectrum compared to newspaper and magazine. Kaolinite and calcium carbonate are also present in the magazine.

Keywords: *paper, ATR-FTIR, age determination.*

INTRODUCTION

Most of the research in document dating has been done in ink analysis that focused on alteration of the handwriting. Only a few analytical methodologies conducted in paper analysis. Difficulties in ink analysis arise since not all documents recovered at the crime scene have ink entries. There are also possibilities that the questioned document received contain a few words or written in unusual form to disguise writer's handwriting that challenge for handwriting comparison. Paper analysis provides information on the paper's origin, source or manufacturer so that it can determine whether two papers or documents have the common origin or different origin. Hence, this study was performed as an alternative to ink studies to estimate the age of documents through paper analysis. Different types of paper were artificially aged for specific period of time and the composition of the papers was analysed with ATR-FTIR spectroscopy. This technique is favoured in forensic application as it is known to be non-destructive to samples, provides rapid analysis and minimal sample preparation (Sharma & Kumar, 2017).

METHODOLOGY

Three types of paper (newspaper, magazine, white paper) were collected from four different years range from 2009-2018. Three boxes of same size were prepared for lightbox preparation. Each box was cleaned and wrapped with aluminium foil inside it to prevent any external light source. The boxes were punched with hole that fix the size of the bulb holder and the bulb was placed in the holder. The wire was connected from the bulb to the adapter and then to the power supply. Each sample was cut into 3×2 cm and been exposed in a lightbox for aging process under a cool daylight bulb. The samples were placed in the lightbox with different time frame for 6, 12, 18, 24, 30, 36, 42, and 48 hours. The estimated age of the documents was measured using Thermo Scientific Nicolet 6700 Fourier Transform Infrared (FTIR) Spectrometer using OMNIC-7 software equipped with Attenuated Total Reflectance (ATR) sampling interface.

FINDINGS

Different documents possess different functional groups which might due to the manufacturer's formulation that consist of various organic, inorganic and synthetic materials to enhance paper performance and gain greater profits. According to Silva *et al*. (2013), cellulose absorption bands at 3300-2900 cm^{-1} were due C-H and O-H stretching, C-H angular bending at 1500-1300 cm^{-1}, and C-O stretching bond at 1030 cm^{-1}.

Colloquium of Chemistry and Environment 2018
Faculty of Applied Sciences, Universiti Teknologi MARA, Shah Alam.

Paper may also contain features by the presence of additives such as calcium carbonate which can be observed at absorption bands of 712 cm^{-1} and 870 cm^{-1}.

Table 4 Comparison of chemical compounds in documents using ATR-FTIR

Compound	**Formula**	**Magazine**	**Newspaper**	**White paper**
Cellulose	(C6H10O5)n	×	×	×
Lipids	R-COOH		×	
1-Hydroxy-2propanone	C3H6O2	×	×	×
Furfural	C5H4O2		×	×
2-Furanmethanol	C5H6O2		×	×
2-Methoxy-phenol	C7H8O2	×		
N-methyl-3propanediamine	C4H10N2	×	×	×
1,4:3,6-dianhydro-α-D-glucopyranose	C6H8O4	×		
5-Hydroxymethylfurfura l	C6H6O3		×	×
Vanillin	C8H8O3	×		
Apocynin	C9H10O3	×		
Kaolinite	Al2Si2O5(OH)4	×		
Calcium carbonate	$CaCO_3$	×		×

For aging of documents, the result showed that there are no significant differences between samples after been artificially aged for 6 hours to 48 hours.

CONCLUSIONS

In conclusion, this study had identified the functional groups present on different types of paper which are magazine, newspaper, and white paper. Newspaper and white paper have the identical chemical composition except for the presence of calcium carbonate in white paper. IR spectrum of magazine was slightly differentiated from the newspaper and white paper besides there are kaolinite and calcium carbonate present in the paper. Age estimation of documents show no significant difference in IR spectrum for all documents after been artificially aged for a specific period. Environmental factors such as presence of microorganism like bacteria and fungi, contaminants, humidity, temperature and light may not strongly influence for deterioration of documents to occur.

REFERENCES

i. Sharma, V. & Kumar, R. (2017). Fourier transform infrared spectroscopy and high performance thin layer chromatography for characterization and multivariate discrimination of blue ballpoint pen ink for forensic applications. *Vibrational Spectroscopy*, *92*, 96-104.
ii. Silva, C.S., Borba, F.D.S.L., Pimentel, M.F., Pontes, M.J.C., Honorato, R.S. & Pasquini, C. (2013). Classification of blue pen ink using infrared spectroscopy and linear discriminant analysis. *Microchemical Journal*, *109*, 122-127.

JUNIOR SCIENCE COMMUNICATION
https://jscfsg.uitm.edu.my/
Volume 2 (2019)
eISSN 2637-0689

Colloquium of Chemistry and Environment 2018
Faculty of Applied Sciences, Universiti Teknologi MARA, Shah Alam.

GREEN APPROACHES TOWARDS SYNTHESIS OF PYRANOPYRAZOLES

Farwieza Alia Farwez Khan, Mohd Fazli Mohammat@ M Yahya*
Faculty of Applied Sciences, UniversitiTeknologi MARA, 40450, Shah Alam, Selangor, Malaysia

*mohdfazli@uitm.edu.my

Abstract*:* Simple and green approaches for the synthesis of pyranopyrazoles was established. The synthesis Was achieved via one pot reaction of methyl acetoacetate, hydrazine hydrate, different aldehydes and malononitrile in under refluxing condition, solvent free condition and by using mortar pestle under non-catalytic system. The procedure used furnished moderate to excellent yields and used easily excess starting materials and displayed operational simplicity. All the synthetic approaches used follow the principles of green chemistry where hazardous substances have been reduced and eliminated, low wastage, shorter reaction time, no purification steps needed and environmental friendly**.**

Keywords: *pyranopyrazoles, green chemistry, one-pot reaction and high percent yield*

INTRODUCTION

In modern days of organic chemistry, efficiency and environmental sustainability are the main issues in order to follow green chemistry principle. As a result, chemist has come out with an effective approach to synthesize the target molecule in a single vessel which is known as one-pot reaction procedure. This method is effective as several chemical transformation and bond-forming steps can be carried out in a single pot without producing much side product. (Hayashi, 2016; Sethurajan *et al.*, 2015; Gu, 2012) Chemically, pyranopyrazole is a fused heterocyclic compound. This synthetic compound possesses the pyran ring fused together with pyrazole ring to form the potentially biologically active pyranopyrazole type compounds. Amongst them, pyrano[2,3c-]pyrazole is the most interesting template in medicinal chemistry and also inorganic chemistryas it has a wide spectrum of biomedical and pharmaceutical applications. (Abdou *et al*., 1961; Ahmad *et al*., 2017) Generally, synthesis of pyranopyrazole compounds takes longer time even though it produces high percentage yield, but sometimes it has low percentage yield. Besides, the usage of method that is not environmental friendly. Therefore, a study was done in order to know either preparation of pyranopyrazole compounds in solvent or solventless method can be done in shorter time and produce high percent yield in green approach.

METHODOLOGY

Synthesis of pyranopyrazole in solventless reaction condition

A 0.6 ml methyl acetoacetate (5.56 mmol) was placed in a 25 ml round-bottomed flask and connected to a reflux condenser, 80%, 0.42 ml hydrazine hydrate (6.95 mmol) was added and refluxed for 15 minutes at 125^{o}C. Next, 0.702 ml benzaldehyde **3a** /0.505 ml propionaldehyde **3b** /0.845 ml 4-methoxybenzaldehyde **3c** (6.95 mmol) (6.95 mmol) and 0.459 g malononitrile (6.95 mmol) were added into the mixture and the reflux continued for additional 30 minutes. After it was completed, as guided by thin layer chromatography,

the reaction mixture was left to cool at room temperature and then was filtered off, washed with water and diethyl ether to obtained white solid.

Synthesis of pyranopyrazole in aqueous condition reaction

To a solution of 0.2 ml methyl acetoacetate (5.56 mmol) in 15ml EtOH **6a** / H_2O **6b** / EtOH:H_2O (8:2) **6c** in a round-bottomed flask of 25 ml connect to a reflux condenser, 80%, 0.14 ml hydrazine hydrate **2** (6.95 mmol) was added and refluxed for 15 minutes. Next 0.235 ml benzaldehyde **3a** / 0.127 ml propionaldehyde **3b** / 0.281 ml 4-methoxybenzaldehyde **3c** (6.95 mmol) and 0.152 g malononitrile 4 (6.95 mmol) were added into the mixture and the reflux continued for additional 30 minutes. After it was completed, as guided by thin layer chromatography, the reaction mixture was left to cool at room temperature and then was filtered off, washed with water and diethyl ether produced white solid.

Synthesis of pyranopyrazole using mortar pastle

To a solution of 0.2 ml methyl acetoacetate **1** (5.56 mmol), 80%, 0.14 ml hydrazine hydrate **2** (6.95 mmol) was added into mortar pestle and grinded. Next, 0.235 ml benzaldehyde **3a** / 0.127 ml propionaldehyde**3b** / 0.281 ml 4-methoxybenzaldehyde **3c** (6.95 mmol) and 0.152 g malononitrile **4** (6.95 mmol) were added into the mixture and continued grinded until solid formed. After it was completed, as guided by thin layer chromatography, the reaction mixture was filtered off, washed with water and diethyl ether to obtained white solid.

FINDINGS

In the first synthetic approach, a solventless one-pot method was performed where methyl acetoacetate and hydrazine hydrate was refluxed for 15 minutes initially. Then, different aldehydes were added along with malononitrile and further refluxed for another 30 minutes to give the title compounds. Nevertheless, the percent yield for all the synthesized pyranopyrazole compounds obtained was moderate ranging from 45% to 69%. Interestingly, upon adding ethanol as the solvent to the system for optimization process significantly increase the yield of the cyclized product to more than 80%. It was reasoned that ethanol contribute to better solubility of the reagents and at the same time act as an acid donor. Finally, as for further green-synthetic exploration methods, different one-pot methods by using grinding of mortar and pestle in solventless system was attempted. The mentioned approaches successfully furnished the pyranopyrazole but again in a moderate yield (23% to 65%). Versatility of all the attempted one-pot approaches was reflected by different range of classes of aldehyde to give different types of the pyranopyrazole in a reasonable yield.

CONCLUSIONS

The best approach in synthesizing pyranopyrazole is by using the aqueous condition reaction of water as it provides excellent yield as compared to other solvent. While mortar pestle come in second as it is the simplest and easiest method to be used. To sum up all the approaches provide good percent yield, no hazardous substances used, low wastage, short time reaction, no purification processes and environmental friendly.

REFERENCES

i. Abdou S., Fahmy S.M., Sadek K.U., Elnagdi M.H. (1961). Activated nitriles in heterocyclic synthesis : A novel synthesis of pyrano[2,3-c]pyrazoles. *Heterocycles*, *16* (12) 217-2180.
ii. Ahmad Reza Moosavi-Zare, Hamid Goudarziafshar, Khadijeh Saki. (2017). Synthesis of pyranopyrazoles using nano-Fe-[phenylsalicylaldiminemethylpyranopyrazole]Cl_2 as new Schiff base complex and catalyst. *Applied Organometallic Chemistry*, *32*(1), e3968
iii. Gu, Y. (2012). Multicomponent reactions in unconventional solvents: state of the art. *Green Chemistry*, *14* (12), 2091-2028.
iv. Hayashi, Y. (2016). Pot economy and one-pot synthesis. *Chemical Science* ,*7*, 866-880
v. Sethurajan, A, Vediappen, P., Nattamai, B (2015) A green and efficient protocol for the synthesis of dihydropyrano[2,3-*c*]pyrazole derivatives via a one-pot, four component reaction by grinding method. *Journal of Advanced Research*, *6*, 975-985
vi. Mandha, S. R., Siliveri, S., Alla, M., Bommena, V. R., Bommineni, M. R., & Balasubramanian, S. (2012). Eco-friendly synthesis and biological evaluation of substituted pyrano[2,3-c]pyrazoles. *Bioorganic & Medicinal Chemistry Letters*, *22*(16), 5272-5278.
vii. Tekale, S. U., Kauthale, S. S., Jadhav, K. M., & Pawar, R. P. (2013). Nano-ZnO Catalyzed Green and Efficient One-Pot Four-Component Synthesis of Pyranopyrazoles. *Journal of Chemistry*, 1-8

JUNIOR SCIENCE COMMUNICATION
https://jscfsg.uitm.edu.my/
Volume 2 (2019)
eISSN 2637-0689

Colloquium of Chemistry and Environment 2018
Faculty of Applied Sciences, Universiti Teknologi MARA, Shah Alam.

THE SYNTHESIS OF THIOSEMICARABZIDE LIGANDS AS CORROSION INHIBITORS ON MILD STEEL IN 1.0 M H_2SO_4

Fazreen Nur Idayu Rosli[1], Karimah Kassim[1,2,*]
[1]Faculty of Applied Sciences, Universiti Teknologi MARA, 40450 Shah Alam, Selangor, Malaysia
[2]Institute of Science, Universiti Teknologi MARA, 40450 Shah Alam, Selangor, Malaysia
[*]karimah@uitm.edu.my

Abstract: This study focuses on corrosion activity due to acid usage on mild steel surface using thiosemicarbazide as corrosion inhibitor. The aims of this study are to synthesize and characterize the thiosemicarbazide ligands as corrosion inhibitor in sulfuric acid solution. The elemental analysis showed the obtained percent of elements were in the acceptable range. The FTIR showed the presence of important peaks of functional groups such as C-N at 1373.45-1292.71 cm^{-1}, C=N at 1603.12-1591.06 cm^{-1}, C=S at 1176.62-1090.63 cm^{-1} and N-H at 3401.59-3369.93 cm^{-1}. NMR spectrum of the ligands showed the presence of NH_2 peaks at 11.34-8.59 ppm, NH at 2.04-1.85 ppm, C=N at 8.12 ppm, CH aromatic at 7.64-4.46 ppm and CH_3 at 2.45-2.22 ppm. Meanwhile for carbon NMR, the important peaks were observed for C=S at 178.83-178.34 ppm, CH_3 at 25.57-21.56 ppm, C=N at 152.32-142.92 ppm and CH aromatic at 148.56-127.05 ppm. These ligands were tested as corrosion inhibitor using weight loss method for 18 days. The concentrations of corrosion inhibitors were varied from 1 $x10^{-4}$ mmol and 1 x 10^{-5} mmol. Then, the mass of mild steels was recorded and used to calculate weight loss. The increasing concentration of corrosion inhibitors and the presence of electron donation group (EDG) increased the percent of inhibition efficiency. The highest IE% was shown on Ligand 3 at 99.62 % in concentration 1 $x10^{-4}$ mmol which supported by the presence of 2 methyl moieties.

Keywords: *Thiosemicarbazide, corrosion inhibitor and inhibition efficiency.*

INTRODUCTION

A corrosion inhibitor is a chemical compound that acts to reduce the corrosion rate of a material such as metal or an alloy. The effectiveness of the corrosion inhibitor for mild steel depends on fluid composition quantity of water, and flow of regime. Coating is a common formation of the mechanism for inhibiting corrosion. Mostly, corrosion inhibitor often acts as a passivation layer that can avoid and prevent the access of the corrosive substance onto the metal. The corrosion inhibitors are additives to the fluids that surround the metal or related object. Corrosion inhibitors are common in industry and can be found as over-the-counter products, typically in spray form in combination with a lubricant and sometimes penetrating oil (Ashassi-Sorkhabi *et al*., 2005). One of the corrosion inhibitors that can be used is thiosemicarbazide. It is commonly used as an antiviral, anti-infective and anti-neoplastic through the binding to copper or iron in cells. Thiosemicarbazide is the analogous compound with sulphur atom in place of oxygen atom. It is in white crystalline powder form with melting point of 183°C and it is soluble in water (O'Neil, 2013). The thiosemicarbazide can act as corrosion inhibitor in its derivative form and combination the with other corrosion inhibitors to enhance the corrosion inhibition on mild steel. In this study, a series of thiosemicarbazide ligands in with 3 starting materials are synthesized as shown in Figure 1.

Colloquium of Chemistry and Environment 2018
Faculty of Applied Sciences, Universiti Teknologi MARA, Shah Alam.

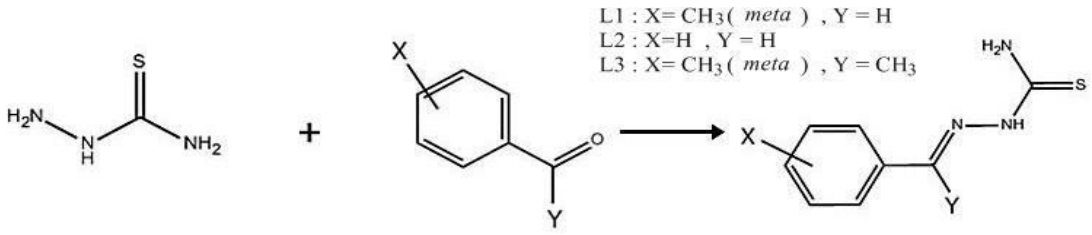

Figure 1 Proposed structure of ligands

METHODOLOGY

Thiosemicarbazide ligands were synthesized from 3 starting materials which were 4-methylbenzaldehyde, benzaldehyde and 4-methylacetophenone in ethanol solvent for 4 hours. These compounds were prepared in 2:1 (aldehyde or ketone: thiosemicarbazide) ratio under refluxed in EtoH for 4 hours (Kumar & Mohana, 2014). The ligands were then filtered off and air dried. The ligands were characterized using Elemental Analyser to determine the percent of elements while FTIR was used to determine the functional groups, and NMR was used to determine the structures of C and H in the ligands. Weight loss method was used to evaluate the IE%. The polished mild steels were immersed in 10 mL of 1.0 M sulphuric acid with added corrosion inhibitor for 18 days. The concentrations of corrosion inhibitors were varied into 1 $x10^{-4}$ mmol and 1 x 10^{-5} mmol. Then, the mass of mild steels was recorded and used to calculate the weight loss using Equation 1;

$$\% IE = \left| \frac{W\ (before) - W'(after)}{W\ (before)} \right| x\ 100 \quad (1)$$

W = weight loss without inhibitor, W' = weight loss with inhibitor

FINDINGS

Based from the results, the percent yield for Ligand 1 and Ligand 3 were 71.94 % and 74.10 %, respectively. Meanwhile, Ligand 2 only yielded 57.00 %. The melting point are 176°C, 163°C, and 165°C for Ligand 1, 2 and 3, respectively. The high value of melting point indicated the purity of the ligands. The elemental analysis showed the obtained percent of each element was in good agreement with theoretical values. The FTIR showed the presence of important peaks of functional groups such as C-N at 1373.45-1292.71 cm^{-1}, C=N at 1603.12-1591.06 cm^{-1}, C=S at 1176.62-1090.63 cm^{-1} and N-H at 3401.59-3369.93 cm^{-1} (Ljubijankić *et al*., 2017). NMR spectrum of the ligands showed the presence of peaks which indicated the structure of C and H in the ligands. In proton-NMR, several peaks were observed, which were NH_2 at 11.34-8.59 ppm, NH at 2.04-1.85 ppm, C=N at 8.12 ppm, CH aromatic at 7.64-4.46 ppm and CH_3 at 2.45-2.22 ppm. Meanwhile for carbon NMR, the important peaks were C=S at 178.83-178.34 ppm, CH_3 at 25.57-21.56 ppm, C=N at 152.32-142.92 ppm and CH aromatic at 148.56-127.05 ppm (Tan *et al*., 2012).

Table 1 The inhibition efficiency of the thiosemicarbazide ligands

Ligands	Concentration (mmol)	Inhibition efficiency, IE (%)
Ligand 1	1 x 10^{-4}	99.44
	1 x 10^{-5}	99.18
Ligand 2	1 x 10^{-4}	99.09
	1 x 10^{-5}	99.32
Ligand 3	1 x 10^{-4}	99.62

Table 1 showed that as the concentration of corrosion inhibitors increases, the inhibition efficiencies of the ligands increased (Badr, 2009). Ligand 3 showed more significant difference between the 2 concentrations while Ligand 2 and Ligand 3 did not show distinctive difference between the concentrations. In the same time, the presence of substituent groups which acted as electron donating group (EDG), CH_3, were also increased the inhibition (Singh *et al*., 2018). Since Ligand 3 had 2 EDGs, the inhibition activity of Ligand 3 was higher than Ligand 2 and Ligand 1.

CONCLUSIONS

Three thiosemicarbazide ligands were successfully synthesized and characterized using 3 instruments which were elemental analyzer, FTIR and NMR. The results obtained showed a great significance between the comparisons between the ligands. The application of corrosion inhibitor on mild steel from the weight loss method was also achievable in which the inhibition efficiencies increased in when the concentration of corrosion inhibitors increased (Musa *et al.,* 2011). The highest IE% was observed in Ligand 3 at 99.62 % at 1 $x10^{-4}$ mmol due to the presence of two methyl groups in the structure Ligand 1.

REFERENCES

i. Ashassi-Sorkhabi, H., Shaabani, B. & Seifzadeh, D. (2005). Corrosion inhibition of mild steel by some schiff base compounds in hydrochloric acid. *Applied Surface Science, 239*(2), 154-164.
ii. Badr, G.E. (2009). The role of some thiosemicarbazide derivatives as corrosion inhibitors for C-steel in acidic media. *Corrosion Science, 51*(11*)*, 2529–2536.
iii. Kumar, C.B.P. & Mohana, K.N. (2014). Corrosion inhibition efficiency and adsorption characteristics of some Schiff bases at mild steel/hydrochloric acid interface. *Journal of the Taiwan Institute of Chemical Engineers, 45(3)*, 1031-1042.
iv. Ljubijankić, N., Tešević, V., Grgurić-Šipka, S., Jadranin, M., Begić, S., Buljubašić, L., Markotić, E. & Ljubijankić, S. (2017). Synthesis and characterization of Ru(III) complexes with thiosemicarbazide-based ligands. *Bulletin of the Chemists and Technologists of Bosnia and Herzegovina, 47*, 1-6.
v. Musa, A.Y., Kadhum, A.A.H., Mohamad, A.B. & Takriff, M.S. (2011). Molecular dynamics and quantum chemical calculation studies on 4,4-dimethyl-3-thiosemicarbazide as corrosion inhibitor in 2.5 M H_2SO_4. *Materials Chemistry and Physics, 129*(1-2), 660-665.
vi. O'Neil, M.J. (2013). The Merck Index - An Encyclopedia of Chemicals, Drugs and Biologicals. *Royal Society of Chemistry*, 3-302.
vii. Singh, A., Ansari K.R., Haque, J., Dohare, P., Lgaz, H., Salghi, R. & Quraishi M.A. (2018). Effect of electron donating functional groups on corrosion inhibition of mild steel in hydrochloric acid: Experimental and quantum chemical study. *Journal of the Taiwan Institute of Chemical Engineers*, *82*, 233-251.
viii. Tan, O.U., Ozadali, K., Yogeeswari, P., Sriram, D. & Balkan, A. (2012). Synthesis and antimycobacterial activities of some new N-acylhydrazone and thiosemicarbazide derivatives of 6-methyl-4,5-dihydropyridazin-3(2H)-one. *Medicinal Chemistry Research, 21*(9), 2388–2394.

JUNIOR SCIENCE COMMUNICATION
https://jscfsg.uitm.edu.my/
Volume 2 (2019)
eISSN 2637-0689

Colloquium of Chemistry and Environment 2018
Faculty of Applied Sciences, Universiti Teknologi MARA, Shah Alam.

ANALYSIS OF HEAVY METALS IN LOCAL COSMETIC PRODUCTS USING ATOMIC ABSORPTION SPECTROSCOPY

Floreni James Parun, Zarila Mohd Shariff *
Faculty of Applied Sciences, Universiti Teknologi MARA, 40450 Shah Alam, Selangor, Malaysia

*zarila@uitm.edu.my

Abstract: Three different types of local cosmetic products (facial moisturizer) purchased from local markets in Shah Alam were analysed for their lead, cadmium and zinc contents. Wet digestion method was employed to all samples and analysed for their heavy metals (lead, cadmium and zinc) by using atomic absorption spectroscopy (AAS). From the observation, all the samples contain high concentration of lead. Sample A has the highest concentration of zinc as compared to sample B and C. However, the concentration of the cadmium (Cd) and zinc (Zn) in the samples are below the international regulations. Moreover, the concentration of lead (Pb) in samples A, B and C are higher than the permissible limit. Although, the concentration of Cd and Zn in the samples are below the limit, the cosmetic products (facial moisturizer) are still not safe to be used due to the high concentration of Pb present in the sample.

Keywords**:** *Atomic absorption spectroscopy, lead, cadmium, zinc*

INTRODUCTION

A cosmetic is defined as any product intended to be sprayed or rubbed on human body or any part for cleansing, beautifying, promoting attractiveness or altering the appearance that includes any product intended for use as a component of cosmetics (Sahu *et al*., 2014). One of the most important skin care product is facial moisturizer. Facial moisturizer is important to keep skin hydrated. It helps increasing the moisture level and preventing our skin from drying out. Facial moisturizer can also protect our skin from sun damage if the moisturizer contain sunscreen. There are concerns regarding the presence of harmful chemical content in the cosmetics including heavy metals. Toxic elements are widely diffuse in coloured make-up products. Heavy metals impurities in cosmetic products are unavoidable due to the nature of these elements, but should be removed wherever technically feasible (Al-Dayel *et al*., 2011). The purpose of this study is to determine the concentration of lead, cadmium and zinc in local facial cream that are available in the Shah Alam market by using calibration curve method and AAS.

METHODOLOGY

One gram of sample was weighed and placed into a 250 ml conical flask. After that, 15 ml of HNO_3, 5 ml of H_2O_2 (30%) and 5 ml HCl (37%) were added into the conical flask. The conical flask was then covered and left to digest for 15 minutes. Next, the sample in the conical flask was heated medium strength on a hot plate in a fume hood until brown fumes ceased. The conical flask was cooled to room temperature. After that, 20 ml of deionized water was added into the conical flask and then the sample was filtered into 100 ml volumetric flask and diluted to the volume with deionized water. Lastly, the sample was transferred into a plastic container and was kept in the chiller for further analysis.

Volume 2 (2019)
eISSN 2637-0689

Colloquium of Chemistry and Environment 2018
Faculty of Applied Sciences, Universiti Teknologi MARA, Shah Alam.

FINDINGS

All samples had high concentrations of lead. In this study, the concentrations of lead were 27.42 ppm, 26.61 ppm and 27.42 ppm for samples A, B and C, respectively. The concentration of cadmium in samples A, B and C were 1.96 ppm, 1.96 ppm and 1.89 ppm, respectively. Sample A has the highest concentration of zinc compared to samples B and C. According to The German Federal Government Regulations heavy metal levels in cosmetic products are considered safe if the value for lead is below 20 ppm and Cd is below 5 ppm.

Meanwhile, the Canadian guideline stated that the limit of the heavy metal in the cosmetics for Pb is 10 ppm and Cd is 3 ppm. Besides that, the USFDA also stated that the limit concentration of lead in the cosmetics should not exceed 20 ppm. All the facial moisturizer samples analysed in this study were found to have lead concentration higher than the German Federal Regulation, Canadian and USFDA guidelines. As for zinc, according to Omolaoye *et al*. (2010) there is no regulation limit given for zinc. However, it is proposed that the concentration of zinc in the cosmetic products must not exceed 100 ppm (Bocca *et al*., 2014). In this study, the highest concentration of the zinc was 10.68 ppm. It shows that the concentration of zinc present in the samples are below the proposed limit. The findings show the concentration of cadmium to be in the range of 1.89 to 1.96 ppm. The amount of cadmium in the facial moisturizers are below the permissible level of the regulations. Figure 1 shows the concentration of lead, cadmium and zinc in the samples with international regulations.

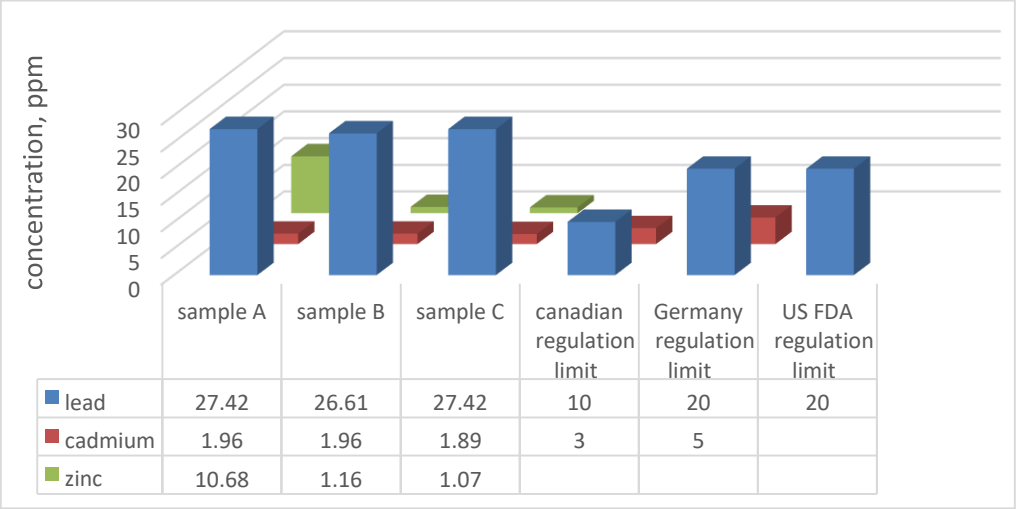

	sample A	sample B	sample C	canadian regulation limit	Germany regulation limit	US FDA regulation limit
lead	27.42	26.61	27.42	10	20	20
cadmium	1.96	1.96	1.89	3	5	
zinc	10.68	1.16	1.07			

Figure 1 Comparison of the concentrations of lead, cadmium and zinc in the samples with international regulations.

CONCLUSIONS

From the analysis, it is revealed that Pb, Cd and Zn are present in sample A, B and C. The concentrations of Cd and Zn in the samples are below the given limits. However, the concentration of Pb in sample A, B and C are higher than the permissible limits. Although, the concentration of Cd and Zn in the samples are below the limits, the facial moisturizer are still not safe to be use due to the high concentration of Pb present in the sample.

REFERENCES

i. Al-Dayel, O., Hefne, J. & Al-Ajyan, T. (2011). Human Exposure to Heavy Metals from Cosmetics. *Oriental Journal of Chemistry*, *27*(1), 1–11.
ii. Bocca, B., Pino, A., Alimonti, A. & Forte, G. (2014). Toxic metals contained in cosmetics: A status report. *Regulatory Toxicology and Pharmacology*, *68*(3), 447–467.
iii. Omolaoye, J.A., Uzairu, A. & Gimba, C.E. (2010). Heavy metal assessment of some eye shadow products imported into Nigeria from China. *Archives of Applied Science Research*, *2*(5), 76–84.
iv. Sahu, R., Saxena, P. & Johnson, S. (2014). *Heavy Metals in Cosmetics*. Retrieved Sep 5, 2019 from http://www.environmentportal.in/files/file/Heavy_Metals_in_Cosmetics_Report.pdf

JUNIOR SCIENCE COMMUNICATION
https://jscfsg.uitm.edu.my/
Volume 2 (2019)
eISSN 2637-0689

Colloquium of Chemistry and Environment 2018
Faculty of Applied Sciences, Universiti Teknologi MARA, Shah Alam.

SYNTHESIS OF TRIMETHYLSILYL CYCLOHEXENE-TRIAZOLE USING CLICK CHEMISTRY

Intan Syazwani Mohd Noor, Mohd Tajudin Mohd Ali*
Faculty of Applied Sciences, Universiti Teknologi MARA, 40450, Shah Alam, Selangor, Malaysia
*tajudinali@uitm.edu.my

Abstract: The synthesis of Trimethylsilyl Cyclohexene-Triazole was achieved through the formation of azide followed by the synthesis of triazole via click chemistry.

Keywords: *Click Chemistry, Triazole*

INTRODUCTION

The concept of click chemistry has been widely used in the area of drug discovery, drug delivery system, polymer chemistry and material science (Meghani *et al*., 2017). The click chemistry is a cycloaddition reaction that involved alkyne and azide to formed 1,4- and 1,5- disubstituted-triazole through few methods (Totobenazara & Burke, 2015). Thus, triazole derivative is useful for the synthesis of γ-butyrolactone triazole which may have potential to inhibit tuberculosis cell line. The product was characterized using NMR spectroscopy and IR spectroscopy. The following are the steps involved in the synthesis.

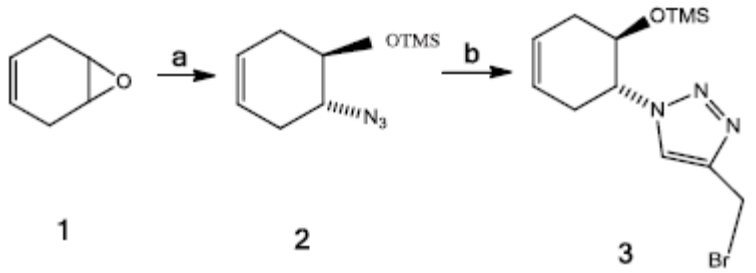

Scheme 1 Synthesis of trimethylsilyl cyclohexene-triazole using click chemistry. Reagents and Conditions: a) Salen complex, TMSN3, Et2O, rt, 46h; b) CuI[P(OEt)3], dry diethyl ether, propagryl bromide, 2 days, rt;

METHODOLOGY

Synthesis of Trimethylsilyl Cylohexene Azide

The formation of azide is mixed of epoxide (0.71 g, 0.0074 mol, 1.0 eq.), diethyl ether and salen complex. This mixture was stirred for 15 minutes. Trimethylsilylazide was added into the mixture and it stirred for 46 hours at room temperature.

Synthesis of Trimethylsilyl Cyclohexene Triazole

Colloquium of Chemistry and Environment 2018
Faculty of Applied Sciences, Universiti Teknologi MARA, Shah Alam.

To stirred solution of propagryl bromide (0.0835 g, 0.000702 mol, 3.0 eq.) in 3ml of diethyl ether was added CuI[P(OEt_3)] followed by mixed of azide and diethyl ether. This reaction was conducted for two days at room temperature.

FINDINGS

For the formation of azide, the azide had synthesized through epoxide which involved ring opening reaction in the presence of Salen Complex. The data for ^{1}H and ^{13}CNMR shows in Table 1. The following is the synthesis of trimethylsilyl cyclohexene-triazole which involved click reaction between azide and propagryl bromide in the presence of Cu as a catalyst and diethyl ether as a solvent. The data for ^{1}H and ^{13}CNMR shows in Table 2.

Table 1 ^{1}H NMR and ^{13}C NMR shift of compound **2**.

Proton	^{1}H NMR Shift (ppm)	Coupling Constant, *J* (Hz)	Multiplicity	Number of Proton	Carbon	^{13}C NMR Shift (ppm)
CH=CH	5.6-5.7	-	S	1H	C=C	124.0
CHN	3.5-3.7	12.0	T	1H	CH_2	31.0
CH_2	2.5-2.6	-	M	2H	CH_2	34.0
CH_2	2.1-2.3	-	M	2H	C-N	64.0
CHO	2.0-2.1	-	S	1H	C-O	77.2
CH_3	0.00	-	S	9H	CH_3	2.00

Table 2 ^{1}H NMR and ^{13}C NMR shift compound 3.

Proton	^{1}H NMR Shift (ppm)	Coupling constant, *J* (Hz)	Multiplicity	Number of Proton	Carbon	^{13}C NMR Shift (ppm)
CH=CH	5.06-5.52	-	S	2H	C=C	122-125
CH_2	1.95-1.99	-	M	1H	C-O	77.03
CHO	4.04-4.35	-	M	1H	C-N	76.61
CHN	3.35-3.45	-	M	1H	CH_2	29.71
CHCBr	1.50-1.70	-	M	1H	CH_3	0.03
CH_3	1.0	-	S	9H	CH_2Br	20.0

CONCLUSIONS

In conclusion, the synthesis of azide and synthesis of cyclohexene-triazole bromide were achieved.

REFERENCES

i. Meghani, N.M., Amin, H.H. & Lee, B.-J. (2017). Mechanistic applications of click chemistry for pharmaceutical drug discovery and drug delivery. *Drug Discovery Today, 22*(11), 1604-1619.
ii. Totobenazara, J. & Burke, A.J. (2015). New click-chemistry methods for 1,2,3-triazoles synthesis: recent advances and applications. *Tetrahedron Letters, 56*(22), 2853-2859.

JUNIOR SCIENCE COMMUNICATION
https://jscfsg.uitm.edu.my/
Volume 2 (2019)
eISSN 2637-0689

Colloquium of Chemistry and Environment 2018
Faculty of Applied Sciences, Universiti Teknologi MARA, Shah Alam.

ADSORPTION OF METHYL ORANGE ON MESOPOROUS SILICA SANTA BARBARA AMORPHOUS SBA-15

Isna Fazliana Mohamed Idrus, Hamizah Md Rasid*
Faculty of Applied Sciences, Universiti Teknologi MARA, 40450 Shah Alam Selangor, Malaysia.

*hamizah7708@uitm.edu.my

Abstract: Synthesis of SBA-15 using TEOS as silica source and Pluronic 123 as the surfactant in the acidic medium were carried out. Characterization of SBA-15 was done using FESEM, XRD, BET and ATR-FTIR. The percentage removal of methyl orange using SBA-15 was observed and the efficiency of the adsorption was determined using batch adsorption studies. This batch studies include the effect of pH, initial concentration and contact time. The adsorption isotherm and kinetic also included in this study. The optimum conditions for this adsorption studies was at pH 5, initial concentration 140 ppm, 40 minutes with 0.05 g of adsorbent dosage at room temperature 27 °C. The isotherm and kinetic data obtained for this adsorption study was best fit the Freundlich isotherm and pseudo-second-order kinetic model.

Keywords: *methyl orange,removal, SBA-15, mesoporous silica*

INTRODUCTION

Synthetic dyes are commonly used in textile and dyeing industries because it involves easy preparation steps and cost-effective production methods. Synthetic dyes have several benefits such as high stability towards light and detergent and can withstand extreme temperature and microbial attack. However, due to the wide application of synthetic dyes, it causes serious environmental, aesthetical and health problems when released into the environment because of its stability and long-lasting colorant, recalcitrant organic molecules which are carcinogenic and toxic. Methyl orange with azo group is a toxic and mutagenic anionic dye (Haque *et al*., 2011; Xing *et al*., 2016). Thus, by using ultraviolet-visible spectroscopy, the adsorption of methyl orange on SBA-15 was determined.

METHODOLOGY

Method discovered by Koh *et al*. (2017) was used to synthesize SBA-15. Amphiphilic triblock polymer of Pluronic P123 ($PEO_{20}PPO_{70}PEO_{20}$) was used as template for the synthesis of SBA-15. Firstly, P123 (4.0 g) was dissolved in deionized water (30.00 mL) and 2 M HCl (120.00 mL). Then, the mixture was stirred at 35 °C for 20 hours. Next, TEOS (8.5 g) was added slowly into the mixture containing the acidic surfactant and was stirred continuously for 15 minutes. Under static conditions at same temperature (35 °C), the mixture was continuously stirred for 20 hours. Then, it was heated in an oven at 90 °C for 24 hours. Next, the solution was filtered, washed and dried at 45 °C for 72 hours. Lastly, the product obtained was calcined at 500 °C for 6 hours.

FINDINGS

The results obtained from this study show the optimum parameters for adsorption study. There are some parameters that have been used in this study which were pH of dye, contact time and initial concentration

of methyl orange (MO). The adsorbent dosage has been fixed at 0.05 g, stirring speed 160 rpm and volume of MO of 0.010 L.

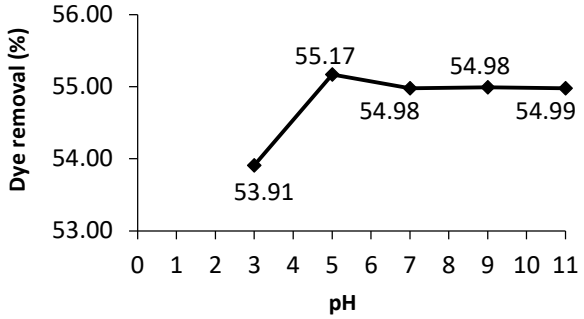

Figure 1 Effect of pH on the adsorption of MO by using SBA-15 (experiment conditions: adsorbent dosage was 0.05 g; initial dye concentration was 80 mg/L; contact time was 30 minutes; volume of MO was 0.010 L; agitation speed was 160 rpm)

From Figure 1, it was observed that adsorption of MO dye for SBA-15 increases from pH 3 to pH 5 but slightly drops at pH 7. The maximum pH for the adsorption of MO occurred at acidic condition which was pH 5. Methyl orange was an anionic dye that reacted more active at acidic condition. While, SBA-15 was also in acidic condition and that caused competition between OH and H group in methyl orange for the surface of SBA-15.

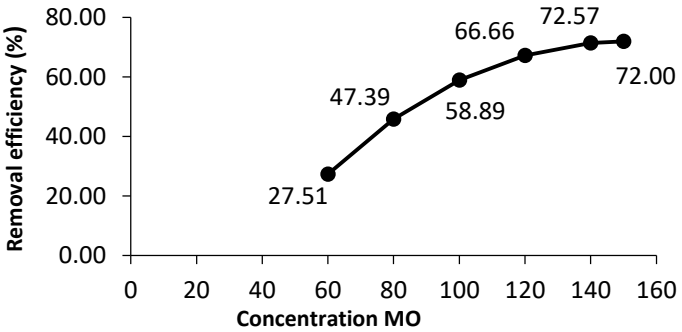

Figure 2 Effect of initial dye concentration on the adsorption of MO by using SBA-15 (experiment conditions: adsorbent dosage was 0.05 g; contact time was 40 minutes; pH of dyes was 5; volume of MO was 0.010 L; agitation speed was 160 rpm)

From Figure 2, we can observe that the percentage removal of dye was proportional with initial concentration of dye. This indicates that the ratio of the dye molecule to the adsorbent sites was higher,

thus increase the potential of dye molecules bind with active sites of the adsorbents. This will cause a low color intensity of MO. But, the percentage removal of dye decreases from 140 mg/L to 150 mg/L. This can be explained according to Mor *et al*. (2007) which stated that an adsorbent has limited number of active sites which would have become saturated above a certain concentration. Thus, at higher concentration, more MO dye molecules were left unadsorbed in the solution due to the saturation of binding sites resulting in decreased of dyes removal percentage.

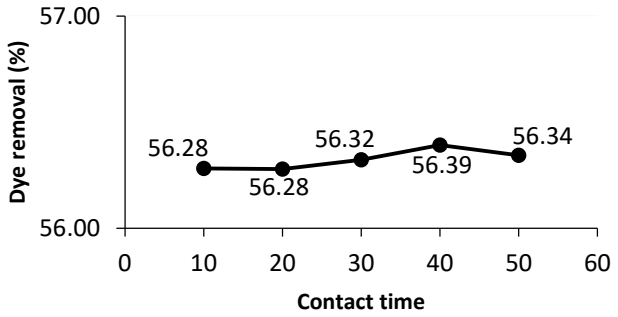

Figure 3 Effect of contact time on the adsorption of MO by using SBA-15 (experiment conditions: adsorbent dosage was 0.05 g; initial dye concentration was 80 mg/L; pH of dyes was 5; volume of MO was 0.010 L; agitation speed was 160 rpm)

From Figure 3, it was observed that adsorption of MO dye for adsorbent increases from 30 minutes to 40 minutes and slightly drops at 50 minutes. The percentage of dye removal for SBA-15 was constant from 10 minutes to 20 minutes. The maximum contact time for adsorption of MO occurred at 40 minutes.

CONCLUSIONS

In conclusion, the optimized conditions from various parameters were obtained. All the analysis was done using 0.05 g of SBA-15, at room temperature 27 °C with 5 mL of methyl orange solution and 160 rpm speed of shaker. The optimized adsorption for 0.05 g of SBA-15 were 140 ppm methyl orange, pH 5 and 40 minutes contact time. For concentration of methyl orange, the highest removal efficiency achieved for 140 ppm of methyl orange was 86.40% at pH 5 and 10 minutes of contact time. The highest removal efficiency at contact time 40 minutes was 56.39% using 80 ppm of methyl orange solution and pH of methyl orange was 5. The pH of the highest removal efficiency obtained at pH 5 was 54.99% at 80 ppm of methyl orange solution and 20 minutes contact time.

REFERENCES

i. Haque, E., Jun, J.W. & Jhung, S.H. (2011). Adsorptive Removal of Methyl Orange and Methylene Blue from Aqueous Solution with a Metal-Organic Framework Material, Iron Terephthalate (MOF-235). *Journal of Hazardous Materials, 185,* 507-511.

ii. Koh, M.H., Haji Azaman, S.A., Hameed, B.H. & Mohd Din, A.T. (2017). Surface Morphology and Physicochemical Properties of Ordered Mesoporous Silica SBA-15 Synthesized at Low Temperature. *IOP Conference Series: Materials Science and Engineering, 206,* 012056.
iii. Mor, S., Ravindra, K. & Bishnoi, N.R. (2007). Adsorption of Chromium from Aqueous Solution by Activated Alumina and Activated Charcoal. *Bioresource Technology, 98,* 954-957.
iv. Xing, X., Chang, P.H., Lv, G., Jiang, W.T., Jean, J.S., Liao, L. & Li, Z. (2016). Ionic-Liquid-Crafted Zeolite for the Removal of Anionic Dye Methyl Orange. *Journal of the Taiwan Institute of Chemical Engineers, 59,* 237-243.

JUNIOR SCIENCE COMMUNICATION
https://jscfsg.uitm.edu.my/
Volume 2 (2019)
eISSN 2637-0689

Colloquium of Chemistry and Environment 2018
Faculty of Applied Sciences, Universiti Teknologi MARA, Shah Alam.

EFFECT OF ELECTRON DONATING GROUP (EDG) IN SCHIFF BASES AS CORROSION INHIBITORS ON MILD STEEL IN 1.0 M HYDROCLORIC ACID

Izyan Yusof[1], Karimah Kassim[1,2]*
[1]Faculty of Applied Sciences, Universiti Teknologi MARA, 40450 Shah Alam Selangor
[2]Institute of Science, Universiti Teknologi MARA, 40450 Shah Alam Selangor

*karimah@uitm.edu.my

Abstract: The use of inhibitors for the protection against the corrosion in acid media has been widely reported. Three Schiff base compounds, *N*-benzylidene-4-metoxyaniline (SB-1), 4-(((4-metoxyphenyl)imino)methyl)phenol (SB-2), and 4-((((4(phenylamino)phenyl)imino)methyl)phenol (SB-3) were synthesized, characterized and applied as potential mild steel corrosion inhibitors in 1.0 M HCl at room temperature. The Schiff bases were synthesized by using aldehyde (benzaldehyde and 4-hydroxybenzaldehyde) with amine (*p*-Anisidine and *N*-phenyl-*p*-phenylenediamine). The characterization of the compounds were carried out using Elemental Analyzer (CHNS/O), Fourier Transform Infrared (FTIR) Spectroscopy, and Nuclear Magnetic Resonance (NMR) Spectroscopy. Important peak, HC=N were found in the IR spectrum (1602-1622 cm^{-1}), ^{1}H NMR (8.42-8.51 ppm), and ^{13}C NMR (158.48-163.20 ppm). The Inhibition Efficiency (IE) were explored and analyzed by weight loss method when the mild steel was immersed in the different concentration of inhibitors for 16 days. The studies shown that as the concentration of inhibitor increased, the inhibition efficiency will increase. The corrosion inhibition performance are strongly depends on the type of functional groups substituted on the benzene ring. Between the three synthesized Schiff bases, the trends of the inhibition efficiency were in order of: SB-3 (87.73%) > SB-1 (73.52%) > SB-2 (63.19%). This is because SB-3 has two stronger activating EDG which are –OH and –NHC6H6 compared to SB-1 (-OMe and NH_2) and SB-2 (-OMe). The results obtained indicate that these Schiff bases have the ability to inhibit the corrosion efficiently.

Keywords: *EDG, Schiff bases, corrosion inhibitors*.

INTRODUCTION

Schiff base ligands can be synthesized from an aliphatic or aromatic amine and a carbonyl compound by nucleophilic addition forming a hemiaminal, followed by a dehydration to generate an imine. Excellent inhibitors will form a non-penetrable layer over the metal surface from the chemical reaction. The inhibitors will work in a mechanical barrier fashion by increasing the viscosity of the corrosive medium. The theory was supported by Muniandy *et al*. (2011), Echem & James (2014), Verma & Quraishi (2014), Chitra *et al*. (2010), and Verma *et al*. (2016) which stated that the percentage of IE will increase when the concentration of inhibitors increases. This study was conducted to study the effect of electron donating group in Schiff bases as corrosion inhibitors. The present study aims to synthesize derived from benzaldehyde, and 4-hydroxybenzaldehyde with *p*-anisidine and *N*-phenyl-*p*-phenylenediamine and to characterize three Schiff base ligand using elemental analyzer (CHNS/O), Fourier Transform Infrared (FTIR), and Nuclear Magnetic Resonance (NMR), and and lastly to study the effect of electron donating group (EDG) of the synthesized ligands on mild steel as corrosion inhibitors in 1.0 M HCl by weight loss method.

METHODOLOGY

Colloquium of Chemistry and Environment 2018
Faculty of Applied Sciences, Universiti Teknologi MARA, Shah Alam.

A mixture of aldehyde and amine were mixed in equivalent mole ratio (1:1) in 30 mL absolute methanol. This mixture was refluxed for 2 hours (Figure 1). The precipitate formed was filtered and dried in room temperature.

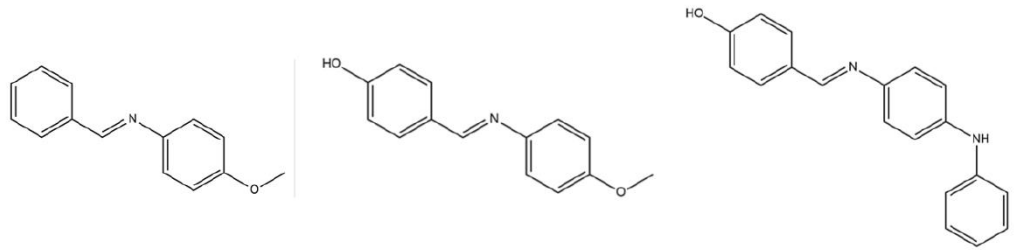

SB-1 SB-2 SB-3

Figure 1 Molecular structures of the synthesized Schiff bases.

The Schiff bases were characterized using Elemental Analyzer (CHNS/O), Fourier Transform Infrared (FTIR), and Nuclear Magnetic Resonance (NMR) spectroscopy. After that, the ligands were prepared at two different concentrations which were 2.5×10^{-4} M and 0.5×10^{-4} M in 50mL 1.0 M HCl. The 1cm x 1cm mild steels were immersed in the blank and different concentrations of inhibitors in 50 mL, 1.0 M HCl for 16 days. The difference in weight of before and after the immersion of mild steel in acid solution were recorded to calculate the weight loss. Finally, the percent inhibition efficiency (%IE) were calculated by using the formula below where, W_o and W_i is the weight loss of the mild steel in the absence and presence of the inhibitors respectively.

$$\%IE = \left|\frac{W_o - W_i}{W_o}\right| \times 100$$

FINDINGS

Three Schiff bases were successfully synthesized namely *N*-benzylidene-4-metoxyaniline (SB-1), 4-(((4metoxyphenyl)imino)methyl)phenol (SB-2), and 4-(((4-(phenylamino)phenyl)imino)methyl)phenol (SB-3). The percent yield of the synthesized Schiff bases was 80% (SB-1), 91% (SB-2), and 58% (SB-3) and the melting point obtained for each ligands were 67-73℃ (SB-1), 233-257℃ (SB-2), and 188-193℃ (SB-3).

The characterization of the Schiff bases had been done by using elemental analyzer, FTIR Spectroscopy, and NMR Spectroscopy. When analyzing using FTIR spectroscopy, few important peaks had been observed. The range of wavenumber for the important bonds are, 1033-1168 cm^{-1} (C-N), 1602-1622 cm^{-1} (C=N), 2836-2840 cm^{-1} (-OCH_3) for SB-1 and SB-2, and 3442 cm^{-1} (-NH) for SB-3. The presence of

phenolic proton in SB-2 and SB-3 are proven by the appearance of singlet peak downfield at the range of 7.02-7.20 ppm because of the deshielding of hydrogen by oxygen atoms (Ramadan *et al*., 2018).

For ^{1}H NMR, the important peaks were observed for the Schiff bases are 8.42-8.51 ppm (HC=N), 3.86-4.03 ppm (OCH_3), 7.02-2.20 ppm (OH), and 9.72 ppm (NH). While for ^{13}C NMR, the important peaks observed were 158.48-163.20 ppm (HC=N), 141.50-144.89 ppm (C-N), and 158.30-160.08ppm (C-OCH_3) for SB-1 and SB-2, or 143.17 ppm (C-NH) for SB-3. The proton and carbon in azomethine group for both ^{1}H and ^{13}C spectrum appeared at the downfield region due to the deshielding effect of the nitrogen atom.

The study shows that the inhibition efficiency will increase when the concentrations of inhibitor increase (Muniandy *et al*., 2011). Between the three synthesized Schiff bases, the trend of the inhibition efficiency was in order of: SB-3 (87.73%) > SB-1 (73.52%) > SB-2 (63.19%). According to Chitra *et al*. (2010), the presence of C=N group on the aromatic ring in the molecules will produce a good corrosion inhibitor due to the presence of electronegative nitrogen, and oxygen atoms. In SB-3, two strongly activating EDG which are –OH and –NHC_6H_6 were present compared to SB-1, which only has –OCH_3, and SB-2 which have –OH and –OCH_3. Even though both functional groups in SB-1 and SB-3 are listed in the strongly activating EDG, –NHC_6H_6 is more EDG activating than –OCH_3 (Hunt, 2019). This is why SB-3 has higher corrosion inhibition efficiency.

Other than that, when comparing the three structures of the Schiff bases, SB-3 has three benzene rings while SB-1 and SB-2 have only two benzene rings. The electron cloud at the C=N bond in SB-3 is bigger than in SB-1 and SB-2 (Brady *et al*., 2015). The situations favoured the N atom to enhance the adsorption of the Schiff bases on the mild steel.

CONCLUSIONS

In conclusion, *N*-benzylidene-4-metoxyaniline, 4-(((4-metoxyphenyl)imino)methyl)phenol, and 4-(((4(phenylamino)phenyl)imino)methyl)phenol were successfully synthesized and characterized. Azomethine group (C=N) was observed in the IR (1602-1622 cm-1), ^{1}H NMR (8.42-8.51 ppm) and ^{13}C NMR (158.48-163.20 ppm) spectra. SB-3 which is 4-(((4-(phenylamino)phenyl)imino)methyl)phenol has two strong activating EDG (-OH and –NHC_6H_6) show the best corrosion inhibition at high concentration (2.5×10-4 M) in 1.0 M HCl. The corrosion inhibition increased when the concentration of the inhibitors increased. The inhibitions efficiency of the inhibitors follows the order of SB-3 > SB-1 > SB-2.

REFERENCES

i. Brady, J., Jespersen, N. & Hyslop, A. (2015). Chemisty (7 ed.): Wiley, 448.
ii. Chitra, S., Parameswari, K. & Selvaraj, A. (2010). Dianiline Schiff Bases as Inhibitors of Mild Steel Corrosion in Acid Media. *International Journal of Electrochemical Science*, *5*(11), 1675-1697.

iii. Echem, O.G. & James, A.O. (2014). Corrosion Inhibitory Effects of A New Synthetic Schiff Base On Aluminium in Sulphuric Acid. *International Journal of Scientific & Engineering Research*, *5*(10), 1054-1063.
iv. Hunt, I. (2019). *Chapter 12: Reactions of Arenes. Electrophilic Aromatic Substitution*. Retrieved Sep 05, 2019, from http://www.chem.ucalgary.ca/courses/350/Carey5th/Ch12/ch12-8b.html
v. Muniandy, M.T., Abdul Rahim, A., Osman, H., Mohd Shah, A., Yahya, S. & Raja, P.B. (2011). Investigation of Some Schiff Bases as Corrosion Inhibitors for Aluminium Alloy in 0.5 M Hydrochloric Acid Solutions. *Surface Review and Letters*, *18*(3-4), 127-133.
vi. Ramadan, R.M., Al-Nasr, A.K.A. & Ali, O.A.M. (2018). Synthesis, spectroscopic, DFT studies and biological activity of some ruthenium carbonyl derivatives of bis-(salicylaldehyde)phenylenediimine Schiff base ligand. *Journal of Molecular Structure*, *1161*, 100-107.
vii. Verma, C., Quraishi, M.A. & Singh, A. (2016). 5-Substituted 1H-tetrazoles as effective corrosion inhibitors for mild steel in 1 M hydrochloric acid. *Journal of Taibah University for Science*, *10*(5), 718-733.
viii. Verma, C.B. & Quraishi, M.A. (2014). Schiff's Bases of Glutamic Acid and Aldehydes as Green Corrosion Inhibitor for Mild Steel: Weight Loss, Electrochemical and Surface Analysis. *International Journal of Innovative Research in Science, Engineering and Technology*, *3*(7), 14601-14613.

JUNIOR SCIENCE COMMUNICATION
https://jscfsg.uitm.edu.my/
Volume 2 (2019)
eISSN 2637-0689

Colloquium of Chemistry and Environment 2018
Faculty of Applied Sciences, Universiti Teknologi MARA, Shah Alam.

TRANSESTERIFICATION OF WASTE COOKING OIL TO BIODIESEL USING CAO AS A HETEROGENOUS BASE CATALYST DERIVED FROM CHICKEN EGG SHELL

Khairunnisa Khrull Azman, Noraini Hamzah*
Faculty of Applied Sciences, Universiti Teknologi MARA, 40450 Shah Alam, Selangor, Malaysia.

*pnoraini@uitm.edu.my

Abstract: Fossil fuel is considered as non-renewable energy source as it will be depleted in the future. Besides that, high use of fossil fuel gives rise to environmental issue such as greenhouse effect. Therefore, fossil fuel needs to be replaced with renewable energy. Biodiesel fuel also known as fatty acid methyl ester (FAME) is a renewable energy that could overcome for this problem in the future. To make biodiesel production more cost effective, waste cooking oil and CaO derived from chicken egg shell were used as feedstock and heterogenous base catalyst, respectively. The effect of catalyst loading and methanol/oil molar ratio were investigated by transesterification of waste cooking oil to biodiesel at constant temperature of 65°C for 2 hours of reaction time with stirring rate of 400 rpm. The result obtained in this study showed that 2.0 wt % of catalyst and 15:1 of methanol/oil molar ratio are the optimum parameter with 77% of biodiesel yield. It was found that CaO derived chicken egg shell have high basicity that contributed good catalytic activity in transesterification of waste cooking oil. Chromatogram of GC-FID shows that major composition of FAME in biodiesel from waste cooking oil were methyl stearate ($C_{19}H_{38}O_2$) and methyl palmitate ($C_{17}H_{34}O_2$). The present work showed that the calcined of waste chicken egg shells at 900°C for 3 hours are suitable catalyst for production of biodiesel via transesterification of waste cooking oil.

Keywords: *waste cooking oil, biodiesel, egg shell, transesterification, GC-FID*

INTRODUCTION

Fossil fuels are one of a non-renewable energy which will be depleted in the future due to heavy consumption as it lasts for a limited time. Therefore, it is important to replace the non-renewable fossil fuels with renewable energy resources. An alternative fuel that can be used from renewable source of energy is biodiesel (Hill *et al*., 2006; Mekhilef *et al*., 2011). However, production of biodiesel required high production cost when using animal fat and vegetable oil as a raw material. To make biodiesel production more cost effective, waste cooking oil were used as feedstock. Recently, heterogeneous catalysts have gain researcher's attention because it has more advantages than homogeneous catalysts. Calcium oxide (CaO) heterogeneous base-catalyst is the most commonly used in transestrification process because of its high basicity, low solubility in biodiesel, easy to handle and non-toxicity (Maneerung *et al*., 2016; Mansir *et al*., 2018). In this study, chicken egg shell will be used as the source of heterogeneous based-catalyst in transesterification of waste cooking oil to fatty acid methyl ester (biodiesel). CaO catalyst from waste material used make biodiesel production more cost effective (Viriya-empikul *et al*., 2010). Effect of methanol/oil molar ratio and catalyst loading were evaluated in transesterification of waste cooking oil to biodiesel yield.

METHODOLOGY

Waste cooking oil as feedstock was collected from the stall in Dataran Cendekia at Universiti Teknologi MARA located in Shah Alam. The transesterification reaction was performed using methanol and egg

Colloquium of Chemistry and Environment 2018
Faculty of Applied Sciences, Universiti Teknologi MARA, Shah Alam.

shell as heterogeneous catalyst. The waste chicken egg shells as a source of CaO were collected from household waste at Pangsapuri Subang Suria. Methanol (99.95%) was bought from Fisher Chemical. Collected chicken egg shells were calcined under air for 3 h at 900 ℃ with a heating rate of 10 ℃/min (Piker *et al*., 2016) while waste cooking oil undergo pre-treatment to remove contaminants. The transesterification reaction was conducted at 65 ℃ with a continuous stirring of 400 rpm for 2 h with varied methanol/oil molar ratio of 9:1, 12:1, 15:1, 18:1 and 21:1 while catalysts loading was varied at 1.0 wt.%, 1.5 wt.%, 2.0 wt.%, 2.5 wt.% and 3.0 wt.%. After separation between FAME and glycerol, crude biodiesel undergoes washing for three times at 50 ^{o}C in separatory funnel. The compositions of FAME present in the biodiesel were determined by GC-FID (Agilent 5975C).

FINDINGS

The effect of catalyst loadings (wt.%) on biodiesel yield via transesterification reaction was investigated using five different amount of catalyst from 1 wt.% to 3 wt.% based on the weight of the catalyst over the volume of waste cooking oil. Figure 1(a) shows the biodiesel yield increased with the increasing of catalyst concentration from 1 wt.% to 2 wt.% that result in the increasing of biodiesel yield from 54.2% to 77.0%. This result displayed that increasing the amount of catalyst could increase the contact between the catalyst and the reactants which then affected the reaction rate. However, for higher amount of catalyst which is more than 2 wt.%, the yield of biodiesel slightly decreased because the number of active site was fully occupied. Therefore, 2 (wt.%) of CaO catalyst from eggshell was optimum catalyst loading in order to achieve high yield of biodiesel for 2 hours.

Figure 1(b) shows the effect of five different methanol/oil molar ratios (9:1, 12:1, 15:1, 18:1 and 21:1) on the percentage of biodiesel yield. The result indicated that increasing of methanol/oil molar ratio from 9:1 to 15:1 leads to the increased of biodiesel yield up to 80%. However, the biodiesel yield decreased with further increasing in methanol to oil ratio from 15:1 to 21:1 due to excessive of methanol. The percentage yield of biodiesel is directly proportional to the methanol to oil molar ratio for egg shell catalyst. In general, molar ratio for methanol/oil molar ratio was 3:1. Excessive methanol is necessary to shift the equilibrium to form higher biodiesel yield. However, when the ratio of oil to methanol is too high, it could give adverse effect to the yield of biodiesel because the concentration of glycerol increase when there is excess methanol in the reaction mixture.

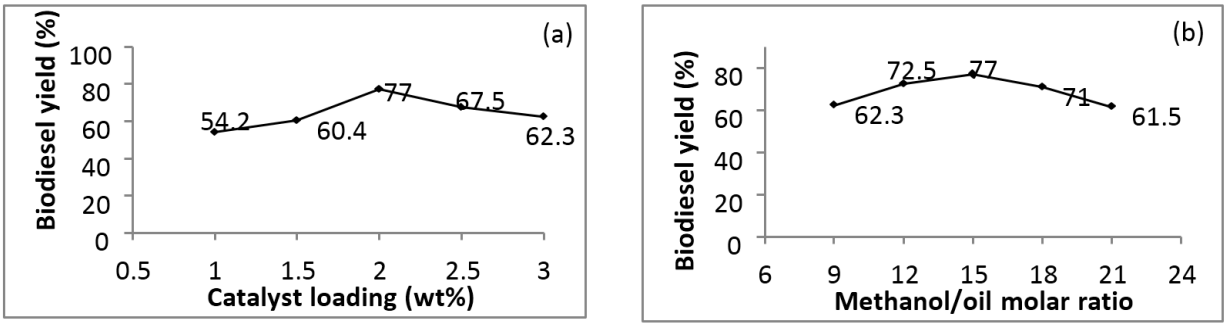

Figure 1(a) Effect of catalyst loading (wt%) (b) effect of methanol/oil molar ratio on biodiesel yield

Colloquium of Chemistry and Environment 2018
Faculty of Applied Sciences, Universiti Teknologi MARA, Shah Alam.

Figure 2(a) shows the chromatogram GC-FID of FAME standard and the retention time of standard FAME was summarized in Table 1. The methyl laurate is the first peak observed due to molar mass of methyl laurate is lower make the compound vaporised faster than other compound.

Table 1 Retention time of peak standard FAME

	Standard FAME				
	Methyl Laurate	Methyl Myristate	Methyl Palmitate	Methyl Stearate	Methyl Linoleate
Retention Time	1.792	2.280	3.208	4.642	4.921

As shown in Figure 2(b), five peaks are observed that confirmed the presence of FAME components which are methyl stearate, methyl palmitate, methyl linoleate, methyl myristate and methyl laurate. The major component of FAME obtained are methyl stearate ($C_{19}H_{38}O_2$) and methyl palmitate ($C_{17}H_{34}O_2$).

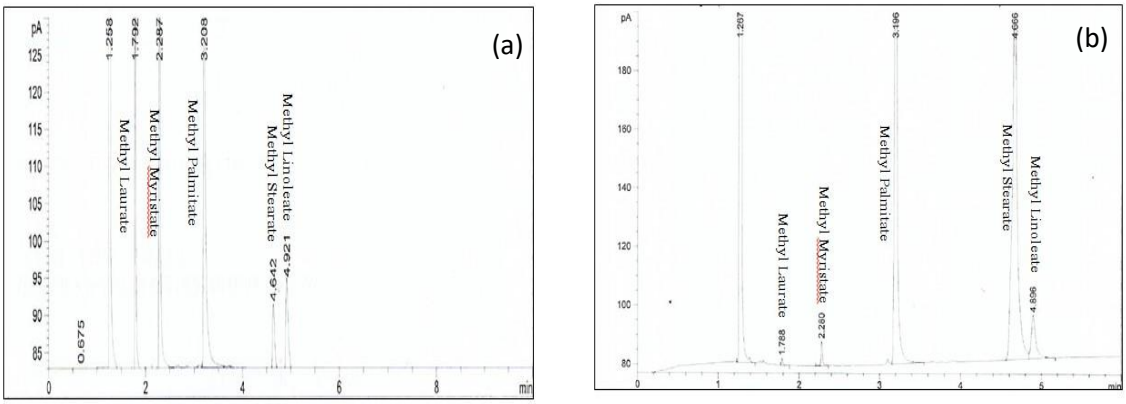

Figure 2 Gas chromatography spectrum of (a) standard FAME and (b) biodiesel product sample

CONCLUSION

Chicken egg shell was successfully used as CaO catalyst for biodiesel production. The obtained CaO catalyst exhibited high catalytic performance for production of biodiesel from transesterification reaction of waste cooking oil with biodiesel where 77% of FAME yield was achieved with optimum condition of 15:1 of methanol/oil molar ratio and 2.0 wt.% of catalyst loading.

Volume 2 (2019)
eISSN 2637-0689

REFERENCES

i. Hill, J., Nelson, E., Tilman, D., Polasky, S. & Tiffany, D. (2006). Environmental, economic, and energetic costs and benefits of biodiesel and ethanol biofuels. *Proceedings of the National Academy of Sciences, 103*(30), 11206-11210.

ii. Maneerung, T., Kawi, S., Dai Y. & Wang, C.-H. (2016). Sustainable biodiesel production via transesterification of waste cooking oil by using CaO catalysts prepared from chicken manure. *Energy Conversion and Management, 123*, 487-497.

iii. Mansir, N., Teo, S.H., Rashid, U., Saiman, M.I., Tan, Y.P., Alsultan, G.A. & Taufiq-Yap, Y.H. (2018). Modified waste egg shell derived bifunctional catalyst for biodiesel production from high FFA waste cooking oil. A review. *Renewable and Sustainable Energy Reviews, 82*, 3645-3655.

iv. Mekhilef, S., Siga, S. & Saidur, R. (2011). A review on palm oil biodiesel as a source of renewable fuel. *Renewable and Sustainable Energy Reviews, 15*(4), 1937-1949.

v. Piker, A., Tabah, B., Perkas, N. & Gedanken, A. (2016). A green and low-cost room temperature biodiesel production method from waste oil using egg shells as catalyst. *Fuel, 182*, 34-41.

vi. Viriya-empikul, N., Krasae, P., Nualpaeng, W., Yoosuk, B., & Faungnawakij, K. (2012). Biodiesel production over Ca-based solid catalysts derived from industrial wastes, Fuel, *92*(1), 239-244.

JUNIOR SCIENCE COMMUNICATION
https://jscfsg.uitm.edu.my/
Volume 2 (2019)
eISSN 2637-0689

Colloquium of Chemistry and Environment 2018
Faculty of Applied Sciences, Universiti Teknologi MARA, Shah Alam.

SYNTHESIS OF CINNAMATE-ZINC LAYERED HYDROXIDE (ZLCA) FOR SUNSCREEN APPLICATION

Maria Amirrah binti Mamnor, Siti Halimah binti Sarijo*
Faculty of Applied Sciences, Universiti Teknologi MARA, 40450, Shah Alam, Selangor, Malaysia.

* sitihalimah@uitm.edu.my

Abstract: The intercalation process of cinnamate acid into zinc-layered hydroxide was successfully performed by direct method using cinnamic acid and zinc oxide as precursor. The intercalated compound, zinc-cinnamic acid layered compound (ZLCA) showed a basal spacing of 12.12 Å. The estimated percentage loading of cinnamate is 38.8% (w/w%) estimated from the TGA thermogram. The FTIR spectra of the intercalated compound ZLCA showed disappearance of ZnO absorption spectra at 445nm.

Keywords: *cinnamic acid, zinc-layered hydroxide, zinc oxide, PXRD, FTIR, TGA, sunscreen, UV.*

INTRODUCTION

Skin is the largest organ of the body and is always exposed to sunlight which causes photoaging and skin cancer. Therefore, sunscreen is widely used to protect skin from UVA and UVB especially in tropical climate. This is because the active ingredients in sunscreen contain organic and inorganic molecule which is capable to absorb, scattered and reflected UV radiation (Cursino *et al*., 2013). However, these molecules can be photo degraded after a period of time, causing it to be ineffective (Yousif & Haddad, 2013). One of the compounds used as a UV absorber is cinnamic acid. It has anti-oxidant and ant- inflammatory properties. Cinnamic acid and its derivatives are capable of absorbing UV radiation of broad range. However, cinnamic acid is easily decomposed at high heat and has some restriction in terms of their stability and toxicity at high concentration. Hence, zinc-layered hydroxide (ZLH) is an ideal precursor to be used as a host for layered nanocomposite. It is a layered hydroxide salts with modification of brucite-like structure that composed of single divalent metal cation which is zinc ion. It has positively charged layers that are capable to expand or contract depending on the nature of the interlayer anions (Arizaga *et al*., 2008). Zinc layered hydroxide is used as a layer to protect from direct contact of concentrated cinnamic acid with the skin and to increase the efficiency of UV blocking functionality.

METHODOLOGY

Methods that were applied to this study involves two steps; synthesis of ZLCA and characterization of the synthesized ZLCA. ZLCA was synthesized by reacting about 0.2g of ZnO with 100 ml of 0.1mol/L cinnamic acid solution. The intercalation compound was titrated with 2 mol/L NaOH until pH 8 before it was stirred continuously for 5 hours at room temperature. Then it was aged in an oil bath at 70°C for 18 hours before being centrifuged and washed with deionized water. The final white solid (ZLCA) was dried under vacuum at 70°C overnight. The intercalated compound, ZLCA was characterized by using Powder X-Ray diffractometer and Fourier Transform Infrared spectroscopy. Powder X-Ray diffraction (PXRD) patterns were recorded at room temperature on Rigaku model Ultima IV Powder Diffractometer using CuK_{α} radiation (λ = 1.540562 Å) at 40 kV and 20mA. The pattern was collected from 2 to 60° at dwell time of

2° min^{-1}. Next characterization was by Fourier Transform Infrared Spectrometer (FTIR). The sample was prepared to a KBr disc and was analyzed over the range of 20 to 400cm^{-1} on FTIR spectrometer Perkin-Elmer Spectrum 100. Last characterization was using Thermogravimetry Analysis (TGA). Approximately 1 to 5 mg of the sample was placed in aluminum pan and was heated up to 1000°C with the heating rate of 10°C/min and under nitrogen gas flow of about 50 $mL.min^{-1}$

FINDINGS

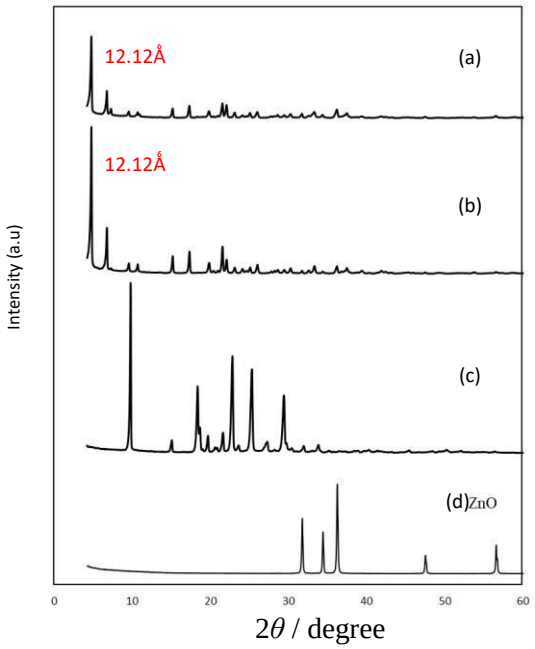

Figure 1 PXRD patterns of (a) 0.05M ZLCA, (b) 0.1M ZLCA, (c) CA and (d) ZnO

Table 4.1 Data from PXRD pattern of 0.05M ZLCA and 0.1M ZLCA

	Basal Spacing (Å)	Peak Intensity (a.u)
0.05M ZLCA	12.12	2624
0.1M ZLCA	12.12	24712

Colloquium of Chemistry and Environment 2018

Faculty of Applied Sciences, Universiti Teknologi MARA, Shah Alam.

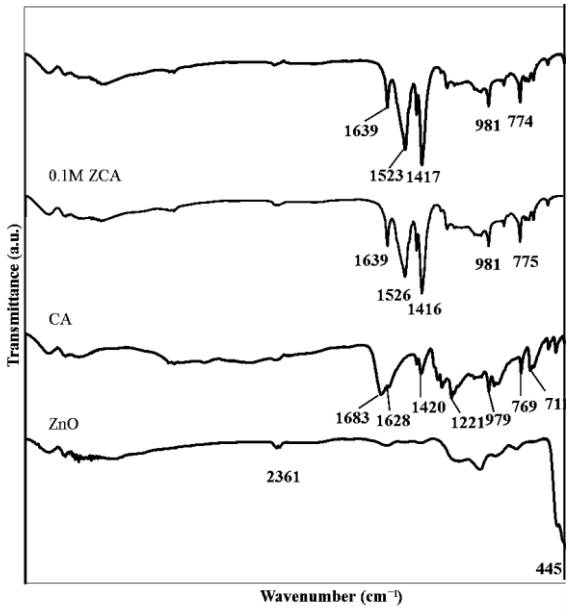

Figure 2 FTIR spectra of ZnO, CA and ZLCA.

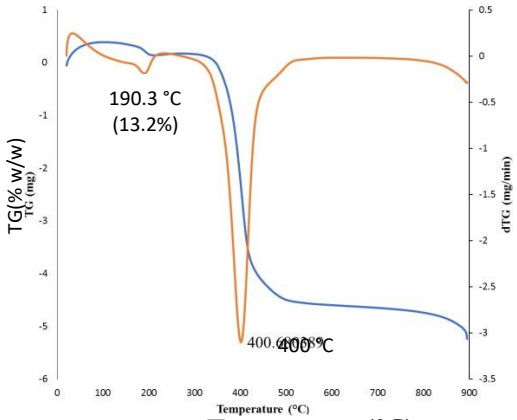

Temperature (°C)

Figure 3 TG and dTG curves for ZLCA

Based on the Figure 1, 3 harmonic patterns were observed for ZLCA intercalation compounds with basal spacing of 12.12Å. It is considered as a successful intercalation. The present finding was similar to previous study which has close value of basal spacing of ZLCA intercalation compound at 13.2Å (Sun *et al*., 2007). Based on Table 1, the diffraction peak of 0.1M ZLCA is more intense than 0.05M ZLCA making 0.1M CA the best concentration to be intercalated with ZLH. According to Figure 2, the FTIR spectrum for both 0.05M and 0.1M ZLCA shows disappearance of broad ZnO peak at 445cm^{-1}. This indicates that all ZnO molecules has reacted with cinnamate anion to form ZLCA. The shifting of COOH from pure cinnamic acid to COO^- is due to cinnamic acid being deprotonated to allow the interaction of negative carboxyl group to the positive interlayer of ZLH. As seen on Figure 3, the thermal analysis curbs revealed 2 steps of decomposition. The first step is due to removal of physiosorbed and interlayer water at 190°C with 13.2% of weight loss. The decomposition of cinnamate ion intercalated compound happens at step 2 at 400°C with weight loss of 38.8%. The estimated percentage loading obtained from this TGA thermogram is 38.8%.

CONCLUSIONS

This research was conducted to synthesize and characterize ZLCA intercalation compounds for sunscreen application. Organic UV absorbing active agent, cinnamate anion has been successfully intercalated into ZLH interlayers spaces from zinc oxide precursor to generate ZCA intercalation compound with a basal spacing of 12.12Å to accommodate cinnamates in a bilayer arrangement.

REFERENCES

i. Arizaga, G.G.C., Mangrich, A.S. & Wypych, F. (2008). Cu^{2+} ions as a paramagnetic probe to study the surface chemical modification process of layered double hydroxides and hydroxide salts with nitrate and carboxylate anions. *Journal of Colloid and Interface Science*, *320*(1), 238-244.

ii. Cursino, A.C.T., Lisboa F.D.S., Pyrrho, A.D.S., Sousa, V.P.D. & Wypych, F. (2013). Layered double hydroxides intercalated with anionic surfactants/benzophenone as potential materials for sunscreens. *Journal of Colloid and Interface Science*, *397*, 88-95.

iii. Sun, W., He, Q. & Luo, Y. (2007). Synthesis and properties of cinnamic acid series organic UV ray absorbents-interleaved layered double hydroxides. *Materials Letters*, *61*(8-9), 1881–1884.

iv. Yousif, E. & Haddad, R. (2013). Photodegradation and photostabilization of polymers, especially polystyrene: review. *SpringerPlus*, *2*(1), 398.

JUNIOR SCIENCE COMMUNICATION
https://jscfsg.uitm.edu.my/
Volume 2 (2019)
eISSN 2637-0689

Colloquium of Chemistry and Environment 2018
Faculty of Applied Sciences, Universiti Teknologi MARA, Shah Alam.

DETERMINATION OF FATTY ACID RATIOS IN LATENT FINGERPRINT USING GC-MS

Izzudeen Zainal, Ezlan Elias*
Faculty of Applied Sciences, Universiti Teknologi MARA, 40450 Shah Alam, Selangor, Malaysia.

*ezlan@uitm.edu.my

Abstract: Besides DNA, fingerprints play an important role as trace evidence in criminal investigations. It is routinely identified from the pattern of fingerprint; thus, it is possible to track the individual appellant. Despite the pattern of fingerprint, it is possible to obtain the information of the appellant from the chemical composition of the fingerprint. In this study, analytical method for the determination of fatty acid ratios in fingerprint using liquid solid extraction (LSE) and gas chromatography (GC) coupled with mass spectrometer (MS) was developed. Solubility test was carried out to test whether dichloromethane, hexane or methanol is the best solvent to extract fatty acid in fingerprint by LSE method. Dichloromethane gives the highest percent efficiency and % RSD which is 58% efficiency and 24% RSD followed by hexane with 52% efficiency and 20% RSD. Methanol did not give any of fatty acid which means methanol cannot be using to extract fatty acid from fingerprint. The higher % efficiency and % RSD, the more suitable solvent to extract the fatty acids. Significant differences in the ratios of fatty acid were found when comparing the individuals of different gender, BMI and personal habit using GC-MS. In conclusion, fatty acid in female fingerprints is higher than male fingerprints, overweight BMI has higher fatty acid than normal BMI and a person who use a cosmetic product will give rise many broad peaks in chromatogram than a person that did not use any cosmetic product.

Keywords: *Latent fingerprint, GC-MS, fatty acid ratios.*

INTRODUCTION

For more than a century, fingerprints have been commonly used in forensic investigations, basically for identification purposes. Fingerprints composition is importance in the development of detection and enhancement techniques. Besides amino acids, water and salt, lipid is one of the important components in the latent fingerprint. Lipids consist of robust component in latent finger-mark since they are hydrophobic and non-volatile nature compound. Lipid fraction provide highly compositional changes based on several factors and it is proved to characterize different individual profile (Cadd *et al.*, 2015). Useful information can be obtained from fingerprints composition such as gender, age, ethnic, personal care products, diet, daily activities and level of oil on the face based on the level of fatty acid . Study shows that, differences in skin surface lipid production are related to age, gender, metabolic disorders and skin pathology which may affect the fingerprint composition (Asano *et al.*, 2002). Environmental factors such as diet, washing and personal care products also will have a result on the chemical composition of the fingerprints. Gas Chromatography Mass Spectrometry (GC-MS) was used to determine the fatty acid ratios in latent fingerprint. Using gas chromatography - mass spectrometry, differences in the ratios of several fatty acid methyl esters will found when comparing individuals of varying race and gender. GC- MS is an important instrument in lipid identification. GC-MS is a very sensitive analytical technique that have been used in a wide range as an application of identification especially forensic and criminal cases (Chauhan *et al.*, 2014).

Volume 2 (2019)
eISSN 2637-0689

METHODOLOGY

Forty donors, between ages of 21 and 25, were selected to give the latent fingerprint samples based on their individual profile (gender, BMI, personal habit). Each of the donors must rub all their fingers to their foreheads at least for 4 seconds. Then the fingers were placed on the filter paper circles (25mm qualitative filter paper, Grade 1: Whatman, UK). The donors were asked to press each fingertip gently to a filter paper circle for approximately 10 seconds. Then, the filter papers that contained the fingermark were wrapped with the aluminium foil and were labelled with specific code. Extraction of fingermark started after an hour of deposition and were extracted from filter paper in a 4 ml glass screw-top vials. The vials first were cleaned with distilled water and were rinsed with dichloromethane. A 750 μL of dichloromethane was poured in the 4 ml glass vials. Samples were immersed in the vials contain dichloromethane and were allowed to extract for at least 2 minutes. In this step, the sample were immersed with gentle manual agitation in order to ensure that the filter papers were completely submerged in the solvent. After 2 minutes, the filter papers were removed and discarded from the vials, and the sample extracts were transferred to 2ml glass crimp top vials (Agilent Technologies, USA). The vials then were sealed at the screw top of vials with aluminium crimp tops. The samples were analysed by GC-MS. Blanks consisting only of clean filter paper were prepared and analysed along with a sample.

FINDINGS

The results obtained from this study shows that difference level of fatty acid ratios between three factors which are gender, BMI and personal habit. As depicted in Figure 1, female shows higher level of fatty acid ratios compared to male. This may be due to the hormone presence in women. According to Brown & Clegg, (2009) oestrogen and progesterone hormone cause increase deposition of fat in female body. The person who have higher BMI shows higher level of fatty acid ratios compared to person who has lower BMI. According to Michalski *et al.* (2012), the body fat percentage in male and female were increased along with increasing in body mass index (BMI). A person who are used cosmetic product will give rise many broad peaks in chromatogram compared to person who did not use any cosmetic product as shown in Table 1. Large variety of fatty acids which usually found in fingerprints are present in cosmetic products such as stearic acid, palmitic acid, lauric acid, oleic acid an myristic acid. According to Ricci & Kazarian (2010), fatty acid presence in latent fingerprint can indicate whether a person applies a cosmetic or not by observing the number of broad peaks present in the chromatogram.

Colloquium of Chemistry and Environment 2018

Faculty of Applied Sciences, Universiti Teknologi MARA, Shah Alam.

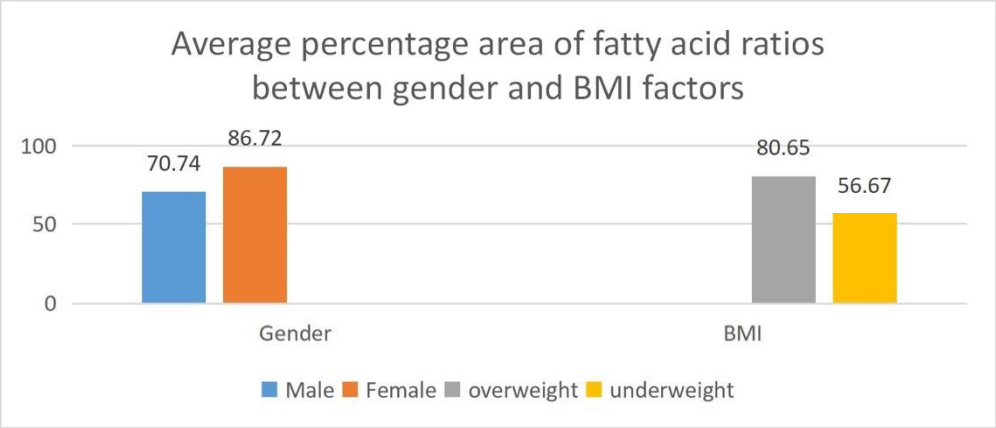

Figure 1 Difference level of fatty acid ratios due to genders and BMI

Table 1 The presence of contaminants in different personal habit of a person

Compound	**Cosmetic product user**	**Non Cosmetic product user**
Squalene	√	√
Hexadecanoic Acid	√	√
Myristic Acid	√	×
Oleic Acid	√	×
Palmitic Acid	√	×
Stearic Acid	√	×

CONCLUSIONS

In summary, the data has shown that fingerprints compose of various fatty acids, and may be differentiated based on gender, BMI and lifestyle. Female showed higher fatty acid mean ratios than male. Person with higher BMI showed higher fatty acid ratios than person lower BMI. Besides that, the personal habit of a person was also differentiated. From the result showed, person who applies cosmetic product to their skin will give rise many broad peaks while a person who did not apply any skin product will give rise a normal peak. This showed that, the skin product can contaminate the fingerprint residue with their chemical components in the skin product.

REFERENCES

i. Asano, K., Bayne, C.K., Horsman, K.M. & Buchanan, M.V. (2002). Chemical Composition of Fingerprints for Gender Determination. *Journal of Forensic Sciences*, *47*(4), 805-807.

Volume 2 (2019)
eISSN 2637-0689

ii. Brown, L.J. & Clegg, D.J. (2009). Central Effects of Estradiol in the Regulation of Adiposity. *The Journal of Steroid Biochemsitry and Molecular Biology, 122*(1-3),65-73.
iii. Cadd, S., Islam, M., Manson, P. & Bleay, S. (2015). Fingerprint composition and aging: A literature review. *Science and Justice, 55*(4), 219–238.
iv. Chauhan, A., Goyal, M.K. & Chauhan, P. (2014). GC-MS Technique and its Analytical Applications in Science and Technology. *Journal of Analytical & Bioanalytical Techniques*, *5*(6), 1000222.
v. Michalski, S., Shaler, R. & Dorman, F.L. (2012). The Evaluation of Fatty Acid Ratios in Latent Fingermarks by Gas Chromatography/Mass Spectrometry (GC/MS) Analysis. *Journal of Forensic Sciences, 58*, S215-S220.
vi. Ricci, C. & Kazarian, S.G. (2010). Collection and Detection of Latent Fingermarks Contaminated with Cosmerics on Nonporous and Porous Surface. *Surface and Interface Analysis, 42*(5), 386-392.

JUNIOR SCIENCE COMMUNICATION
https://jscfsg.uitm.edu.my/
Volume 2 (2019)
eISSN 2637-0689

Colloquium of Chemistry and Environment 2018
Faculty of Applied Sciences, Universiti Teknologi MARA, Shah Alam.

ANT REPELLENT ACTIVITY OF *Polygonum mınus* AND *Etlıngera elatıor*

Nadia Abu Samah and Faridahanim Mohd Jaafar*
Faculty of Applied Sciences, Universiti Teknologi MARA, 40450 Shah Alam, Selangor, Malaysia.

*faridahanim@uitm.edu.my

Abstract: Ants are considered as pests when they enter buildings in search of food and water or when they build their nests in buildings or gardens. Synthetic pest repellents may repulse these pests effectively, however the accumulation of the residue of the synthetic repellents can be toxic to human and the environment. Hence, natural repellents are perceived as safe and better alternatives in comparison to the synthetic repellents. In this study, essential oils extracted from the leaves of *P. minus* and the flower parts of *E. elatior* were tested for ant repellency activity while their chemical composition were analyzed using gas chromatography-mass spectrometry (GC–MS) and infrared spectroscopy (IR). The extraction of the essential oil was carried out by hydrodistillation method using the Clevenger-type apparatus for four hours at 100°C. Filter paper test were conducted to evaluate the ant repellent activity of the essential oil of both plants on odorous house ant, *Tapinoma sessile* for three hours of exposure respectively. The findings revealed that the essential oils of both plants *P. minus* and *E. elatior* effective repel the ants by which the essential oil of *E. elatior* showed a higher mean repellency with 89.58% inhibition compared to *P. minus* with 84.03% inhibition. The analysis of the essential oil of *P. minus* revealed the presence of 81 compounds with 0.20% yield and the major compounds were γ-sitosterol (34.01%), dodecanal (7.74%), cyclododecane (5.40%), decanal (2.50%), caryophyllene (1.52%) and 1-decanol (1.20%). A total of 41 compounds were identified from the essential oil of *E. elatior* with 0.14% yield and the main compounds were dodecanal (10.08%), thymol (5.31%), caryophyllene (3.45%), dodecanol (2.86%), ß-Longipinene (1.59%) and germacrene D (1.58%).The compounds were found to have possible repellent properties in the essential oil of both plants were β-caryophyllene, p-cymene, humulene, decanol, dodecanal, thymol, germacrene D, α-Pinene, and dodecanol. These compounds were identified as insect repellents based on previous studies. Therefore, the essential oils of *P. minus* and *E. elatior* have the potential as natural ant repellents.

Keywords: *Ant repellent, filter paper test, P. minus and E. elatior.*

INTRODUCTION

Repellents are substances that are widely used to solve problems involving pests and insects. Repellents can be identified as synthetic or natural repellents. However, the excessive use of the chemicals has led to many problems. Hence, natural repellents are considered as an alternative way towards green technology and a healthy environment. There are several studies on the essential oils from plants that are used as insect repellents such as *Murraya koenigii*, *Curcuma longa* (Das *et al*., 2015) and *Polygonum hydropiper* (Maheswaran & Ignacimuthu, 2013). This study focused on the ant repellent potential of *Polygonum minus* and *Etlingera elatior*. The response (stimuli) of the ant towards the essential oil was the main focus of this experiment. The results will show whether these essential oils are more effective or just as effective against a specific ant compared to synthetic repellents. The study emphasized on the extraction of the essential oils from the leaves of *P. minus* and flower part of *E. elatior* by hydrodistillation. The oils were subjected to FTIR and GC-MS analysis to determine their chemical composition. The ant repellency ability of both essential oils were measured and compared to distinguish the efficiency of the oils as natural ant repellents while the ants' species are limited to household ants.

METHODOLOGY

First, the fresh leaves of *P. minus* and fresh inflorescence of *E. elatior* were collected at the wet market of Section 6, Shah Alam, and washed using deionized water to remove any dirt or contaminant. The plant

samples were chopped into small pieces and 300 g of each plant samples were blended with 1500 ml of deionized water using an electric blender. The extraction of the essential oil was carried out by hydro-distillation method using the Clevenger-type apparatus. About 500 ml of the plant-water mixture were poured into a round bottom flask attached to a heating mantle. The distillation was conducted for 4 hours at 100°C to extract the essential oil completely from the mixture. The volatile compounds containing water soluble fractions were allowed to settle for 30 minutes and collected in a beaker. The essential oils collected were dried using anhydrous sodium sulphate to remove excess water. The anhydrous sodium sulphate was removed from the oils then the hexane containing the oils was removed by using the rotary evaporator. The oils were weighed and kept in airtight vials covered with aluminium foil at 4°C before further analysis. The oils were subjected to FTIR, GC-MS analysis and ant repellent activity test.

FINDINGS

The results obtained from this study showed the mean percentage of repellency (%) of the essential oil of *E. elatior* was 89.58 ± 4.17 (mean ± SD) while the mean percentage of repellency (%) of the essential oil of *P. minus* was 84.03 ± 1.20. The percentage of repellency values between the essential oils of the two plants and repellent product showed that the essential oil of *E. elatior* is more effective in repelling household ants compared to that of *P. minus* while the repellent product of "Serai Wangi Natural Repellents" act as positive control in this study and showed 100% ant repellency. The essential oils of both plants were effective in repelling household ants. Dodecanal and caryophyllene were present in both of the essential oils of *P. minus* and *E. elatior* as the major constituents in the oils. There were seven compounds in total present in essential oils of *E. elatior* including thymol, germacrene D, α-Pinene and dodecanol while five compounds with repellent properties were determined including decanol and p-cymene. The compounds were found to have possible repellent properties based on several previous studies. The total percentage of essential oil recovery collected from the leaves of *P. minus* was collected at 0.20% yield with yellowish colour appearance compared to that of *E. elatior* which was collected at 0.14% with strong smell of oil and translucent appearance. However, only the flower of *E. elatior* which is known as pink torch was used for hydrodistillation. The essential oil of *E. elatior* collected were higher as compared to that of previous study with 0.05% while the essential oil of *P. minus* collected was found to be lower as compared to that of previous study of 0.48%. The amount of the essential oils yield may be affected by several factors such as solvent used in extraction, part of plant extracted and temperature of extraction. The analysis of the essential oil of *P. minus* identified 81 compounds and the major compounds were γ-sitosterol (34.01%), dodecanal (7.74%), cyclododecane (5.40%), decanal (2.50%), caryophyllene (1.52%) and 1- decanol (1.20%). A total of 41 compounds were identified from the essential oil of *E. elatior* and the main compounds were dodecanal (10.08%), thymol (5.31%), caryophyllene (3.45%), dodecanol (2.86%), ß-longipinene (1.59%) and germacrene D (1.58%). The compounds found to have possible repellent properties in the essential oil of both plants were β-caryophyllene, p-cymene, humulene, decanol, dodecanal, thymol, germacrene D, α-Pinene, and dodecanol. These compounds were previously identified as insect repellents.

CONCLUSIONS

In conclusion, essential oils of both plants *P. minus* and *E. elatior* were effective in repeling the ants in which the essential oil of *E. elatior* showed a higher mean repellency with 89.58% as compared to *P. minus* with 84.03%. The "Serai Wangi Natural Repellents" was used as positive control for the ant repellent

activity with mean percentage of repellency (%) of 100 ± 0.00 (mean ± SD). The analysis of the essential oil of *P. minus* identified 81 compounds with 0.20% yield and the major compounds were γ-sitosterol (34.01%), dodecanal (7.74%), cyclododecane (5.40%), decanal (2.50%), caryophyllene (1.52%) and 1-decanol (1.20%). A total of 41 compounds were identified from the essential oil of *E. elatior* with 0.14% yield and the main compounds were dodecanal (10.08%), thymol (5.31%), caryophyllene (3.45%), dodecanol (2.86%), ß-Longipinene (1.59%) and germacrene D (1.58%). The compounds found to have possible repellent properties in the essential oil of both plants were β-caryophyllene, p-cymene, humulene, decanol, dodecanal, thymol, germacrene D, α-Pinene, and dodecanol. These compounds were identified as insect repellents based on previous reported studies. Therefore, the essential oils of *P. minus* and *E. elatior* have the potential as natural ant repellents.

REFERENCES

i. Das, N.G., Dhiman, S., Talukdar, P.K., Rabha, B., Goswami, D. & Veer, V. (2015). Synergistic mosquito-repellent activity of *Curcuma longa*, *Pogostemon heyneanus* and *Zanthoxylum limonella* essential oils. *Journal of Infection and Public Health*, *8*(4), 323-328.

ii. Maheswaran, R. & Ignacimuthu, S. (2013). Bioefficacy of essential oil from *Polygonum hydropiper* L. against mosquitoes, *Anopheles stephensi* and *Culex quinquefasciatus*. *Ecotoxicology and Environmental Safety*, *97*, 26-31.

JUNIOR SCIENCE COMMUNICATION
https://jscfsg.uitm.edu.my/
Volume 2 (2019)
eISSN 2637-0689

Colloquium of Chemistry and Environment 2018
Faculty of Applied Sciences, Universiti Teknologi MARA, Shah Alam.

PHARMACEUTICAL AS POTENTIAL CHEMICAL MARKERS IN WASTEWATER

Nadihaa Binti Azman, Rozita Binti Osman*
Faculty of Applied Sciences, Universiti Teknologi MARA, 40450, Shah Alam, Selangor, Malaysia

*rozit471@uitm.edu.my

Abstract: This study evaluates the potential of common pharmaceuticals (caffeine, acetaminophen, carbamazepine, naproxen and ibuprofen) as chemical markers for wastewater. The online solid phase extraction liquid chromatography (SPE-LC) method was used to provide rapid analysis for pharmaceuticals in wastewater. The instrumental limits of detection and limit of quantification ranged from 2.23 - 7.30 μg/L and 6.75 - 22.11 μg/L, respectively. A satisfactory recovery was obtained between 53-102% with % RSD of 1.4-2.7%. The calibration curves were linear with correlation coefficient (r2) in the range of 0.994 to 0.999. The online SPE-LC analytical method performance showed satisfactory accuracy and precision. The method was applied to analyse pharmaceuticals in wastewater treatment plant in Klang area. Acetaminophen could be a possible chemical marker for human waste contamination in surface water because it showed good correlation with population density and is source specific.

Keywords: *Monolaurin, virgin coconut oil, antimicrobial, and disc diffusion test.*

INTRODUCTION

Pharmaceuticals are classified as emerging contaminants has been used widely in developed country. There are many factors that have been investigated by the previous studies about how pharmaceuticals residue polluted the aquatic environment. A collection of chemical marker has been recommended to trace contamination caused by private and local activity. The chemical markers can be gathered into various group, for example, pharmaceuticals, hormones, drugs, cleansers, pesticides and manures. Caffeine has been proposed as a good chemical anthropogenic marker for monitoring human fecal contaminants in source water (Kosma *et al.* 2010). Caffeine is one of the fundamental components of food and medicine and is the most extensively utilized substance (Kurisserya, 2012). As the presence of pharmaceuticals are relatively low in complex environmental sample, an efficient and fast analytical method needs to be developed to isolate and pre-concentrate these pharmaceuticals from the complex wastewater. Using online SPE-LC, the eluted analytes are directly transferred into the analytical column for separation and quantitation. Therefore, this approach has the advantages of significant reduction in sample preparation time and less human handling which result in high sensitivity and accuracy. In this study, analysis of selected pharmaceuticals including caffeine, acetaminophen, carbamazepine, ibuprofen and naproxen was conducted using online SPE-LC prior to assessment of suitability of these pharmaceuticals used as chemical marker for wastewater.

METHODOLOGY

Five selected pharmaceuticals (caffeine, carbamazepine, naproxen, ibuprofen, and acetominophen) with purity between 98% to 101% and methanesulfonic acid (MSA) were purchased from Sigma Aldrich. Acetonitrile (HPLC grade) was purchased from Merck (Darmstadt, Germany). Water samples were

collected from three wastewater treatment plants (WWTPs) around Klang area. Grab sampling technique was used to collect influent and effluent wastewater samples (vertical grab sampler 5 L, Ocean test Equipment, Florida USA). The sample was transferred into a 1.0 L amber bottle. Water samples were collected twice and acidified using 3 M hydrochloric acid (2-3 drops). This is done to prevent biological activities. After collection had been made, the water sample was immediately filtered using 0.45 µm glass fibre to get rid of suspended matter. Majority, collection and filtration of the water sample and sample enrichment could not be performed on the same day. In such cases, filtered water samples were kept in the dark and stored at 4˚C to be analyzed within one week of collection. The concentration of studied pharmaceuticals in the wastewater sample were determine by using online SPE-HPLC.

FINDINGS

The analytical performance of online SPE-LC methods was validated based on linearity, accuracy, precision, LOD and LOQ for the studied pharmaceuticals as tabulated in Table 1.

Table 1 Analytical performance of online SPE-LC methods

Pharmaceuticals	Linear range (µg/L)	Coefficient of determination R^2	LOD (µg/L)	LOQ (µg/L)	Recovery (%)	RSD (%)
Caffeine	0.5-50	0.999	2.23	6.75	102.0	2.7
Acetaminophen	0.5-50	0.994	5.40	16.36	53.0	1.9
Carbamazepine	1.0-50	0.996	4.33	13.13	99.2	1.4
Naproxen	0.1-50	0.999	7.30	22.11	94.1	1.4
Ibuprofen	0.1-50	0.994	5.36	16.26	101.0	1.6

Table 2 shows the concentration of pharmaceuticals in influent and effluent wastewater collected in three different wastewater treatment plants in Klang area. Removal efficiencies of pharmaceuticals were compound-specific. Anti-inflammatories and analgesics were very well removed in the WWTP treatment. Acetaminophen and caffeine presented high removal rates (>90%) as reported by Subari *et al.* (2017). Though, the extended aeration system in WWTPs of Klang was not able to completely remove most of the detected pharmaceuticals. Acetaminophen could be a possible chemical marker for human waste contamination in surface water because it showed good correlation with population density and is source specific (Ismail, 2014).

Colloquium of Chemistry and Environment 2018
Faculty of Applied Sciences, Universiti Teknologi MARA, Shah Alam.

Table 2 Concentration of pharmaceuticals (µg/L) in influent and effluent wastewater collected in three different wastewater treatment plant (WWTP) in Klang area

Pharmaceuticals	WWTP 1		WWTP2		WWTP 3	
	Influent	Effluent	Influent	Effluent	Influent	Effluent
Caffeine	8.13	0.18	11.87	0.13	68.84	0.11
Acetaminophen	11.05	0.76	8.83	0.24	5.01	0.18
Carbamazepine	n.d	n.d	n.d	n.d	n.d	n.d
Naproxen	1.3	n.d	n.d	n.d	n.d	n.d
Ibuprofen	n.d	n.d	n.d	n.d	n.d	n.d

CONCLUSIONS

The online SPE-LC method was able to provide rapid analysis for pharmaceuticals in wastewater with good reproducibility and accuracy. In this study, the potential of selected pharmaceuticals (caffeine, acetaminophen, carbamazepine, naproxen and ibuprofen) as chemical marker was evaluated. Caffeine and acetaminophen were detected consistently in all samples. This suggests that these two pharmaceuticals can be good chemical markers for wastewater.

REFERENCES

i. Ismail, L (2014). Pharmaceuticals as potential Chemical Markers in Wastewater MSc Thesis Universiti Teknologi MARA.
ii. Kurissery, S., Kanavillil, N., Verenitch, S., and Mazumder, A (2012). Caffeine as an anthropogenic marker of domestic waste: A study from Lake Simcoe watershed. *Ecological Indicators, 23*, 501-508.
iii. Kosma, C. I., Lambropoulou, D. A. & Albanis, T. A. (2010). Occurrence and removal of PPCPs in municipal and hospital wastewater in Greece. *Journal of Hazardous Material, 179*, 804-807.
iv. Subari, S. N., Osman, R., Saim, N. (2017). Evaluation of Acetaminophen as Chemical Marker for Wastewater Contamination. *Science Letter, 11*(2):11-19.

JUNIOR SCIENCE COMMUNICATION
https://jscfsg.uitm.edu.my/
Volume 2 (2019)
eISSN 2637-0689

Colloquium of Chemistry and Environment 2018
Faculty of Applied Sciences, Universiti Teknologi MARA, Shah Alam.

BETULINIC ACID FROM THE LEAVES OF *Macaranga hosei*

Nadira Nadzir[1]*, Norizan Ahmat [1,2], M. Hamizan M. Isa[1,2]
[1]Faculty of Applied Sciences, Universiti Teknologi MARA, 40450 Shah Alam, Selangor, Malaysia.
[2]Atta-ur-Rahman Institute for Natural Product Discovery, Universiti Teknologi MARA, Cawangan Selangor, Kampus Puncak Alam, 42300 Bandar Puncak Alam, Selangor, Malaysia

*noriz118@uitm.edu.my

Abstract: The genus of *Macaranga* is one of the family of Euphorbiacae which contains about 300 species and widely distributed in Peninsular Thailand, Peninsular Malaysia, Sumatra and borneo. The genus of *Macaranga* is known to produces phenolic compounds, flavonoids and stilbenoids. The leaves of *Macaranga hosei* collected from Lenggong, Perak subected to various chromatographic tecniques including column chromatography (CC), vacuum liquid chromatography (VLC) and thin layer chromatography (TLC) and it was subjected to various spectroscopic methods to identify the chemical constituents in the leaves of *Macaranga hosei*. Phytochemical study on the leave of *M. hosei* lead to isolation of betulinic acid. The compound was elucidated by using spectroscopic methods which are UV, IR, and NMR.

Keywords: *Macaranga hosei, pentacyclic terpene, betulinic acid, NMR*

INTRODUCTION

Natural products, either as pure compounds or as standardized extracts will provide unlimited opportunities for some new drug discoveries because of the unmatched availability of chemical diversity. Asian peoples rely more on traditional medicine for their primary healthcare needs. Plants that were used for traditional medicine contain wide range of substances that can be used to treat wide range of diseases such as chronic diseases as well as infectious diseases. Thousands of phytochemicals from plants that are safe and broadly effective with less adverse effect were found. Natural herbal products provide many beneficial biological activities such as anticancer, antimicrobial, wound healing activity and many more benefits were reported. There are many cases where people claims that natural herbal products contain good benefit. *Macaranga* is the large genus of Old World trees classified in the family Euphorbiaceae and the genus consists over 300 species. It was reported that 27 species of *Macaranga* can be found in Malaysia from the total of 280 species worldwide (Magadula, 2014). *M. hosei* is a large tree that can grow up to 20 to 30 m tall with a bluishgreen appearance.

METHODOLOGY

Extraction and isolation

The leaves of *M. hosei* were collected from reserved forest Lenggong, Perak, Malaysia. The sample was identified and the plant voucher (SK2865/15) was deposited at Universiti Putra Malaysia. The dried powdered leaves of *M. hosei* was macerated in methanol for 24 hours and the extraction process was repeated for 7 days. All the obtained extracts were concentrated under reduced pressure. Then, the crude methanolic extract was fractionated by using vacuum liquid chromatography (VLC) to give seven major fractions (MH1-MH7) by using combination of hexane and ethyl acetate as solvent system. The TLC of the crude and fractions were monitored under UV lamp at 254 nm and cerric sulphate was used as spraying reagent. MH2 (6.4551g) was further fractionated into five subfractions by using VLC with solvent system of hexane and ethyl acetate. MH25 (486.5 mg) was further fractionated by using column chromatography

with the solvent system of hexane and ethyl acetate and yielded 7 subfractions. MH257 was chosen to be further purified and 0.8 mg of MH257-1 (betulinic acid) was isolated by using recrystallization method.

Elucidation and characterization

The isolated compounds were elucidated by using 600 MHz NMR, ATR-FTIR and UV.

Compound **MH257-1**. (betulinic acid) – White amorphous powder (5.7 mg) UV λmax =228 in Acetonitrile. ATR-IR ν_{max}= 3204.71, 2945.24, 1713.22, 1696.35, 1631.62 1468.59. 1H NMR (600 MHz, CDCl3) δ 4.77 (s, 1H, H-29b), 4.63 (s, 1H, H-29a), 3.22 (dd, *J* = 11.5, 4.7 Hz, 1H, H-3), 3.03 (td, *J* = 10.8, 4.9 Hz, 1H, H-19), 1.72 (s, 3H, H-30), 1.002 (s, 3H, H-26), 0.992 (s, 3H, H-27), 0.96 (s, 3H, H-23), 0.85 (s, 3H, H-25), 0.78 (s, 3H, H-24). 13C NMR (151 MHz, CDCl3) δ 178.33 (C28), 150.39 (C20), 109.69 (C29), 79.02 (C3), 56.22 (C17), 55.38 (C5), 50.57 (C9), 49.30 (C19), 46.87 (C18), 42.46 (C14), 40.73 (C8), 38.87 (C4), 38.74 (C1), 38.38 (C13), 37.23 (C22), 37.01 (C10), 34.36 (C7), 32.16 (C16), 30.55 (C15), 29.71 (C21), 27.99 (C23), 27.42 (C2), 25.53 (C12), 20.88 (C11), 19.37 (C30), 18.30 (C6), 16.13 (C24), 16.03 (C25), 15.34 (C26), 14.70 (C27).

FINDINGS

Phytochemical study on the leaves of *Macaranga hosei* has resulted in the isolation of a lupane triterpene namely betulinic acid (**MH257-1**). This compound was isolated from the slightly non-polar fraction of methanolic leaf extract of *M. hosei*. Betulinic acid was conventionally purified by using recrystallization technique.

MH257-1 is a pentacyclic terpene namely betulinic acid which was firstly discovered in outer bark of plant species. The proton spectrum of the compound showed the presents of 5 methyl groups at δH 1.002 (s, 3H, H-26), 0.992 (s, 3H, H-27), 0.96 (s, 3H, H-23), 0.85 (s, 3H, H-25), and 0.78 (s, 3H, H-24). One isopropenyl moiety was also presented as a set of one singlet for the proton at carbon C-30 at δH 1.72 (s, 3H, H-30) together with two signals which represented the vinyl proton at δH 4.77 (brs, 1H, H-29b), 4.63 (brs, 1H, H-29a). The proton spectrum of the compound also showed a proton that is attached to C-3 hydroxy group as a doublet of doublet at δH 3.22 (dd, *J* = 11.5, 4.7 Hz, 1H, H-3) and proton at C-19, exhibited a signal as a triplet of doublet at δH 3.03 (td, *J* = 10.8, 4.9 Hz, 1H, H-19).

The carbon spectrum of the compound showed 30 signals which represented the total carbons in betulinic acid structure. One signal at a very downfield region represents the carboxyl group of C-28. The vinyl carbon signals of C-20 and C-29 were shown at δc 150.39 and 109.69, respectively. At a slight upfield region, one signal for which hydroxyl group was attached can be observed at δc 79.02 (C-3). The other signals were distributed into six methyls, eight methylenes, nine methines and three quaternary carbons.

Betulinic acid is a pentacylic triterpenoid and it is widely distributed in the plant kingdom. It is commonly available in the outer bark of variety tree species. Betulinic acid is a known natural product which has gained a lot of attention from researchers since it exhibits a variety of biological and medicinal properties such as antioxidant (Wu *et al*., 2018), anti-inflammatory (Moghaddam *et al*., 2012) and antitumor and anticancer activities (Chintharlapalli *et al*., 2011).

Colloquium of Chemistry and Environment 2018
Faculty of Applied Sciences, Universiti Teknologi MARA, Shah Alam.

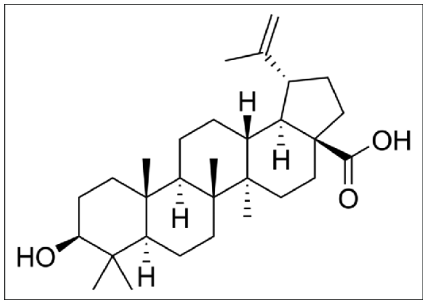

CONCLUSIONS

In conclusion, phytochemical study of *Macaranga hosei* leaves resulted in the isolation of a pentacyclic triterpene namely betulinic acid.

REFERENCES

i. Wu, L., Xiong, W., Hu, J.-W., Li, X.-H., Fu, J.-P., Si, C.-L., & Wang, J. (2018). Chemical Constituents of Xylem of *Sophora japonica* Roots. *Chemistry of Natural Compounds*, *54*(3), 610-612
ii. Magadula, J. J. (2014). Phytochemistry and pharmacology of the genus Macaranga: A review. Journal of Medicinal Plants Research, *8*(12), 489–503
iii. Moghaddam, M.G., Ahmad, F. & Samzadeh-Kermani, A. (2012). Biological Activity of Betulinic Acid: A Review. *Pharmacology & Pharmacy*, *3*(2), 119-123.
iv. Chintharlapalli, S., Papineni, S., Lei, P., Pathi, S. and Safe, S. (2011). Betulinic acid inhibits colon cancer cell and tumor growth and induces proteasomedependent and -independent downregulation of specificity proteins (Sp) transcription factors. *Biomedical Central Cancer*, *371*(11), 1471-2407.

JUNIOR SCIENCE COMMUNICATION
https://jscfsg.uitm.edu.my/
Volume 2 (2019)
eISSN 2637-0689

Colloquium of Chemistry and Environment 2018
Faculty of Applied Sciences, Universiti Teknologi MARA, Shah Alam.

SYNTHESIS, CHARACTERIZATION AND ANTIBACTERIAL ACTIVITY OF THIOUREA LIGANDS DERIVED FROM 4-METHOXYBENZOYL CHLORIDE

Nik Nur Khairunnisa Khalilullah[1], Amalina Mohd Tajuddin[1,2*]
[1]Faculty of Applied Sciences, Universiti Teknologi MARA, 40450 Shah Alam, Selangor, Malaysia
[2]Atta-ur-Rahman Institute for Natural Products Discovery, Universiti Teknologi MARA, Cawangan Selangor, Kampus Puncak Alam, 42300 Bandar Puncak Alam, Selangor, Malaysia.

*amalina9487@uitm.edu.my

Abstract: Three thiourea ligands (T1, T2 and T3) have been successfully synthesized using condensation reactions. The ligands have been characterized using elemental analysis, FTIR, ^{1}H NMR and UV-Vis spectroscopy. The percentage of C, H and N, the observable signals of ^{1}H NMR spectral as well as the electronic transitions in UV-Vis spectrum and also the important peaks of FTIR spectra have been analyzed and discussed. FTIR spectra showed strong peaks at 1149-1175 cm^{-1} indicated the C=S stretching vibrations. Antibacterial activity of ligands was evaluated against two Gram-positive strains, *S. aureus* and *S. haemolyticus* and two Gram-negative strains, *E. coli* and *S. flexneri*. The percentage of cell inhibition of T3 for strains except *E. coli* was higher than T1 and T2.

Keywords: *Thiourea, benzoyl chloride, ligands, antibacterial*

INTRODUCTION

Thiourea is a compound which has general chemical formula of $SC(NH_2)_2$, first synthesized by Neuki in 1873 (Normark & Normark, 2002). It has the active groups of C=S and N-H to react with the C=O and P groups on bacteria surface. They displayed high biological activities such as antimicrobial (Said *et al*., 2015; Zhao, 2013), antioxidant, antitumor (Yeşilkaynak *et al*., 2017) and antituberculosis (Plutín *et al*., 2016). Bacterial resistance increases as the bacteria becoming less affected by the existing of antibacterial agents due to increases of bacterial resistance (Abbas *et al*., 2013; Krajacic *et al*., 2009). New development of antibacterial agents is progressing slower than expected. This study reports the synthesis and characterization of thiourea ligands derived from 4-methoxybenzoyl chloride using physico-chemical and spectral methods and investigation of the effect of ligands on antibacterial activity on Gram-positive and Gram-negative bacteria.

MATERIALS AND METHOD

Chemicals were 4-methoxybenzoyl chloride, sodium thiocyanate and three primary amines, i.e. aniline, *p*-anisidine and 4-chloroaniline. Acetone was used as solvent. The chemicals were analytical grade and purchased from Sigma Aldrich and used without further purification.

Colloquium of Chemistry and Environment 2018
Faculty of Applied Sciences, Universiti Teknologi MARA, Shah Alam.

Synthesis of Ligand

A solution of 4-methoxybenzoyl chloride was added dropwise to a stirring acetone solution of sodium thiocyanate. The solution was stirred for 30 minutes. A solution of aniline in acetone was added to the resulting mixture. Then, the solution was refluxed at 55°C for 2 hours. The solution was kept in chiller overnight. White precipitate was formed, collected by filtration and washed with cold ethanol. The compound was labelled as T1 with 72.4% yield. This method was repeated to synthesize ligands T2 and T3 using different amines which were *p*-anisidine and 4-chloroaniline with 74 and 83% yields, respectively. M.p.

Antibacterial Screening

All ligands were screened using Resazurin microtiter-based assay method against four strains of bacteria i.e. *Staphylococcus aureus* ATCC 25923 (*S. aureus*), *Staphylococcus haemolyticus* ATCC 29970 (*S. haemolyticus*), *Escherichia coli* ATCC 25922 (*E. coli*) and *Shigella flexneri* ATCC 25931 (*S. flexneri*). Several antibiotics such as erythromycin, chloramphenicol, nalidixic acid, tetracylin and streptomycin were used as positive control and dimethyl sulfoxide (DMSO) as negative control. The ligands were dissolved in DMSO solvent at 1 mg/mL and were transferred into 96-well microtiter plate. Each strain bacteria were transferred to microtiter plate and incubated at 37°C for 18-24 hours. After incubation, the plates were analyzed using microplate reader and percentage of cell inhibition were calculated.

FINDINGS

All ligands were successfully synthesized and characterized using elemental analysis, FTIR, ^{1}H NMR and UV-Vis spectroscopy. Figure 1 shows the structure of ligands.

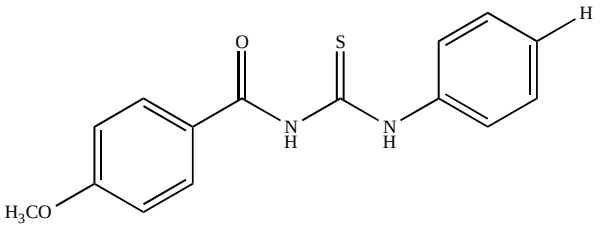

4-methoxy-*N*-(phenylcarbamothioyl)benzamide (T1)

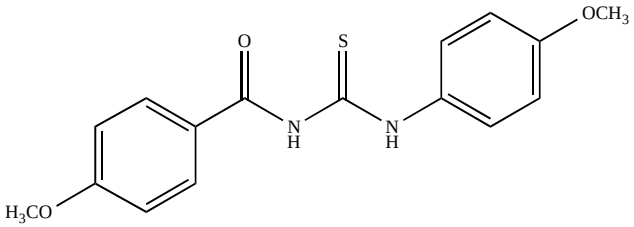

4-methoxy-*N*-((4-methoxyphenyl)carbamothioyl)benzamide (T2)

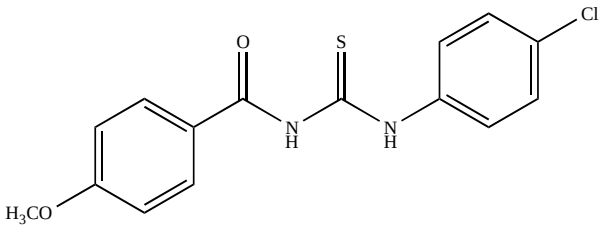

N-((4-chlorophenyl)carbamothioyl)-4-methoxybenzamide (T3)

Figure 1 The structure of thiourea ligands

The theoretical data were compared with experimental data for elemental analysis. Results showed that percentage of C, H and N for T2 and T3 were acceptable due and in a good agreement with calculated values. In the FTIR spectra, the vibrations found at 3296 to 3391 cm^{-1} indicate the N-H groups (Ghazal *et al*., 2018). Presence of peak in the region of 1656 to 1664 cm^{-1} indicate the functional group of C=O while peaks at 1149 to 1175 cm^{-1} are for C=S stretching vibrations (Soni *et al*., 2014). The frequency of C=N group was ascribed to the higher frequency range 1257 to 1241 cm^{-1} that appeared in the spectra. From ^{1}H NMR, the data demonstrate the presence of methoxy group as singlet at 3.70 to 4.00 ppm and the aromatic protons as multiplet at range 7.00 to 8.00 ppm. Singlet peak of amine proton appeared at very downfield between 11.00 to 13.00 ppm (Halim & Ngaini, 2016) because of deshielding of N proton resulted by the electronegative atoms of O and S. Based on UV-Vis spectra, electronic transition of $\pi \rightarrow \pi^*$ of aromatic benzene appeared at range of 205 to 226 nm while 280 to 289 nm were assigned as $n \rightarrow \pi^*$ electronic transition of the C=N and C=S of thiourea (Orysyk *et al*., 2012). For antibacterial, all ligands have very small activities due to the ligands might not have enough ability to penetrates into lipid membranes of cell.

CONCLUSION

Three thiourea ligands derived from 4-methoxybenzoyl chloride were successfully synthesized and characterized using physico-chemical and spectral methods. The results of antibacterial activity were negative for all ligands.

REFERENCES

i. Normark, B. H., & Normark, S. (2002). Evolution and spread of antibiotic resistance. *Journal of Internal Medicine, 252,* 91–106.
ii. Said, M., Ahmad, J., Rehman, W., Badshah, A., Khan, H., Khan, M., Spasyuk, D.M. (2015). Synthesis, structural characterization and antibacterial studies of trisubstituted guanidines and their copper(II) complexes. *Inorganica Chimica Acta, 434,* 7-13.
iii. Zhao, M.-M. (2013). Antibacterial Studies of Copper(I) Complexes with Benzoylthiourea Derivatives. *Asian Journal of Chemistry, 25*(14), 1-3
iv. Yeşilkaynak, T., Muslu, H., Özpınar, C., Emen, F.M., Demirdöğen, R.E., & Külcü, N. (2017). Novel thiourea derivative and its complexes: Synthesis, characterization, DFT computations, thermal and electrochemical behavior, antioxidant and antitumor activities. *Journal of Molecular Structure, 1142,* 185-193.
v. Plutín, A.M., Alvarez, A., Mocelo, R., Ramos, R., Castellano, E.E., da Silva, M.M., Batista, A. (2016). Anti-mycobacterium tuberculosis activity of platinum(II)/*N*,*N*-disubstituted-*N*′-acyl thiourea complexes. *Inorganic Chemistry Communications, 63,* 74-80.
vi. Abbas, S.Y., El-Sharief, M.A., Basyouni, W.M., Fakhr, I.M., & El-Gammal, E.W. (2013). Thiourea derivatives incorporating a hippuric acid moiety: synthesis and evaluation of antibacterial and antifungal activities. *European Journal of Medicinal Chemistry, 64,* 111-120.
vii. Krajacic, M.B., Novak, P., Dumic, M., Cindric, M., Paljetak, H.C., & Kujundzic, N. (2009). Novel ureas and thioureas of 15-membered azalides with antibacterial activity against key respiratory pathogens. *European Journal of Medicinal Chemistry,, 44*(9), 3459-3470.
viii. Ghazal, K., Shoaib, S., Khan, M., Khan, S., Rauf, M. K., Khan, N., Rehman, A.-u. (2018). Synthesis, characterization, X-ray diffraction study, in-vitro cytotoxicity, antibacterial and antifungal activities of nickel(II) and copper(II) complexes with acyl thiourea ligand. *Journal of*

Molecular Structure, 1177, 124-130.

ix. Soni, L. K., Narsinghani, T., & Jain, R. (2014). Synthesis and antibacterial screening of some 1-Aroyl-3-aryl thiourea derivatives. *ISRN Medicinal Chemistry, 2014*, 1-6.

x. Abd Halim, A.N., & Ngaini, Z. (2016). Synthesis and bacteriostatic activities of bis(thiourea) derivatives with variable chain length. *Journal of Chemistry, 2016*, 1-7.

xi. Orysyk, S.I., Bon, V.V., Obolentseva, O.O., Zborovskii, Y.L., Orysyk, V.V., Pekhnyo, V.I., Vovk, V. M. (2012). Synthesis, structural and spectral characterization of Zn(II) complexes, derived from thiourea and thiosemicarbazide. *Inorganica Chimica Acta, 382*, 127-138.

JUNIOR SCIENCE COMMUNICATION
https://jscfsg.uitm.edu.my/
Volume 2 (2019)
eISSN 2637-0689

Colloquium of Chemistry and Environment 2018
Faculty of Applied Sciences, Universiti Teknologi MARA, Shah Alam.

CHARACTERIZATION OF BACTERIAL CELLULOSE PREPARED FROM *Medusomyces gisevii*

Noor Fazlin, Maryam Husin*
Faculty of Applied Sciences, Universiti Teknologi MARA, 40450 Shah Alam, Selangor, Malaysia.

*marya911@uitm.edu.my

Abstract: Bacterial cellulose (BC) from *Medusomyces gisevii* (scoby fiber) has been isolated and characterized in this project using FTIR, FESEM, TGA, and XRD. The BC was treated with three different treatments which were single-step sodium hydroxide (6% NaOH), single-step hydrogen peroxide (6% H_2O_2) and the two-step (6% NaOH and 6% H_2O_2) at 80℃-100℃ for 2 h. The effect of treatments on the percentage yield, colour changes, morphology, crystallinity, and thermal stability of BC were determined. FTIR results showed that the different chemical treatments did not induce chemical changes. A network like structure was observed in FESEM analysis. Based on characterization, single-step treatment gave the best result in terms of crystallinity, thermal stability and percentage yield. While two-step treatment gave the optimum result in term of physical appearance (white colour) although it gave lower percentage yield, crystallinity and thermal stability.

Keywords: *Bacterial cellulose, Acetobacter xylinus, alkali treatment, bleaching treatment*

INTRODUCTION

Medusomyces gisevii is well known as tea mushroom, Manchurian mushroom, and scoby fiber. Scoby fiber is a fermented beverage made by fermenting sugared black or green tea drinks using a symbiotic culture of bacteria and yeasts (SCOBY) as drinking water that give beneficial health effects. According to Gabr *et al*. (2010), BC is of extremely high purity and exhibits a higher degree of polymerization and crystallinity (60%-70%) than the cellulose obtained from the plant sources where they are embedded with lignin, hemicelluloses, and other impurities. Lignin and hemicellulose that make up the cell wall components of plants is hard to evacuate during purification process. Bacterial cellulose could be processed further to improve the percentage yield, colour changes, morphology, crystallinity, and thermal stability without any toxic chemicals being released to the environment.

METHODOLOGY

The scoby fiber obtained was washed and cut into small pieces and dried in the oven at 100℃ for 1 day. The scoby fiber was characterised to obtained the percent yield of BC by treating the scoby fiber (5 g) with 200 ml of NaOH (17% w/v) and left for 30 min. After 30 min, 100 ml of distilled water was added followed by stirring for 1 min and left for 29 min. Later, it was filtered and washed with distilled water until all NaOH solution is removed. Subsequently, it was mixed with 1 M CH_3COOH for 5 min followed by filtration and washing with distilled water. The content of cellulose was determined. Next, the raw scoby fiber was characterised to study the effect of treatment by treating 10 g of scoby fiber with three different treatments which were single-step 6% NaOH, single-step 6% H_2O_2 and two-step treatment (6% NaOH and

6% H_2O_2) in a water bath set at 80℃-100℃ for 2 h. After the reactions were completed, the treated scoby fiber was washed with enough distilled water until normal pH was obtained. All the reactions were repeated for three times and the final product was dried in an oven at 100℃ for 6 h. The dried treated scoby and untreated scoby fiber was subjected to characterization using FTIR, FESEM, XRD, and TGA.

FINDINGS

The amount of cellulose obtained from scoby fiber at 95% confidence interval are summarised in Table 1.

Table 1 The amount of bacterial cellulose (BC) from scoby fiber

Compound	Percent yield (%)
Raw scoby fiber	88.63 ± 0.06
Single-step Treated (6% NaOH)	75.46±0.05
Single-step Treated (6% H_2O_2)	75.10±0.01
Two-step Treated	59.72±0.04

The colour changes upon treatment were also observed. Initially, the colour of dried scoby fiber was dark brown and upon single-step treatments, it changed to yellowish colour product. While two-step treatment gives a pure white colour product. Based on FTIR analysis, the extracted cellulose has similar peaks indicating that the structure was not influenced by different chemical treatment applied. All samples showed significant peaks of cellulose functional groups at approximately 3400 cm^{-1}, 2900 cm^{-1}, 1430 cm^{-1}, 1370 cm^{-1}, 890 cm^{-1}. Based on diffraction curves, the bacterial cellulose from scoby fiber exhibited semi crystalline structures. Both single-treatments gave almost similar crystallinity and a slight increase in crystallinity was noted with two-step treatment. Table 2 summarizes the crystallinity index of cellulose.

Table 2 The degree of crystallinity of bacterial cellulose

Sample	Crystallinity index (CI), %
Untreated sample	77.95%
Single-step treated BC (6% H_2O_2)	85.88%
Single-step treated BC (6% NaOH)	85.75 %
Two-step treated BC	86.82%

TGA analysis revealed that the two-step treated bacterial cellulose illustrated different thermal degradation pattern ranging from 250℃-350℃. The first degradation occurred at 311.6℃, while the second stage occurred at 351.1℃. According to Husin *et al*. (2017) and Yang *et al.* (2007), this is due to the degradation of cellulose. However, for treated samples, the single-step treatment of 6% NaOH and 6% H_2O_2 showed similar degradation profile of degradation cellulose at 339.7℃ and 334.8℃ respectively.

Volume 2 (2019)
eISSN 2637-0689

CONCLUSIONS

In this study, the amount of bacterial cellulose from scoby fiber was 88.63 ± 0.06 %. Among the three treatments conducted, the single step treatments gave the best results in all terms of characterization. According to FTIR spectra, all samples exhibit significant peaks of cellulose functional groups. Comparing the treatments applied, single-step treatments were chosen as the most reliable method to purify the BC from scoby fiber due to good crystallinity, thermal stability and high yield of BC after treatment.

REFERENCES

i. Gabr, M. H., Elrahman, M. A., Okubo, K., & Fujii, T. (2010). A study on mechanical properties of bacterial cellulose/epoxy reinforced by plain woven carbon fiber modified with liquid rubber. *Composites Part A: Applied Science and Manufacturing*, *41*(9), 1263-1271.

ii. Husin, M., Li, A. R., Ramli, N., Romli, A. Z., Hakimi, M. I., & Ilham, Z. (2017). Preparation and characterization of cellulose and microcrystalline cellulose isolated from waste *Leucaena leucocephala* seeds. *International Journal of Advanced and Applied Sciences*, *4*(3), 51–58.

iii. Yang, H., Yan, R., Chen, H., Lee, D. H., & Zheng, C. (2007). Characteristics of hemicellulose, cellulose and lignin pyrolysis. *Fuel*, *86*(12–13), 1781–1788.

JUNIOR SCIENCE COMMUNICATION
https://jscfsg.uitm.edu.my/
Volume 2 (2019)
eISSN 2637-0689

Colloquium of Chemistry and Environment 2018
Faculty of Applied Sciences, Universiti Teknologi MARA, Shah Alam.

EFFECT OF TEMPERATURE AND TIME ON BIODIESEL YIELD USING CaO DERIVED FROM CHICKEN EGG SHELL AS HETEROGENOUS CATALYST

Noor Hasinah Hamizi, Noraini Hamzah*
Faculty of Applied Sciences, Universiti Teknologi MARA, 40450 Shah Alam, Selangor, Malaysia.

*pnoraini@uitm.edu.my

Abstract: The decrement in the fossil fuels reserves triggers the need to look for the alternative source of energy. One of the renewable sources of energy that could be considered to substitute traditional fossil fuels is biodiesel. In this study, biodiesel was synthesized from waste cooking oil (WCO) through transesterification with egg shell derived CaO as a catalyst. The chicken egg shells were washed, dried and ground. The process proceeded with calcination in a furnace at a temperature of 900°C for 3 hours. The egg shell was completely converted into CaO catalyst, proven by the characterisation with XRD. BET analysis revealed that the catalyst is mesoporous with surface area of 1.1152 m^2/g. SEM images showed that the morphology of the catalyst is more regular and the size of particles become smaller after calcination. WCO analysis indicated the percentage of free fatty acid (FFA) was 0.4% before undergoing transesterification. GC-FID chromatogram showed that biodiesel synthesized from transesterification of waste cooking oil is composed of methyl laurate ($C_{13}H_{26}O_2$), methyl myristate ($C_{15}H_{30}O_2$), methyl palmitate ($C_{17}H_{34}O_2$), methyl stearate ($C_{19}H_{38}O_2$) and methyl linoleate ($C_{19}H_{34}O_2$). The optimum temperature and reaction time were 65℃ and 5 hours, respectively, with the biodiesel yield between 76% and 89%. This study revealed that CaO derived from chicken egg shell has good catalytic activity in transesterification of waste cooking oil into fatty acid methyl ester (FAME).

Keywords: *Waste cooking oil, chicken egg shell, transesterification, and biodiesel*

INTRODUCTION

The fossil fuel consumption is rising in the world because of industrialization and rise in population. The decrement in the fossil fuels reserves has triggered the need to look for the alternative source of energy. One of the renewable sources of energy that could be considered to substitute traditional fossil fuels is biodiesel. Mansir *et al*. (2018) stated that manufacturing of biodiesel at commercial scale remains the prime barrier nowadays because it is expensive compared to the fossil fuels. Its high cost of production is assigned to the cost of raw materials and labour; hence the fundamental policy of biodiesel is not yet accomplished (Adepoju *et al*., 2014). Besides, the non-availability of raw materials and productive catalytic system are the leading problems of commercialization of biodiesel to fulfil the global demand. In order to solve the problems, the synthesis of biodiesel from transesterification of waste cooking oil in the presence of monohydric alcohol and CaO derived from egg shells as catalyst is being studied.

METHODOLOGY

First, the chicken egg shells collected from a local area in Shah Alam, Selangor were washed, dried and ground. The egg shells were then calcined in a furnace at a temperature of 900°C for 3 hours. The catalyst derived from the egg shells was characterized with XRD, BET and SEM. The waste cooking oil also collected from a local area in Shah Alam was treated by filtering, heating and titrating with KOH in order to calculate the percentage of FFA which was 0.4%. The transesterification reaction was performed in a

Colloquium of Chemistry and Environment 2018
Faculty of Applied Sciences, Universiti Teknologi MARA, Shah Alam.

250ml of three-neck round-bottom flask fitted with a water-cooled condenser and thermometer. The catalyst was first activated by dispersing it in methanol at 50°C with constant stirring for 5 minutes. About 15.0 g of pre-treated oil with methanol to oil ratio (15:1) was then added into the reactor and the reaction was carried out using 2 wt % of catalyst loading at 50°C for 2 hours. The mixture was refluxed with stirring at 400 rpm. After the reaction, the product was transferred into a separatory funnel and left overnight to obtain two distinct phases. The lower layer which is glycerol was discarded, while the upper layer that is biodiesel was purified by using boiled water three times. The biodiesel yield was weighed and the percentage yield was calculated. The transesterification reactions were repeated at 50^0C, 55°C, 60°C, 65°C and 70°C. Transesterification reaction times of 2, 3, 4, 5 and 6 hours were also investigated. The obtained products were analysed with GC-FID.

FINDINGS

The results obtained for the effect of temperature on biodiesel yield is shown in Figure 1. Figure 1 indicates the biodiesel yield increases as the reaction temperature increases and the optimum temperature was 65℃ in which the biodiesel yield was the highest at 76.29%. However, the biodiesel yield began to reduce upon further increase in the temperature beyond 65℃. Usually at high temperatures the methanol vaporizes and forms bubbles which might inhibit the reaction on the interface.

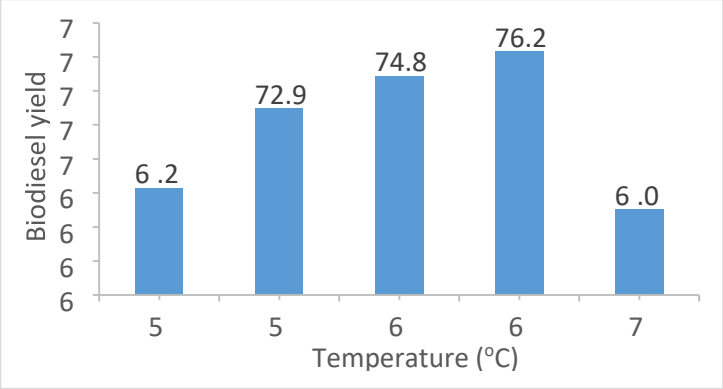

Figure 1 Effect of temperature on biodiesel yield

Figure 2 shows the effect of reaction time on biodiesel yield. Based on the Figure 1, the biodiesel yield increases as the reaction time increases. The longer the reaction time, the oil could react more with methanol. The optimum reaction time was 5 hours with biodiesel yield of 88.50% as the biodiesel yield beyond the time became almost constant. Transesterification reaction is a reversible reaction; therefore, the biodiesel yield remains constant because the reverse reaction and forward reaction have achieved equilibrium.

Colloquium of Chemistry and Environment 2018
Faculty of Applied Sciences, Universiti Teknologi MARA, Shah Alam.

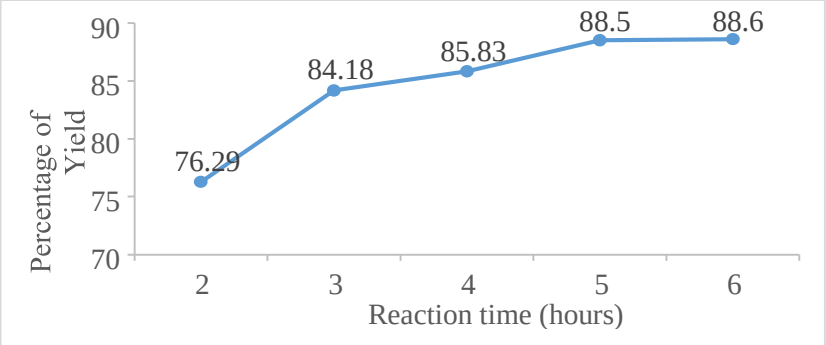

Figure 2 Effect of reaction time on biodiesel yield

CONCLUSION

CaO catalyst was successfully synthesized from chicken egg shells for biodiesel production. After calcination of the egg shells at 900℃, $CaCO_3$ in the egg shells was converted into CaO and it was confirmed by XRD analysis. BET analysis revealed that this catalyst is mesoporous with surface area and pore diameter of 1.1152 m^2/g and 48.2nm. Images of SEM analysis show that the morphology of the chicken egg shells after calcination were more regular and the size of particles were smaller than the egg shells before calcination. The obtained CaO catalyst exhibited high activity towards the transesterification of waste cooking oil with methanol to produce biodiesel. At optimum conditions of 65℃ and 5 hours, biodiesel yield was about 76% and 89%, respectively, and were obtained by maintaining the oil to methanol molar ratio at 1:15 and 2.0 wt% of catalyst loading. GC-FID analysis confirmed that the biodiesel produced from transesterification reaction consists of methyl laurate, methyl myristate, methyl palmitate, methyl stearate and methyl linoleate when compared to the chromatogram of FAME standard.

REFERENCES

i. Adepoju, T. F. & Olawale, O. (2014). Acid-Catalyzed Esterification of Waste Cooking Oil with High FFA for Biodiesel Production. *Chemical and Process Engineering Research*, *21*, 80–86.
ii. Mansir, N., Teo, S. H., Rashid, U., Saiman, M. I., Tan, Y. P., Alsultan, G. A., & Taufiq-Yap, Y. H. (2018). Modified waste egg shell derived bifunctional catalyst for biodiesel production from high FFA waste cooking oil. A review. *Renewable and Sustainable Energy Reviews*, *82*, 3645–3655.

JUNIOR SCIENCE COMMUNICATION
https://jscfsg.uitm.edu.my/
Volume 2 (2019)
eISSN 2637-0689

Colloquium of Chemistry and Environment 2018
Faculty of Applied Sciences, Universiti Teknologi MARA, Shah Alam.

ANALYSIS OF SOIL PROPERTIES FOR GINGER AGRICULTURE

Noor Ul- Hana Saifuddin, Zainiharyati Mohd Zain*
Faculty of Applied Sciences, Universiti Teknologi MARA, 40450 Shah Alam, Selangor, Malaysia.

*zainihar@uitm.edu.my

Abstract: Ginger production in Malaysia is low which limit the export capacity due to lack of suitable soil for ginger cultivation. In this study, two types of soil from Bukit Tinggi, Bentong, Pahang and Sekinchan, Selangor were analysed in determine certain important properties of soil such as pH, moisture, carbon, nitrogen and nutrients such as Zn, Mg and Fe. The carbon content was determined using Walkley-Black method which undergoes oxidation with a known excess of potassium dichromate solution in concentrated sulfuric acid. Then, Kjedahl instrument is also used in this study to determine the percentage of nitrogen content in the soil. In addition, Flame Atomic Absorption Spectroscopy was used in to determine the concentration of nutrients in the soil. All the determined soil parameters from Bukit Tinggi, Bentong, Pahang show properties suitable for ginger cultivation.

Keywords: *Ginger, soil properties*

INTRODUCTION

Zingiber officinale Roscoe or normally known as ginger is a member of Zingiberaceae family. In Asia, India, Europe, and the Middle East, ginger is normally used in treating arthritis, stomach upset, asthma, diabetes, and menstrual irregularities (Singletary, 2010). Salahin *et al.* (2013) stated that ginger plants are usually cultivated in the highland and other hilly areas with sandy soil. The ginger plant needs about 16 nutrients for perfect growth. These nutrients can be divided into two types which are macro elements such as nitrogen, magnesium and micro elements such as iron and zinc (Mohd & Manas, 2012). There are many factors that will affect the growth of ginger plant especially the soil properties like type of soil, organic content in the soil, carbon content, humidity and pH. Mineral nutrients in the soil is very important to improve the production of plant and it also can be used as tools to produce the quality of herbal medicines (Singh *et al.*, 2014). Hence, in this study the two types of soil used in ginger cultivation which were silt soil from Bukit Tinggi, Bentong, Pahang and peat soil from Sekinchan, Selangor. The soils were analysed to determine the certain properties and organic nutrient content such as pH, moisture, carbon, nitrogen and organic nutrients (Zn, Mg, Fe). From this study, information on the nutrient content in the soil for proper ginger cultivation can serve as a guideline to farmers on how to prepare the soil suitable for ginger cultivation.

METHODOLOGY

pH Analysis

About 10 g of soil was put in a beaker and 25ml of distilled water was added. Then, the mixture was shaken for 30 minutes using electronic shaker. Next, the pH meter was calibrated with pH 4 and pH 7 of buffer solution prior to pH reading of the soils was recorded.

Moisture Analysis

An empty silica crucible was weighted and then 10 grams of soil sample was placed in it. The crucible was dried in oven at 105 ºC to 110 ºC for 24 hours. Then, the crucible was cooled in the desiccator before being weighed again to determine percent of moisture.

Colloquium of Chemistry and Environment 2018
Faculty of Applied Sciences, Universiti Teknologi MARA, Shah Alam.

Walkley- Black Method
The carbon present as an organic material in the sample was estimated by oxidizing it with a known excess of $K_2Cr_2O_7$ solution in concentrated H_2SO_4. Diphenylamine was used as indicator to titrate the unutilized dichromate with ferrous ammonium sulphate (FAS).

Organic matter
The samples were digested in a microwave digester. Then, the samples were filtered using filter funnel and diluted in a 100 ml volumetric flask. After that, the standard solution of zinc, iron and magnesium was prepared. Sample and standard solutions were analysed using Flame Atomic Absorption Spectroscopy (FAAS).

Kjedahl Method
About 0.5 g of samples were put in the test tube and 30ml of H_2SO_4 were added with two pellets of Kjedahl catalyst for the digestion process. This process took 5-6 hours in order to ensure all the samples were completely digested. Then, it was left overnight before distillation and titration processes. The ammonia is determined by back titration with NaOH solution of a known concentration. The results can be expressed in % N, % NH_3 or protein (%N x factor).

FINDINGS
Based on result, pH of sample B soil (Bukit Tinggi) was 5.71 which is in optimum range for used in a ginger cultivation while pH of soil sample A (Sekinchan) was 5.20. High moisture content indicates that the size of particles in the soil is small so it has large surface area and can hold more water. Ginger growth is not suitable in overly saturated or waterlogged soil because it is grown beneath the soil. Sample A has high carbon content of 95.7% while sample B had 22.5%. Darker coloured soils tend to have higher carbon content compared to other soils. Sample B had 0.0553% nitrogen content while sample A had 0.0290% nitrogen content. High nitrogen content is important in ginger growth to produce high quality ginger. High percentage of carbon in the soil will increase the organic matter in the soil. However, the amount of organic nutrients must in the optimum range so the ginger can grow perfectly. Results from soil analysis are summarised in Table 1:

Table 1 Summary of Sample A and Sample B soil parameters

Soil properties	**Sample A (Sekinchan, Selangor)**	**Sample B (Bukit Tinggi, Pahang)**
pH	5.20	5.71
Moisture (%)	40.6	18.3
Carbon (%)	95.7	22.5
Nitrogen (%)	0.0290	0.0553
Mg (ppm)	9.33	3.33
Zn (ppm)	10.40	7.33
Fe (ppm)	50.9	209

Colloquium of Chemistry and Environment 2018
Faculty of Applied Sciences, Universiti Teknologi MARA, Shah Alam.

CONCLUSION

The properties of soil such as pH, moisture, carbon, nitrogen and certain nutrients in two types of soil used in ginger cultivation were determined. From this study, silt soil (Sample B) is more suitable for ginger growth because the structure of silt soil is not compact as compared to peat soil. So, the root plant like ginger can easily grow beneath the soil and this makes it very suitable for ginger cultivation.

REFERENCES

i. Mohd, Y. S., & Manas, M. A. (2012). Commercial ginger production using fertigation system, *1*, 97–105.
ii. Salahin, N., Begum, R. A., Hossain, S., Ullah, M. M., & Alam, M. K. (2013). Degradation of Soil Properties Under Ginger, Turmeric, Aroid, And Jhum Rice Cultivation in Hilly Areas of Bangladesh, (July).
iii. Singletary, K. (2010). Ginger Review. *Food Science*, *45*(4), 171–183.
iv. Singh, A.K. (2015). Efficacy of fungicides for the control of leaf spot disease of ginger under the field conditions of Chhattisgarh (India). *African J. of Agricultural Research, 10* (11), 1301-1305

JUNIOR SCIENCE COMMUNICATION
https://jscfsg.uitm.edu.my/
Volume 2 (2019)
eISSN 2637-0689

Colloquium of Chemistry and Environment 2018
Faculty of Applied Sciences, Universiti Teknologi MARA, Shah Alam.

EXTRACTIVE-OXIDATIVE DESULFURIZATION FOR REMOVAL OF DIBENZOTHIOPHENE IN MODEL FUEL USING MOLYBDATE SUPPORTED ON ACTIVATED CARBON CATALYST

Nor Atikah Pauzi[1]. Mohd Lokman Ibrahim[1, 2, *], Mohd Sufri Mastuli [1, 2], Sabiha Hanim Saleh[1]
[1]Faculty of Applied Sciences, Universiti Teknologi MARA, 40450 Shah Alam, Selangor, Malaysia.
[2]Centre for Nanomaterials Research, Institute of Science, Universiti Teknologi MARA, 40450 Shah Alam Selangor, Malaysia.

*mohd_lokman@uitm.edu.my

Abstract: Sulphur is one of the major pollutants that brings harm to human and can be removed by extractive and oxidative desulfurization which enhanced by addition of catalyst such as molybdenum (Mo). The Mo supported on the activated carbon rubber seed shell (Ac-RSS) with different metal loading were prepared and their surface morphology and characteristics were characterized by using FESEM, BET (nitrogen adsorption and desorption technique), and XRF. The desulfurization process was conducted by using model fuel that contain DBT and oxidize by using H_2O_2. The effects of catalyst and addition of H_2O_2 on the desulfurization process were investigated and analysed by using GC-FID.

Keywords: *Extractive desulfurization, Oxidative desulfurization, activated carbon, molybdenum, dibenzothiophene*

INTRODUCTION

Hydrodesulfurization was not preferable method for sulphur removal as it requires high temperature and unable to remove complex and bulky dibenzothiophene (DBT) (Liu *et al*., 2019). Common alternative method such as oxidative desulfurization (ODS) can be used as it effective to remove sulphur in mild condition (Kang *et al.*, 2018). ODS process can be enhanced by the presence of metal oxide catalyst such as Mo where it has active phase of d-block elements that able to remove out organic compound (Sikarwar *et al*., 2018). Activated carbon is an amorphous solid with large surface area and high porosity (Saleh & Danmaliki, 2016). Combination of Mo with activated carbon can increase efficiency of sulphur adsorption via polar group interaction (Saleh *et al*., 2017).

METHODOLOGY

Rubber seed shell (RSS) was treated with 2% KOH before calcined at 500°C to produce activated carbon which was then different amount of Mo (5% and 15%) impregnated onto it. The surface morphology was characterized by FESEM, while the surface area, pore size and pore diameter were characterized using the N_2 sorption analysis of BET. Meanwhile, the presence of Mo on the surface of the Ac-RSS was confirmed by using the XRF elemental analysis. Furthermore, the desulfurization analysis was done by addition of the prepared catalyst into 500ppm of DBT in iso-octane as a model fuel together with H_2O_2 and methanol. The mixture was then stirred and heated at 60°C for 2 hours. The desulfurization product was characterized by using GC-FID.

FINDINGS

Colloquium of Chemistry and Environment 2018
Faculty of Applied Sciences, Universiti Teknologi MARA, Shah Alam.

The surface morphology and active species distribution of the catalyst are important in order to determine the activity of catalyst. From raw RSS to 15% metal loading, the pores formation was increased, showing that the pores of Ac-RSS became wider after been treated with KOH solution and metal loading as shown in FESEM images in Figure 1 and BET analyses in Table 1. The increasing number of pore formation had led to increasing surface area and volume of pore. Table 1 also shows the presence of Mo analyzed by the XRF elemental analysis hence confirming the impregnation of the Mo metal on the Ac-RSS.

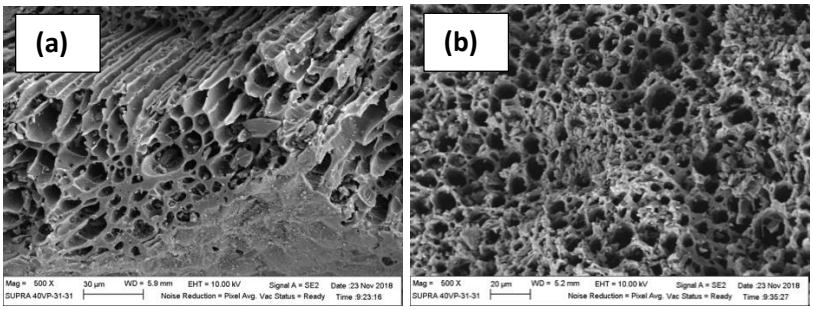

Figure 1 Images of **(a)** Ac-RSS 5% and **(c)** Ac-RSS 15% at 500 x magnifications.

Table 1 Summary of surface area, total pore volume, pore diameter and the Mo content of the catalysts.

Catalyst	**BET surface area (m^2/g)**	**Total pore volume (cm^3/g)**	**Pore diameter (nm)**	**Mo content (wt. %)**
Treated RSS	0.30	0.002	27.75	-
Ac-RSS 5%	5.27	0.003	2.51	0.14
Ac-RSS **15**%	7.52	0.004	2.29	0.51

For desulfurization process, the efficiency of sulphur removal increased as increased number of metal loading onto Ac-RSS as shown in Figure 2. It was revealed that the overall sulphur removal by oxidative desulfurization (ODS) was lower than extractive desulfurization (EDS) techniques. The result obtained might be affected by the amount of H_2O_2 that added during ODS which also affected the dispersive capacity of catalyst in oil. The amount of H_2O_2 which was oxidant in this process must be higher than saturated adsorption capacity of catalyst that causing only lower efficiency for desulfurization due to poor mass transfer between catalyst, oxidant and the reactant.

Volume 2 (2019)
eISSN 2637-0689

Colloquium of Chemistry and Environment 2018
Faculty of Applied Sciences, Universiti Teknologi MARA, Shah Alam.

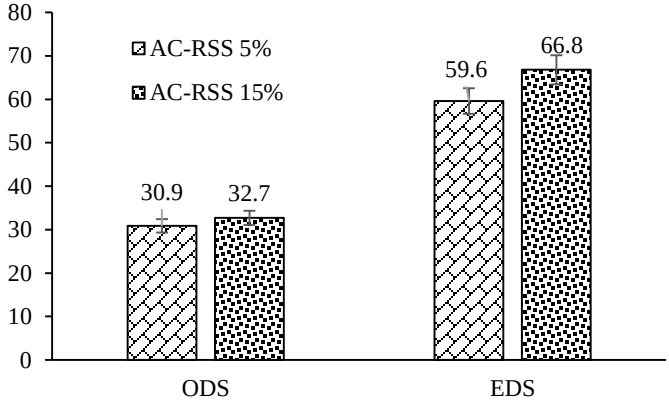

Figure 2 Effect of catalyst on EDS and ODS

CONCLUSIONS

This work has showed the preparation of Mo supported on the Ac-RSS in order to enhance the sulfur removal process from model fuel. Different type catalysts had been prepared that consist different of metal loading of 5% and 15%. These heterogeneous activated carbon catalysts were characterized by using FESEM, BET and XRF. It was found that the surface area of RSS was increased after the chemical treatment by KOH and the impregnation of Mo metal. In order to analyze the efficiency of the catalyst, two (2) types of desulfurization methods were carried out; which are ODS and EDS methods. Chromatographic analysis showed that sulfur removal by ODS was lower than EDS. The maximum sulfur removal was achieved over 66.8 % by EDS.

REFERENCES

i. Kang, L., Liu, H., He, H., & Yang, C. (2018). Oxidative desulfurization of dibenzothiophene using molybdenum catalyst supported on Ti-pillared montmorillonite and separation of sulfones by filtration. *Fuel*, *234*, 1229–1237.

ii. Liu, Y., Leus, K., Sun, Z., Li, X., Depauw, H., Wang, A., Voort, P. Van Der. (2019). Catalytic oxidative desulfurization of model and real diesel over a molybdenum anchored metal-organic framework. *Microporous and Mesoporous Materials*, *277*, 245–252.

iii. Saleh, T. A., Al-hammadi, S. A., Tanimu, A., & Alhooshani, K. (2017). Ultra-deep adsorptive desulfurization of fuels on cobalt and molybdenum nanoparticles loaded on activated carbon derived from waste rubber. *Journal of Colloid And Interface Science*, *513*, 779– 787.

iv. Saleh, T. A., & Danmaliki, G. I. (2016). Adsorptive desulfurization of dibenzothiophene from fuels by rubber tyres-derived carbons: Kinetics and isotherms evaluation. *Process Safety and Environmental Protection*, *15*4, 401–412.

v. Sikarwar, P., Kumar, U. K. A., Gosu, V., & Subbaramaiah, V. (2018). Catalytic Oxidative Desulfurization of DBT Using Green Catalyst (Mo/MCM- 41) Derived from Coal Fly Ash. *Biochemical Pharmacology*, *6*, 1736-1744.

JUNIOR SCIENCE COMMUNICATION
https://jscfsg.uitm.edu.my/
Volume 2 (2019)
eISSN 2637-0689

Colloquium of Chemistry and Environment 2018
Faculty of Applied Sciences, Universiti Teknologi MARA, Shah Alam.

CHEMICAL CONSTITUENTS FROM THE DICHLOROMETHANE CRUDE EXTRACT OF *Goniothalamus lanceolatus* (ROOT)

Nor Salwani Che Muda, Nur Vicky Bihud*
School of Chemistry and Environment, Faculty of Applied Sciences, Universiti Teknologi MARA, 40450 Shah Alam, Selangor

*vicky@uitm.edu.my

Abstract: The root of *Goniothalamus lanceolatus* belonging to the family of Annonaceae was investigated for its chemical constituents. The study focused on the fraction of dichloromethane extract (root) of *G. lanceolatus*. The isolation and purification of chemical constituents were done using preparative recycling HPLC while structure elucidation using modern spectroscopic techniques such as NMR, HR-TOF-MS, and IR spectrometry. From the study, three compounds were isolated and identified as goniodiol, 8-chlorogoniodiol and 9-deoxygoniopypyrone.

Keywords: *Goniothalamus lanceolatus, goniodiol, 9-deoxygoniopypyrone, 8-chlorogoniodiol*

INTRODUCTION

Goniothalamus lanceolatus is an endemic plant used by native of Sarawak to cure cancer and fever (Iqbal *et al*., 2018). This study focused on isolating chemical constituents from the root of this plant. To date, not much phytochemical study has been done on this plant. The only published work on *G. lanceolatus* was reported by Rasol *et al*. (2018) which described some alkaloid constituents from the root. Previous studies on the genus *Goniothalamus* reported two type of compounds which contributed to their cytotoxic properties, known as acetogenins and styryl-lactone. Therefore, this study may lead to isolation of compounds which are biologically active and can be used as drug template in the future. The identification of chemical constituents can provide scientific information to support its medicinal usage.

METHODOLOGY

Modern chromatographic technique was utilized to obtain pure compounds. Recycling HPLC was used over ODS column, in an isocratic solvent system of methanol:water to separate the compounds. The 1D and 2D NMR were used to elucidate and characterize the compound's structure. The structures were further confirmed using the IR and HR-TOF-MS.

FINDINGS

Fourier Transform Infarared Analysis

The results revealed the presence of strong absorption peaks of hydroxyl group at 3480 cm^{-1} and carbonyl group at 1689 cm^{-1} for Compound 1. For Compound 2, the result showed strong absorption peak of hydroxyl group at 3445 cm^{-1} and carbonyl group at 1724 cm^{-1}. Compound 3 also showed the presence of a hydroxyl group at 3449 cm^{-1} and carbonyl group at 1719 cm^{-1}.

Mass Spectrum

The molecular formula of Compound 1 was determined as $C_{13}H_{14}O_4$ based on HR-TOF-MS (*m/z* 235.0907 $[M+H]^+$).

The molecular formula of Compound 2 was determined as $C_{13}H_{13}ClO_3$ based on HR-TOF-MS (m/z 253.0733 $[M+H]^+$). The molecular formula of Compound 3 was determined as $C_{13}H_{14}O_4$ based on HR-TOF-MS (m/z 235.0968 $[M+H]^+$).

^{1}H and ^{13}C NMR spectra

The ^{1}H-NMR spectrum of Compound 1 showed five aromatic proton signals between δ 7.34-7.44, which indicated the presence of a mono-substituted phenyl moiety. Two olefinic protons resonated at δ 6.02 and δ 6.93 typical of α,β-unsaturated δ-lactone ring and were assigned as H-3 and H-4, respectively. Three oxygenated methine protons at δ 4.84, δ 3.74 and δ 4.97 were attributable to H-6, H-7 and H-8, and a pair of methylene geminal protons at δ 2.22 and δ 2.84, belonged to H-5a and H-5b, were observed. The ^{13}C-NMR spectrum revealed the presence of a downfield signal resonated at δ 163.7, a characteristic signal of carbonyl at C-2, belonging to α,ß-unsaturated δ-lactone carbonyl group (Lan *et al*., 2005). Six aromatic carbons of phenyl ring [δ 126.6 (C-10, C-14), δ 128.7 (C-11, C-13), δ 128.3 (C-12) and δ 140.8 (C-9)], two olefinic carbons [δ 120.6 (C-3) and δ 146.2 (C-4)], three oxygenated methine carbons [δ 76.8 (C-6), δ 75.0 (C-7) and δ 73.7 (C-8)], and a methylene carbon at δ 26.0 (C-5) were observed.

The ^{1}H-NMR spectrum of Compound 2 showed five aromatic proton signals between δ 7.39-7.48, which indicated the presence of a mono-substituted phenyl moiety. Two olefinic protons resonated at δ 6.11 and δ 7.04 typical of α,β-unsaturated δ-lactone ring and were assigned as H-3 and H-4, respectively. Three oxygenated methine protons at δ 5.21, δ 5.19 and δ 4.00 were attributable to H-6, H-7 and H-8, and a pair of methylene geminal protons at δ 2.38 and δ 2.95, belonged to H-5a and H-5b, were observed. The ^{13}C-NMR spectrum revealed the presence of a downfield signal resonated at δ 163.5, a characteristic signal of carbonyl at C-2, belonging to α,ß-unsaturated δ-lactone carbonyl group (Lan *et al*., 2005). Six aromatic carbons of phenyl ring [δ 128.1 (C-10, C-14), δ 129.0 (C-11, C-13), δ 129.1 (C-12) and δ 140.8 (C-9)], two olefinic carbons [δ 120.9 (C-3) and δ 138.0 (C-4)], three oxygenated methine carbons [δ 75.6 (C-6), δ 75.4 (C-7) and δ 60.0 (C-8)], and a methylene carbon at δ 26.2 (C-5) were observed.

The ^{1}H-NMR spectrum of Compound 3 showed four one-proton signals at δ 3.98, δ 4.56, δ 4.98 and δ 4.90, belonged to oxygen bearing methine protons of H-8, H-5, H-7 and H-1, and another four one-proton signals were observed in the upfield region at δ 1.86, δ 2.64, δ 2.88 and δ 2.99, assignable to two pairs of methylene protons, H-9 and H-4, respectively. A multiplet at δ 7.35-7.45 were attributable to five aromatic protons (H-11 to H-15) from a *mono*-substituted phenyl moiety. The ^{13}C-NMR spectrum showed signals of thirteen carbons. The presence of mono-substituted phenyl ring was confirmed from the signals at δ 136.7 (C-10), δ 126.1 (C-11, C-15), δ 128.3 (C-13) and δ 128.9 (C-12, C-14). Two methylene carbon signals were observed at δ 23.9 and δ 36.3. A downfield-shifted carbonyl signal at δ 169.2 (C-3) suggested the presence of a saturated δ-lactone moiety (Tai *et al*., 2010). The oxymethine carbon signals at δ 66.1 (C-5), δ 68.2 (C-8), δ 70.5 (C-7), δ 74.6 (C-1), and a carbonyl carbon of C-3 were reminiscent of a pyranopyrone moiety with hydroxyl function.

CONCLUSIONS

Comparison of ^{1}H-NMR and ^{13}C-NMR data for all compounds with literature values identified Compounds 1, 2 and 3 as goniodiol (Lan *et al*., 2005), 8-chlorogoniodiol (Lan *et al*., 2003) and 9-deoxygoniopypyrone (Tai *et al.*, 2010).

REFERENCES

i. Iqbal, E., Lim, L. B. L., Salim, K. A., Faizi, S., Ahmed, A., & Mohamed, A. J. (2018). Isolation and characterization of aristolactam alkaloids from the stem bark of Goniothalamus velutinus (Airy Shaw) and their biological activities. *Journal of King Saud University - Science*, *30*(1), 41–48.

ii. Lan, Y. H., Chang, F. R., Yu, J. H., Yang, Y. L., Chang, Y. L., Lee, S. J., & Wu, Y. C. (2003). Cytotoxic styrylpyrones from Goniothalamus amuyon. *Journal of Natural Products*, *66*(4), 487–490.

iii. Rasol, N. E., Ahmad, F. B., Lim, X. Y., Chung, F. F. L., Leong, C. O., Mai, C. W., … Ismail, N. H. (2018). Cytotoxic lactam and naphthoquinone alkaloids from roots of Goniothalamus lanceolatus Miq. *Phytochemistry Letters*, *24*, 51–55.

iv. Lan, Y. H., Chang, F. R., Liaw, C. C., Wu, C. C., Chiang, M. Y., Wu, Y. C. (2005). Digoniodiol, Deoxygoniopypyrone A, and Goniofupyrone A: Three New Styryllactones from *Goniothalamus amuyon*. *Planta Med.*, *71*, 153-159.

v. Tai, B. H., Huyen, V. T., Huong, T. T., Nhiem, N. X., Choi, E. M., Kim, J. A., Long, P. Q., Cuong, N. M., Kim, Y. H. (2010). New pyrano-pyrone from *Goniothalamus tamirensis* enhances the proliferation and differentiation of osteoblastic MC3T3-E1 cells. *Chemical and Pharmaceutical Bulletin*, *58* (4), 521-525.

JUNIOR SCIENCE COMMUNICATION
https://jscfsg.uitm.edu.my/
Volume 2 (2019)
eISSN 2637-0689

Colloquium of Chemistry and Environment 2018
Faculty of Applied Sciences, Universiti Teknologi MARA, Shah Alam.

DETERMINATION OF HEAVY METALS IN HAIR DYE PRODUCTS AND HENNA LEAVES USING FLAME ATOMIC ABSORPTION SPECTROMETRY

Norafydza Joha, Zuraidah Abdullah Munir*
Faculty of Applied Sciences, Universiti Teknologi MARA, 40450 Shah Alam, Selangor, Malaysia.

*zurai394@.uitm.edu.my

Abstract: This study was conducted to determine the amount of heavy metals (cadmium, copper, lead, iron and nickel) in hair dye products and henna leaves. The hair dye samples used were HD1, HD2, HD3 and henna leave sample, HL4. The heavy metal contents in the samples were extracted using wet digestion method followed by detecting the metals by flame atomic absorption spectrometer (FAAS). The quantification of metal content was determined from standard calibration method. The result from this study showed the mean concentrations of the heavy metals ranged from 4.80-5.11 μg/g for Pb, 1.32-1.84 μg/g for Fe, 0.16-0.18 μg/g for Cd, 0.61-0.74 μg/g for Cu and 1.99-2.02 μg/g for Ni.

Keywords**:** *heavy metals, atomic absorption spectrometer*

INTRODUCTION

Despite the challenging economic situation in Malaysia, there is a continuous demand of cosmetic products due to increased desire to improve the appearance as well as an alternative way to increase self-esteem (Kim *et al*., 2016). Commercial hair colouring products consist of a mixture of complex compounds, with varying components and formulas which differ from one manufacturer to another (Hussein, 2015). In Malaysia, other traditional alternative that is also popularly used to dye hair is by using leaves of henna tree or scientifically known as *Lawsonia inernis.* The heavy metal in cosmetics may be present in negligible amount compared to sources such as water, air or foods. However, their health toxicities should be considered because hair dyes, if being applied frequently may lead to heavy metal poisoning as they will eventually be absorbed into our body and accumulated. Thus, evaluation of hair dye products along with their components has to be done in order to inspect the ingredients and to ensure their safety to consumer.

METHODOLOGY

Three imported hair dye products and a sample of locally planted henna leaves were used in this study. The henna leaves sample were dried and ground to powder form. All samples were digested using wet digestion method. Chemicals used for digestion were analytical grade nitric acid, HNO_3 (65% w/w, Sigma Aldrich), 30% (w/v) hydrogen peroxide (H_2O_2), concentrated hydrochloric acid (HCl) (37%) and 1000 µg/g standard stock solution of GFS Fishers' AAS Reference Standard of lead, iron, cadmium, copper and nickel. The concentrations of heavy metals in the samples were analyzed using Pelkin Elmer Analyst 400 Atomic Absorption Spectrometer.

Volume 2 (2019)
eISSN 2637-0689

Preparation of samples

About 2-3 g of the dried powdered Henna leaves was placed into a conical flask and digested with 30 mL nitric acid. The digestion was continued until the nitrogen oxide fumes ceased. After the sample has cooled to room temperature, 2 mL hydrogen peroxide was added. Then it was again heated to concentrate the solution. Meanwhile, about 1 g sample of hair dye were heated with 15 mL nitric acid, 5 mL hydrogen peroxide and 5 mL hydrochloric acid until all nitrous oxide subsided. The henna leaves and hair dye samples were then cooled, filtered and transferred into 250 mL and 100 mL volumetric flasks respectively. Both henna and dye samples were replicated five times.

FINDINGS

Table 1 shows the mean values of heavy metals in each sample. As shown in Table, lead is the heavy metal with the highest amount in all samples, followed by nickel, iron, copper and cadmium. The order of the amount of heavy metals in these samples is as follow: Pb>Ni>Fe>Cu>Cd. The amount of all heavy metals in each sample whether from commercial hair dye products or henna leaves are still within the permissible limits (Alsaffar, 2014; Iwegbue, 2016; Ekere, 2014; Lodyga-Chruscinska *et al*., 2018 & Ayenimo *et al*., 2010). HL 4 which represents the henna leaves, contains the highest amount of Pb, Fe, Cd and Cu. Fe and Cu are essential elements but they can be potentially toxic if persist in high concentration in our body (Ayenimo *et al*., 2010). Higher amount of Fe in henna leaves might show that it is an iron accumulating plants while the presence of Pb is due to environmental pollution which is absorbed by the leaves (Ahmad *et al*., 1994). In addition, Ahmad *et al.*, (1994) emphasized that the amount of heavy metals in plants are also affected from the geochemical area of the plant itself.

Table 1 Mean amounts of heavy metals (µg/g) in samples based on analysis using FAAS (mean±SD).

	HD1 (µg/g)	**HD2 (µg/g)**	**HD3 (µg/g)**	**HL4 (µg/g)**
Lead (Pb)	4.95±0.00	4.86±0.82	4.80±0.00	5.11±0.00
Iron (Fe)	1.32±0.02	1.50±0.06	1.52±0.12	1.84±0.10
Cadmium (Cd)	0.16±0.01	0.17±0.01	0.17±0.00	0.18±0.01
Copper (Cu)	0.64±0.01	0.61±0.01	0.70±0.03	0.74±0.01
Nickel (Ni)	1.99±0.01	2.01±0.01	2.03±0.01	2.00±0.01

Table 2 shows the value of limit of detection (LOD) and limit of quantification (LOQ) for Pb, Cd, Fe, Ni and Cu calculated at 95% confidence level. Al metals detected were above the LOD.

Table 2 LOD and LOQ of Pb, Cd, Fe, Ni and Cu.

	LOD	**LOQ**
	µg/g	**µg/g**
Lead (Pb)	0.66	2.01
Cadmium (Cd)	0.09	0.28
Iron (Fe)	0.13	0.39
Nickel (Ni)	0.50	1.51
Copper (Cu)	0.24	0.72

CONCLUSIONS

This study was conducted to determine the amount of selected heavy metals in hair dye products and henna leaves. Based on results, the amount of heavy metals in these samples is as follow: Pb>Ni>Fe>Cu>Cd. All amounts are within the permissible limits.

REFERENCES

i. Ahmad, I., Siddiqui, M. H., & Khan, Z. A. (1994). The major, minor and trace elements in Henna leaves. *Jour. Chem. Soc. Pak. Vol*, *16*(1), 29-31.
ii. Alsaffar, N. and Hussein, H. (2014). Determination of heavy metals in some cosmetics available in locally markets. IOSR Journal of Environmental Science, *Toxicology and Food Technology*, *8*(8), 9-12.
iii. Ayenimo, J. G., Yusuf, A. M., Adekunle, A. S., & Makinde, O. W., 2010. Heavy metal exposure from personal care products. *Bulletin of environmental contamination and toxicology*, *84*(1), 8-14.
iv. Ekere, N. R., Ihedioha, J. N., Ogbuefi, F. I., & Ayogu, J. (2014). Assessment of some heavy metals in facial cosmetic products. Journal of Chemical and Pharmaceutical Research, *6*(8), 561-564.
v. Hussein, H. J. (2015). Evaluation of Some Heavy Metals in Hair Dyes in Baghdad. *International Journal of Science and Research (IJSR)*, *4*(9), 687-691.
vi. Iwegbue, C. M. A., Emakunu, O. S., Obi, G., Nwajei, G. E., & Martincigh, B. S. (2016). Evaluation of human exposure to metals from some commonly used hair care products in Nigeria. *Toxicol Rep*, *3*, 796-803.
vii. Kim, K. H., Kabir, E., & Jahan, S. A. (2016). The use of personal hair dye and its implications for human health. *Environ Int*, *89-90*, 222-227.
viii. Lodyga-Chruscinska, E., Sykula, A., & Wiedlocha, M. (2018). Hidden Metals in Several Brands of Lipstick and Face Powder Present on Polish Market. Cosmetics, *5*(4), 57.

JUNIOR SCIENCE COMMUNICATION
https://jscfsg.uitm.edu.my/
Volume 2 (2019)
eISSN 2637-0689

Colloquium of Chemistry and Environment 2018
Faculty of Applied Sciences, Universiti Teknologi MARA, Shah Alam.

DETERMINATION OF VOLATILE COMPOUNDS IN *Mangifera odorata* BY HEAD-SPACE SOLID-PHASE MICROEXTRACTION AND GAS CHROMATOGRAPHY-MASS SPECTROMETRY

Norashikin Md Jamil, Norashikin Saim*
Faculty of Applied Sciences, Universiti Teknologi MARA, 40450 Shah Alam, Selangor, Malaysia.

* noras691@uitm.edu.my

Abstract: In this study, the volatile compounds present in whole fruit and pulp of *Mangifera odorata* obtained from different sources were analyzed and compared. Extraction and analysis were achieved using head-space solid-phase microextraction (HS-SPME) and gas chromatography-mass spectrometer (GC-MS). HS-SPME was chosen in this study as it is a simple, solvent-less, non-destructive and fast extraction technique for the determination of volatile compounds that contribute to the aroma of the fruit. *M.odorata* fruit samples were obtained from two sources, Shah Alam and Jeram, Selangor. The analysis on the pulp of *M.odorata* was done using two approaches, sliced and blended. ß-myrcene and linalool are major compounds extracted from whole fruit of M.odorata while major compounds extracted from the pulp sample were 3-carene and α-pinene. Significant difference in the amount of extracted compounds was observed from *Mangifera odorata* obtained from different sources.

Keywords: *Mangifera odorata, volatile compounds, SPME, and GC-MS.*

INTRODUCTION

M. odorata mango species is native to tropical Asia and commonly planted in orchards or around village houses (Wong & Ong, 1993). Fruit aroma is a complex mixture of large number of volatile compounds which are specific to species (El Hadi *et al.*, 2013). Previously, simultaneous extraction method was used in the extraction of volatile compounds from *M. odorata*. However, the method required large volume of solvent with long extraction time that may cause loss of important volatile compounds that contribute to the aroma of the fruit. Thus, in this study, HS-SPME and GC-MS were used in determining the volatile compounds present in whole fruit and pulp of *M. odorata* and fruit samples obtained from different sources.

METHODOLOGY

The volatile compounds from *M. odorata* were extracted from the whole fruit, sliced pulp and blended pulp using HS-SPME using polydimethyl siloxane/divinylbenzene (PDMS/DVB) fiber based on the method developed by Zakaria *et al.* (2017), The volatile compounds were analyzed using a GC-MS system (Agilent Technologies 5973 Inert Mass Selective Detector and Agilent 7683 Series Injecto) with helium as the carrier gas (1.2 mL/min) and HP-5MS capillary column (Agilent 19091S-433, 0.25mm x 30m 0.25m) under the following GC conditions; column temperature of 40˚C - 150˚C ($5^{\circ}C \cdot min^{-1}$) and increased to 250˚C ($100^{\circ}C \cdot min^{-1}$) with final time of 5 mins, injector temperature of 280˚C, and interface temperature: 280˚C. Extracted compounds were identified by comparing their spectra with those available in the NIST digital library.

FINDINGS

Colloquium of Chemistry and Environment 2018

Faculty of Applied Sciences, Universiti Teknologi MARA, Shah Alam.

Figure 1 shows the chromatogram obtained from whole fruit sample from Shah Alam. Major compounds extracted from whole fruit sample from both sources is shown in Figure 2. ß-myrcene is the most abundant compound extracted from whole fruit sample from Shah Alam while linalool is the most abundant compound identified in whole fruit sample from Jeram.

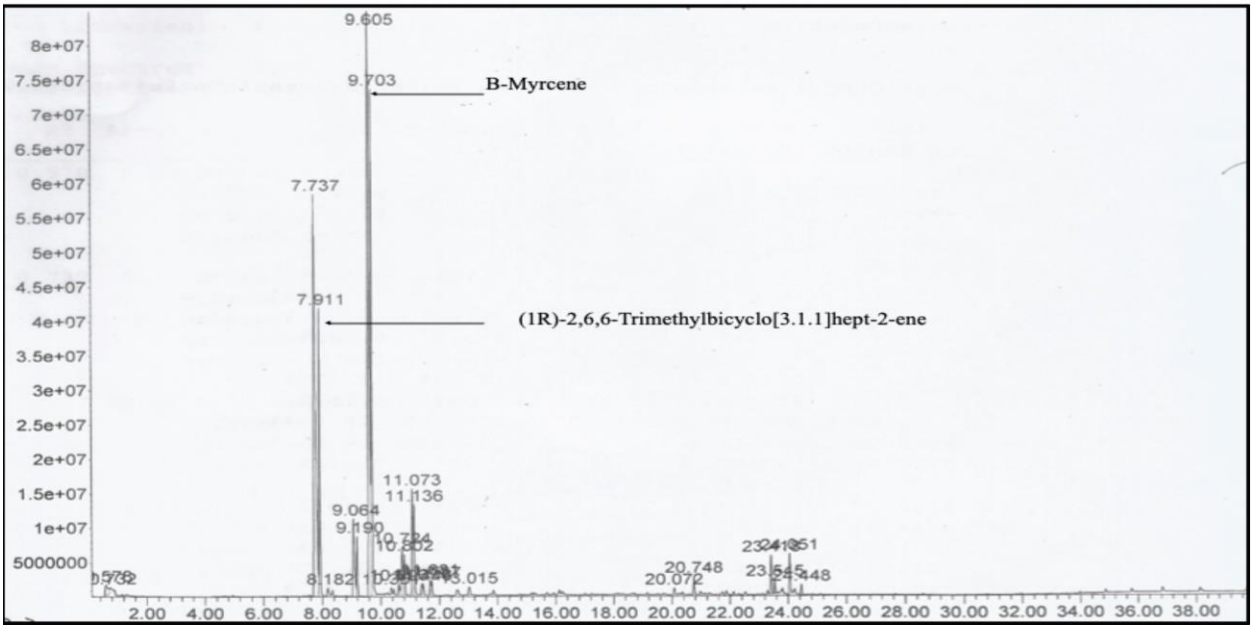

Figure 1 Chromatogram of whole fruit sample from Shah Alam

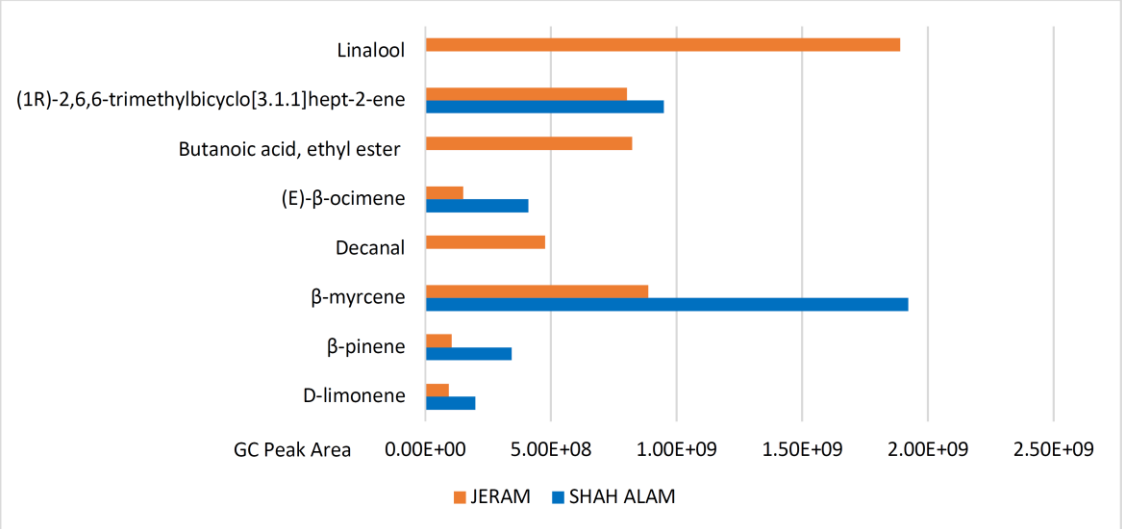

Figure 2 Major volatile compounds in whole fruit sample from different sources.

For pulp sample, significant difference is observed between sliced pulp and blended pulp sample from Shah Alam. The most abundant compound identified in sliced sample is linalool while 3-carene is the most abundant compound in blended sample. This study shows that the sample preparation technique may contribute to the differences in the detected compounds. Pino *et al.* (2005), stated that sample preparation can cause variation in volatile compounds of the fruit. β-pinene was found in both sliced and pulp sample in significant amount. Wijaya *et al.* (1999) reported α-pinene as the most abundant compound in pulp sample of *M. odorata*. This compound was detected in blended pulp.

CONCLUSIONS

Similar compound extracted in whole and pulp of *M. odorata* include ß-pinene, α-pinene, 3-carene, β-myrcene, linalool, (1r)-2,6,6-trimethylbicyclo[3.1.1]hept-2-ene and 2-butenoic acid, ethyl ester. These compounds may contribute to the distinguished aroma of this fruit. There are differences in the composition of volatile compounds in fruits from different sources.

REFERENCES

i. El Hadi, M. A. M., Zhang, F. J., Wu, F. F., Zhou, C. H., & Tao, J. (2013). Advances in fruit aroma volatile research. Molecules, *18*(7), 8200–8229.
ii. Pino, J. A., & Mesa, J. (2006). Contribution of volatile compounds to mango (Mangifera indica L .) aroma, Flavour and Fragrance journal *21*(2), 207–213
iii. Wijaya, C. H., A. Apriyantono, T. May, H. Raharja, and T. A. Ngakan. "Flavor of Kweni (Mangifera odorata Griff), an exotic tropical fruit." In Flavor Chemistry of Ethnic Foods, pp. 119-125. Springer, Boston, MA, 1999.
iv. Wong, K. C., & Ong, C. H. (1993). Volatile components of the fruits of bachang (Mangifera foetida Lour.) and kuini (Mangifera odorata Griff.). Flavour and Fragrance Journal, *8*(3), 147–151.
v. Zakaria, S. R., Tajuddin, R., Osman, R., Saim, N., & Saaid, M. (2017). Optimization of Headspace Solid Phase Microextraction (HS-SPME) for the Extraction of Volatile Organic Compounds (VOCs) in Mangoes (Harumanis cv.) Using 2 Stages Multivariate Analysis. *Pertanika J. Sci. & Technol*, *25*, 167–174.

JUNIOR SCIENCE COMMUNICATION
https://jscfsg.uitm.edu.my/
Volume 2 (2019)
eISSN 2637-0689

Colloquium of Chemistry and Environment 2018
Faculty of Applied Sciences, Universiti Teknologi MARA, Shah Alam.

PREPARATION AND CHARACTERIZATION OF CELLULOSE FROM *Leucaena leucocephala* SEED BY ALKALINE TREATMENT

Nur Aini Nabilah, Maryam Husin*
Faculty of Applied Sciences, Universiti Teknologi MARA, 40450 Shah Alam, Selangor, Malaysia.

*marya911@.uitm.edu.my

Abstract: In this study, the matured *Leucaena leucocephala* seed (LLS) was used as a raw material to extract cellulose. Different concentration of NaOH which are 2%, 4% and 6% were studied to extract cellulose. The highest amount of cellulose extracted was from 4% NaOH treatment which is 23.7%. Meanwhile, in terms of colour, 6% NaOH treatment shows the best result. Several analytical methods were also used to study the structural characteristic, crystallinity and morphology of the cellulose. FTIR spectrum of all treated samples shows the peaks of cellulose. The highest crystallinity index of cellulose was obtained from 6% NaOH treatment which is 76.04%. Under FESEM images, the cellulose appeared in fibrils-like structure with an average diameter less than 9.0 µm.

Keywords: *Leucaena leucocephala,* cellulose, NaOH

INTRODUCTION

Leucaena leucocephala is a legume and in Malaysia it is locally known as *petai belalang* that has a potential to be used as lignocellulosic raw materials. The seed are used as animal feeds, however the present of mimosine believes can cause negative effects. The use of *L. leucocephala* woods' in paper industry get attentions due to present of low lignin content and producing high pulp yield. In the past few years, cellulose has been an interesting research subject due to its non-toxicity, biodegradability, high mechanical strength and low density. Cellulose is made up of long chain of β-d-glucopyranose units and linked by β-1,4-glycosidic bond (Zhao *et al*., 2018). Cellulose can be obtained from various sources such as natural source which is plant, agricultural residue, bacteria and more. Cellulose are normally extracted by using alkali treatment followed by acid hydrolysis to remove hemicellulose, lignin and other trace materials.

METHODOLOGY

A 10.0 g of LLS powder was mixed with 200 mL of 2 wt% NaOH solution at temperature of 80°C for 2 hrs. The steps were repeated with 4 wt% and 6 wt% NaOH. The alkali treated sample was then mixed with 200 ml of 2 wt% H_2O_2. The mixture was stirred for 2 hours at temperature of 80–100°C. Then, the solution was filtered and washed before being repeated for three times. The product was dried and weighed. FTIR was used to obtain the spectra of samples under frequency range 400-4000 cm^{-1} with four number of scans. FESEM was used to analyse the microstructure of the raw and treated samples. The diffraction pattern of the different treated samples was analysed by XRD instrument and the crystallinity index (CI) of each of sample was calculated by using Segal formula.

Volume 2 (2019)
eISSN 2637-0689

Colloquium of Chemistry and Environment 2018
Faculty of Applied Sciences, Universiti Teknologi MARA, Shah Alam.

FINDINGS

The average amount of holocellulose, cellulose, hemicellulose and lignin obtained in percent yield at 95% confidence interval were summarised in Table 1.

Table 1 The yield of holocellulose, cellulose, hemicellulose and lignin.

Compound	Percent yield (%)
Holocellulose	37.29 ± 7.38
Cellulose	28.29 ± 3.07
Insoluble lignin	8.30 ± 0.67

The average yield of cellulose from 2 wt%, 4 wt% and 6 wt% of NaOH were 22.62 %, 23.70 % and 22.44 %, respectively. The difference between cellulose amount in all three treatments is less than 1.3%. Hence, it is concluded that the amount of cellulose extracted from different NaOH concentration are almost the same. Figure 1 showed the effect of treatments on the colour of cellulose obtained. After the alkaline treatment, the LLS turn to dark brown then changes to yellowish and white product depends on the concentration of NaOH used.

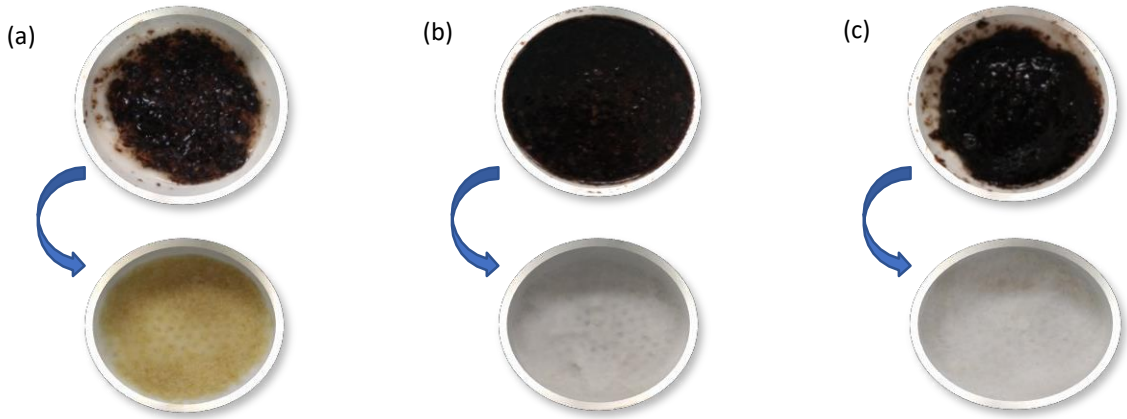

Figure 1 The changes in colour during the treatments (a) 2% (b) 4% c) 6% of NaOH followed by bleaching.

Based on the FTIR spectra, the treated samples showed broad peak of O-H, C-H stretching of aromatic functional group, O-H bond of water absorption, C-C stretching band and C-O-C vibrational pyranose ring band. In the spectra of the LLS, a small peak at 1746.32 cm^{-1} which corresponding to the C=O stretching of acetyl and ester group of hemicellulose or carboxylic acid in the lignin group (Frone *et al*., 2017). This peak was unseen in all three alkaline treated samples. LLS treated with 2%, 4% and 6% NaOH gives CI value of 71.14%, 70.50% and 76.40% respectively. The FESEM analysis showed that

the LLS had a globular structure while treated samples appear to be fibril-like structure. The difference in morphology are due to the removal of hemicellulose, lignin and others non-cellulosic compounds (Husin *et al*., 2017). In average, the diameter of fibrils is less than 9.0 µm in all treated samples.

CONCLUSIONS

Treatment with 4 % NaOH solution obtained the highest amount of the cellulose which is 23.70 %. In term of whitening, 6 % NaOH coupled with bleaching treatment using H_2O_2 is the most excellent compared to others. FTIR results for all treated LLS shows a significant peak of cellulose. The highest crystallinity index calculated based on the XRD data is 76.04 % for cellulose treated with 6 % NaOH.

REFERENCES

i. Frone, A. N., Chiulan, I., Panaitescu, D. M., Nicolae, C. A., Ghiurea, M. & Galan, A. M. (2017). Isolation of cellulose nanocrystals from plum seed shells, structural and morphological characterization. *Materials Letters*, *194*, 160–163.
ii. Husin, M., Li, A. R., Ramli, N., Romli, A. Z., Hakimi, M. I. & Ilham, Z. (2017). Preparation and characterization of cellulose and microcrystalline cellulose isolated from waste Leucaena leucocephala seeds. *International Journal of Advanced and Applied Sciences*, *4*(3), 51-58.
iii. Zhao, T., Chen, Z., Lin, X., Ren, Z., Li, B., & Zhang, Y. (2018). Preparation and characterization of microcrystalline cellulose (MCC) from tea waste. *Carbohydrate Polymers*, *184*, 164–170.

JUNIOR SCIENCE COMMUNICATION
https://jscfsg.uitm.edu.my/
Volume 2 (2019)
eISSN 2637-0689

Colloquium of Chemistry and Environment 2018
Faculty of Applied Sciences, Universiti Teknologi MARA, Shah Alam.

SYNTHETIC STUDY TOWARDS ISAGARIN DERIVATIVE

Nur Aliah Diyana Rahmat, Fazni Susila Abdul Ghani*, Najmah P.S.Hassan
Faculty of Applied Sciences, Universiti Teknologi MARA, 40450 Shah Alam, Selangor

*fazni542@uitm.edu.my

Abstract: This study was carried out to synthesized a pyranonapthoquinone antibiotics from isagarin derivatives **39**. This synthesis includes preparation of salt, coupling of salt, radical alkylation, ketone reduction and spontaneous cyclization. The product, pyridinium salt **32** was successfully synthesized from pyridine **34** and 4-phenylphenacyl bromide **33** with percentage yield of 64.14%. Pyridinium salt **32** obtained was coupled with menandione**40** producing compound **35** with percentage yield of 13.53%. Coupling of pyridinium salt **32** with naphthoquinone **2** was unsuccessful, thus step ofradical alkylation was planned to be executed. Preparation of acrylic acid **36** was needed in this synthesis to be reacted with naphthoquinone **2**. Acrylic acid **36** was attempted under 2 conditions which are basic and acidic condition by hydrolysis of ester, methyl acrylate **41**. Saponification process produced conjugate addition product **43** while in acid hydrolysis of ester **41** gave acid **44**. Both basic and acidic hydrolysis steps failed to give the desired acrylic acid **36**. An attempt to produce halogenated naphthoquinone **42** using bromine absorbed on alumina also failed.

Keywords:*pyridinium, menandione, naphthoquinone and phenylphenacyl bromide.*

INTRODUCTION

Antibiotics is a type of chemicals that always being used in medical world. Antibiotics have ability to inhibit and slowing down the growth of microbial but give a minimal effect to the anchor person (Bhattacharjee, 2016). Isagarin**9** was said to have antibiotics properties that can use to treat skin dieases like scabies and skin mycosis. It can be obtained naturally from isolating the roots of *Pentas longiflora* Oliv. from the Rubiaceae (Jacobs *et al*.,2010). Due to its biological properties present, chemists were called to synthesis isagarin from quinone**1** and naphhoquinone **2**. It was reported that quinone**1** has the best antibiotics properties in it which act as the anticancer agent while Naphthoquinone **2** play main role in biological activities such as anti-fungal, anti-cancer and anti-microbial (Griesback, 2014). There are several ways of synthesizing isagarin based on previous study. For example, Fernandes and his co-worker said in 2011 in order to synthesize isagarin, they used a Dotz annulation reaction process. Other that, sharpless assymetric dihydroxylation process by Heravi, *et al*., 2017 to obtain isagarin. Purpose of this study are to synthesis isagarin derivative from quinone, to isolate and purify the substituted isagarin derivative and lastly to identify the compound by using spectroscopy method.

METHODOLOGY

The synthesis was begun with synthesis of pyridinium salt **32** from 4-phyenylphenacyl bromide **33** with pyridine **34**. The mixture was set to reflux for 5 days. After reaction was completed, the mixture was filtered for purification steps. The product obtained was dried overnight and done with the analytical analysis once it dried. Compound produce is pyridinium salt **32**. The synthesis was further by coupling the pyridinium salt **32** with substituted naphthoquonine, menandione **40**. Triethylamine was added in the mixture under nitrogen gas environment. It was then set to reflux for 24 hours to let the reaction complete. The reaction

Colloquium of Chemistry and Environment 2018
Faculty of Applied Sciences, Universiti Teknologi MARA, Shah Alam.

mixture was worked up to extract the target analytes from it. Rotary evaporator was used to evaporate off the solvent to give crude product **35**. Crude **35** was purified by using column chromatography to give pure compound **35**. Hydrolysis of ester, methyl acrylate **41**, was done under 2 conditions, basic (saponification) condition and acidic condition. Saponification used sodium hydroxide added into methyl acrylate **41** in methanol and distilled water. After reflux for 16 hours, the mixture was worked up by using liquid-liquid extraction technique to obtain acrylic acid **36**. The solvent was evaporated by using rotary evaporator. Next, in acidic condition, methyl acrylate **41** was added in concentrated hydrochloric acid, distilled water and tetrahydrofuran (THF) and refluxed for 5 hours. After reaction completed, the mixture was work up as in saponification process. Solvent was evaporated by using rotary evaporator to remove it. The results obtained were further with analysis process by using NMR spectroscopy and FTIR-ATR instrument to identify the structure and characteristic of compound.

FINDINGS

The synthesis of pyridinium salt **32** met successful by producing yellow solid powder compound with the melting point of pyridinium salt **32** is between 237-238˚C. The percentage yield of the compound is 64.14%. This compound structure was confirmed by observing and analysing the spectra of 1H NMR, 13C NMR and FTIR-ATR. From pyridinium salt **32**, compound **35** was obtained from the coupling of pyridinium salt **32** with menandione**40** under nitrogen environment. This coupling was successful yield compound **35** in form of orange-yellow solid powder with the melting point between 109-117˚C. The percentage yield of compound **35** obtained is 13.53%. This compound structure was also confirmed by observing and analysing the spectra of spectroscopy method. However, the synthesis of acrylic acid **36** in both basic and acidic condition met failure. Compound **43** was produced for synthesis by using basic condition instead while in acidic condition, compound **44** was obtained. There were no expected peaks appears on the spectra that show the presence of acrylic acid **36** for both condition.

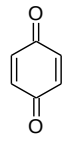

1

Quinone **1**

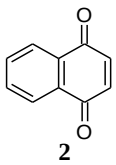

2

Naphthoquinone **2**

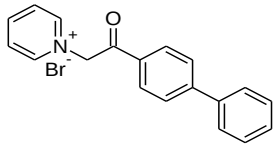

32

Compound **32**.

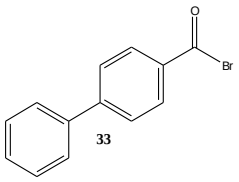

33

4-phenylphenacyl bromide **33**

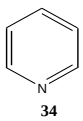

34

Compound **34**

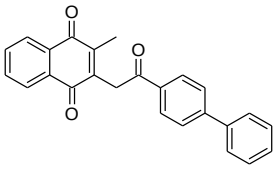

35

Compound **35**.

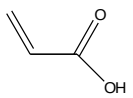

36

Acrylic acid **36**

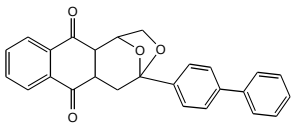

39

Compound **39**

Colloquium of Chemistry and Environment 2018
Faculty of Applied Sciences, Universiti Teknologi MARA, Shah Alam.

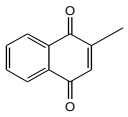

40
Menadione **40**

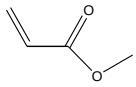

41
methyl acrylate **41**

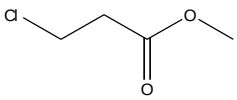

43
Compound **43**

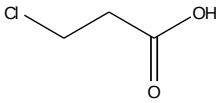

44
Compound **44**

CONCLUSIONS

In conclusion, the synthesis of pyridinium salt **32** from reaction of 4-phenylphenacyl bromide **33** with pyridine **34** was successful with percentage yield of 64.14%. Since coupling of pyridinium salt **32** with naphthoquinone **2** based on previous study met failure, another route of coupling salt which is coupling of salt **32** with menandione **40** instead was successful. It gives compound **35** with a percentage yield of 13.53%. However, the synthesis of acrylic acid under both acidic and basic condition were failed to give expected acrylic acid **36**. Compound **43** and compound **44** were produced instead. Suggested recommendation for future study, Quinone 1 is a type of compound that has highly sensitivity towards light, able to degrade when it exposed to the light. Due to its characteristic, a precaution steps must be done during handling quinone**1** to minimized the exposure towards light. Alternative way to avoid a rapid degradation of naphthoquinone **1** is via, a reductive methylation, the coupling product of compound **33** and compound **35**. While, for synthesizing of acrylic acid **36**, the monitoring steps should be done using HPLC instead of TLC. The TLC monitoring step was not effective to monitor the reaction.

REFERENCES

i. Bhattacharjee, M. K. (2016). Chemistry of Antibiotics and Related Drugs: Introduction to Antibiotics. Springer, Switzerland
ii. Fernandes, R. A., & Ingle, A. B. (2011). A Concise Stereoselective of the Tetracyclic Naphthoquinone Isagarin. *J.Org.Chem, 33*, 6624-6627
iii. Griesback, A. G. (2014). Compound with two carbon- Heteroatom Bonds: Quinones and Heteroatom Analogues. *Science of Synthesis: Houben-Weyl Methods of Molecular Transformation, 28*, 1-12.
iv. Heravi, M. M., Zadsirjan, V., Esfandyari, M., Lashaki, T. B. (2017). Applications of sharpless asymmetric dihydroxylation in the total synthesis of natural products. *Tetrahedron: Asymmetry, 28*(8), 987-1043.
v. Jacobs, J., Claessens, S., De Mol, E., El Hady, S., Minguillón, C., Álvarez, M., & De Kimpe, N. (2010). First Enantioselective Synthesis of Isagarin, A Natural Product Isolated from PentasLongifloraOliv. *Tetrahedron, 66*(27-28), 5158-5160.

JUNIOR SCIENCE COMMUNICATION
https://jscfsg.uitm.edu.my/
Volume 2 (2019)
eISSN 2637-0689

Colloquium of Chemistry and Environment 2018
Faculty of Applied Sciences, Universiti Teknologi MARA, Shah Alam.

STABILITY OF STIRRED OIL-IN-WATEREMULSION SYSTEM: THE EFFECT OF CORN STARCH AND VIRGIN COCONUT OIL

Nur Amira Izzati Ramli, Hairul Amani Abdul Hamid*
Faculty of Applied Sciences, Universiti Teknologi MARA, 40450, Shah Alam, Selangor, Malaysia.

*h.amani@uitm.edu.my

Abstract: This study was carried out in order to determine the effect of corn starch and virgin coconut oil (VCO) on the stirred oil-in-water (O/W) emulsions as well as to characterize the emulsion mixtures using two different techniques. The tensiometer is used to measure the interfacial tension of the emulsion mixtures, and the rheometer is used to measure the average viscosity of the O/W emulsions. The most stable sample was observed in 6% w/v of corn starch as it has the lowest surface tension of 27.5 mN/m. On the other hand, the emulsion mixture consists of 40% v/v of VCO is the most stable emulsion that shows the highest surface tension of 27.8 mN/m. Furthermore, the O/W emulsion at 6% w/v of corn starch also has the highest average viscosity of 0.00589 mPa.s, however, emulsion mixture with 40% v/v of VCO has the lowest average viscosity of 0.01560 mPa.s.

Keywords**:** *Oil-in-Water Emulsions, Corn Starch, Virgin Coconut Oil Surface Tension, Rheology*

INTRODUCTION

Oil-in-water emulsions are thermodynamically unstable which caused the destabilization of emulsion mixtures, thus decreased the quality of the product. Corn starch acts as a co-surfactant to improve the stability of the emulsion (Sadeghi *et al.*, 2017). In addition, virgin coconut oil is essential as it gives oil-in water emulsion. Thus, this study was conducted to determine the effects of corn starch and virgin coconut oil on the stirred O/W emulsions.

METHODOLOGY

The oil-in-water (O/W) emulsions were prepared manually by mixing different compositions of corn starch (0-6% w/v) and virgin coconut oil (10-40% v/v) with methyl-α-*D*-glucopyranoside (5% w/v), salicylic acid (1% w/v), and distilled water. Moreover, the emulsion mixtures were mixed thoroughly for five seconds by using a vortex mixer and stored in small vials with samples labelled from A to H.

FINDINGS

Figure 1 and 2 illustrate the surface tension of the emulsion mixtures against concentrations of corn starch and virgin coconut oil, respectively. As the concentration of corn starch increases, the surface tension decreases. On the other hand, as the virgin coconut oil increases, the surface tension of emulsion mixtures increase. Figure 3 and 4 depict an average viscosity against concentration of corn starch and VCO, respectively. The highest average viscosities were observed at 6% w/v of corn starch and 10% v/v of VCO. According to Castel *et al.*, (2017), the adsorption of protein component at the interface will lower the interfacial tension and increase the viscosity. On the other hand, the highest surface tension and lowest average viscosity are due to flocculation of the droplet will be observed at high amount of oil content (Onsaard *et al.*, 2006; Taherian *et al.*, 2006).

Colloquium of Chemistry and Environment 2018
Faculty of Applied Sciences, Universiti Teknologi MARA, Shah Alam.

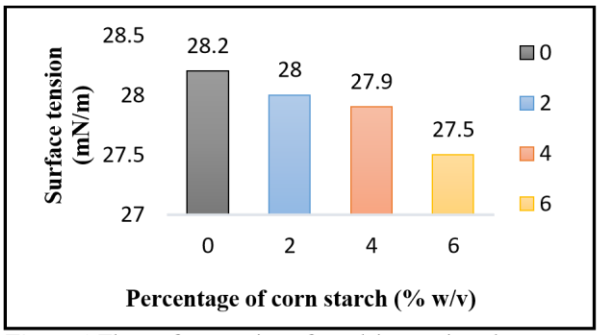

Figure 1 The surface tension of emulsion against the percentage of corn starch

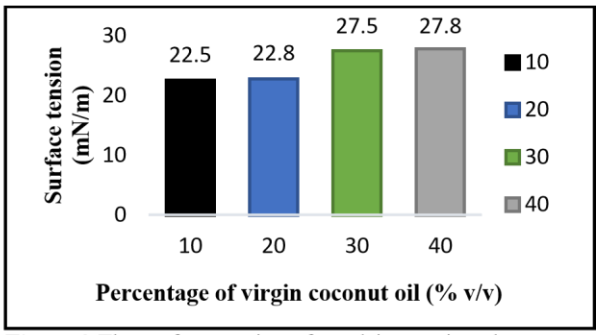

Figure 2 The surface tension of emulsion against the percentage of virgin coconut oil

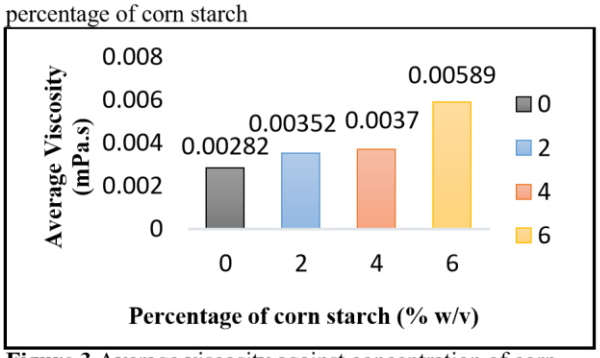

Figure 3 Average viscosity against concentration of corn starch

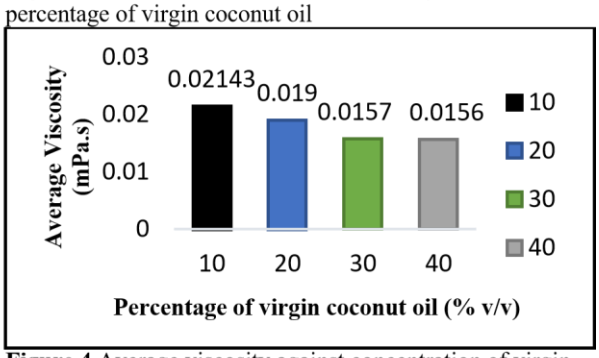

Figure 4 Average viscosity against concentration of virgin coconut oil

CONCLUSIONS

As a conclusion, the effects of corn starch and virgin coconut oil in the O/W emulsion were studied and characterized by using tensiometer and rheometer. The most stable emulsions were observed in samples which contain 6% w/v of corn starch and 40% v/v of VCO. Sample with 6% w/v of corn starch shows the lowest surface tension and the highest average viscosity, however, sample with 40% v/v of VCO produces the highest surface tension and the lowest average viscosity.

REFERENCES

i. Castel, V., C.Rubiolo, A. and R. Carrara, C., (2017). Droplet size distribution, rheological behavior and stability of corn oil emulsions stabilized by a novel hydrocolloid (Brea gum) compared with gum Arabic. *Food Hydrocolloids, 63*, 170-177.

ii. Onsaard, E., Vittayanont, M., Srigam, S. and McElements, D.J., (2006). Comparison of properties of oilin-water emulsions stabilized by coconut cream proteins with those stabilized by whey protein isolate. *Food Research International, 39*, 78-86.

iii. Sadeghi, R., Daniella, Z., Uzun, S. and Kokini, J., (2017). Effects of starch composition and type of nonsolvent on the formation of starch nanoparticles and improvement of curcumin stability in aqueous media. *Journal of Cereal Science, 76*, 122-130.

iv. Taherian, A.R., Fustier, P. and Ramaswamy, H.S., (2006). Effect of added oil and modified starch on rheological properties, droplet size distribution, opacity and stability of beverage cloud emulsions. *Journal of Food Engineering, 77*, 687-696.

JUNIOR SCIENCE COMMUNICATION
https://jscfsg.uitm.edu.my/
Volume 2 (2019)
eISSN 2637-0689

Colloquium of Chemistry and Environment 2018
Faculty of Applied Sciences, Universiti Teknologi MARA, Shah Alam.

SYNTHETIC STUDY TOWARDS ELEUTHERIN DERIVATIVE

Nor Amirah Abdullah, Najmah P.S.Hassan*, Fazni Susila Abdul Ghani
Faculty of Applied Sciences, Universiti Teknologi MARA, 40450 Shah Alam, Selangor, Malaysia.

*najma902@uitm.edu.my

Abstract: Eleutherin **11** is one of the simplest pyranonaphthoquinone compound that exhibits anticancer and antibacterial properties. This study describes synthetic strategies towards preparation of an eleutherin **11** derivative that belong to pyranonaphthoquinone family. The synthesis includes preparation of salt, salt coupling, radical alkylation, and ketone reduction and lastly spontaneous cyclization. The pyridinium salt **50** was successfully prepared from pyridine **49** and 4-bromophenacyl bromide **48** with 64 % yield. Salt **50** was coupled with substituted naphthoquinone **5** producing compound **56** in 13 % yield. Coupling of salt **50** with naphthoquinone **2** was unsuccessful thus radical alkylation step was planned to be executed. Preparation of acrylic acid **52** needed for this step was attempted using both basic and acidic conditions. Hydrolysis of methyl acrylate **57** in basic condition produced conjugate addition product **58** in 68 % yield. The acid hydrolysis of ester **57** gave acid **59** in 6 % yield. Both basic and acidic hydrolysis steps failed to give desired acrylic acid **52**. The synthesized compounds were characterized by Nuclear Magnetic Resonance (NMR) spectroscopy and Infrared (IR) spectroscopy.

Keywords: *Pyranonaphthoquinone, Eluetherine, substituted naphthoquinone.*

INTRODUCTION

Eleutherine **11** is isolated from the bulbs of *Eleutherine americana* Merr., a medicinal plant, which widely found in South East Asia (Insanu *et al*., 2014). The pyranonaphthoquinone compound, such as eleutherin **11**, is reported to possess good antibacterial activity (Prachayasittikul *et al*., 2014) and exhibit a field of biological activities with medicinal potential such as anticancer (Heapy *et al*., 2013). A revised synthetic methodology towards this compound can lead to new drug discovery. Previous study reports eleutherin **11** molecule can be synthesized through various strategy such as biomimetic synthesis, electrophilic cyclization, intramolecular oxymercuration of naphthalenol (Brimble *et al*., 2000), cycloaddition (Sperry *et al*., 2008) and a Dötz annulation reaction with a chiral alkyne followed by an oxa-Pictet Spengler reaction (Fernandes *et al*., 2008). The study described herein involves the efforts towards preparation of an eleutherin **11** derivative, from pyranonaphthoquinone family of antibiotics.

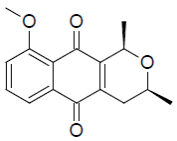

Eleutherine **11**

METHODOLOGY

The synthesis involved the preparation of pyridinium salt **50** by the reaction of 4-bromophenacyl bromide **48** (5.27 g, 19.16 mmol) with pyridine **49** (1.85 ml, 22.99 mmol) in tetrahydrofuran solvent under refluxed

condition. The salt **50** then coupled with menandione **5** (3.00 g, 8.40 mmol) in nitrogen environment with acetonitrile (10 ml) followed with trimethylamine (0.30 ml) after cooled with ice. The mixture was stirred vigorously for 24 hours, and then the desired compound **56** was extracted using liquid-liquid extraction and purified using column chromatography.

Hydrolysis of acrylic ester **57** were undertaken using both basic and acidic conditions. In basic condition, sodium hydroxide (2.09 g, 52.28 mmol), was added to methyl acrylate **57** (3.16 ml, 34.85 mmol) in water (2.8 ml) and methanol (50 ml) and the mixture was refluxed for 16 hours. The mixture was diluted with water (100 ml), acidified with 2M hydrochloric acid and was washed with ethyl acetate. For acididc condition, concentrated HCl (3.56 ml) was added to methyl acyralate **57** (5.26 ml, 58.08 mmol) in water (68.60 ml) and dioxane (192.60 ml) and refluxed for 5 hours. The reaction mixture was neutralized with saturated sodium bicarbonate and washed with ethyl acetate. All the reactions were observed using thin layer chromatography (TLC). All synthesized compounds were characterized by NMR spectroscopy and IR spectroscopy.

FINDINGS

The pyridinium salt **50** was obtained in 64 % yield in the formed of yellow solid with melting point of 237.00 – 238.00 °C. The following coupling of salt **50** with menandione **5** produced compound **56** in the form of orange crystals in 13 % yield with melting point of 156.00 – 157.90 °C. Coupling of salt **50** with 1,4-naphthoquinone **2** to produce compound **51** was unsuccessful thus radical alkylation step was planned to be executed.

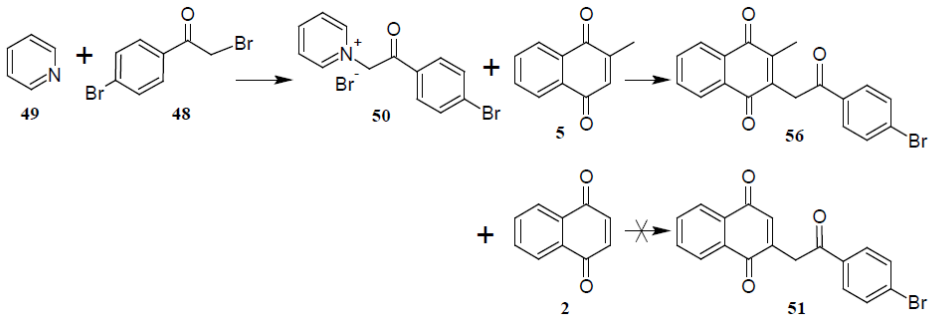

Scheme 1 Preparation of pyridinium salt **50** and coupling with menadione **2**

Preparation of acrylic acid **52** needed for this step was attempted via hydrolysis of methyl acrylate **57**. The hydrolysis of methyl acrylate **57** in basic and acidic condition produced conjugate addition product **58** in 68 % and carboxylic acid **59** in 6 % respectively. The structure of compound **58** was distinguished from compound **59** by the presence of methyl group signals in ^{1}H-NMR and ^{13}C-NMR, while for compound **59**, the IR spectrum showed a broad absorption band for hydroxyl group.

Colloquium of Chemistry and Environment 2018
Faculty of Applied Sciences, Universiti Teknologi MARA, Shah Alam.

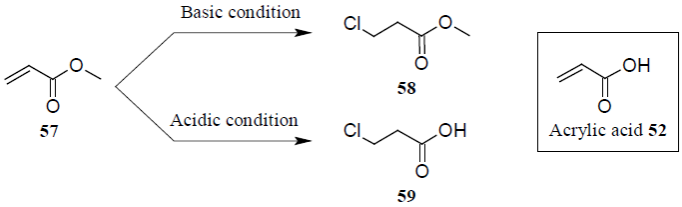

Scheme 2 Hydrolysis of methyl acrylate **57**

CONCLUSIONS

In conclusion, the synthesis work successfully gave pyridinium salt **50** with 64 % yield and coupling product **56** with 13 % yield. Attempts to couple salt **50** with unsubstituted naphthoquinone **2** were unsuccessful. Hydrolysis of methyl acrylate **57** did not produce the expected acrylic acid **52**, however delivered the conjugate addition products **58** (68 %) and **59** (6 %).

REFERENCES

i. Brimble, M. A. (2000). Synthetic studies toward pyranonaphthoquinone antibodies. *Pure and Applied Chemistry*, *72*(9), 1635–1639.
ii. Fernandes, R. A., Chavan, V. P., & Ingle, A. B. (2008). A short enantioselective synthesis of (+)-eleutherin, (+)-allo-eleutherin and a formal synthesis of (+)-nocardione B. *Tetrahedron Letters*, *49*(44), 6341-6343.
iii. Heapy, A. M., Patterson, A. V., Smaill, J. B., Jamieson, S. M. F., Guise, C. P., Sperry, J., Brimble, M. A. (2013). Synthesis and cytotoxicity of pyranonaphthoquinone natural product analogues under bioreductive conditions. *Bioorganic & Medicinal Chemistry*, *21*(24), 7971-7980.
iv. Pracayasittikul, V., Pingaew, R., Worachartcheewan, A., Nantasenamat, C., Pracayasittikul, S., Ruchirawat, S., & Pracayasittikul, V. (2014). Synthesis, anticancer activity and QSAR study of 1,4-naphthoquinone derivatives. *Europian Journal of Medicinal Chemistry, 84*, 247-263.
v. Sperry, J., Bachu, P., & Brimble, M. A. (2008). Pyranonaphthoquinones-isolation, biological activity and synthesis. *The Royal Society of Chemistry*, *25*(2), 376-400.
vi. Insanu, M., Kusmardiyani, S., & Hartati, R., (2014). Recent studies of the phytochemicals and pharmacological effects of *Eleutherine americana Merr*. *Procedia Chemistry*, *13*, 221-228.

JUNIOR SCIENCE COMMUNICATION
https://jscfsg.uitm.edu.my/
Volume 2 (2019)
eISSN 2637-0689

Colloquium of Chemistry and Environment 2018
Faculty of Applied Sciences, Universiti Teknologi MARA, Shah Alam.

ACETYLCHOLINESTERASE INHIBITORY, RADICAL SCAVENGING ACTIVITY(DPPH) AND PHYTOCHEMICAL SCREENING OF *Nigella sativa* (BLACK CUMIN) EXTRACTS

Nur'Amirah Binti Kamaruddin[1]*, Norizan Ahmat [1,2], M. Hamizan M. Isa[1,2]
[1]Faculty of Applied Sciences, Universiti Teknologi MARA, 40450 Shah Alam, Selangor, Malaysia.
[2]Atta-ur-Rahman Institute for Natural Product Discovery, Universiti Teknologi MARA, Cawangan Selangor, Kampus Puncak Alam, 42300 Bandar Puncak Alam, Selangor, Malaysia.

*noriz118@uitm.edu.my

Abstract: *Nigella sativa* in an annual flowering plant that comes from Ranunculacea family and it is widely distributed in the Middle East and Southeast Asia. İt is also known as black seed and and widely used as herbal medicine for the treatment of asthma, and possess antioxidants, antimicrobial, antidiabetic and other activities. This study investigates the antioxidant activity, neurodegenerative effect and the compounds present during phytochemical screening of the extracts. The seeds of *Nigella sativa* were purchased in Mecca, Saudi Arabia somewhere in 2012. The solvents used for the extraction technique was hexane, chloroform, ethyl acetate, methanol and water. Five extracts (hexane, chloroform, ethyl acetate, methanol and aqueous) were successfully extracted using sequential solvent extraction technique and subjected to phytochemical screening, antioxidant and acetylcholinesterase inhibitory activities. These extracts were tested against AChE inhibition and DPPH radical scavenging activities and phytochemical screening. The phytochemical screening result showed that tannin and terpene presence in four out of five extracts. This is further supported by the presence of their peaks in the NMR spectra of chloroform and ethyl acetate extracts. For acethylcholinesterase (AChE) inhibition activity, hexane extract showed the highest inhibition which was 64%. For DPPH radical scavenging activity, hexane and chloroform showed the highest inhibitions which were 65% and 53%, respectively. From the results obtained, the seed of *Nigella sativa* can give different antioxidant and AchE profile when extracted with different solvents. All five extracts of the *Nigella sativa* seeds showed both ability of inhibiting the DPPH radical scavenging and acetylcholinesterase activities. Chloroform extract exhibited the highest AchE inhibition and DPPH radical scavenging activities at 49.52% and 53.00%, respectively. From the ^{1}H NMR spectra, it showed the presence of flavonoid, sugar and carbohydrate, olefinic, hydroxyl group, -OH and aromatic ring in the extracts.

Keywords: *Nigella sativa, acethylcholinesterase (AchE), DPPH, antioxidant, neurodegeneration.*

INTRODUCTION

Nigella sativa is an annual flowering plant that is widely distributed in Middle East and Southeast of Asia (Kooti *et al*., 2016). Its characteristics include white, pale blue or pale purple delicate flowers of 5-10 petals, black seeds with whitish interior follicles within fruits (Majdalawieh & Fayyad, 2016). The black seeds also known as "Habba Al-Sauda" have many pharmacological effects such as anti-inflammatory, antimicrobial, antioxidant and anticancer (Aljabre *et al*, 2015). According to study done by Farag *et al.* (2014), *Nigella sativa* produces phytochemicals such as proteins, flavonoids, glycosides, alkaloid and saponins. The action of antioxidant enzymes was improved by *Nigella sativa* and acts as free radical scavenger (Gholamnezhad *et al*., 2015).

METHODOLOGY

Colloquium of Chemistry and Environment 2018
Faculty of Applied Sciences, Universiti Teknologi MARA, Shah Alam.

First, the seeds of *Nigella sativa* were extracted using five different sequential solvent extractions to produce hexane, chloroform, ethyl acetate, methanol and aqueous extracts. The seeds were submerged into each solvent used overnight and then dried using rotary evaporator. The extracts were kept in room temperature prior to analysis. The extracts were filtered and then subjected to phytochemical screenings which compose of Shinoda test for flavonoid, Mayer test for alkaloid, saponin test, tannin test and test for terpenoid to determine the presence of the compounds. The extracts were tested against acetylcholinesterase inhibitory activity (AChE) using acetylthiocholine as the substrate and DTNB was used as measurement of the AChE activity. Yellow colour solution was the result of DTNB react with tiocholine, catalyzed by enzyme in a 96-well microplate reader. The experiment was carried out in triplicates. DPPH radical scavenging activity was carried out to determine the antioxidant property. This was also done in a 96-wall microplate reader in which stock sample of 4 mg/ml were prepared. Seven dilutions ranging from 2000 to 31.24 µg/ml was prepared with final volume reached 100 µl. DPPH solution added to each well and incubated in dark for 30 minutes. The absorbance was read at 517nm and the results were expressed as IC_{50}. NMR spectra were acquired for all extracts to correlate with the phytochemical screening done.

FINDINGS

Phytochemical screening

The phytochemical screening results were shown in Table 1. The presence of tannin and terpene were detected in four out of five extracts and their presence were supported by the peaks present in the NMR spectrum of chloroform, ethyl acetate and methanol. Terpene showed highest content in the methanol extract. Flavonoid, saponin and tannin were also found in methanol extract in moderate amount.

Table 1 Phytochemical screening on extracts of *Nigella sativa*

Tests / Solvent Extract	Flavonoid	Alkaloid	Saponin	Tannin	Terpenoid
Hexane, H	-	-	-	-	-
Chloroform, C	+	-	-	+	++
Ethyl acetate, EA	+	-	-	++	++
Methanol, M	++	-	++	++	+++
Aqueous, Aq	-	-	+	++	-

Acetylcholinesterase inhibitory activity

The results obtained from this study shows that the seeds of *Nigella sativa* gave different antioxidant and AcHE inhibition profile when extracted using different type of solvent. Acetylcholinesterase assay results are shown in Table 2, the highest inhibition with value of 64.1% was shown by the hexane extract, while methanol extract showed the lowest inhibition with 30.04%. This value is better than value given by serine (positive control). Study done by Ahmed *et al*. (2013) showed that the compounds present in the hexane extract which is normally terpene had the potential of AChE inhibitory activity thus making it a promising candidate to be used as cholinesterase inhibitors.

Table 2 Percent inhibition of Nigella sativa seed extract on AChE activity

Sample extract	% inhibition
Hexane (H)	64.10
Chloroform (C)	49.52
Ethyl acetate (EA)	32.42
Methanol (M)	30.04
Aqueous (Aq)	40.66
Eserine (Positive control)	55.54

DPPH Radical Scavenging Activity

The DPPH radical scavenging activity result is shown in Table 3, hexane and chloroform extracts showed the highest radical scavenging activity with value of 65.15% and 53%, respectively. This suggest that non polar and moderately polar compound attribute to the good radical scavenging. According to study done by Brewer (2011), the compounds present in the extracts which are phenolic, diterpenes and flavonoid can inhibit the radical formation and interrupt propagation of autoxidation and these compounds were found in the extracts.

Table 3 Percent inhibition of DPPH radical scavenging activity on the seed extracts

Sample extract	% Inhibition
Hexane	65.15
Chloroform	53.00
Ethyl acetate	43.95
Methanol	29.81
Aqueous	2.83

CONCLUSIONS

In conclusion, the seeds of *Nigella sativa* gave different phytochemical screening results when extracted with different type of solvents. The extracts showed both ability on inhibiting the DPPH radical scavenging and cholinesterase activity. The highest value of inhibition of 64.1% was shown by hexane extract on the AChE inhibitory activity. For DPPH activity, hexane and chloroform showed 65.15% 53.00% inhibition, respectively, which supports the connection between antioxidant and neurodegenerative properties. From the ^{1}H NMR spectra, it showed the presence of flavonoid, sugar and carbohydrate, olefinic, hydroxyl group, -OH and aromatic ring in the extracts. Hexane extract of *Nigella sativa* was found to possess the potential to be used to treat Alzheimer's subject for further research.

REFERENCES

i. Ahmed, F., Ghalib, RM., Sasikala, P. & Ahmed K. K. (2013). Cholinesterase inhibitors from botanicals. *Pharmacogn Review*, *7*(14), 121-130.
ii. Aljabre, S.H.M., Alakloby, O. M. & Randhawa M.A. (2015). Dermatological effects of Nigella sativa. *Journal of Dermatology & Dermatologic Surgery*, *19*, 92-98.

iii. Brewer, M. S. (2011). Natural Antioxidants: Sources, Compounds Mechanisms of Action, and Potential Applications. *Comprehensive Reviews in Food Science and Food Safety*, *10*(4), 221-247.
iv. Farag, M.A., Gad, H.A., Heiss, A.G. & Wessjohann, L.A. (2014). Metabolomics driven analysis of six Nigella species seeds via UPLC-qTOF-MS and GC-MS coupled to chemometrics. *Food Chemistry*, *151*, 333–342.
v. Gholamnezhad, Z., Keyhanmanesh, R., & Boskabady, M.H. (2015). Anti-inflammatory, antioxidant, and immunomodulatory aspects of Nigella sativa for its preventive and bronchodilatory effects on obstructive respiratory disease. *Journal of Functional Foods*, *17*, 910–927.
vi. Kooti, W., Hasanzadeh-Noohi, Z., Sharafi-Ahvazi, N., Asadi-Samani M. & Ashtary-Larky, D. (2016). Phytochemistry, pharmacology, and therapeutic uses of black seed (nigella sativa). *Chinese Journal of Natural Medicines*, *14*(10), 732-745.
vii. Majdalawieh, A.F. & Fayyad, M.W. (2016). Recent advances on the anti-cancer properties of Nigella sativa, a widely used food additive. *Journal of Ayurveda and Integrative Medicine*, 7(3), 173-180.

JUNIOR SCIENCE COMMUNICATION
https://jscfsg.uitm.edu.my/
Volume 2 (2019)
eISSN 2637-0689

Colloquium of Chemistry and Environment 2018
Faculty of Applied Sciences, Universiti Teknologi MARA, Shah Alam.

ANALYSIS OF VOLATILE COMPOUNDS IN DIFFERENT VARIETIES OF PINEAPPLE USING HEADSPACE SOLID PHASE MICROEXTRACTION (HS-SPME) AND GAS CHROMATOGRAPHY-MASS SPECTROMETRY DETECTOR (GC-MSD)

Nur Fatin Najwa Mohd Isa and Rozita Osman*
Faculty of Applied Sciences, Universiti Teknologi MARA, 40450 Shah Alam, Selangor, Malaysia.

*rozit471@uitm.edu.my

Abstract: This study was conducted to identify the volatile compounds in different varieties of pineapples (Josephine, Morris, Sarawak and MD2) using headspace solid phase microextraction and gas chromatography-mass spectrometry (HS-SPME-GC-MS). The volatile compounds from these samples were extracted using CAR/PDMS SPME fiber prior to GC-MS analysis. The volatile compounds extracted from these varieties were compared. Josephine pineapple consist of 35 volatile compounds, while 18 and 28 volatile compounds were identified from Morris and MD2 pineapples, respectively. Less volatile compounds (10) volatile compounds were found in Sarawak pineapple. Similarities and differences of different pineapple varieties were observed. The major volatiles composition in pineapple was from ester group. Four similar compounds from this group were identified, which were methyl hexanoate, methyl butyrate, methyl-2-methylbutyrate and methyl octanoate. The differences of those pineapples were only Josephine pineapple consist of alkane compounds, while MD2 pineapple contains alkene and alcohol compounds. Moreover, Sarawak pineapple has only amine and ester groups as compared to other varieties of pineapple that consist of more than two functional groups.

Keywords: *Pineapple, Headspace Solid Phase Microextraction, Gas Chromatography*

INTRODUCTION

Pineapple (*Ananas comosus* L.) is widely cultivated in tropical countries including Malaysia (Yapo *et. al*, 2011). This plant is cultivated predominantly for its fruit and one of the commercially important fruit crops in Malaysia. The volatile organic compounds in the pineapple is responsible on giving the pineapple's flavor, sweetness and odour. The quality control and classification of pineapple in Malaysia is based on physical appearance made by the agricultural officer. Some extraction methods have been used to extract the volatile compounds from pineapples are hydro-distillation and liquid-liquid extraction. However, these techniques often required large amounts of solvent and time-consuming. Thus, the environmental friendly sample pretreatments technique must be employed as well as fast chemical analysis. Solid phase microextraction (SPME) method technique was applied for extraction as it is faster, easier and solventless sampling. This approach was proved to be the most favorable technique as it has been used by many researchers in extracting volatile compounds in different part of pineapple (Wei *et al*., 2011; Pino & Quieris, 2010). In this study, SPME technique was applied in extracting volatile compounds from four pineapple varieties (Josephine, Morris, Sarawak and MD2) prior to identification of the compounds by gas chromatography-mass spectrometry.

METHODOLOGY

Colloquium of Chemistry and Environment 2018
Faculty of Applied Sciences, Universiti Teknologi MARA, Shah Alam.

The pineapples were peeled, sliced and homogenized using a blender to become a pulp. Pineapple pulp (5 g) and 2 g of deionized water was placed into 12 mL SPME vial. The vial was capped and placed into hot water bath at 55℃ for 34 minutes. Then, the fiber was desorbed into GC-MS the injector port with desorption time of 20 minutes. The identification of volatile compound was conducted by comparing the mass spectra obtained with database in National Institute Standard and Technology 14 (NIST14) library with the percent quality above 80%.

FINDINGS

Common volatile compounds that contributed to the flavor of pineapple were grouped as alcohols, esters, aldehydes, ketones and terpenes functional groups. In this study, the volatiles compounds obtained from four pineapple varieties (Josaphine, Morris, MD2 and Sarawak) were classified into ester, alkene, terpene, alkane, amine, amide, alcohol and phenyl functional groups. Ester and terpenes are the major functional groups for these varieties as shown in Figure 1. Josephine pineapple has the highest number of terpene compounds, while no terpene was detected in Sarawak variety. MD2 pineapple has the highest number of ester compounds followed by Morris and Sarawak varieties. Zemlicka *et al.*, (2013) reported the volatile compounds that contribute to the aroma of MD2 is mainly from ester group. Other than ester, alkene and alcohol compounds was only detected in MD2 pineapple variety.

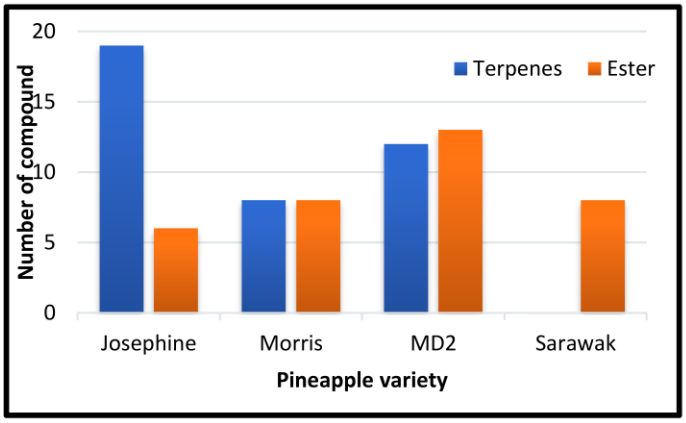

Figure 1 Major functional groups of volatile compounds in different varieties of pineapple

Different varieties of pineapple have different amounts and profile of volatile compounds. Similarity and dissimilarity of these varieties can be observed. Figure 2 shows the chromatographic fingerprints obtained from each variety of pineapple. Josephine pineapple consist of 35 volatile compounds, while 18 and 28 volatile compounds were identified from Morris and MD2 pineapples, respectively. Less volatile compounds (10) volatile compounds were found in Sarawak pineapple. Four similar compounds were identified in all varieties of pineapple which were methyl butanoate, methyl-2-methyl butanoate, methyl

hexanoate and methyl octanoate. Similar observation were reported by Calderon *et al*., (2010) and Tokitomo *et al*., (2005).

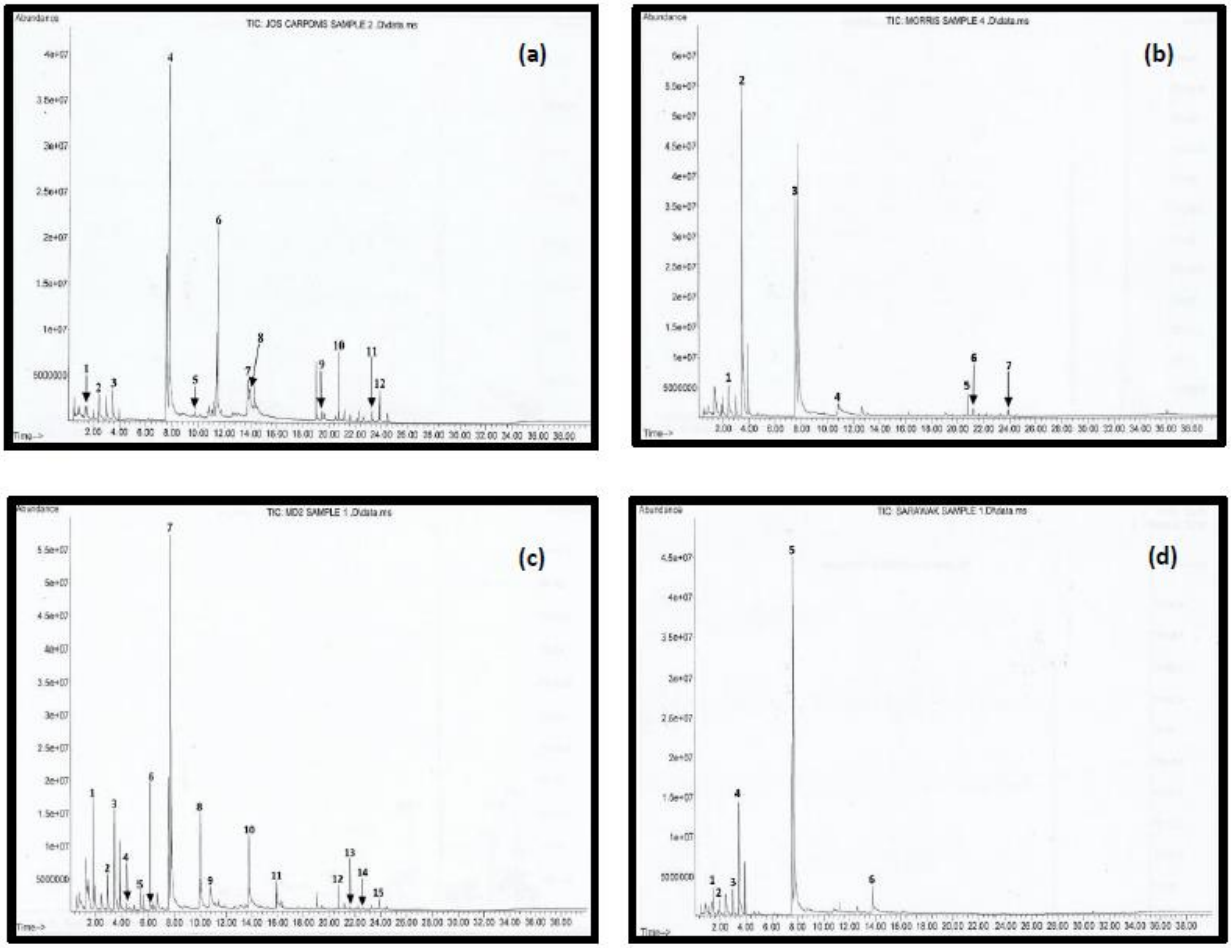

Figure 2 Chromatographic fingerprints of pineapple varieties: Josaphine (a), Morris (b), MD2 (c) and Sarawak (d).

CONCLUSIONS

The highest number of volatile compounds in the pineapple varieties are from ester group. These compounds contributed to the aroma and flavour of the pineapple. Methyl butyrate, methyl-2-methyl butyrate, methyl hexanoate and methyl octanoate were detected in all pineapple varieties. Different varieties of pineapple have different volatile compounds, thus, the distinctive compounds can be used as marker compounds for that particular type of pineapple.

Volume 2 (2019)
eISSN 2637-0689

REFERENCES

i. Calderón, M., Rojas-Graü, M. A., & Martín-Belloso, O. (2008). Effect of packaging conditions on quality and shelf-life of fresh-cut pineapple (Ananas comosus). *Postharvest biology and technology*, *50*(2-3), 182-189.
ii. Pino, J. A., & Queris, O. (2010). Analysis of volatile compounds of pineapple wine using solid-phase microextraction techniques. *Food Chemistry*, *122*(4), 1241-1246.
iii. Yapo, E.S., Kouakou, H.T., Kouakou, L.K., Kouadio, J.Y., Kouame, P., Mérillon, J. (2011) Phenolic profiles of pineapple fruits (Ananas comosus L. Merrill) Influence of the origin of suckers. *Australian Journal of Basic and Applied Sciences*, *5*, 1372-1378.
iv. Tokitomo, Y. M. S., Andrea Büttner & Peter Schieberle (2005). Odor-Active Constituents in Fresh Pineapple (*Ananas comosus* [L.] Merr.) by Quantitative and Sensory Evaluation. *Bioscience Biotechnology Biochemistry*, *69*(7), 1323–1330.
v. Wei, C. B., Liu, S. H., Liu, Y. G., Lv, L. L., Yang, W. X., & Sun, G. M. (2011). Characteristic aroma compounds from different pineapple parts. *Molecules*, *16*(6), 5104-5112.
vi. Žemlička, L., Fodran, P., Kolek, E., & Prónayová, N. (2013). Analysis of natural aroma and flavor of MD2 pineapple variety (*Ananas comosus* [L.] Merr.). *Acta Chimica Slovaca*, *6*(1), 123-128.

JUNIOR SCIENCE COMMUNICATION
https://jscfsg.uitm.edu.my/
Volume 2 (2019)
eISSN 2637-0689

Colloquium of Chemistry and Environment 2018
Faculty of Applied Sciences, Universiti Teknologi MARA, Shah Alam.

DETERMINATION OF FATTY ACID IN FRESH COOKING OIL AND USED COOKING OIL

Nur Fatima Mohd Arsad, Zuraidah Abdullah Munir*
School of Chemistry, Faculty of Applied Sciences, Universiti Teknologi MARA, 40450 Shah Alam, Selangor.

*zurai394@uitm.edu.my

Abstract: Fatty acid in fresh and used (1-5 times) cooking oil was determined by using gas chromatography flame ionization detector (GC-FID) and gas chromatography mass spectrometry detector (GC-MSD). The injector port and detector temperatures for GC-FID analysis were 25˚C with 70.0 mLs^{-1} carrier gas flow, while for GC-MSD analysis, the injector port and detector temperatures were 200˚C and 300˚C, respectively, with 1.0 $mLmin^{-1}$carrier gas flow. The concentrations of fatty acid; methyl laurate, methyl myristate, methyl palmitate, methyl stearate and methyl linoleate in fresh cooking oil and used (1-5 times) cooking oil were compared. The FRESH cooking oil sample has the highest amount of fatty acids which were methyl laurate (71.3 ppm), methyl myristate (1505.7 ppm), methyl palmitate (355973.7 ppm), methyl stearate (63702.7 ppm) and methyl linoleate (12894.6 ppm). The cooking oil for COOK4 sample (used four times) has the lowest amount of fatty acids which were methyl laurate (14.5 ppm), methyl myristate (203.3 ppm), methyl palmitate (43635.8 ppm), methyl stearate (7265.1 ppm) and methyl linoleate (2074.6 ppm). Based on this study, the fatty acid content decreases after using one time, then increases for 2nd and 3rd times using the oil. The pattern repeats to 5th time using the oil.

Keywords: *concentration of fatty acid, fresh cooking oil, used cooking oil*

INTRODUCTION

Palm oil is derived from the flesh of the fruit of the oil palm species *E. guineensis*. Palm oil has a balanced fatty acid composition in which the level of saturated fatty acids is almost equal to that of the unsaturated fatty acids (Ibrahim, 2013). Cooking palm oil is commonly used for frying and since it is so frequently used, people tend to reuse it several times. Reusing cooking oil after frying food can be very harmful to health. A study conducted by the students of Surgical Gastroenterology Department at the Madras Medical College (MMC) revealed that 90% of patients suffering from oesophagus cancer are due to consuming food prepared with reused cooking oil. The food cooked with reused oil can be carcinogenic (Adavi, 2015). As frying oil can cause some of unsaturated fatty acid in the oil to polymerize, thus, reusing the oil can cause imbalance to the fatty acid composition.

METHODOLOGY

Six samples of cooking palm oil (fresh and 1-5 times used) were collected from the local street vendor for this analysis. A 0.5 M methanolic solution and esterification reagent were added into each sample and refluxed for 3 to 4 minutes. The mixture was then transferred into a separatory flask. Next, saturated NaCl and diethyl ether were added and the mixture was shaken vigorously for 2 minutes. The aqueous layer was discarded and the organic layer was transferred into a vial. Five standard solutions of fatty acid methyl esters (FAME) were prepared with different concentrations. The standard fatty acids for this study were methyl laurate, methyl myristate, methyl palmitate, methyl stearate and methyl linoleate. A 0.4 µL of each standard esters and derivatized samples were injected into the column and the injection were repeated to

Colloquium of Chemistry and Environment 2018
Faculty of Applied Sciences, Universiti Teknologi MARA, Shah Alam.

get reproducible peak areas. Using the data from the standard esters, the amount of each fatty acid in the samples was calculated. The GC-FID was used to determine the fatty acid contents in the cooking oil samples while the GC-MSD was used to detect presence of other volatile compounds in the samples.

FINDINGS

FRESH cooking oil sample had the highest amount of each fatty acid while COOK4 cooking oil had the lowest amount of each fatty acid. Figure 1 compares the amount of fatty acids in cooking oil samples.

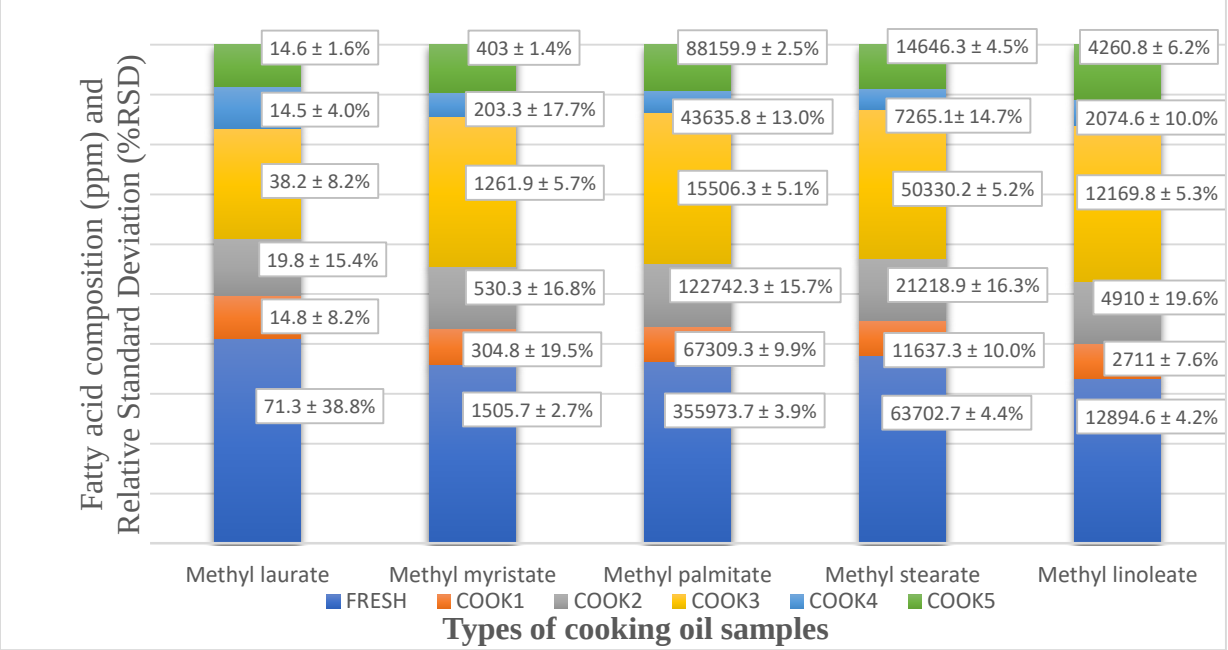

Figure 1 Average amount of fatty acid (ppm) and relative standard deviation (%RSD) in cooking oil samples

Figure 1 shows the decrease trend of fatty acid after 1 time used, followed by increased amount at 2 and 3 times using the oil. The pattern repeats to 5 times using the oil. The fatty acid content decreases thus reduce its nutritional values. According to Choe and Min, (2007), frying time and temperature during frying could affect the deterioration of oil. Frying time will increase the contents of free fatty acid while high frying temperature will accelerate the thermal oxidation and polymerization of oils (Mazza and Qi, 1992). Since the oil samples were taken from local street vendor, the temperature for each time the oil sample was used was not fixed, therefore may cause the decreasing trend of fatty acid not being consistent. During the process of frying, new compounds are formed as a result of oxidation, polymerization and hydrolysis, which substantially modify the composition of the oil and its nutritional quality (Dobarganes *et al*., 2000). Spanish

researchers found that people who re-used any types of oil many times are more likely to have high blood pressure than people who always change their cooking oil (Atherton, 2003).
Other major compounds were also determined for different number of times the cooking oil was used. Table 1 shows other major compounds in each cooking oil sample.

Table 1Other major compounds in six types of cooking oil samples

Volatile Compounds	Common name	Cooking oil samples					
		FRESH	COOK1	COOK2	COOK3	COOK4	COOK5
Pentadecanoic acid	Pentadecylic acid	/	/	/	/	/	/
9-Octadecenoic acid (z)	Oleic acid	/	/	/	/	/	/
Eicosanoic acid	Arachidic acid	/					
Butylated hydroxytoluene	**Butylhydroxy toluene**					/	/

For instance, eicosanoic acid compound can only be found in FRESH cooking oil sample. Eicosanoic acid helps in increasing the muscle mass (Markworth and Cameron-Smith, 2012). On the other hand, butylated hydroxytoluene was only found in COOK4 and COOK5 (used 4 and 5 times) samples. Butylated hydroxytoluene is cancer risk, can cause asthma and behavioural issues in children (Cancer, 1994).

CONCLUSIONS

Based on this study, all five fatty acids analysed were present in all samples. FRESH cooking oil sample had the highest amount for each fatty acid while COOK4 cooking oil sample had the lowest amount for each fatty acid. Eicosanoic acid which is beneficial was found only in FRESH cooking oil sample while butylated hydroxytoluene which can cause cancer was found in COOK4 and COOK5, but not in the first three batches of used cooking oil. Based on this study, it can be concluded that in general the more times the cooking oil was used, the lower the fatty acid content, the lower the quality of the oil and the higher the risk of danger to our health due to presence of high risk compounds.

Volume 2 (2019)
eISSN 2637-0689

REFERENCES

i. Adavi, P. (2015). Reusing Cooking Oil? Not a Great Idea. Retrieved from http://www.indiajournal.com
ii. Atherton, M. (2003). Heart Attack Warning. Retrieved from http://www.preventdisease.com
iii. Cancer, I.A.f.R.o. (1994). IARC monographs on the evaluation of carcinogenic risks to humans, Vol 59 (International Agency for Research on Cancer).
iv. Choe, E., and Min, D. (2007). Chemistry of deep-fat frying oils. *Journal of food science 72*.
v. Dobarganes, C., Márquez-Ruiz, G., and Velasco, J. (2000). Interactions between fat and food during deep-frying. *European Journal of Lipid Science and Technology 102*, 521-528.
vi. Ibrahim, N.A. (2013). Characteristics of Malaysian palm kernel and its products. *Journal of Oil Palm Research 25*, 245-252.
vii. Markworth, J.F., and Cameron-Smith, D. (2012). Arachidonic acid supplementation enhances in vitro skeletal muscle cell growth via a COX-2-dependent pathway. *American Journal of Physiology-Cell Physiology 304*, C56-C67.
viii. Mazza, G., and Qi, H. (1992). Effect of after-cooking darkening inhibitors on stability of frying oil and quality of French fries. *Journal of the American Oil Chemists Society 69*, 847-853.

JUNIOR SCIENCE COMMUNICATION
https://jscfsg.uitm.edu.my/
Volume 2 (2019)
eISSN 2637-0689

Colloquium of Chemistry and Environment 2018
Faculty of Applied Sciences, Universiti Teknologi MARA, Shah Alam.

BIODIESEL PRODUCTION VIA ESTERIFICATION OF PALM FATTY ACID DISTILLATE OVER SUPERACID SO_4^{2-}/SnO_2 CATALYST

Nur Nabihah Mohammad Fauzi[1], Mohd Sufri Mastuli[1,2]*

[1]Faculty of Applied Sciences, Universiti Teknologi MARA, 40450 Shah Alam, Selangor, Malaysia.
[2]Centre for Nanomaterials Research, Institute of Science, Universiti Teknologi MARA, 40450 Shah Alam, Selangor, Malaysia

*mohdsufri@uitm.edu.my

Abstract: Fatty acid methyl ester (FAME) produced by esterification reaction of palm fatty acid distillate (PFAD) is considered as environmental friendly process for the production of biodiesel, a sustainable alternative fuel to replace the dependency on the petroleum. In this work, SO_4^{2-}/SnO_2 catalyst via self-propagating combustion (SPC) was successfully synthesized and used to convert the FFA of the PFAD into FAME. It was found that SO_4^{2-}/SnO_2 catalyst rendered high FFA conversion up to 90 %, indicating high strong acidic sites plays key role in esterification of PFAD. The physico-chemical properties of SO_4^{2-}/SnO_2 catalysts were characterized by using X-ray diffraction (XRD), temperature programmed desorption-ammonia (TPD-NH_3) and Brunauer–Emmett–Teller (BET) surface area. The total acidity and specific surface area of catalysts were increased significantly after being treated by chlorosulfonic acid (HSO_3Cl). From this study, it was found that an optimum biodiesel yield of 98.94% can be attained at following reaction condition: 1) methanol to PFAD molar ratio: 9:1, 2) catalyst loading: 4 wt%, 3) reaction temperature: 100 °C and 4) reaction time: 3 h.

Keywords**:** SO_4^{2-}/SnO_2, Biodiesel, PFAD, Esterification, Catalyst

INTRODUCTION

Excessive use of non-renewable fuel in transportation and industry, leads to the twin crises of fossil fuel depletion and environmental degradation. As the fossil fuels are limited and it takes million of years to be produced, their availability may be prolonged by decreasing overall consumption. Following this issue, various renewable sources of energy have successfully been tested to replace the dependency on fossil fuel consumption. However, the alternate resources of biodiesel from edible oils lead to the hurdle of foods versus fuel and higher production cost is spent compared to the diesel production. Thus, attempts are constantly being made to lower the feedstock cost by using palm fatty acid distillate (PFAD). PFAD contains more than 80% of free fatty acid (FFA), so it is compulsory to use superacid catalyst in esterification for the biodiesel production. Various heterogenous catalysts based on transition metals (mixed oxides, supported oxides, sulfated) have been used during the esterification reaction (Kapor *et al*., 2017). However, these transition metal oxide catalysts are expensive. Herein, the SO_4^{2-}/SnO_2 as superacid solid catalyst was synthesized using a self-propagating combustion (SPC) method. Their catalytic performances were evaluated in esterification of PFAD feedstock into biodiesel.

Colloquium of Chemistry and Environment 2018
Faculty of Applied Sciences, Universiti Teknologi MARA, Shah Alam.

METHODOLOGY

Self-propagating combustion (SPC) method was used to synthesize the SnO_2 catalyst and the sulfated SnO_2 was prepared according to the reported method (Wang *et al*. 2018). Various techniques were used to characterize the synthesized catalysts such as X-Ray diffraction (XRD), Brunauer-Emmett-Teller (BET) method and temperature-programmed desorption of ammonia (TPD-NH_3). Esterification reaction of PFAD with methanol was carried out in a reflux setup that equipped with thermometer. About 5.0 g of PFAD was added into 100 mL round-bottom flask, followed by the addition of methanol and small amount of catalyst before connected to reflux system. The catalyst was separated from the solid catalyst by centrifugation at 500 rpm for 5 min and followed by the methanol recovery process. The reaction parameters involved in this process was methanol to oil feedstock molar ratio, catalysts loading, temperature and time.

RESULTS & DISCUSSION

Figure 1(a) shows the XRD patterns for the studied catalysts and indexed to the tetragonal crystal structure with space group of P42/mnm as agreed in ICDD No. 01-077-0448. All the catalysts found to be pure without the presence of impurities. However, the crystallinity for both SnO_2 catalysts are decreased after sulfated indicating the presence of SO_4^{2-} ion on the surface of the SnO_2 catalysts. It means that the specific surface area for both catalysts would decreased as expected in Table 1. The SO_4^{2-}/SnO_2-spc has high acid density of 4986.0 μmol g-1 as compared to 1775.5 μmol g-1 for the SO_4^{2-}/SnO_2-com. In addition, both sulfated catalysts have high acidity strength (SO_4^{2-}/SnO_2-spc > SO_4^{2-}/SnO_2-com) as appeared at temperature of above 700 °C that can be seen clearly from the TPD-NH_3 profiles (Figure. 1(b)). It is worthy to mention that the SO_4^{2-}/SnO_2-spc exhibited higher density and strength of acid active sites compared to the other catalysts. The superacid SO_4^{2-}/SnO_2-spc catalyst was used to esterify the PFAD feedstock. It has found that 98.94 % of FFA conversion can be achieved at 9:1 of methanol to PFAD molar ratio, 4 wt.% of catalyst, 100 °C of temperature and 3 h of reaction time

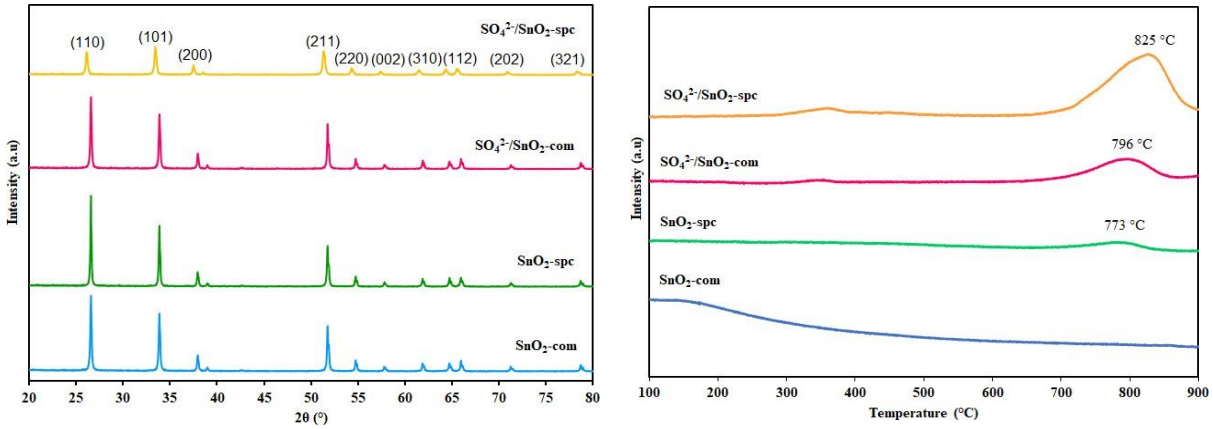

(a) **(b)**

Figure 1 (a) XRD patterns and (b) TPD-NH_3 profiles of commercialized and synthesized SnO_2 catalysts.

Colloquium of Chemistry and Environment 2018
Faculty of Applied Sciences, Universiti Teknologi MARA, Shah Alam.

Table **1** Textural properties of SnO_2 based catalysts.

Catalyst	Specific surface area[a] ($m^2 g^{-1}$)	TPD-NH_3[b]	
		Temperature (°C)	Amount of acidity ($\mu mol\ g^{-1}$)
SnO_2-com	6.76	ND*	ND*
SnO_2-spc	7.46	773	72.6
SO_4^{2-}/SnO_2-com	6.70	796	1775.5
SO_4^{2-}/SnO_2-spc	2.03	825	4986.0

*Not detected.
[a]Calculated by BET analysis.
[b]Determined by TPD-NH_3.

CONCLUSIONS

Superacid solid catalysts such as SnO_2-com, SnO_2-spc, SO_4^{2-}/SnO_2-com and SO_4^{2-}/SnO_2-spc were synthesized using a self-propagating combustion (SPC) method. Among the catalysts, the SO_4^{2-}/SnO_2-spc catalyst has the highest density of active sites and the strongest of acidity strength that beneficial for the esterification of PFAD feedstock resulted 98.94% of FFA conversion.

REFERENCES

i. Kapor, A., Zaheera, A., Gaanty, R. M., Ab.Rahim, M. H. and Yusoff, M. M. (2017). Palm Fatty Acid Distillate as a Potential Source for Biodiesel Production-a Review, *Journal of Cleaner Production, 143*,1–9.

ii. Wang, Tianqi, Xu, Y., He, Z., Zhou, M., Yu, W., Shi, B., Song, C. and Huang, K. (2018). Fabrication of Sulphonated Hollow Porous Nanospheres and Their Remarkably Improved Catalytic Performance for Biodiesel Synthesis, *Reactive and Functional Polymers*, *132*, 98–103.

JUNIOR SCIENCE COMMUNICATION
https://jscfsg.uitm.edu.my/
Volume 2 (2019)
eISSN 2637-0689

Colloquium of Chemistry and Environment 2018
Faculty of Applied Sciences, Universiti Teknologi MARA, Shah Alam.

ANALYSIS OF VOLATILE HYDROCARBON COMPOUNDS OF DIESEL IN SOIL

Nur Shahz Ereena Zulkifli[1*], Muhammad Afiq Huri[2], Reena Abd Rashid[1]
[1]Faculty of Applied Science, Universiti Teknologi MARA, 40450, Shah Alam, Selangor, Malaysia.
[2]Faculty of Science, Universiti Teknologi Malaysia, 81310, Skudai, Johor Bharu, Malaysia.

*reena1572@uitm.edu.my

Abstract: Diesel tends to be the most common ignitable liquid used in arson after petrol. Besides fire debris, soil are considered to be a prominent evidence in arson cases as the fire debris will eventually land on the ground and it can be transported using shoes sole or by adhering to other materials. Detection of diesel residue from the soil can provide an important information to link evidence with the fire scene in arson cases. Thus this study was conducted to identify and quantify volatile diesel hydrocarbons present in soil and to observe the decomposition rate of diesel volatile hydrocarbons in soil over a specific period of time (5 days). The procedures begin by spiking the diesel to ten grams of soil sample. On day 1, day 3 and day 5, sample are extracted using liquid-liquid extraction method (LLE) which involved hexane and ultrapure water. The extract will later be analyzed using Gas Chromatography-Mass Spectrometry to identify five most prominent hydrocarbon peaks and will be considered to be used as standard. The five compound was later prepared in 50 to 300ppm to be analyzed using GC-Flame Ionization Detector (GC-FID). Calibration curve of the standards was plotted to obtained the concentration of the five prominent hydrocarbon in soil sample. Calibration curve for each five individual hydrocarbon standard has R^2 value > 0.99. Diesel hydrocarbon compound exhibit decreasing value from day 1 to day 5 and diesel decomposition rate in soil for day 1, day 3 and day 5 after exposure, was observed based on the decreasing value in soil pH, electrical conductivity and moisture value.

***Keywords*:** *Diesel residue, Ignitable liquid (IL), Volatile diesel hydrocarbon and Liquid-liquid extraction method (LLE).*

INTRODUCTION

Soil sample from crime scenes in arson cases are commonly collected from loose soil evidence transported by shoes or vehicles and soil evidence from open field of the crime (Fitzpatrick *et al*., 2008) In most arson cases, accelerants are used to fuel the flame and causes the charred materials burn to ashes or fire debris and land on the ground. Volatile hydrocarbons from the accelerant or ignitable liquid such as diesel, petrol and kerosene can be firmly absorbed onto soil organic matter and is shown to be resistant to loss or alteration by minimal land activity (Sadler *et al*., 2016). Diesel are the second most used accelerant in arson cases in Malaysia after petrol, due to long lasting burning, inexpensive and can be easily obtain from shelf of a store. The detection of the accelerant has been widely studied using GC-MS, with extraction using SPME on remaining fire debris. This study is to observe the decomposition rate of diesel volatile hydrocarbons in soil over a specific period of time (5 days). And secondly, to identify and quantify the volatile hydrocarbons of diesel present in the soil sample.

METHODOLOGY

Ten gram of soil sample was collected and spiked with 2.0 mL diesel in a crucible and exposed it to room temperature for day 1 to day 5. All samples are prepared in triplicates including blank samples. On day 1,3, and 5, soil pH, electrical conductivity and moisture level was measured to study soil decomposition

rate. Volatile hydrocarbon compound from soil sample were also extracted on sample day 1, day 3 and day 5 using liquid-liquid extraction method (LLE) method with hexane and ultrapure water. Detection of the volatile hydrocarbon was conducted using Gas Chromatography coupled with Mass Spectrometry (GC-MS). Hydrocarbon compounds of diesel were identified based on the chromatogram. Five hydrocarbons which gives the most abundance peak using GC-MS were identified and used to prepare the hydrocarbon standards. The calibration curve for the hydrocarbon standards were prepared at the following concentration of 50 ppm, 100 ppm, 150 ppm, 200 ppm, 250 ppm and 300 ppm and analyzed using Gas Chromatography coupled with Flame Ionization Detector (GC-FID).

FINDINGS

The decomposition rate of diesel in soil sample from day 1 to day 5 was studied based on soil pH, electrical conductivity (EC) and soil moisture. Soil pH increases from pH 5.5 to pH 5.9 which indicate decreasing of hydrogen ions in soil samples caused by deteriorating microbial activity in soil due to presence of diesel. EC can measure the relationship between microorganism and salinity. EC reading showed increasing value from 800 to 1000 S/m which indicate increase in soil salinity caused by decreasing microbial activity (Xu *et al*., 2014). Soil moisture content from from 4% to 0.5% as oil contamination highly increases soil hydrophobicity (Adams *et al*., 2008). Soil sample from day 1, day and day 5 were analyzed using GCMS. Five major volatile hydrocarbon compounds of diesel which give the most abundance peak on the chromatogram for all sample was identified as octadecane, nonadecane, eicosane, docosane and tetracosane. These five major compound were then analyzed using GC-FID and used to plot the calibration curve. Concentration of the volatile hydrocarbons were calculated using the calibration curve and tabulated in Table 1, including Percentage (%) recovery, Limit of Detection (LOD) and Limit of quantification (LOQ). Concentration of all hydrocarbon compound in soil sample decreased from day 1 to day 5. Day 5 still exhibit the detection of the volatiles compound under room temperature exposure.

Table 1 Concentration of five major hydrocarbons of diesel in soil sample using GC-MS (*n=3*)

Hydrocarbon	t_R (min)	Day	Concentration (ppm)	% Recovery	LOD	LOQ
Octadecane	21.54	1	189.14	29.33	30.99	103.33
		3	185.72			
		5	123.2			
Nonadecane	23.63	1	1431.38	121.16	26.69	88.96
		3	1193.37			
		5	941.25			
Eicosane	25.69	1	1070.50	80.92	26.02	86.76
		3	1036.79			
		5	679.50			
Docosane	29.58	1	772.93	61.84	25.83	86.13
		3	749.23			
		5	488.84			
Tetracosane	33.19	1	499.04	21.74	27.02	90.07
		3	473.09			
		5	330.83			

CONCLUSION

The diesel composition in soil from day 1 to day 5 for each hydrocarbon standard was observed based on the decreasing value in soil pH, electrical conductivity and moisture value. The five major hydrocarbon compound in diesel ignitable liquid in soil sample are identified as octadecane, nonadecane, eicosane, docosane and tetracosane extracted using LLE and analyzed by GC-MS. Concentration of the hydrocarbon compound were calculated using the calibration curve, where the amount for all five compound indicate inclination from day 1 to day 5.

REFERENCES

i. Adams, R. H, Osorio, F. G., Cruz J.Z., (2008) Water repellency in oil contaminated sandy and clayey soils. *International Journal of Environmental Science and Technology*, *5* (4), 445-454
ii. Fitzpatrick, R. Rave, M., Forrester, F., (2008). A criminal case study involving transference of acid sulfate soil material from a crime scene to forensic evidence, Inland Acid Sulfate Soil System Across Australia, pp. 151-161
iii. Sadler, R, Maetam, B., Edokpolo, B., ConnelL, D., Yu, J., Stewart, D., Gray, D., Laksono, B., (2016) Health risk assessment for exposure to nitrate in drinking water from village wells in Semarang, Indonesia, *Environmental Pollution*, *216*, 738-745
iv. Xu, H.M, Tam, N. F., Zan, Q, J., Bai, M, Shin, P. K., Vrijmoed L.L.P., Cheung S. G., Liaw., W.B., (2014), Effects of salinity on anatomical features and physiology of a semi-mangrove plant Myoporum bontoiodes, *Marine Pollution Bulletins*, *5*(2), 738-46.

JUNIOR SCIENCE COMMUNICATION
https://jscfsg.uitm.edu.my/
Volume 2 (2019)
eISSN 2637-0689

Colloquium of Chemistry and Environment 2018
Faculty of Applied Sciences, Universiti Teknologi MARA, Shah Alam.

METHYL ORANGE REMOVAL FROM AQUEOUS MEDIUM USING MESOPOROUS SILICA MCM-41

Nur Zabirah Zabi, Wan Nazihah Wan Ibrahim*
School of Chemistry and Environment, Faculty of Applied Sciences, Universiti Teknologi MARA, 40450 Shah Alam Selangor

*wannazihah@uitm.edu.my

Abstract: The mesoporous silica MCM-41 was prepared and the removal of methyl orange (MO) using calcined MCM-41 was observed and the efficiency of the adsorption was determined using batch adsorption studies. The batch studies that were studied on was the effect of pH, initial concentration as well as contact time and it is analysed using UV-Vis spectrophotometer. The optimum conditions for this adsorption study were at pH 3, 30 minutes of contact time with initial concentration of 60 ppm with removal percentage of 40.79%. The isotherm and kinetic data obtained from this adsorption study best fit Langmuir and pseudo-second-order kinetic model.

Keywords: *methyl orange, MCM-41, UV-Vis*

INTRODUCTION

Dye is a molecule that contain chromophore and auxochrome structure. There are many types of dyes produced such as acidic, basic, disperse, azo, anthraquinone based and metal complex dyes. Azo dyes are commonly used in food and MO is one of known azo dyes (Lafi & Hafiane., 2016). All of these dyes are usually disposed to the water as it is the easiest way to remove it from the factory. These azo dyes are known to be carcinogenic organic substances due to the presence of benzidine. Besides affecting health, dyes will become major threat to aquatic life because it reduces light penetration and will eventually reduce photosynthetic activity in water (Nidheesh *et al*., 2018). Thus, removal of these dyes is required to improve the quality of water. Mobil Composition of Matter-41(MCM-41) is a good adsorbent to remove different types of dyes as the surface of the adsorbent can be easily modified. Other than that, surface area of MCM-41 is large and size of pore ranges from 20 to 100 Å (Lee *et al*., 2007).

METHODOLOGY

Method for synthesizing MCM-41 is based on the study done by Hadi *et al*. (2003). For removal experiment, 0.05 g calcined MCM-41 was added to 10 mL of dye solutions (60 -140 ppm) respectively under stirring for a certain time (10-50 min) at room temperature. The mixed solution was extracted and subsequently centrifuged to separate MCM41 and dye solution at 2500 rpm for 2 min. The concentration after various intervals of time and initial concentration were monitored immediately by measuring absorbance of the supernatant at 463 nm using a UV –Vis spectrophotometer (Lambda 35-Perkin Elmer).

Colloquium of Chemistry and Environment 2018
Faculty of Applied Sciences, Universiti Teknologi MARA, Shah Alam.

FINDINGS

Batch adsorption studies of MO using calcined MCM-41

Effect of pH

The study on effect of changing pH (3, 5, 7, 9 and 11) on percentage removal of MO was done using 80 ppm with 30 minutes contact time at room temperature. The pH of solution affected every adsorption process especially for dyes since pH controls the magnitude of electrostatic charges after dye molecules has been ionized (Salahshoor *et al*., 2014). At pH 3, the highest percentage removal of MO was obtained (58%). In acidic condition, there was high concentration of H^+ which eventually change the surface of adsorbent used and this leads to better adsorption of MO that have negative charge (Alkan *et al*., 2004). However, percentage removal of MO slightly dropped at higher pH due to competitive interaction between MO and OH^- on surface and also in the pores in the adsorbent.

Effect of initial concentration

The study on effect of using different initial concentration of MO solution (60 ppm, 80 ppm, 100 ppm, 120 ppm and 140 ppm) on percentage removal of MO was done with adsorbent dosage of 0.05 g, at pH 3 and contact time was set to 30 minutes. Initial concentration of dye will affect the amount of adsorption for dye removal. The amount of dye being adsorbed onto the adsorbent highly depends on available sites on adsorbent surface. This shows that as the concentration increases, percentage removal of dye will decrease. This is because the adsorption site is already concentrated with dye (Yagub *et al*., 2014). The optimum initial concentration is 60 ppm with percentage removal of 100%.

Effect of contact time

Efficiency of adsorbent to remove MO depends on equilibrium time. Based on contact time it can predict the mechanism of removal process (El Gamal *et al*., 2015). In this batch of study, 0.05 g of adsorbent used with pH 3 and 60 ppm of initial concentration used. The optimum contact time is 30 minutes. The percentage removal of MO at 30 minutes is 53%. At beginning of adsorption, MO concentration is high which causes the driving force between calcined MCM-41 and MO solution become larger (Lafi *et al*., 2016). Efficiency of removing dye increases to a certain extent along with increasing the contact time but further increase in contact time does not increase the adsorption rate between adsorbent and MO. Figure 1 shows the graph of percentage removal for each batch studies.

Colloquium of Chemistry and Environment 2018
Faculty of Applied Sciences, Universiti Teknologi MARA, Shah Alam.

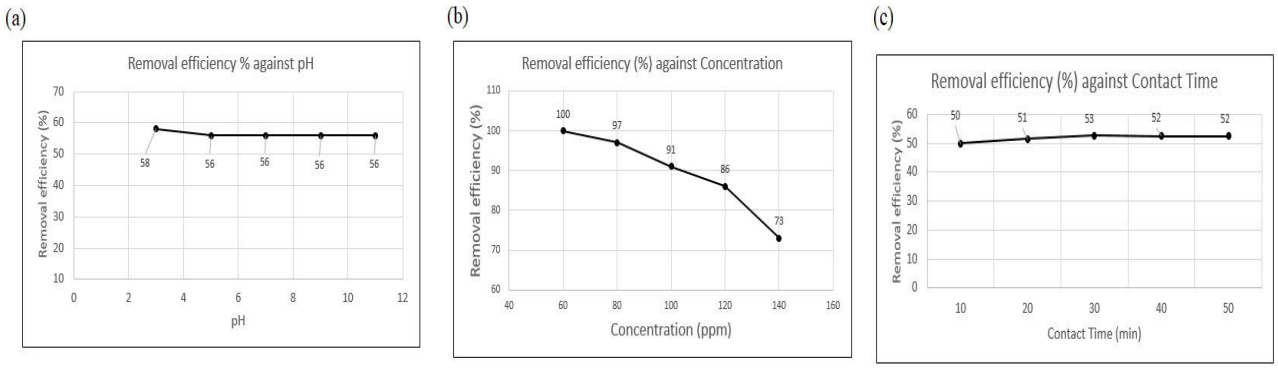

Figure 1 Graph of percentage removal for each batch studies (a) pH, (b) initial concentration and (c) contact time

Adsorption isotherm

Adsorption isotherm determine whether the adsorption reaction occurred monolayer or multilayer. It determined the ability of the adsorbent by predicting the number of adsorbate required to cover the surface of adsorbent and also internal surface of adsorbent with single molecular layer. There were two isotherm models that were studied to determine the adsorption behaviour for this study which were Langmuir and Freundlich. These two isotherm models evaluated the distribution of MO on surface of calcined MCM-41. Based on the graph, linear regression correlation coefficient, R^2 value for each isotherm model was obtained to define which model was suitable to explain the behaviour of the adsorption occur throughout the adsorption process. The R^2 value for Langmuir model was 0.9742 while Freundlich model was 0.7587. This shows that the adsorption process for removal of MO using calcined MCM-41 is best describe by Langmuir model where monolayer adsorption was taken placed during this study.

Adsorption kinetic

There are two kinetic modesl that is common in kinetic study which is pseudo-first-order and pseudo-second-order. These two kinetic models were used to investigate mechanism of adsorption and rate of adsorption that occurred during the adsorption process. The determination of types of kinetic model were based on the linear regression correlation coefficient, R^2 value. Based on the graph, R^2 values for pseudo-first-order and pseudo-second order were 0.5209 and 0.9999 respectively. Hence, it can be said that the adsorption studies in removing MO fit better with pseudo-second-order. This shows that the mechanism of reaction is more towards chemisorption instead of physisorption.

CONCLUSION

Optimum value for each parameter has been obtained which was pH 3 with initial concentration of 60 ppm and 30 minutes of contact time. The adsorption isotherm model chosen for this study is Langmuir isotherm

and the adsorption kinetic that is the most suitable to represent the mechanism kinetic data is pseudo-second-order.

REFERENCES

i. Alkan, M., Demirbas, O., & Dogan, M. (2004). Removal of Acid Yellow 49 from Aqueous Solution by Adsorption. *Fresenius Environmental Bulletin*, *13*(11a), 1121.
ii. El-Gamal, S. M. A., Amin, M. S., & Ahmed, M. A. (2015). Removal of methyl orange and bromophenol blue dyes from aqueous solution using Sorel's cement nanoparticles. *Journal of Environmental Chemical Engineering*, *3*(3), 1702-1712.
iii. Hadi, N., Guan, L. C., Endud, S., & Hamdan, H. (2003). Quantitative measurement of a mixture of mesophases cubic MCM-48 and hexagonal MCM-41 by C-13 CP/MAS NMR. *Material Letters*, *58*, 1971-1974.
iv. Lafi, R., & Hafiane, A. (2016). Removal of methyl orange (MO) from aqueous solution using cationic surfactants modified coffee waste (MCWs). *Journal of the Taiwan Institute of Chemical Engineers*, *58*, 424-433.
v. Lee, C. K., Liu, S. S., Juang, L. C., Wang, C. C., Lin, K. S., & Lyu, M. D. (2007). Application of MCM-41 for dyes removal from wastewater. *J Hazard Mater*, *147*(3), 997-1005.
vi. Nidheesh, P. V., Zhou, M., & Oturan, M. A. (2018). An overview on the removal of synthetic dyes from water by lectrochemical advanced oxidation processes. *Chemosphere*, *197*, 210-227.
vii. Salahshoor, Z., & Shahbazi, A. (2014). Review of the use of mesoporous silicas for removing dye from textile wastewater. *European Journal of Environmental Sciences*, *4*(2), 116-130.
viii. Yagub, M. T., Sen, T. K., Afroze, S., & Ang, H. M. (2014). Dye and its removal from aqueous solution by adsorption: A review. *Adv Colloid Interface Sci*, *209*, 172-184.

JUNIOR SCIENCE COMMUNICATION
https://jscfsg.uitm.edu.my/
Volume 2 (2019)
eISSN 2637-0689

Colloquium of Chemistry and Environment 2018
Faculty of Applied Sciences, Universiti Teknologi MARA, Shah Alam.

SYNTHESIS AND CHARACTERIZATION OF MCM-41 FROM POWER PLANT BOTTOM ASH

Nurul Azimah Edrus, Mohammad Noor Jalil*
Faculty of Applied Sciences, Universiti Teknologi MARA, 40450 Shah Alam, Selangor, Malaysia.

* moham423@uitm.edu.my

Abstract: This study reports a synthetic method for preparing mesoporous silica MCM-41 from coal bottom ash as silica source and using cetyl trimethyl ammonium bromide (CTAB) as surfactant. For comparison, the MCM-41 was also synthesized from pure silica which is tetraethyl orthosilicate (TEOS). The samples were characterized by X-Ray Diffraction (XRD) and Scanning Electron Micrograph (SEM). It was confirmed that the synthesized material using XRD exhibits mesoporous characteristics by having an intense peak around diffraction angle of 1.5-2°. The SEM images, exhibited large aggregations meanwhile the BAMCM-41 shows a smaller aggregation.

Keywords: *Coal bottom ash, Mesoporous silica, MCM-41, Synthesis, Characterization*

INTRODUCTION

Mobil Corporation had discovered a new family of mesoporous silica sieves which is MCM-41 that can be synthesized using an inorganic silicate in the 1990s (Zhao *et al*., 1996). Besides, the materials show their potential in many industries including adsorption, separation, catalysis and fuel cells. Researchers had considerable interest in conversion of coal bottom ash into MCM-41 (Park *et al*., 2012). The synthesis of MCM-41 has been done by many researchers but synthesis of MCM-41 from power plant bottom ash is not commonly known. In this study, the synthesis of MCM-41 from coal bottom ash will be compared with MCM-41 using TEOS as silica source. MCM-41 will be characterized by X-Ray Diffraction (XRD) and Scanning Electron Micrograph with Energy Dispersive X-Ray (SEM-EDX) analyses.

METHODOLOGY

Alkali fusion and silicate extraction.

Method of extracting silica from bottom ash was taken from Chandrasekar *et al*. (2008). First, bottom ash was mixed well with NaOH powder at a 1:1.2 weight ratio and fused at 550°C for 1 hour. The obtained fused mass was cooled to room temperature. Then, the fine powder was mixed with water at a weight ratio 1:4 and this was stirred for 24 hours. The resulting suspensions was then centrifuged and filtered to separate the suspended particles and the supernatant was used for the synthesis of MCM-41.

Synthesis of MCM-41.

A 1.2 g of cetyltrimethylammonium bromide (CTAB) was dissolved in 15 g of water and 1.0 g ammonium hydroxide (NH_4OH). Thereafter, 40 ml of BA supernatant was slowly added to the mixture under stirring and continue for 2 hours. The pH was adjusted to 10 using dilute acetic acid followed by further stirring for 30 minutes. Finally, the gel was heated in an oven at 100°C for 48 hours. The solid product obtained was filtered, washed and dried at 100°C and then calcined at 550°C for 8 hours using furnace. TEOS was used as a pure silica source same as previous procedure.

Colloquium of Chemistry and Environment 2018
Faculty of Applied Sciences, Universiti Teknologi MARA, Shah Alam.

FINDINGS

X-Ray Diffraction (XRD)

From the XRD pattern, there was one major peak for MCM-41 and BAMCM-41 samples which at around diffraction angle of 1.5-2°. The characteristic reflection (100) was observed in the XRD pattern of MCM41 and BAMCM-41 as shown in Figure 1, which was the characteristic of a typical hexagonal pore structure of mesoporous silica MCM-41 (Pirouzmand *et al.*, 2013).

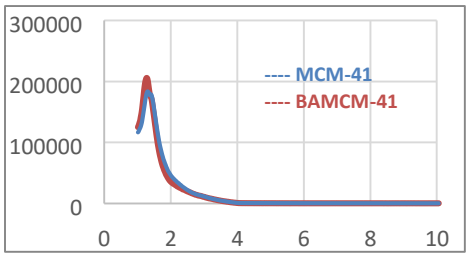

Figure 1 XRD pattern of MCM-41 and BAMCM-41

Scanning Electron Micrograph (SEM)

Figure 2 shows the morphology image of MCM-41 and BAMCM-41. It revealed that the morphologies of the both materials were different. According to Figure 2 (a), it proved that the shapes of MCM-41 nanoparticles are spherical with mean size about 1-10 µm. Moreover, MCM-41 exhibited large, monolith aggregates. In contrast, BAMCM-41 in Figure 2 (b) showed smaller aggregation which is in close agreement with previous researchers (Liu *et al.*, 2014).

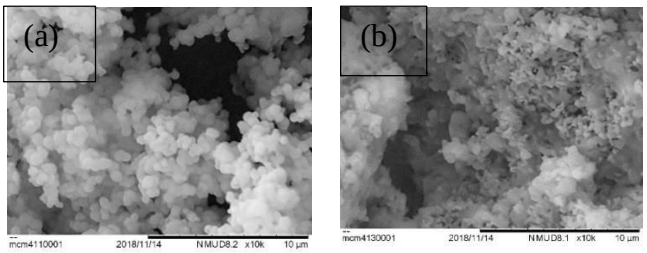

Figure 2 SEM images of (a) MCM-41 and (b) BAMCM-41

CONCLUSIONS

MCM-41 was prepared successfully using bottom ash supernatant. XRD patterns of both MCM-41 and BAMCM-41 show the regular mesoporous hexagonal structure of typical MCM-41. The morphology of BAMCM-41 particles was smaller compared to MCM-41.

REFERENCES

i. Zhao X. S., Lu G. Q. M. & Millar G. J. (1996). Advances in Mesoporous Molecular Sieve MCM-41. *Industrial & Engineering Chemistry Research, 35*(7), 2075–2090.
ii. Park J. E., Youn H. K., Yang S. T. & Ahn W. S. (2012). CO_2 capture and MWCNTs synthesis using mesoporous silica and zeolite 13X collectively prepared from bottom ash. *Catal. Today, 190*(1), 15–22.
iii. Chandrasekar G., You K. S., Ahn J. W. & Ahn W. S. (2008). Synthesis of hexagonal and cubic mesoporous silica using power plant bottom ash. *Microporous Mesoporous Mater, 111*(1–3), 455–462.
iv. Pirouzmand M., Amini M. M., Safari N. & Hamoule T. (2013). Immobilization of Cobalt Phthalocyanine and Tetrasulfophthalocyanine onto MCM-41 and MCM-48: Effect of Immobilization Method on Catalytic Activity. *Journal of the Brazilian Chemical Society, 24*(11) 1864–1870.
v. Liu Z. S., Li W. K. & Huang C. Y. (2014). Synthesis of mesoporous silica materials from municipal solid waste incinerator bottom ash. *Waste Management, 34*(5), 893–900.

JUNIOR SCIENCE COMMUNICATION
https://jscfsg.uitm.edu.my/
Volume 2 (2019)
eISSN 2637-0689

Colloquium of Chemistry and Environment 2018
Faculty of Applied Sciences, Universiti Teknologi MARA, Shah Alam.

EFFECT OF SiO_2 FILLER ON FILLER-SALT-POLYMER INTERACTION AND IONIC CONDUCTIVITY OF PMMA/PEG ELECTROLYTES

Nurul Dhabitah Basri, Sharil Fadli Mohamad Zamri*
Faculty of Applied Sciences, Universiti Teknologi MARA, 40450 Shah Alam, Selangor, Malaysia

*sharil7240@uitm.edu.my

***Abstract*:** Poly(methylacrylate) (PMMA) is a hard, brittle polymer material with poor conductivity. In this study, Poly(ethylene glycol) was used as a secondary polymer and plasticizer to improve the film properties and silicon dioxide (SiO_2) as filler to improve ionic conductivity of PMMA/PEG electrolytes system. PMMA and PEG were blended and doped with lithium tetrafluoroborate ($LiBF_4$) with addition of various amount of SiO_2 filler. The samples were prepared by solvent casting method with tetrahydrofuran (THF) as solvent. The PMMA/PEG electrolytes film were characterized using fourier transform infrared spectroscopy (FTIR) analyis, and electrochemical impedance spectroscopy (EIS) analysis. The result showed that PEG successfully give better formation of film and SiO_2 filler successfully improve ionic conductivity which exhibit the highest ionic conductivity 5.55 X 10^{-6} S cm^{-1} given by polymer electrolytes containing 3wt. % filler at room temperature

***Keywords*:** *poly(methylmethacrylate), poly(ethylene glycol), SiO_2, polymer electrolytes*

INTRODUCTION

Composite polymer electrolytes (CPE) has attracted the attention of researchers in the past decade as the inert filler particles present in the polymer system can give higher ionic conductivity. In this study PMMA was used due to its superior characteristics such as high resistance and electrochemical properties (Zamri & Latif, 2015). Unfortunately, PMMA is hard, brittle, exhibits poor electrode-electrolyte contact and is unable to give reasonable ionic conductivity (Zamri & Latif, 2015). To overcome this limitation, PMMA is blended with PEG and addition of various amount of SiO_2 filler. SiO_2 was has been chosen because it can increase the ionic conductivity of polymer electrolytes.

METHODOLOGY

PMMA (0.5 g) and PEG (0.5 g) were dissolved separately in THF. $LiBF_4$ (0.2 g) salt was added and various amount of weight percentage of SiO_2 (0, 1, 3, 5 and 7) were then added to each mixture and stirred for 24 hours. The solutions were then casted into Teflon dish and left to dry under nitrogen gas flow at room temperature. Obtained films were peeled off and dried in an oven at 50°C for 12 hours.

FINDINGS

Fourier Transform Infrared Analysis

Figure 1 shows that after adding filler into the system, the C=O, O-CH_3 and C-O-C peaks become less intense and shifted to lower wavenumber. This implies that Li^+ ion in the system were probably coordinated

with oxygen atom in carbonyl group of PMMA and ether of PEG. The peak that was observed at 728 cm^{-1} probably belong to BF_4^- and confirms dissociation of $LiBF_4$ salts in polymer blends. Additionally, it was noted the intensity of the peaks decreased with increased amount of SiO_2. This indicates interaction between filler, salt, and polymer.

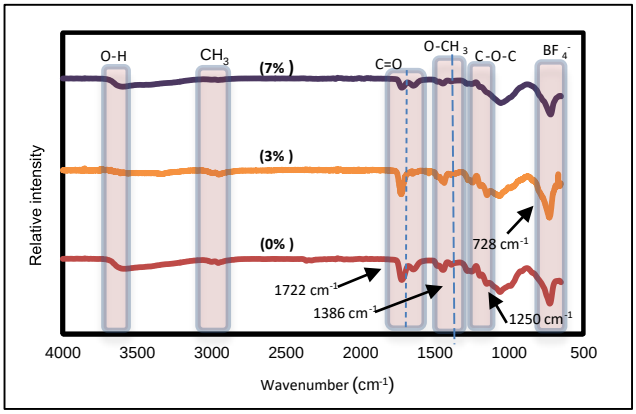

Figure 1 FTIR spectra of PMMA/PEG/$LiBF_4$ with various SiO_2 weight percent filler

Electrochemical Impedance Spectroscopy Analysis

Figure 2 depicts the ionic conductivities with respect to the amount of SiO_2 filler added into polymer blend electrolyte. The ionic conductivity increases with the addition of the filler up to 3 wt.%. The highest value of ionic conductivity of 5.55 X 10^{-6} S cm^{-1} was obtained with 3 wt.% of filler because the filler can help in dissociation of salt. Zamri & Latif (2013) also observed a similar trend for PMMA/ENR blends with the highest conductivity for 3wt. % of SiO_2 filler. The decrease in ionic conductivity for 5wt. % and 7wt. % of filler were attributed to the massive agglomeration of nano-filler in the film. This reduces the number of ions involved in conduction and causes the decrease in ionic conductivity at 5wt. % of SiO_2 filler. As result, the movement of Li^+ ion was obstructed by the filler and hence induces to a decrease in ionic conductivity (Sharma *et al*., 2015).

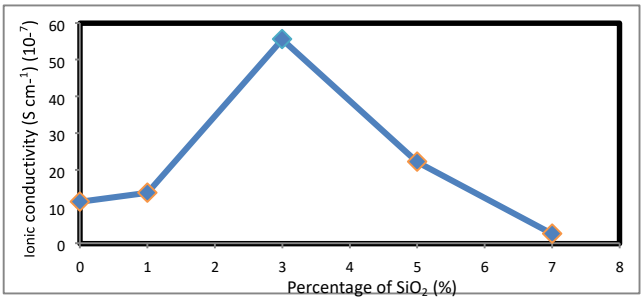

Figure 2 Effect of SiO_2 on the ionic conductivity of PMMA/PEG electrolytes at room temperature

Colloquium of Chemistry and Environment 2018
Faculty of Applied Sciences, Universiti Teknologi MARA, Shah Alam.

CONCLUSIONS

PMMA/PEG electrolyte systems were successfully prepared using solvent casting method. FTIR spectra confirmed the interaction between filler-salt-polymer interactions. The highest conductivity value of 5.55 X 10^{-6} Scm^{-1} at room temperature was obtained when 3wt.% of filler was added into the PMMA/PEG electrolytes system.

REFERENCES

i. Sharma, P., Kanchan, D. K., & Gondaliya, N. (2012). Effect of Nano-Filler on Structural and Ionic Transport Properties of Plasticized Polymer Electrolyte. *Open Journal of Organic Polymer Materials*, *2*(2), 38–44.

ii. Zamri M. S. F. & Abdul Latif, F. (2015). Effects of Acid Modified SiO_2 on Ionic Conductivity and Blend Properties of $LiBF_4$ Doped PMMA/ENR 50 Electrolytes. *Advanced Materials Research*, *1107*, 187–193.

JUNIOR SCIENCE COMMUNICATION
https://jscfsg.uitm.edu.my/
Volume 2 (2019)
eISSN 2637-0689

Colloquium of Chemistry and Environment 2018
Faculty of Applied Sciences, Universiti Teknologi MARA, Shah Alam.

SYNTHESIS, CHARACTERIZATION AND ANTIBACTERIAL STUDIES OF COPPER(II) SCHIFF BASE COMPLEXES DERIVED FROM SALICYLALDEHYDE

Nurul Izzati Shahariman[1], Amalina Mohd Tajuddin[1,2]*
[1]Faculty of Applied Sciences, Universiti Teknologi MARA,40450 Shah Alam, Selangor, Malaysia.
Atta-ur-Rahman Institute for Natural Product Discovery, Universiti Teknologi MARA, Cawangan Selangor, Kampus Puncak Alam, 42300 Bandar Puncak Alam, Selangor, Malaysia.

*amalina9487@uitm.edu.my

Abstract: A Schiff base was synthesized between salicylaldehyde and phenylenediamine and coordinate with Ni(II) and Cu(II). Elemental analysis (CHN), Fourier Transform Infrared (FTIR), Proton Nuclear Magnetic Resonance (^{1}H- NMR) and Ultraviolet-Visible spectroscopies (UV-Vis) were characterization that have been performed. In IR spectra, azomethine linkage was observed around 1600-1620 cm^{-1}. All compounds have no ability as an antibacterial toward bacteria of *S. aureus, S. haemolyticus, S. flexneri* and *E. coli.*

Keywords: *Schiff base, salicylaldehyde, nickel, copper, antibacterial.*

INTRODUCTION

Schiff bases were discovered by Hugo Schiff, 1864 (Yousif *et al.,* 2017). The ligands were obtained by reaction between aldehyde and the amine (Habibi *et al.,* 2017). In characterization Kılınç & Şahin (2018), stated that peaks of Schiff base ligands at 1621 cm^{-1} indicates azomethine group This peak were observed to shift due to the linkage between nitrogen and metal ions. Schiff base ligands and their metal complexes are important in biological field especially in antibacterial activity. They have ability as antibacterial based on the lipophilicity to enter the cell wall and destroy the bacteria (Yamgar, *et al.,* 2014). Parsaee & Mohammadi (2017) explained that, Schiff base complexes soluble in lipid. Therefore, they can penetrate into the cell membrane, blocking enzyme binding sites and kills the bacteria effectively. Therefore, this study was to develop a new type of antibiotics of Schiff base complexes to replace the common antibacterial. The objectives of this study were to synthesize and characterize Schiff base ligands and their metal complexes then, investigate the antibacterial activity on selected bacteria.

METHODOLOGY

Salicylaldehyde (30 mmol, 3.66 g) was mixed with *o*-phenylenediamine (15 mmol, 1.62 g) in ethanol and heated under reflux for one hour before filtered to form colored precipitates. Then, the ethanolic ligand (5 mmol, 1.58 g) was mixed with Cu(II) ions (5 mmol, 0.91 g) and refluxed for another two hours before cooling to form precipitates and characterized using selected techniques. The compounds then were screened for antibacterial activity using Resazurin Microbial Assay.

Colloquium of Chemistry and Environment 2018
Faculty of Applied Sciences, Universiti Teknologi MARA, Shah Alam.

FINDINGS

All compounds were successfully synthesized. Table 1 tabulates the IR data for L1 and CuL1 in Figure 1.

L1 CuL1

Figure 1 General Structure of L1 and CuL1.

Table 1 IR analysis of L1 and CuL1

Compound	Wave number (cm^{-1})			
	v(C=N)	**v(C-O)**	**v(M-N)**	**v(M-O)**
L1	1613	1191	-	-
CuL1	1608	1187	535	475

Based on the data, L1 having a strong peak on 1613 cm^{-1} for azomethine group (C=N). The band was shifted to lower wavenumber upon complexation due to the nitrogen that coordinated to metal ion. Peak of (C-O) in free ligands appeared on 1191 cm^{-1} and shifted due to the coordination of oxygen with metal ions (Kılınç & Şahin, 2018). New peak also appeared which to confirm the ligand was successfully coordinated with metal ions. In biological activity, all compounds give negative results toward bacteria. It concluded that the compounds not fully soluble to pass through the membrane and destroy the cell (Taylor & Triggle, 2007).

CONCLUSIONS

All compounds were successfully synthesized. For IR analysis, the significant IR peaks for Schiff bases are 1600- 1620 cm^{-1} for C=N and 1185-1200 cm^{-1} for C-O stretching that shifted in metal complexes. In antibacterial screening, there is no compound inhibited bacterial growth of *S. aureus, S. haemolyticus, S. flexneri* and *E. coli*.

REFERENCES

i. Habibi, M., Beyramabadi, S. A., Allameh, S., Khashi, M., Morsali, A., Pordel, M., & Khorsandi-Chenarboo,
M. (2017). Synthesis, experimental and theoretical characterizations of a new Schiff base derived from pyridincarboxaldehyde and its Ni (II) complex. *Journal of Molecular Structure*, *1143*, 424-430.

ii. Kılınç, D., & Şahin, Ö. (2018). Synthesis of polymer supported Ni (II)-Schiff Base complex and its usage as a catalyst in sodium borohydride hydrolysis. *International Journal of Hydrogen Energy*, *43*(23), 10717- 10727.

iii. Parsaee, Z., & Mohammadi, K. (2017). Synthesis, characterization, nano-sized binuclear nickel complexes, DFT calculations and antibacterial evaluation of new macrocyclic Schiff base compounds. *Journal of Molecular Structure*, *1137*, 512-523.

iv. Taylor, J. B., & Triggle, D. J. (2007). *Comprehensive medicinal chemistry II*. Amsterdam: Elsevier.

v. Yamgar, R. S., Nivid, Y., Nalawade, S., Mandewale, M., Atram, R. G., & Sawant, S. S. (2014). Novel Zinc(II) Complexes of Heterocyclic Ligands as Antimicrobial Agents: Synthesis, Characterisation, and Antimicrobial Studies. *Bioinorganic Chemistry and Applications*, 1-10.

vi. Yousif, E., Majeed, A., Al-Sammarrae, K., Salih, N., Salimon, J., & Abdullah, B. (2017). Metal complexes of Schiff base: Preparation, characterization and antibacterial activity. *Arabian Journal of Chemistry*, *10*, S1639-S1644.

JUNIOR SCIENCE COMMUNICATION
https://jscfsg.uitm.edu.my/
Volume 2 (2019)
eISSN 2637-0689

Colloquium of Chemistry and Environment 2018
Faculty of Applied Sciences, Universiti Teknologi MARA, Shah Alam.

ADSORPTION OF CADMIUM (II) IONS USING *Ananas comosus* MERR (PINEAPPLE) PEEL AS AN ADSORBENT

Nurul Nadirah Suliman, Sabrina M. Yahaya*
Faculty of Applied Sciences, Universiti Teknologi MARA, 40450 Shah Alam, Selangor, Malaysia.

*sabrina@uitm.edu.my

Abstract: In this study, the ability of pineapple peel as an adsorbent in removal of Cd (II) ions from aqueous solution was investigated. The objectives of this study are to determine the percentage removal of Cd (II) ions and to study the surface morphology of pineapple peels adsorbent. The adsorbent was prepared by soaking 12 g of pineapple peel in potassium permanganate and sulphuric acid. The peels were then stirred, filtered and dried in oven. Experiments were conducted at various pH, contact time, adsorbent dosage and different concentrations of metal solution. The removal of metal ions was analysed using Atomic Adsorption Spectroscopy (AAS). The optimum conditions for adsorption of Cd (II) ions were obtained at pH 11 of solution, 16 hours of contact time and 0.5 g of adsorbent dosage. In this study, the result showed that the percentage removal of metal ions decreased with increasing initial concentration of cadmium solution. The surface morphology of the adsorbent was characterized by Scanning Electron Microscopy (SEM).

Keywords**:** *Pineapple peel, adsorbent, percentage removal, surface morphology, parameter*

INTRODUCTION

Heavy metal is a toxic substance that is discharged together with waste products from industrial activities. Adsorption is a mass transfer process which involves the transfer of substance from the liquid phase to the solid surface which is the adsorbent (Barakat, 2011). The conventional techniques that have been used before in the removal of heavy metal process require high capital, maintenance and operational costs (Fu & Wang, 2011). Hence, the adsorption technique was selected as an effective and economical method for the removal of heavy metal. Pineapple peel was used as and adsorbent because it has the ability as a good adsorbent that require simple technique and low-cost operation (Ahmad *et al*., 2016).

METHODOLOGY

A series of cadmium standard solutions were prepared by diluting the stock solution (1000 ppm) with distilled water. The adsorbent was prepared by soaking 12 grams of pineapple peel in 100 mL of potassium permanganate and 100 mL of sulphuric acid. The peels were then stirred at 60^{o}C for 24 hours and then was filtered and dried in oven for 24 hours. Experiments were conducted at various pH (pH 1-14), contact time (0-72 hours), adsorbent dosage (0.1-0.5 grams) and different concentration of metal solutions (5-25 ppm). The removal of metal ions was analysed using Atomic Adsorption Spectroscopy (AAS). The surface morphology of the adsorbent was characterized by Scanning Electron Microscopy (SEM).

Colloquium of Chemistry and Environment 2018
Faculty of Applied Sciences, Universiti Teknologi MARA, Shah Alam.

FINDINGS

Scanning Electron Microscopy Analysis

The results indicate that highly porous surface structure of pineapple peels was potentially helpful in increasing the adsorption efficiency

Atomic Adsorption Spectroscopy Analysis

The removal of metal ions increased as the pH of solution increased and slightly decrease towards pH 14 due to the hydroxide precipitation. It is because of the increasing concentration of OH^- that cause the adsorbent surface to be negatively charged, hence, increase the adsorption of metal ions. The percentage removal also increased with increase in contact time until the equilibrium was reached about 16 hours. Besides, the removal of Cd (II) ions increased with increasing adsorbent dosage due to the increasing number of binding sites. Table 1 shows the optimum parameters obtained in this study. Furthermore, the optimized parameters were used to study the effect on different concentration of cadmium solution. The percentage removal of heavy metal decreased as initial concentration of cadmium solution increased. Figure 1 shows the effect of optimum parameters on different concentrations of cadmium solution.

Table 1 Optimum condition for each parameter

Parameters	Optimize condition	% removal
pH	pH 11	96.42 %
Contact time	16 hours	99.94 %
Adsorbent dosage	0.5 g	94.38 %

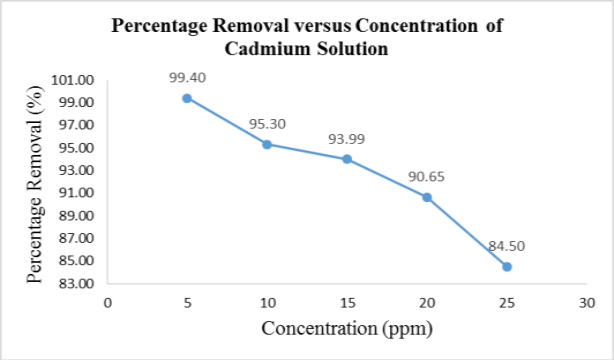

Figure 1 The effect of optimum parameters on different concentration of cadmium solution

CONCLUSIONS

Adsorption observations on the ability of modified pineapple peel reported in this study indicate that the adsorbent has high application potential in removal of cadmium ions. The surface morphology of the adsorbent was characterized by Scanning Electron Microscopy (SEM). The results indicate the highly porous structure on the surface of pineapple peels was potentially helpful in increasing the adsorption efficiency.

REFERENCES

i. Ahmad, A., Khatoon, A., Mohd-Setapar, S.-H., Kumar, R., & Rafatullah, M. (2016). Chemically oxidized pineapple fruit peel for the biosorption of heavy metals from aqueous solutions. *Desalination and Water Treatment*, *57*(14), 6432–6442.
ii. Barakat, M. A. (2011). New trends in removing heavy metals from industrial wastewater. *Arabian Journal of Chemistry*, *4*(4), 361–377.
iii. Fu, F. & Wang, Q. (2011). Removal of heavy metal ions from wastewaters: A review. *Journal of Environmental Management*, *92*(3), 407–418.

JUNIOR SCIENCE COMMUNICATION
https://jscfsg.uitm.edu.my/
Volume 2 (2019)
eISSN 2637-0689

Colloquium of Chemistry and Environment 2018
Faculty of Applied Sciences, Universiti Teknologi MARA, Shah Alam.

ANALYSIS OF VOLATILE COMPOUNDS IN DIFFERENT VARIETIES OF BANANA USING HEADSPACE-SOLID PHASE MICROEXTRACTION (HS-SPME) WITH GAS CHROMATOGRAPHY MASS SPECTROMETRY (GCMS)

Puteri Batrisyia Ab Ghaffar, Rozita Osman*
Faculty of Applied Sciences, Universiti Teknologi MARA, 40450 Shah Alam, Selangor, Malaysia.

*rozit471@uitm.edu.my

Abstract: Banana fruit contains a lot of aroma profile which contribute to its good flavour. Different varieties of banana may contain similarities and differences in their volatile compounds. In this study, headspace solid phase microextraction (HS-SPME) technique coupled with gas chromatography mass spectrometry (GC-MS) was used in analysing the volatile compounds. The performance of two SPME fibers (PDMS/DVB/CAR and PDMS/DVB) was compared. PDMS/DVB/CAR fiber was selected due to its high sensitivity and reproducibility in extracting the volatile compounds. Extraction temperature and extraction time used were 55ºC and 34 minutes, respectively. Four varieties of banana (Pisang Berangan, Pisang Emas, Pisang Cavendish and Pisang Nangka) were chosen. The chromatographic fingerprint obtained for each sample was compared to determine the similarities and differences in each variety. Hexanal and 2-hexenal were detected in all banana varieties. Sixteen volatile compounds were identified in Pisang Berangan, while Pisang Emas and Pisang Cavendish contain eight and six volatile compounds, respectively. Pisang Nangka has the lowest number of volatile compounds whereby only three compounds were identified.

Keywords: *Banana, HS-SPME and GC-MS, chromatographic fingerprint*

INTRODUCTION

Fruits provide us with a lot of nutritional benefits for our health. According to World Health Organisation (WHO), sufficient quantities of fruit and vegetables should become part of the daily diet in all countries. Banana fruit contains a lot of aroma profile which contribute to its good flavour. Aroma of volatile compounds is most probable to play a crucial function in the discernment as well as the acceptableness of products by consumers as aroma is one of the predominant valued for the characteristics of food. Aroma is a complex combination of numerous amounts of VOCs, which make-up is specific to a certain species and usually to the fruits variety. Even though all fruits despite it types have the same aromatic compounds, a particular fruit has a specific aroma that dependent on the combination of the VOCs. Esters followed by aldehydes are the highest rated compounds that contribute to the aroma of banana. Selli *et al*., (2012) and Pino & Febles (2013) stated that isoamyl acetate and 2-pentanol acetate were the main esters in banana. The major VOCs that can be found in "Cavendish" banana in acetoin and "Plantain" were (E)-2-hexenal (E)-2-hexenal and hexanal, respectively (Aurore *et al*., 2011).

METHODOLOGY

Four varieties of banana (Pisang Berangan, Pisang Emas, Pisang Cavendish and Pisang Nangka) were used in this study. The banana was sliced and homogenized using a blender. Then, the pulp sample was

Colloquium of Chemistry and Environment 2018
Faculty of Applied Sciences, Universiti Teknologi MARA, Shah Alam.

transferred into SPME extraction vial for the extraction of volatile compounds. The SPME extraction vial was placed inside a beaker containing hot water. Extraction temperature of 55ºC and extraction time of 34 minutes were used based on optimum conditions reported by Zakaria *et al*. (2017). PDMS/DVB/CAR fibre was selected due to reproducible results as it can efficiently adsorb the volatile compounds as stated in previous study (Pino & Febles, 2013).

FINDINGS

Different varieties of banana (Pisang Berangan, Pisang Emas and Pisang Cavendish and Pisang Nangka) showed similarities and differences in volatile profiles. The volatile compounds were selected based on the percent quality higher than 80%. Shiota (1993) reported isoamyl and isobutyl esters were the major volatile components in banana fruit. The number of volatile compounds raise according to the ripeness of the banana. During ripening, most of volatile compounds increase in their concentration. The type of banana also contribute to this factor whereby if the banana is a dessert banana, which can be eaten raw such as Pisang Emas, Berangan and Cavendish, they have relatively higher number of esters compared to 'Plantain' or cooked banana such as Pisang Nangka. There were 16 volatile compounds extracted from Pisang Berangan. For Pisang Emas and Pisang Cavendish, the number of volatile compounds extracted were 8 and 6, respectively. Pisang Nangka has the lowest number of volatile compounds which were only 3 (Figure 1).

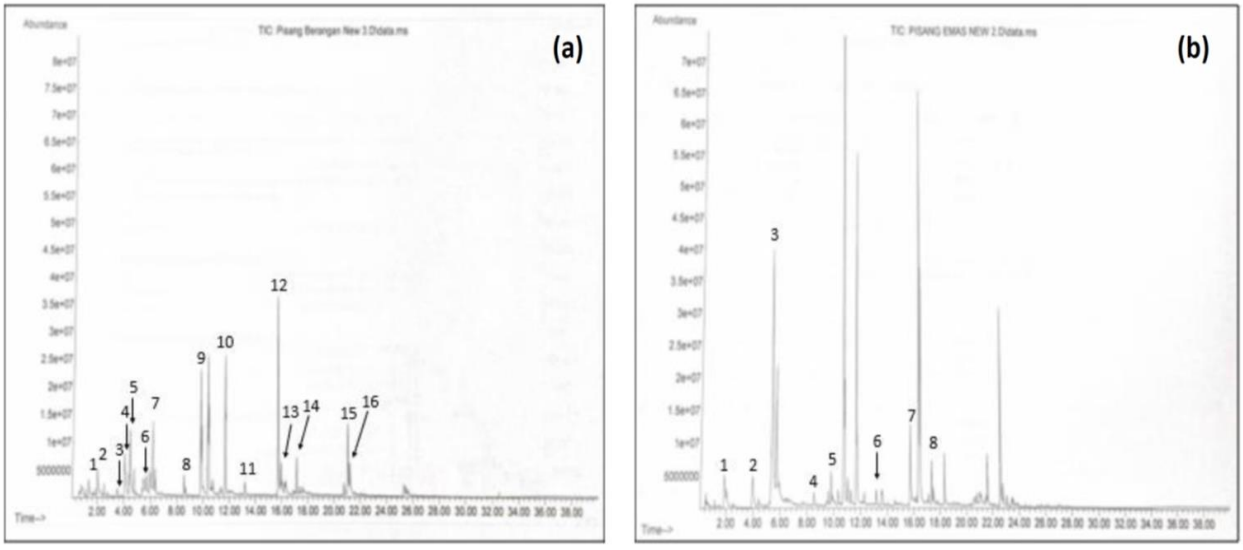

Colloquium of Chemistry and Environment 2018
Faculty of Applied Sciences, Universiti Teknologi MARA, Shah Alam.

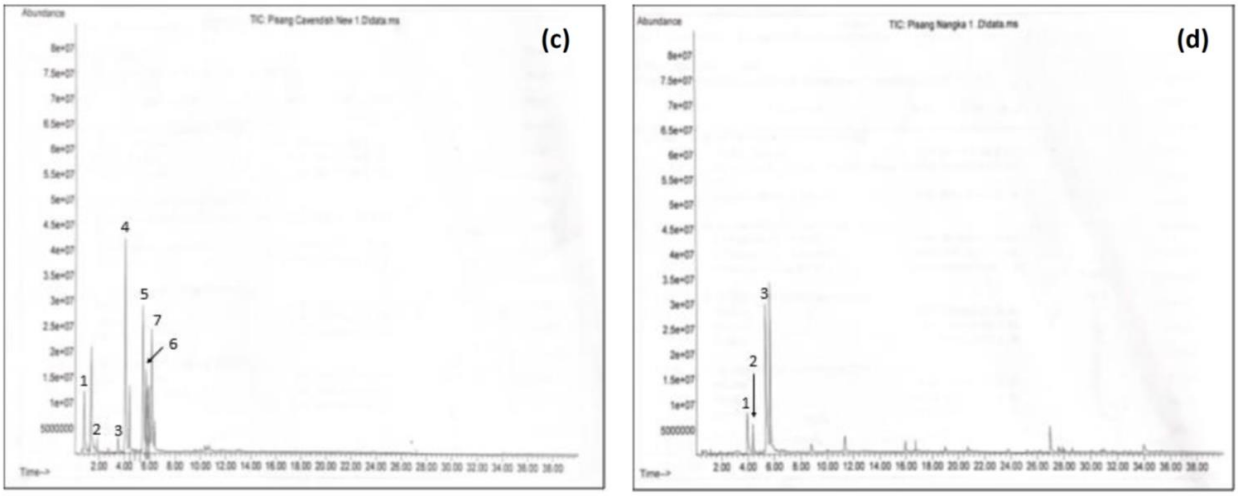

Figure 1 Volatile compounds extracted from different varieties of banana. Pisang Berangan (a), Pisang Emas (b), Pisang Cavendish (c) and Pisang Nangka (d)

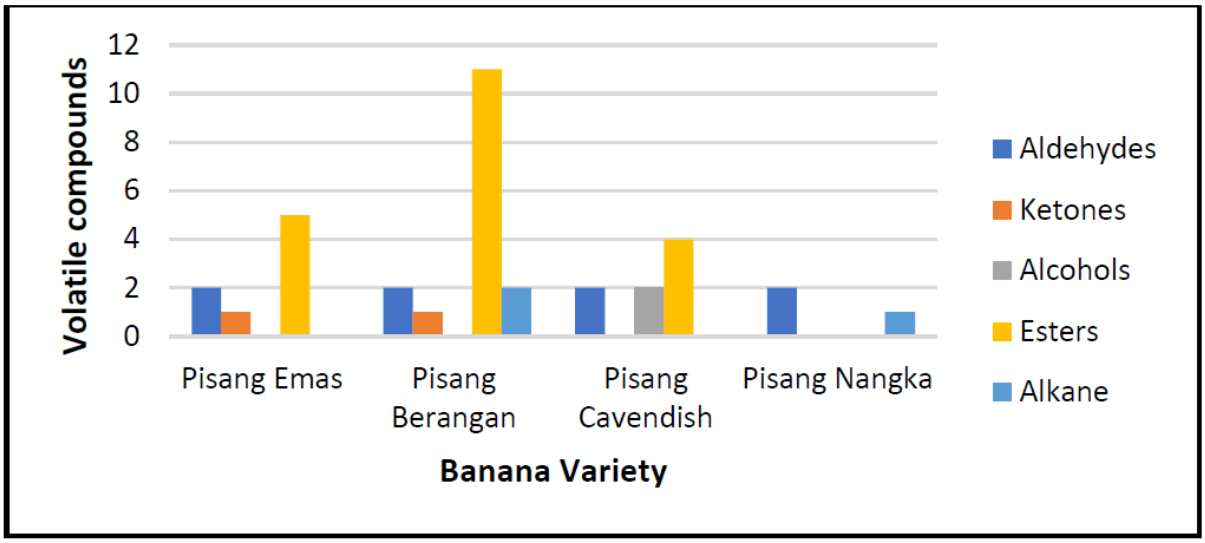

Figure 2 Volatile compounds in different varieties of banana

CONCLUSIONS

Different varieties of banana have different number and functional group of volatile compounds. Esters compounds showed the highest number in each varieties of banana. Therefore, esters were considered as the most important volatile compound that contributed to the odour of banana. The ripeness of banana also determined the amount of volatile compounds present. The riper the fruit, the higher number of volatile

compounds specifically esters. Increasing number of esters during ripening promotes the aroma of the fruit. Chromatographic fingerprint obtained from banana of different varieties can be used to assess the similarities and differences of volatile compounds that could be a good alternative technique in ensuring quality control and authenticity of the banana products.

REFERENCES

v. Aurore, G., Ginies, C., Ganou-Parfait, B., Renard, C. M. & Fahrasmane, L. (2011). Comparative study of free and glycoconjugated volatile compounds of three banana cultivars from French West Indies: Cavendish, Frayssinette and Plantain. *Food chemistry*, *129*(1), 28-34.

vi. Pino, J. A. & Febles, Y. (2013). Odour-active compounds in banana fruit cv. Giant Cavendish. *Food chemistry*, *141*(2), 795-801.

vii. Selli, S., Gubbuk, H., Kafkas, E. & Gunes, E. (2012). Comparison of aroma compounds in Dwarf Cavendish banana (Musa spp. AAA) grown from open-field and protected cultivation area. *Scientia horticulturae*, *141*, 76-82.

viii. Shiota, H. (1993). New esteric components in the volatiles of banana fruit (Musa sapientum L.). *Journal of Agricultural and Food Chemistry*, *41*(11), 2056-2062.

ix. Zakaria, S. R., Tajuddin, R., Osman, R., Saim, N. & Saaid, M. (2017). Optimization of Headspace Solid Phase Microextraction (HS-SPME) for the Extraction of Volatile Organic Compounds (VOCs) in Mangoes (Harumanis cv.) Using 2 Stages Multivariate Analysis. *Pertanika Journal of Science & Technology*, *25*, 167-174.

JUNIOR SCIENCE COMMUNICATION
https://jscfsg.uitm.edu.my/
Volume 2 (2019)
eISSN 2637-0689

Colloquium of Chemistry and Environment 2018
Faculty of Applied Sciences, Universiti Teknologi MARA, Shah Alam.

SYNTHESIS OF N-Boc-3-KETOPROLINE ETHYL ESTER AS ORGANOCATALYST

Siti Hajar Wan Burhadin, Noraishah Abdullah*
Faculty of Applied Sciences, Universiti Teknologi MARA, 40450 Shah Alam, Selangor, Malaysia.

*noraishah6748@uitm.edu.my

Abstract: In this research, glycine ethyl ester hydrochloride, diethyl-2-azabutane-1,4-dicarboxylate and 3-(tert-butoxycarbonyl-ethoxycarbonylmethyl-amino)-propionic acid ethyl ester were used as the starting material to produce N-Boc-3-ketoproline ethyl ester in respective reactions. This synthesis was done by three step reactions. Firstly, glycine ethyl ester hydrochloride was reacted with ethyl acrylate to produce diethyl-2-azabutane-1,4-dicarboxylate. Then the product from previous step which is diethyl-2-azabutane-1,4-dicarboxylate was reacted with Boc anhydride in the second reaction. Boc anhydride was used to protect the nitrogen of the amino acids from reacting with other compounds to produce N-Boc protected diesters which is 3-(tert-Butoxycarbonyl-ethoxycarbonylmethyl-amino)-propionic acid ethyl ester. The third reaction was the cyclization of N-Boc diesters by using LiHMDS in the presence of THF as the solvent. The mixtures were then stirred and the completion of the reaction was determined by TLC analysis. The structure of N-Boc-3-ketoproline ethyl ester was elucidated and confirmed using a modern spectroscopic technique which is NMR spectroscopy.

Keywords: proline, N-Boc, organocatalyst, NMR

INTRODUCTION

Organic synthesis has historically been dominated by transition metal catalysis. A d block metal ion gives the transition metal catalysis its own unique properties. These catalysts can activate substrates and accelerate reactions by means of coordination, ligand exchange, insertion, elimination, and so on, leading to the cleavage or formation of H−H, C−H, and C−C bonds. The activity and selectivity of transition-metal catalysts can be tuned by modification of their ligands, and numerous transition-metal catalysts have been developed and used in diverse fields (Zhong & Shi, 2010). Organocatalysts is the demanding area of research in organic synthesis. One of the most used compound in organocatalysis is proline. Proline exists in two conformer which are *L*-Proline and *S*-Proline. Proline is proteinogenic amino acid with a secondary amine. The primary amine on the α carbon of glutamate semialdehyde forms a Schiff base with the aldehyde which is then reduced, producing proline. It can be synthesized by the body through the breakdown of L-glutamate, another amino acid and it is non-essential amino acid (List, 2002). Chemists use organocatalysts which are more stable, readily available and can be applied in less demanding reaction conditions. A highly diverse structural features are available because of the many catalysts currently available. There are undeniably many successful organic catalysts reported derived from proline. However, they are still limited in regards to hydroxyproline and its applications in asymmetric reactions. In this research, we are going to focus on one of the derivatives of proline which is N-Boc-3-ketoproline ethyl ester.

METHODOLOGY

In this study, the synthesis of N-boc-3-ketoproline ethyl ester which has potential as organocatalyst was focused. There were three steps involved in the synthesis. The steps were Michael Addition reaction, N-Protection reaction and Dieckmann cyclization reaction. Glycine ethyl ester hydrochloride, diethyl-2-

azabutane-1,4-dicarboxylate and 3-(tert-Butoxycarbonyl-ethoxycarbonylmethyl-amino)-propionic acid ethyl ester were used as starting materials in respective reactions. Glycine ethyl ester hydrochloride was readily available whereas the other two starting materials were synthesized during first and second step. Glycine ethyl ester hydrochloride was reacted with ethyl acrylate and diethyl-2-azabutane-1,4-dicarboxylate was subjected to N-Protection using Boc anhydride with the presence of sodium hydroxide. As for 3-(tert-Butoxycarbonyl-ethoxycarbonylmethyl-amino)-propionic acid ethyl ester underwent cyclization to yield N-boc-3-ketoproline ethyl ester. The results were obtained from all the reactions involved.

FINDINGS

^{1}H and APT ^{13}C NMR result of N-Boc-3-ketoproline ethyl ester is tabulated in the Table 1. The crude product underwent column chromatography which the compounds of N-Boc-3-ketoproline ethyl ester was obtained for about 21.29 %.

Table 1 ^{1}H and APT ^{13}C NMR data of N-Boc-3-ketoproline ethyl ester

^{1}H NMR($CDCl_3$,400 MHz)	**Multiplicity**	**Chemical shift (ppm)**
3H, CH_3	t	1.13
9H, 3 X CH_3	s	1.42
2H, CH_2	m	2.55
2H, CH_2	m	3.41
2H, CH_2	m	4.05

APT ^{13}C NMR($CDCl_3$,100 MHz)	**Chemical shift (ppm)**
CH_3-CH_2	14.1
CH_3-C	28.2
CH_2-N	36.2
CH_2-CH_2	41.0
CH_2-CH_3	60.9
C=O-N	154.2
C=O-CH	169.5
C=O-CH_2	204.2

CONCLUSIONS

In conclusion, N-Boc-3-ketoproline ethyl ester has been successfully synthesized using three step reactions which are Michael Addition reaction, N-Protection reaction and Dieckmann cyclization reaction. As expected, the yield for the desired compound in Michael Addition reaction is satisfactorily at 36.64 % whereas N-Protection reaction and Dieckmann cyclization reaction gives 38.49 % and 21.29 % respectively. It proves that this synthesis step was effective enough to be done. All synthesized compounds were successfully characterized by ^{1}H and ^{13}C NMR spectroscopy

REFERENCES

i. List, B. (2002). Proline-catalyzed asymmetric reactions. *Tetrahedron, 58*(28), 5573-5590.
ii. Zhong, C., & Shi, X. (2010). When Organocatalysis Meets Transition-Metal Catalysis. *Europian Journal of Organic Chemistry, 16*, 2999-3025.

JUNIOR SCIENCE COMMUNICATION
https://jscfsg.uitm.edu.my/
Volume 2 (2019)
eISSN 2637-0689

Colloquium of Chemistry and Environment 2018
Faculty of Applied Sciences, Universiti Teknologi MARA, Shah Alam.

ENHANCEMENT IN ELECTROCHEMICAL DETECTION OF MEFENAMIC ACID BY GOLD NANOPARTICLES FABRICATED ON MODIFIED SPCE

Siti Norawatif Zolkapali, Rossuriati Dol Hamid*
Faculty of Applied Sciences, Universiti Teknologi MARA, 40450 Shah Alam, Selangor, Malaysia.

*rossuriati2996@uitm.edu.my

Abstract:
Mefanamic acid (MFA) is among common pharmaceuticals detected in waste water as the treatment plant in Malaysia cannot remove completely this pollutant. It is very challenging to quantitate MFA in natural water system as its concentration is very low (at the ppt level). Traditionally, liquid chromatography coupled with mass spectrometry (LC-MS) is used to quantitate the MFA. However, this method required a longer time analysis with a tedious sample pre-treatment and expensive mass detector. Screen-printed carbon based electrodes (SPCEs) is an electrochemical sensor that has gained popularity lately for pharmaceuticals detection in environmental matrices. The SPCEs provide a simple electrochemical set up, low cost and faster of time analysis compared to the LC-MS. The oxidation peak of mefenamic acid on bare SPCE and modified gold nanoparticles screen-printed carbon electrode (AuNPs-SPCE) were compared in this study. The mefenamic acid oxidation was observed on both electrodes approximately at 0.6 V. Our preliminary data showed the mefenamic acid signal on the AuNPs-SPCE was enhanced by 1.5 times when compared on the bare SPCE. The enhanced signal probably contributed from high conductivity and surface area of the gold nanoparticles.

INTRODUCTION

Mefenamic acid (MFA) is chemically known as 2-(2, 3-dimethylphenyl) amino benzoic acid and categorized under fenamate class of nonsteroidal acidic anti-inflammatory drugs (NSAIDs) (Tarlekar and Chatterjee, 2017). The MFA is ubiquitous in Malaysia natural water system (Al-Odaini *et al.*, 2013) and it has been reported as one of the top most consumed drugs in Malaysia (Mussa *et al.*, 2019). Although the concentration of mefenamic acid is very low in the environment, it can cause threat to the human and aquatic organisms (Collard et *al.*, 2013). This considering the continuous use of the drug and the incapability of the wastewater treatment plant technology to remove it. Therefore, it is important to monitor the concentration of MFA in environment. LC-MS is the common method for quantitate the MFA owing to its high sensitivity and selectivity (Pugajeva *et al.*, 2017). However, this method has a lot of disadvantages such as tedious sample pre-treatment (Rouini *et al.*, 2004). Screen printed electrodes (SPEs) are disposable sensors based on the screen-printing technology. The production of the SPEs using this technology offers high volume production of inexpensive, highly reproducible, reliable sensors and providing precise control over the SPCEs dimensions (Couto *et al.*, 2015). Carbon material is commonly used in the construction of the working electrode of the SPEs as the material has low background current, wide potential window, inexpensive and chemically inert (McCreery, 2008; Lawal, 2015; Kachoosangi *et al.*, 2008). However, the high resistivity of the carbon material in the SPCE can reduce the electron-transfer kinetics at the electrode-electrolyte interface that lead to poor detection of target analyte. Gold nanoparticles is among the potential materials to fabricate on the modified SPCE, as the material has high conductivity (Tu *et al*., 2018). Therefore, this study compares the oxidation peak of mefenamic acid on the bare SPCE and modified AuNPs-SPCE.

Volume 2 (2019)
eISSN 2637-0689

Colloquium of Chemistry and Environment 2018
Faculty of Applied Sciences, Universiti Teknologi MARA, Shah Alam.

METHODOLOGY

The MFA solution with 0.5 mg/L was prepared in 0.1 M phosphate buffer solution. The electrodeposition of 1 mM $HAuCl_4$ solution in 0.5 M H_2SO_4 on bare SPCE was carried out using cyclic voltammetry potentiostat method at the potential rate from -0.8 to 0.0 V in 10 cycles. The morphology of the modified AuNPs-SPCE was obtained from FESEM image. The oxidation peak of the MFA on both electrodes were measured by cyclic voltammetry at pH of 5.3 and scan rate of 50 mV/s.

FINDINGS

Figure 1 shows that FESEM image of the bare SPCE and the modified AuNPs-SPCE. The bare SPCE shows a flake like aggregate on its surface (Figure 1a). The Au-NPs can be clearly seen distributed on the surface of the modified AuNPs-SPCE (Figure 1b). The oxidation peak of the MFA was observed approximately at 0.6 V for both electrodes (Figure 2). This value close to the oxidation peak of MFA reported on glassy carbon electrode, multi-wall carbon nanotube/glassy carbon electrode and single-wall carbon nanotube/glassy carbon electrode (Tarlekar & Chatterjee, 2017). It was found that the modified AuNPs-SPCE resulted with a better signal detection of the MFA than the bare SPCE. The MFA oxidation peak on the modified AuNPs-SPCE is enhanced by 1.5 times when compared with the bare SPCE. The high conductivity and high surface area of the AuNPs that cause a higher electrochemical activity of the mefenamic acid on the modified AuNPs-SPCE than the bare SPCE (Alonso-Lomillo *et al.*, 2017).

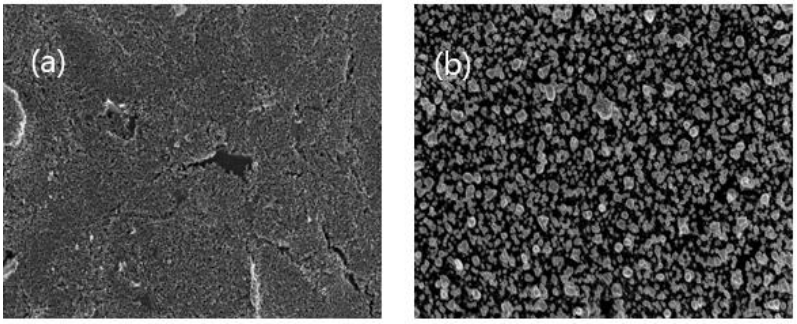

Figure 1 FESEM image of (a) bare SPCE and (b) modified Au-NPs-SPCE

Colloquium of Chemistry and Environment 2018
Faculty of Applied Sciences, Universiti Teknologi MARA, Shah Alam.

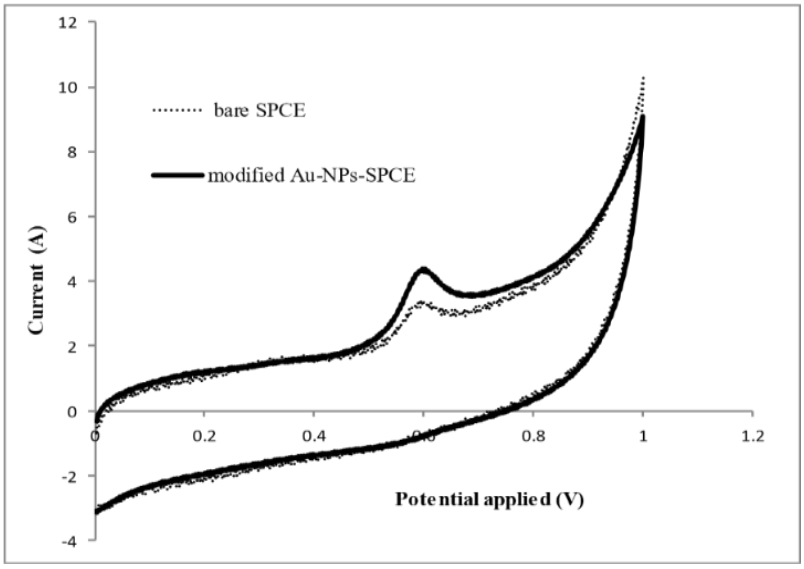

Figure 2 Cyclic voltammogram of MFA recorded at pH 5.3 and scan rate of 50 mV/s on both electrodes investigated in this study.

CONCLUSIONS

Both SPCE and modified AuNPs-SPCE can detect oxidation peak of the MFA. However, the modification of the SPCE with Au-NPs resulted with a better signal detection.

REFERENCES

i. Al-Odaini, N. A., Zakaria, M. P., Yaziz, M. I., Surif, S. & Abdulghani, M. (2013). The occurrence of human pharmaceuticals in wastewater effluents and surface water of Langat River and its tributaries, Malaysia. *International Journal of Environmental Analytical Chemistry, 93*, 245-264.

ii. Alonso-Lomillo, M. A., Dominguez-Renedo, O., Saldana-Botin, A. & Arcos-Martinez, M. J. (2017). Determination of ascorbic acid in serum samples by screen-printed carbon electrodes modified with gold nanoparticles. *Talanta, 174*, 733-737.

iii. Couto, R. A. S., Lima, L. F. C. J. & Quinaz, M. B. (2015). Screen-printed electrode based electrochemical sensor for the detection of isoniazid in pharmaceutical formulations and biological fluids. *International Journal of Electrochemical Science*, *10*, 8738-8749.

iv. Collard, H. R., Ji, K., Lee, S., Liu, X., Kang, S., Kho, Y., Ahn, B., Ryu, J., Lee, J. & Choi, K. (2013). Toxicity and endocrine disruption in zebrafish (Danio rerio) and two freshwater invertebrates (Daphnia magna and Moina macrocopa) after chronic exposure to mefenamic acid. *Ecotoxicology and Environmental Safety*, *94*, 80-86.

v. Kachoosangi, R. T., Wildgoose, G. G. & Compton, R. G. (2008). Carbon nanotube-based electrochemical sensors for quantifying the "heat" of chili peppers: The adsorptive stripping voltammetric determination of capsaicin. *Analyst*, *133*, 888-895.

vi. Lawal, A.T. (2015). Synthesis and utilisation of graphene for fabrication of electrochemical sensors. *Talanta*, *131*, 424-443.
vii. McCreery, R. L. (2008). Advanced carbon electrode materials for molecular electrochemistry. *Chemical Reviews*, *108*, 2646-2687.
viii. Mussa, Z. H., Al-Qaim, F. F., Yuzir, A. & Latip, J. (2019). Electro-transformation of mefenamic acid drug: a case study of kinetics, transformation products, and toxicity. *Environmental Science and Pollution Research*, *26*, 10044–10056.
ix. Pugajeva, I., Rusko, J., Perkons, I., Lundanes, E. & Bartkevics, V. (2017). Determination of pharmaceutical residues in wastewater using high performance liquid chromatography coupled to quadrupole-Orbitrap mass spectrometry. *Journal of Pharmaceutical and Biomedical Analysis*, *133*, 6474.
x. Rouini, M.-R., Asadipour, A., Ardakani, Y. H. & Aghdasi, F. (2004). Liquid chromatography method for determination of mefenamic acid in human serum. *Journal of Chromatography B*, *800*, 189-192.
xi. Tarlekar, P. & Chatterjee, S. (2017). Enhancement in sensitivity of non-steroidal anti-inflammatory drug mefenamic acid at carbon nanostructured sensor. *Journal of Electroanalytical Chemistry*, *803*, 51-57.
xii. Tu, J., Gan, Y., Liang, T., Wan, H. & Wang, P. (2018). A miniaturized electrochemical system for high sensitive determination of chromium(VI) by screen-printed carbon electrode with gold nanoparticles modification. *Sensors and Actuators, B: Chemical*, *272*, 582–588.

JUNIOR SCIENCE COMMUNICATION
https://jscfsg.uitm.edu.my/
Volume 2 (2019)
eISSN 2637-0689

Colloquium of Chemistry and Environment 2018
Faculty of Applied Sciences, Universiti Teknologi MARA, Shah Alam.

ADSORPTION OF METHYLENE BLUE BY MESOPOROUS SILICA MCM-41

Siti Syairah Mat Salleh, Wan Nazihah Wan Ibrahim*
Faculty of Applied Sciences, Universiti Teknologi MARA, 40450 Shah Alam, Selangor, Malaysia.

*wannazihah@uitm.edu.my

Abstract: The mesoporous silica MCM-41 was prepared and characterized using FTIR, FESEM and Isotherm and Surface Area Analysis for adsorption process. The performance of prepared adsorbent for methylene blue (MB) removal was assessed using UV-Vis spectrometer. The optimum condition obtained from this study through effect of pH, initial concentration and contact time are pH 7 with 80 ppm of MB concentration for 10 minutes. Based on the results MCM-41 exhibited on all three batch studies, it has the potential adsorbent on MB removal in aqueous medium.

Keywords: *MCM-41, methylene blue and UV-Vis.*

INTRODUCTION

A global issue arises from the ecological problem due to the negative impact on public health as the quick expansion of industrial sector. İt can affect health through air, soil and water (Miyah *et al*., 2018). Methylene blue (MB) is the common substances used in textile industry which affect mammals and human through inhalation, oral and dermal exposure lead to breathing difficulty, nausea, allergy, mutation and cancer. Thus, the solution of this problem is to employ Mobile Composition Matter No. 41 (MCM-41) for MB removal. It has large surface area, nanometer pore sized, cylindrical pore structure, high degree of pore symmetry and negative charge density due to the presence of SiO and Si-OH groups. This is because adsorption is the most prominent method that can be used for all type of dyes. Determination of prepared adsorbent for MB removal involve analysis done by Ultraviolet-Visible Spectroscopy (UVVis).

METHODOLOGY

The method of synthesis MCM-41 was adopted from previous study by Kamaruzaman *et al*. (2013). Before the batch studies, different concentrations of MB were prepared, and this was done by mixing 1000 mg of MB powder with 1L of distilled water as the stock solution (1000 mg/L). Next, serial dilution was conducted and five different concentrations of MB (60 mg/L, 80 mg/L, 100 mg/L, 120 mg/L and 140 mg/L) were obtained. The parameters used were pH (3 – 11), initial concentration of MB solution (60 – 140 mg/L) and contact time (5 – 50 min). The controlled parameters were adsorbent dosage (0.05 g), shaker speed (160 rpm), temperature (25°C) and volume of MB (0.01 L). Each of the sample was prepared in triplicates. The concentration of target elements after adsorption were determined by a UV-Vis spectroscopy (Perkin Elmar Lamda 35).

FINDINGS

The results obtained from this study shows that MB adsorption by MCM-41 using effect of pH, initial concentration of MB solution and contact time. As depicted in Figure 1(a), at lower pH (acidic), there is competition between H^+ and MB ions for -OH and -COOH groups on MCM-41, respectively. Thus, amount of the MB adsorbed was decreased but at the higher pH values $-COO^-$ and O^- exist, the electrostatic

attraction between MB and the adsorbent increasing ensuing increased MB adsorption capacity (Akpotu & Moodley, 2016). The more alkaline condition of the solution, increases removal of MB hence, optimum pH is 7. Meanwhile in the Figure 1(b), the rate of MB being adsorbed is faster at lower concentration initially and dropped when MB concentration was increased due to the saturation of adsorption sites on the adsorbent surface (Yagub *et al*., 2014). The highest removal efficiency is 100.06% for 80 mgL^{-1} initial concentration of MB solution. Lastly, Figure 1(c) shown the optimum contact time of MB adsorption obtained was at 10 min. The ability of MCM41 to adsorb MB decreased after 10 min till 50 min due to the saturation of the active sites on the adsorbent surface as it was filled with MB ions thus, leave the excessive MB ions in the solution. However, at 5 min to 10 min, when the adsorption contact was increased so, the collision between particle of adsorbate and adsorbent also increased as there was accessed to the vacant of adsorbent sites with removal efficiency from 99.91% to 99.94%.

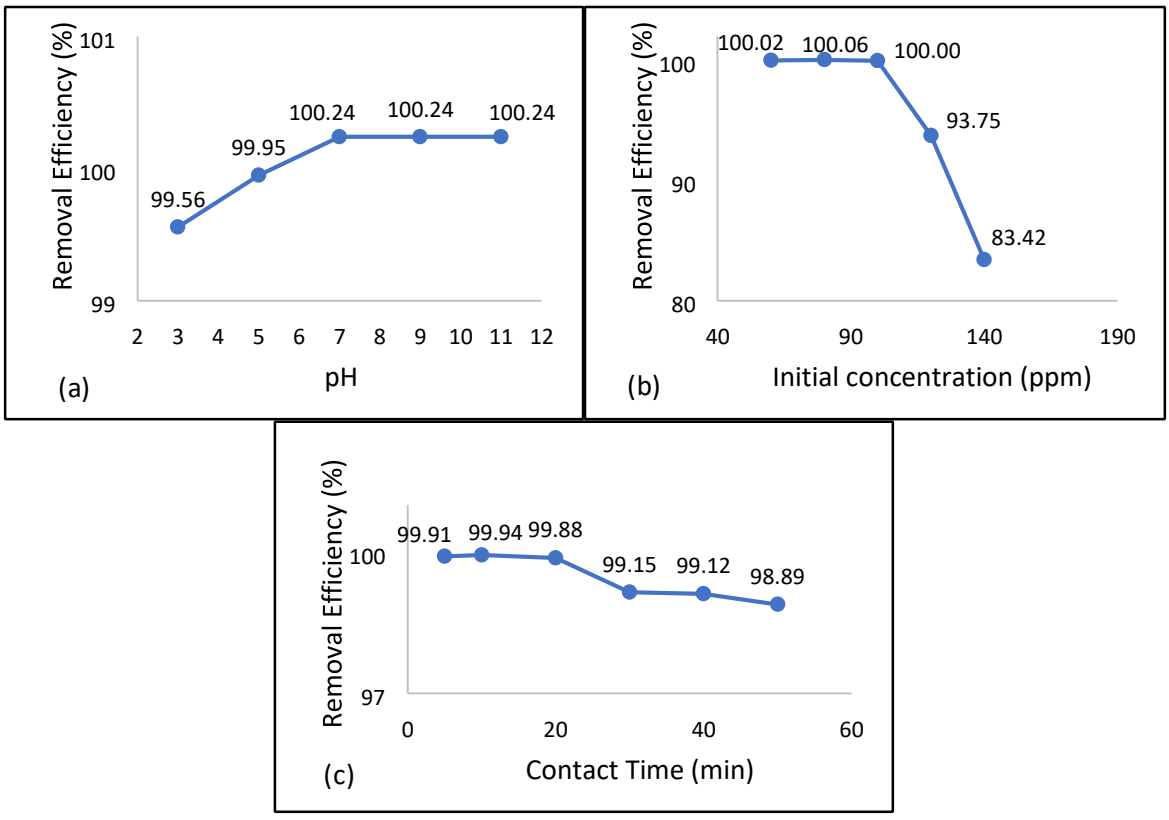

Figure 1 Removal efficiency with effect of (a) pH, (b) initial concentration and (c) contact time

The adsorption isotherm model represented for this study is Langmuir isotherm as the R^2 value is 0.9974 as shown in the Figure 2(a). This show that the adsorption of MB on MCM-41 takes place as monolayer adsorption on a surface which homogenous in adsorption affinity. From Figure 2(b), the pseudo-second-

order model is employed for kinetic mechanism as R^2 value is found to be equal to 1. The mechanism of the reaction more towards chemisorption of MB onto MCM-41 than physisorption.

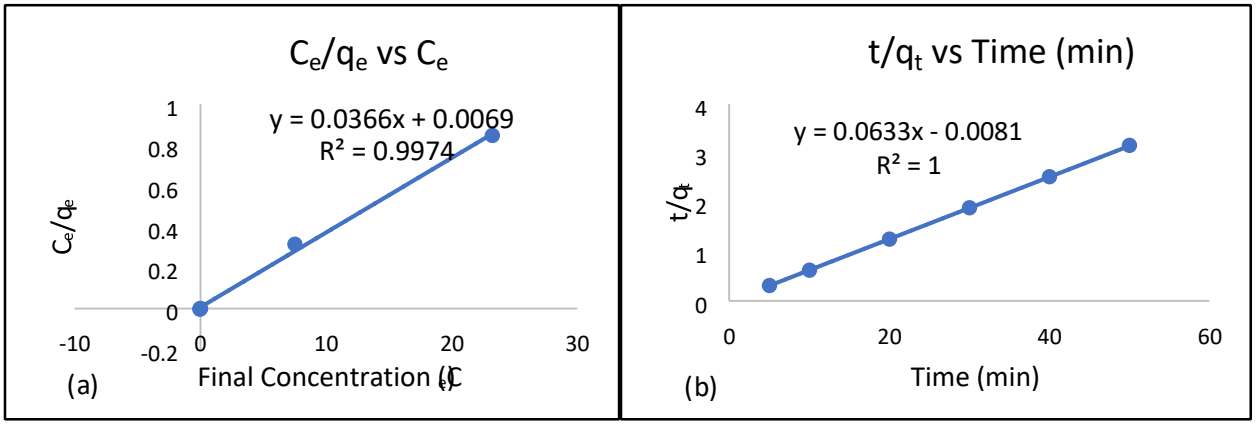

Figure 2 The adsorption (a) Langmuir isotherm and (b) Pseudo-second-order kinetic model

CONCLUSIONS

In conclusion, the analysis on the removal efficiency was completed by batch adsorption studies. The highest efficiency removal achieved based on the optimum condition chosen from all the batch studies are pH 7 at 25°C with 0.05 g of adsorbent dosage using 80 ppm of MB solution as the initial concentration and 10 minutes of contact time.

REFERENCES

i. Akpotu, S. O. & Moodley, B. (2016). Synthesis and characterization of citric acid grafted MCM-41 and its adsorption of cationic dyes. *Journal of Environmental Chemical Engineering, 4*(4), 4503-4513.
ii. Kamaruzaman, S., Sanagi, M. M., Endud, S. & Wan Ibrahim, W. A. & Yahaya, N. (2013). MCM-41 solid phase membrane tip extraction combined with liquid chromatography for the determination of non-steroidal anti-inflammatory drugs in human urine. *Journal of chromatography. B, Analytical technologies in the biomedical and life sciences*, *940*. 59-65.
iii. Miyah, Y., Lahrichi, A., Idrissi, M., Khalil, A. & Zerrouq, F. (2018). Adsorption of methylene blue dye from aqueous solutions onto walnut shells powder: Equilibrium and kinetic studies. *Surfaces and Interfaces, 11*, 74-81.
iv. Yagub, M. T., Sen, T. K., Afroze, S. & Ang, H. M. (2014). Dye and its removal from aqueous solution by adsorption: a review. *Advances in Colloid and Interface Science, 209*, 172-184.

JUNIOR SCIENCE COMMUNICATION
https://jscfsg.uitm.edu.my/
Volume 2 (2019)
eISSN 2637-0689

Colloquium of Chemistry and Environment 2018
Faculty of Applied Sciences, Universiti Teknologi MARA, Shah Alam.

ADSORPTION BEHAVIOR AND PHYSICAL PROPERTIES OF NICOTINAMIDE AND CINNAMIC ACID BY CO-CRYSTALLIZATION METHOD

Sonja Sheena Jacob, Hamizah Mohd Zaki*
Faculty of Applied Sciences, Universiti Teknologi MARA, 40450 Shah Alam, Selangor, Malaysia.

*hamiz410@uitm.edu.my

Abstract: The interaction of Active Pharmaceutical Ingredient (API) with other compounds will influence drugs stability, toxicity, dissolution rate and bioavailability or it may form a new compound with a different crystal structure through the process of adsorption. Adsorption at the liquid or solid interface can be performed by cocrystallization method. Nicotinamide (NCT), also known as Vitamin B3 was mixed with cinnamic acid (CA) to obtain a new phase of interactions leading to a new compound phase. NCT-CA was prepared by using liquid assisted grinding, precipitation and slow evaporation method at stoichiometry of 1:1 molar ratio. The interaction and the physical properties of NCT-CA were characterized by Attenuated Total Reflectance (ATR-IR). NCT-CA exhibits N-H stretching at 3121.80 cm^{-1} and 3316.47 cm^{-1}, C=O stretching at 1655.93 cm^{-1} and N-H bending at 1600.69 cm^{-1} which gives precipitation method as the best method to prepare NCT-CA mixture.

Keywords: *active pharmaceutical ingredients, adsorption, nicotinamide, and cinnamic acid.*

INTRODUCTION

It is a basic concept in the pharmaceutical industry to either find the optimal form of the active pharmaceutical ingredients (API) Adsorption on solid surfaces is involved in every aspect of pharmaceutical development, from formulation design, process development, and manufacturing to store the finished dosage forms (Dą browski, 2001). Adsorption is a phenomenon of attracting and retaining the molecules of a substance on the surface of a liquid or solid which results into higher concentration of molecules on the surface. To achieve content uniformity, especially for low-dose drugs, will exhibit challenge in the manufacturing of solid dosage formulations. Adsorption involves a process where chemicals such as pharmacological drugs bind to nutrients so that they cannot be taken up in the body. The process of adsorption can be done through co-crystallization method. In order for adsorption process to occur, surface is needed. Surface area and porosity are two important physical characteristics that affect the quality and utility of solid phase chemicals including agrochemicals and active pharmaceutical ingredients (Zielinski & Kettle, 2013). Differences in the surface area and porosity of particles within the material will have a big impact to its performance as surface area and porosity plays a vital part in the purification, processing, blending of chemical products as well as product function, efficacy and stability.

METHODOLOGY

Physical mixing.

Physical mixture was obtained by gentle mixing of NCT and CA in a 1:1 molar ratio in a mortar and pestle. 3-5 drops of ethanol solvent were added and the mixture was ground again and the dried solid was collected for further analysis.

Colloquium of Chemistry and Environment 2018
Faculty of Applied Sciences, Universiti Teknologi MARA, Shah Alam.

Precipitation.
A 15mL of ethanol solvent was added to the physical mixture of NCT and CA (1:1 molar ratio). A rotary evaporator with 50°C waterbath, 50 atm and 100 rpm was used to evaporate the solvent. The dried solid was collected for analysis.
Slow Evaporation.
A 5mL of acetone solvent was added to the physical mixture of NCT and CA (1:1 molar ratio). The solution was sonicated at 40°C. The clear solution was left in a petri dish to evaporate at room temperature for 48hr. The dried solid was collected for further analysis.

FINDINGS

Figure 1 shows the ATR-IR spectra of CA, NCT and CA-NCT. The FTIR spectrum of CA showed characteristic peak with high intensity at 1667.79cm^{-1}, presenting C=O functional group (**Fig. 1**). The NCT spectrum exhibited the N-H stretching at 3356.99 cm^{-1} and 3146.93 cm^{-1} and C=O functional group at 1673.91 cm^{-1} and N-H bend at 1575.03 cm^{-1}. The spectrum of precipitation showed characteristic peaks of NCT-CA (1:1) at 3121.80 cm^{-1}, 3316.47 cm^{-1}, 1655.93 cm^{-1} and 1600.69 cm^{-1} which permits the best method to interact these two compounds.

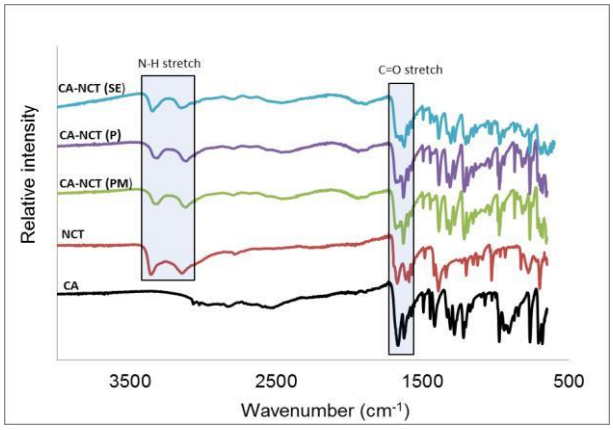

Figure 1 ATR-IR spectra of CA, NCT and CA-NCT prepared by three different methods

CONCLUSION

NCT-CA exhibits N-H stretching at 3121.80 cm^{-1} and 3316.47 cm^{-1}, C=O stretching at 1655.93 cm^{-1} and N-H bending at 1600.69 cm^{-1} which gives precipitation method as the best method to prepare NCT-CA mixture.

REFERENCES

i. Dąbrowski, A. (2001). Adsorption - From theory to practice. *Advances in Colloid and Interface Science*, *93*(1– 3), 135–224. https://doi.org/10.1016/S0001-8686(00)00082-8
ii. Zielinski, J. M., & Kettle, L. (2013). Physical Characterization: Surface Area and Porosity. *Whitepaper: Intertek Chemicals and Pharamaceuticals*, (April), 1–7. https://doi.org/Intertek Chemicals & Pharmaceuticals, Allentown, USA

JUNIOR SCIENCE COMMUNICATION
https://jscfsg.uitm.edu.my/
Volume 2 (2019)
eISSN 2637-0689

Colloquium of Chemistry and Environment 2018
Faculty of Applied Sciences, Universiti Teknologi MARA, Shah Alam.

ANALYSIS OF CADMIUM AND LEAD IN INSTANT NOODLES

Suaidah Sahira Saharudin, Haliza Kassim*
Faculty of Applied Sciences, Universiti Teknologi MARA, 40450 Shah Alam, Selangor, Malaysia.

*haliza893@uitm.edu.my

Abstract: The purpose of this research is to determine the content of cadmium and lead metals in four different brands of instant noodles identified as Sample A, B, C and D, which were manufactured in three different countries which are Indonesia, Korea and Malaysia. In this study the concentration of lead and cadmium were investigated from four different brands of instant noodles to determine which of the four brands obeyed the food safety regulation permissible limit. The samples were prepared using acid digestion method with addition of nitric acid and hydrogen peroxide. Atomic absorption spectroscopy was used in determining the cadmium and lead metals by using standard addition method. The results obtained showed that the four samples contained cadmium and lead metals in different concentrations. Lead was found in every sample higher than cadmium concentration with the highest value being 0.1 mg/kg. Cadmium concentration in each sample were very low and was considered safe compared to the permissible limits listed by WHO, CODEX, EFSA and FSAI. However, lead concentration in all samples exceeded the permissible limit by WHO. Sample D contained the highest amount of lead and cadmium compared to other instant noodles, while Sample C contained the lowest value of both heavy metals.

Keywords**:** *Atomic Absorption Spectroscopy, cadmium, lead, heavy metals and instant noodles.*

INTRODUCTION

There are several types of heavy metals in food and these metals eventually have the tendency to accumulate in selected tissues (Onyema *et al*., 2014). The main source of food contamination is in the raw materials that had been used in production of the food itself. The raw material may have been contaminated from the start, even in minute concentrations (Harcourt, 2018). People nowadays are consuming instant noodles regularly. The aim of the study is to determine and compare the concentration of lead and cadmium present in the four different brands of instant noodles. Furthermore, both heavy metal concentration found in the noodles will be compared with the food safety regulation permissible limits. The samples were digested using acid digestion method and analyzed using Atomic Absorption Spectroscopy (AAS).

METHODOLOGY

Five gram of each samples were digested with 20 ml of concentrated nitric acid for 24 hours. Then, the samples were heated at 120ºC until the production of nitrogen fumes ceased and cooled down to room temperature. A 2 ml of hydrogen peroxide was added and the samples were reheated until concentrated. The sample solutions were filtered, diluted to 250 ml and stored in PTF bottles at below 4ºC. From 1000 mg/L of stock solution of both metals, 0.2 to 1.0 mg/L of standard solutions of cadmium and 2.0 to 10.0 mg/L of the standard solutions of lead were prepared. The calculated volumes were added into five separate 50.0 ml plastic volumetric flasks. A 5.0 ml of the prepared sample solution was added into each flask and was diluted to the mark with deionized water. Blank solution was prepared by adding 5.0 ml of sample into a 50 ml plastic volumetric flask and then was diluted to mark with deionized water. The sample solutions

were tested by using Atomic Absorption Spectroscopy (AAS) to obtain the absorbance reading for determination of lead and cadmium concentration based on standard addition method.

FINDINGS

The amount of cadmium and lead found in Sample A are 0.0067 mg/kg and 0.078 mg/kg, respectively. For Sample B, amount of cadmium and lead are 0.0081 mg/kg and 0.09 mg/kg, respectively. Sample C contains cadmium and lead at 0.0066 mg/kg and 0.068 mg/kg, respectively. Lastly, the amount of cadmium and lead in Sample D were 0.0084 mg/kg and 0.1 mg/kg, respectively.

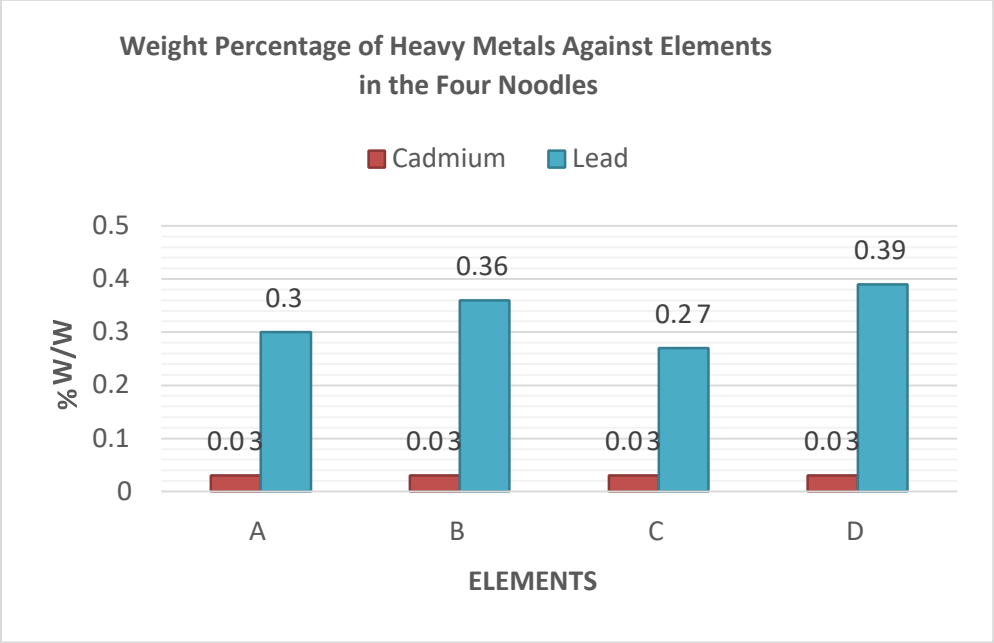

Figure 1 Weight percentage of cadmium and lead in sample A, B, C and D

As shown in Figure 1, all samples have the same weight percentage of cadmium which was 0.03%. However, there was a wide range of weight percentage of lead in each instant noodle, where sample D contained the highest weight percent which was 0.39% while sample C has the lowest one with 0.27%. There was a slightly different mass percent of lead in sample A and C instant noodles, and also between samples B and D. The range percent of lead between the highest and the lowest was about 0.12%. Lead had higher concentration compared to cadmium in every sample. Cadmium levels were all below the permissible limit stated by the organizations selected. Agricultural contaminations from fertilizers, herbicides and insecticides ingredients may elevate lead contamination in instant noodles (Abebe *et al.,* 2017).

Volume 2 (2019)
eISSN 2637-0689

CONCLUSIONS

Sample D was manufactured from Korea has the highest amount of lead and cadmium whereas Sample C from Malaysia has the lowest amount of lead and cadmium. Further recommendation to improve the study is the sample preparation for the instant noodles can be changed by observing heavy metals between raw and cook instant noodles.

REFERENCES

i. Abebe, A., Chandravashi, B. S., & Debebe, A. (2017). Assesment of essential and non-essential metals in popcorn and cornflakes commercially available in Ethiopia. *Chemistry International 3(3),* 268-276.
ii. Harcourt, P. (2018). Health risk assessment of instant noodles commonly consumed, 2580–2587.
iii. Onyema, C. T., Ekpunobi, U. E., Edowube, A. A., Odinma, S., & Sokwaibe, C. E. (2014). Quality Assessment of Common Instant Noodles Sold in Nigeria Markets. *American Journal of Analytical Chemistry, 05*(17), 1174–1177.

JUNIOR SCIENCE COMMUNICATION
https://jscfsg.uitm.edu.my/
Volume 2 (2019)
eISSN 2637-0689

Colloquium of Chemistry and Environment 2018
Faculty of Applied Sciences, Universiti Teknologi MARA, Shah Alam.

CHARACTERIZATION STUDIES OF PAPER PRODUCED BY USING PALAS LEAVES AND BANANA PEELS

Wan Nor Syahira Amylia Wan Ali, Shariff Che Ibrahim*
Faculty of Applied Sciences, Universiti Teknologi MARA, 40450 Shah Alam, Selangor, Malaysia.

*sha88@uitm.edu.my

Abstract: The net paper consumption has increased over the years leading to a higher demand for wood fibre. Non-wood fibres have been chosen as an alternative to help reduce this problem. This study aims to use waste materials of non-wood plants as raw material for paper making industry. The potential of Palas leaves and banana peels as an alternative fibre for paper making was investigated on its basic and physical properties. The basic properties which are grammage, thickness, moisture content and surface morphological properties was investigated according to the TAPPI test method and for the physical properties for tensile strength and tear strength was conducted based on ASTM standard. Scanning Electron Microscope (SEM) was used to observe the morphological of the produced paper sheet. In order to determine whether the alternative fibre used is suitable for paper making, the results obtained are compared with the value from TAPPI standards and the other published literatures. In conclusion, based on the test conducted shows that paper sheet made from palas leaves have better strength compared to banana peels.

Keywords: Papermaking, non-wood fibre, alternative fibre

INTRODUCTION

The net paper consumption in Malaysia is approximately 3 million metric ton in 2007 (Goyal, 2010) and the amount of usage is expected to increase. Cellulose fibers has many benefits as it is recyclable, environmental friendly and less expensive to produce (Li *et al.*, 2010). The rapid decrease in wood resources has led to the search for an alternative source of fiber for paper. Fibers obtained from non-wood resources also can help to reduce the impact on environment (Zawawi *et al*., 2014). Woody fibres used in paper production also increase the usage of virgin materials, chemical usage and the time taken for the pulping process. So, in order to reduce this problem, this non-wooden plant which is Palas leaves and banana peels was studied to determine whether it can be replace for raw material in paper making besides helps to reduce the waste materials and cost of production process.

METHODOLOGY

200 g of raw materials was cut and washed. Then it was put into oven for 24 hours. 32 g of dried materials was boiled with 8 g of sodium hydroxide pellets in 300 ml distilled water for one hour. Next, bleaching process was done by soaking the fibre into 100ml sodium hypochlorite for 2 hours. Pulps produced were blend with 150 ml distilled water and 6 grams of talc. Lastly, screening and drying were done to remove the water content from the pulp. For paper properties testing, several testing was done based on TAPPI standard for grammage, thickness and moisture content. While for tensile strength and tear strength were conducted based on ASTM standard.

FINDINGS

Basic and physical properties

Colloquium of Chemistry and Environment 2018
Faculty of Applied Sciences, Universiti Teknologi MARA, Shah Alam.

Table 1 shows the tensile strength and tear strength is higher in palas leaves paper sheet than banana peels paper sheet due to the different amounts of fibre present in the materials.

Table 1 The basic and physical properties

Pulp used	Grammage (g/m^2)	Thickness (μm)	Moisture content (%)	Tensile strength (Nm/g)	Tear strength (mN.m2/g)
Palas leaves	317.464	1193	4.1	40.01	2.49
Banana peels	337.06	600	5	19.41	0.39

Surface morphological analysis

According to Bidin *et al.* (2015), to produce a paper with a higher tensile strength property, the fibers need to be long and also the interfiber bonding must be considered. Figure 1 shows the paper sheet produced by from palas leaves and banana peels respectively. It can be observed from the SEM images that fibre in the palas leaves paper sheet has denser fibres compared to the banana peels paper sheet and has clearer fibre structure which makes the palas leaves paper produced more applicable for papermaking. However, paper sheet produced from banana peels gave a better coverage and smoother compared with paper sheet made from palas leaves.

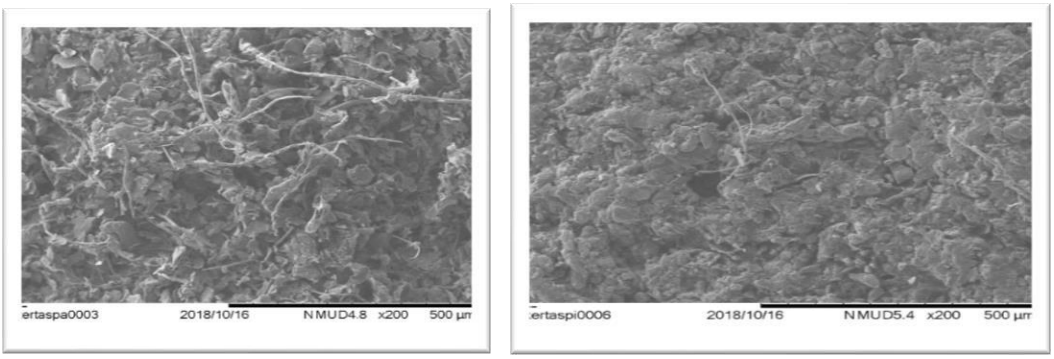

Figure 1 Paper produced by using palas leaves(left) and banana peels(right).

CONCLUSION

In conclusion, based on test conducted shows that the tensile strength and tear strength is higher for paper made from palas leaves compared to banana peels. The basic and physical testing shows that both palas leaves and banana peels paper can be used to make paperboard, blotting paper, tissue or office paper. An abundance and availability of these plants can provide sustainable raw materials in pulping and paper production.

REFERENCES

i. Bidin, N., Zakaria, M. H., Bujang, J. S. & Abdul Aziz N.A. (2015). Suitability of Aquatic Plant Fibers for Handmade Papermaking. *International Journal of Polymer Science*, *1*, 1-9.

Volume 2 (2019)
eISSN 2637-0689

ii. Goyal, H, 2010. Paper and paperboard production and consumption for Malaysia. Assessed on Sep 5, 2019 from http://www.paperonweb.com/Malaysia.htm
iii. Li, K., Fu. S., Zhan, H., Zhan, Y., & Lucia, L.A. (2010). Banana Pseudo-stem Chemistry, Structure. *BioResources, 5*(2), 576-588.
iv. Zawawi, D., Mohd, Z. M. H., Angzzas, S. M. K., Halizah, A. & Ashuvila, M. A. (2014). Exploring of agro waste (pineapple leaf, corn stalk and napier grass) by chemical composition and morphological study. *BioResources*, *9*(1), 872-880.

JUNIOR SCIENCE COMMUNICATION
https://jscfsg.uitm.edu.my/
Volume 2 (2019)
eISSN 2637-0689

Colloquium of Chemistry and Environment 2018
Faculty of Applied Sciences, Universiti Teknologi MARA, Shah Alam.

CHEMICAL CONSTITUENTS FROM THE DICHLOROMETHANE EXTRACT OF *Goniothalamus lanceolatus* (STEMBARK)

Wan Nor Julia Eliana Wan Zamili, Nur Vicky Bihud*
Faculty of Applied Sciences, Universiti Teknologi MARA, 40450 Shah Alam, Selangor, Malaysia.

*vickybihud@uitm.edu.my

Abstract: The stembark of *Goniothalamus lanceolatus*, belonging to the family of Annonaceae, was investigated for its chemical constituents. The study focused on fraction CC62-72 of dichloromethane crude extract from the stembark of *Goniothalamus lanceolatus*. The compounds obtained were isolated and purified by using recycling preparative high performance liquid chromatography (RHPLC) followed by identification using spectroscopic method such as ^{1}H NMR, ^{13}C NMR, COSY, HMBC, IR and HR-TOF-MS. This study has yielded two compounds identified as goniodiol and 9-deoxygoniopypyrone.

Keywords: *Goniothalamus lanceolatus, goniodiol, 9-deoxygoniopypyrone*

INTRODUCTION

According to Wiart (2007), there are about 22 out of 160 species of the *Goniothalamus* species had been scientifically studied. Genus *Goniothalamus* is one of the largest genera in the Annonaceae family (Aslam *et al*., 2016). According to Saunders (2002), the most conventional species are *G. giganteus*, *G. gardneri*, *G. macrophyllus*, *G. amuyon*, *G. griffithii*, *G. tamirensis* and *G. cheliensis*. Wiart (2007) stated that few-leaved slender treelets or shrubs with smooth, thin and fibrous and strongly aromatic bark and upright blackish cylindrical trunk were the botanical characteristic to recognize the *Goniothalamus* species in the rainforest. *G. lanceolatus*, an endemic plant from Sarawak, Malaysia, is used by natives in treating various illnesses such as cancer, fever and skin diseases, however, the plant has limited study on its phytochemical properties to date. This project aims to investigate the chemical constituents from the stembark of *G. lanceolatus*, focusing on dichloromethane crude extract. A modern chromatographic technique, utilizing preparative recycling HPLC was used in the isolation and purification procedures. The pure isolates were characterized using NMR, HR-TOF-MS, and IR.

METHODOLOGY

The fraction CC62-72 was diluted with methanol:water (50:50) to 4 mL. The sample was injected twice (2mL each injection) into RHPLC over ODS (isocratic solvent system methanol:water (50:50); flow rate 4.0 mL/min; UV detector 215 nm). The separated peaks were collected. The isolates were diluted in 0.55 ml to 0.70 ml of deuterated solvent ($CDCl_3$) and the ^{1}H-NMR was analyzed using Bruker AscendTM 600 MHz.

FINDINGS

IR Analysis

Compound 1 showed strong absorption peaks of hydroxyl and carbonyl group at 3840 cm^{-1} and 1689 cm^{-1}. Compound 2 showed strong absorption peaks of hydroxyl and carbonyl group at 3449 cm^{-1} abd 1719 cm^{-1}.

Mass Spectrum

The molecular formula of compound 1 was determined as $C_{13}H_{14}O_4$ based on HR-TOF-MS (*m/z* 235.0950, $[M+H]^+$). The molecular formula of compound 2 was determined as $C_{13}H_{14}O_4$ based on HR-TOF-MS (m/z 235.0968 $[M+H]^+$).

^{1}H and ^{13}C NMR Spectra

The ^{1}H-NMR spectrum of Compound 1 showed multiplet signals between δ7.34-7.44 (5H) corresponding to a mono-substituted phenyl ring, two olefinic protons at δ 6.00 (dd, *J*=9.6, 2.4 Hz, H-3) and δ 6.93 (ddd, *J*=9.6, 6.0, 1.8 Hz, H-4), three oxygenated methine protons at δ 4.80 (ddd, *J*=13.2, 3.6, 2.4 Hz), δ 3.72 (dd, *J*=7.2, 2.4 Hz) and δ 4.95 (d, *J*=7.2) and methylene geminal protons at δ 2.17 and δ 2.78 assigned as H-5a and H-5b. The ^{13}C-NMR spectrum revealed the presence of a carbonyl group (δ 163.7, C-2), which is a characteristic of an α,β-unsaturated δ-lactone in the styrylpyrones (Lan *et al*., 2005), six aromatic carbons of phenyl ring [δ 126.6 (C-10, C-14), δ 128.7 (C-11, C-13), δ 128.3 (C-12) and δ 140.8 (C-9)], two olefinic carbons [δ 120.6 (C-3) and δ 140.8 (C-4)], three oxygenated methine carbons [δ 76.8 (C-6), δ 75.1 (C-7) and δ 73.7 (C-8)], and a methylene carbon at δ 26.1 (C-5).

The ^{1}H-NMR spectrum of Compound 2 showed four one-proton signals at δ 3.98 (br, s), δ 4.55 (m), δ 4.98 (br, s) and δ 4.89 (m), belonged to oxygen bearing methine protons of H-8, H-5, H-7 and H-1, and another four one-proton signals were observed in the upfield region at δ 1.86 (dd, *J*=14.2, 3.9 Hz), δ 2.61 (ddd, *J*=14.2, 3.9, 2.0 Hz), δ 2.88 (dd, *J*=19.2, 4.8 Hz) and δ 2.99 (dd, *J*=19.8, 1.2 Hz), assignable to two pairs of methylene protons, H-9 and H-4, respectively. A multiplet at δ 7.28-7.41 were attributable to five aromatic protons (H-11 to H-15) from a *mono*-substituted phenyl moiety. The ^{13}C-NMR spectrum showed signals of thirteen carbons. The presence of mono-substituted phenyl ring was confirmed from the signals at δ 136.7 (C-10), δ 126.1 (C-11, C-15), δ 128.3 (C-13) and δ 128.9 (C-12, C-14). Two upfield signals due to methylene carbons were observed at δ 23.9 and δ 36.3. The presence of a saturated δ-lactone moiety was suggested by a slight downfield-shifted carbonyl signal at δ 169.2 (C-3) (Tai *et al*., 2010). The oxymethine carbon signals at δ 66.1 (C-5), δ 68.2 (C-8), δ 70.5 (C-7), δ 74.7 (C-1), and a carbonyl carbon of C-3 were reminiscent of a pyranopyrone moiety with hydroxyl function.

CONCLUSIONS

Comparison of ^{1}H-NMR and ^{13}C-NMR data of both compounds with literatures (Lan *et al*., 2005; Tai *et al*., 2010) indeed confirmed the similarity of Compound 1 as Goniodiol and Compound 2 as (+)-9-deoxygoniopypyrone.

REFERENCES

i. Aslam, M.S., Ahmad, M.S., Mamat, A.S., Ahmad, M.Z. & Salam, F. (2016). Goniothalamus: Phytochemical and Ethnobotanical Review. *Recent Advances in Biology and Medicine, 2*, 34-47.
ii. Saunders, R. M. K. (2002). The genus Goniothalamus (Annonaceae) in Sumatra. *Botanical Journal of the Linnean Society*, *139*(3), 225–254.
iii. Wiart, C. (2007). Goniothalamus species: A source of drugs for the treatment of cancers and bacterial infections. *Evidence-Based Complementary and Alternative Medicine*, *4*(3), 299–311.

JUNIOR SCIENCE COMMUNICATION
https://jscfsg.uitm.edu.my/
Volume 2 (2019)
eISSN 2637-0689

Colloquium of Chemistry and Environment 2018
Faculty of Applied Sciences, Universiti Teknologi MARA, Shah Alam.

CHARACTERIZATION AND ELECTROCATALYTIC PERFORMANCE OF HIGH SURFACE AREA GOLD ELECTRODES SYNTHESIZED VIA TWO STEP PROCESS (ELECTRODEPOSITION AND DEALLOYING)

Wan Simpaimun, Yusairie Mohd*
Faculty of Applied Sciences, Universiti Teknologi MARA, 40450 Shah Alam, Selangor. Malaysia.

*yusairie@uitm.edu.my

Abstract: In this study, screen printed carbon electrode(SPCE) was modified with gold alloy (AuCu) by two different electrochemical deposition methods; cyclic voltammetry (CV) and chronoamperometry (CA) followed with dealloying process by CA at +0.80 V for 15 minutes. The synthesized Au alloys were characterized by FESEM, EDX and CV. It was found that AuCu alloy prepared by CV is smoother and AuCu particles are more uniformly distributed on the SPCE surface than by CA. The dealloying process did not give significant effect on the removal of Cu as well as the morphology of Au coating. The AuCu prepared by CA has shown the highest surface area (i.e.: 53.18 cm^2) and the highest catalytic performance (i.e : onset potential = +0.153 V) than other alloyed Au and dealloyed Au samples.

Keywords: **:** *SPCE, gold electrode, electrochemical deposition, dealloying, surface area*

INTRODUCTION

Nanostructured materials such as nanorods, nanowires, nanoparticles have attracted great attention in a wide application including catalysis, chemical sensors, fuel cells, etc. due to their high surface area (Siyu *et al.*, 2010). High surface area of material is important to improve the sensitivity and low detection limits as sensor (Collinson, 2013). Electrochemical erosion, electrochemical oxidation/chemical reduction processes, chemical dealloying of alloys, electrochemical alloying/dealloying and template synthesis are several methods that can be used to prepare high surface area sensing materials (Siyu *et al.*, 2010). In this study, high surface area gold electrodes are synthesized by depositing AuCu alloy on SPCE using electrodeposition method followed with dealloying process.

METHODOLOGY

AuCu alloy was synthesized via a two-step process; electrodeposition and dealloying. Prior to dealloying, the AuCu alloy was deposited on carbon substrate using 0.5 M H_2SO_4 solution containing 10 mM $HAuCl_4$, and 10mM $CuSO_4$. The process of deposition was conducted in a 3-electrode electrochemical cell by applying cyclic voltammetry and chronoamperometry using Autolab Potentiostat. After deposition, dealloying process of gold alloy was carried out in 1 M H_2SO_4 by applying a constant potential of +0.8V for 15 minutes. All the synthesized gold electrodes were characterized by FESEM for surface morphology, EDX for chemical composition and CV for electrocatalytic performance.

Volume 2 (2019)
eISSN 2637-0689

Colloquium of Chemistry and Environment 2018
Faculty of Applied Sciences, Universiti Teknologi MARA, Shah Alam.

FINDINGS

Surface Morphology Analysis by FESEM

Figure 1 (a) shows the deposition of AuCu coating prepared by CV showing small particles of Au formed on the top layer of the coating believed to be Cu particles. The morphology was slightly changed after dealloying as shown in Figure 1 (b) by removing the strange particles. However, the deposition by CA at -0.45 V has produced large granules of AuCu as shown in Figure 1 (c) than AuCu prepared by CV. Meanwhile, after dealloying process, the AuCu coating was slightly changed with dendritic particles formed on the SPCE. Figure 1 (d) shows the dendritic particles was noticed dealloyed AuCu images.

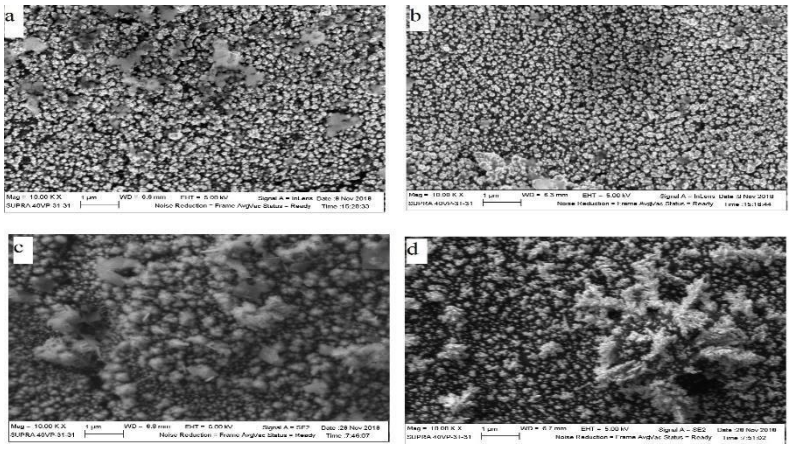

Figure 1 FESEM images of (a)AuCu prepared by CV(b) dealloyed AuCu (prepared by CV) (c) AuCu prepared by CA at -0.45 V (d) dealloyed AuCu (prepared by CA)

Energy Dispersive X-Ray (EDX) Spectroscopy

Table 1 revealed that the removal of Cu was very minimal due to the percentage of Cu present after dealloying process. The highest removal of Cu was higher for AuCu prepared by CA with 12.33% than by CV. The effective surface area of Au electrode was determined by cyclic voltammograms from -0.2 V to 0.6 V at various scan rate (i.e.: 25 mV/s, 50 mV/s, 75 mV/s, 150 mV/s,200 mV/s 250 mV/s). Randless Sevcik equation was used to calculate the surface area of Au electrode. $Ip= (2.69 \text{ X } 10^5) n^{3/2} AD^{1/2} v^{1/2}c$. The highest surface area belonged to the AuCu alloy prepared at -0.45 V with 53.81 cm^2 as shown at Table 1.

Colloquium of Chemistry and Environment 2018
Faculty of Applied Sciences, Universiti Teknologi MARA, Shah Alam.

Table 1 Percentage composition of Au and Cu on SPCE before and after dealloying process and the surface area of gold electrode.

AuCu Alloy Sample		**Element Composition (wt %)**			**Surface area (cm^2)**
		Au		**Cu**	
Blank		-		-	14.67
Prepared by CV	Before dealloying After dealloying	89.70 93.41		10.30 6.59	34.24 39.13
Prepared by CA (-0.45 V)	Before dealloying After dealloying	56.44 69.07		14.42 2.09	53.81 39.13

Behaviour of gold electrodes in $Fe(CN)_6^{3}$ solution

Electrochemical behaviour of Au was investigated by performing cyclic voltammetry in the range of -0.2 V to 0.6 V versus Ag/AgCl in 1 M KNO_3 solution containing 10mM $K_3Fe(CN)_6$ at scanning rate 50mV/s. Based on the result, it was found that SPCE gave the least activity towards Fe(ll)/Fe(lll) reactions. The present of Au on SPCE has enhanced the catalytic activity for Fe (ll)/Fe(lll) reactions. The highest electrochemical performance was shown by AuCu alloy prepared by CA at -0.45V as shown by its onset potential (i.e.: +0.153 V) as shown in Figure 2.

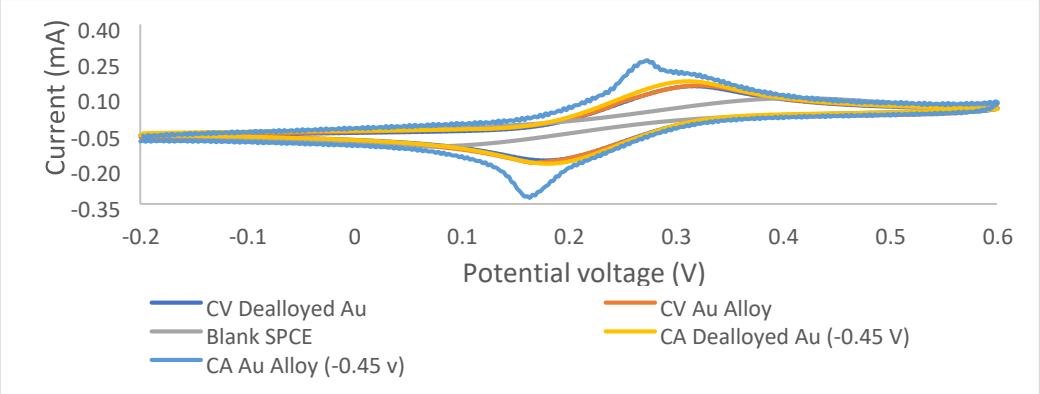

Figure 2 Cyclic voltammograms of gold samples in 1M KNO_3 solution containing 10mM $K_3Fe(CN)_6$ at -0.2 V to 0.6 V at scan rate 50mV/s

CONCLUSIONS

This study focuses on the synthesis of high surface area gold electrode via two-step process (electrodeposition and dealloying). Two deposition methods were used to synthesize AuCu alloys on SPCE; by CA at -0.45 V and CV (by scanning from 0V to -0.50 V at 50 mV/s for 45 cycles). After that, dealloying process was conducted using chronoamperometry to remove Cu element by applying a constant potential

of +0.80 V for 600 s. The morphology of Au alloys at -0.45 V has produced a compact and non-homogenous AuCu deposits. Meanwhile, deposition by CV has produced few strange particles on the surface of SPCE. Based on EDX results, the highest percentage composition of Cu element removed from Au alloy after dealloying process was about 12.33%. Among all the Au alloys, AuCu alloy deposited by CA at -0.45 V showed the best catalytic activity as shown by its highest surface area (53.10 cm^2) and its earliest onset potential (i.e. +0.153V).

REFERENCES

i. Collinson, M. M. (2013). Nanoporous Gold Electrodes and Their Applications in Analytical Chemistry. *ISRN Analytical Chemistry*, 1–21.
ii. Siyu, H., Xinyu, L., Qingyu, L., Mianwu, M., Tengfa, L., Hongqiang, W., & Zhiliang, J. (2010). The preparation of nanoporous gold electrodes by electrochemical alloying/dealloying process at room temperature and its properties. *Materials Letters*, *64*(21), 2296–2298.

JUNIOR SCIENCE COMMUNICATION
https://jscfsg.uitm.edu.my/
Volume 2 (2019)
eISSN 2637-0689

Colloquium of Chemistry and Environment 2018
Faculty of Applied Sciences, Universiti Teknologi MARA, Shah Alam.

EFFECT OF SUTCHI CATFISH (*Pangasius hypophthalmus*) SKIN GELATIN COATING ON BEEF MEAT DURING STORAGE

Normah Ismail*, Nurhaziqah Salikin
Faculty of Applied Sciences, Universiti Teknologi MARA, 40450, Shah Alam, Selangor, Malaysia

*norismel@salam.uitm.edu.my

Abstract: The freshness of beef meat depends on it appearance, aroma and colour. The shelf life of beef cut can be extended by coating in gelatin. In this study, the beef cut (2.5 x 2.5 x 1.5 cm) was double dipped in sutchi catfish gelatin to determine the effect of gelatin coating on the total plate count and physicochemical characteristics during storage for 28 days at -18°C. Results showed that beef cut coated with sutchi catfish gelatin had highest water holding capacity (49.37%) and moisture content (82.14%) while lowest in total plate count (log 7.22 CFU/g) compared to beef cut coated with commercial bovine gelatin and control. Although protein bands started to fade for all samples at day 28 as shown in SDS-PAGE result, more intense bands were observed in sutchi catfish gelatin coated beef cut. Hence, the application of sutchi catfish gelatin coating on beef cuts reduced the deterioration of beef cut when stored at -18°C.

***Keywords*:** sutchi catfish, gelatin, beef cut, storage

INTRODUCTION

Meat is considered as a highly recommended and nutritious food. However, it is easily spoilt due to its nutritional contents which are able to assist growth of many types of microorganisms. For fresh meat, biochemical changes continue during storage causing meat to turn into unacceptable flavour and texture although no microorganisms are present (Egan *et al*., 1988). Gelatin which derived from the partial degradation of collagen has formerly been used to study the effect on shelf life extension of various meat products. A study by Antoniewski *et al*. (2007) showed that meat coated with gelatin remained darker and redder compared to control. Gelatin-coated beef also recorded lower microbial count during storage (Batttisti *et al*., 2017). Coating will prolong the shelf life of beef which make it safe and suitable for consumption provided that the food has been stored in accordance with suitable storage conditions. This study will evaluate the effect of sutchi catfish gelatin coating on the physicochemical characteristics of beef cut during storage.

METHODOLOGY

Gelatin from sutchi catfish skin was extracted according to Normah and Muhamad Fahmi (2015). The beef meat (2.5 x 2.5 x 1.5 cm) was coated with sutchi catfish gelatin and commercial bovine gelatin and then dried in a cabinet drier at 60°C for 30 minutes according to Utami *et al*. (2017). Samples were then stored for 28 days at -18°C. Water holding capacity (WHC), moisture, total plate count were analysed at the interval of 14 days (Köhn *et al*., 2015, AOAC, 2000, Utami *et al.,* 2017). SDS-PAGE was performed for molecular weight distribution analysis.

RESULTS AND DISCUSSION

Both WHC and moisture content decreased during storage with control beef cut WHC sharply decreased compared to others while beef cut coated with sutchi catfish gelatin had highest WHC and moisture content

throughout the storage period (Figure 1). The size of free space where the water is retained in the protein structure and the existence of charged molecules which allows the dipole-dipole interactions influenced the water holding capacity (Ee *et al.*, 2009). Gelatin acts as a barrier to reduce moisture, weight and purge loss (Battisti *et al.*, 2017, Jridi *et al.*, 2018, Herring *et al.*, 2010). Gelatin is rich in hydrophilic amino acids and contains some hydrophobic amino acids that are able to retain water (Jridi *et al.*, 2018). Microbial growth increased with storage as indicated by increased in total plate count with sutchi catfish gelatin coated beef cut exhibiting the lowest count (Figure 1). Gelatin acts as protein bio-film around samples preventing oxygen diffusion and bacterial escalation (Jridi *et al.*, 2018). Protein was degraded during storage (Figure 2). This can be seen by faded protein bands at day 28. Beef cut coated with sutchi catfish gelatin retained most of the bands followed by beef coated with commercial bovine gelatin and control. The bands for all the samples remain similar from day 0 to 14. The accelerated denaturation of protein might have resulted in increased disulfide bond formation (Adeyemi *et al.*, 2014). Protein starts to degrade when the temperature was below -20°C (González-Ferrero *et al.*, 2018).

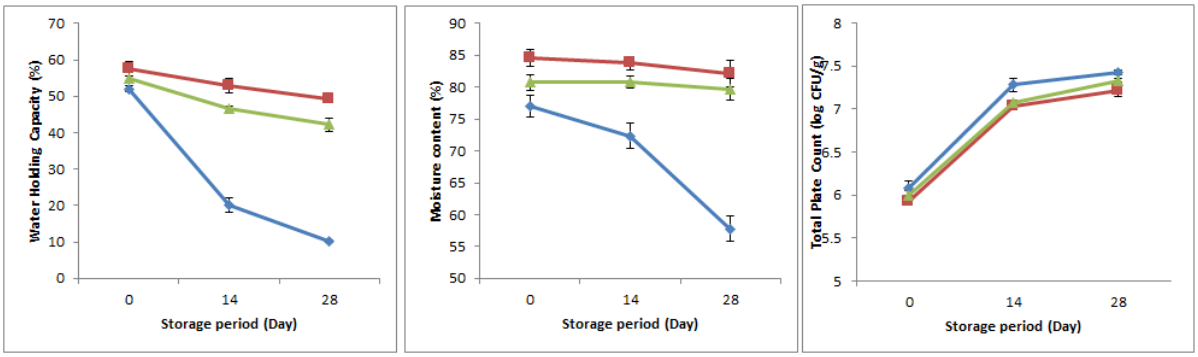

Figure 1. Water holding capacity (%), moisture content (%) and total plate count (log CFU/g) during the 28 days storage of control (—◆—), beef cut coated with sutchi catfish gelatin (—■—) and beef cut coated with commercial bovine gelatin (—△—)

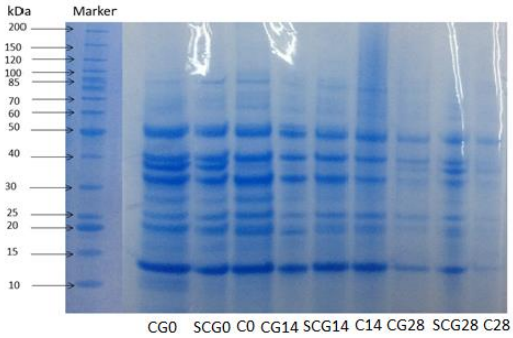

Figure 2. SDS-PAGE of proteins from beef cut coated with commercial bovine gelatin at Day 0 (CG0), Day 14 (CG14) and Day 28 (CG28); beef cut coated with sutchi catfish gelatin at Day 0 (SCG0), Day 14 (SCG14) and Day 28 (SCG28) and control at Day 0 (CO), Day 14 (C14) and Day 28 (C28).

CONCLUSIONS

Coating beef cut with sutchi catfish gelatin preserved the physicochemical characteristics and delayed deterioration due to bacteria.

REFERENCES

i. Adeyami, K.D., Mislan, N., Aghwan, Z.A., Sarah, S. A., & Sazili, A. Q. (2014). Myofibrillar protein profile of Pectoralis major muscle in broiler chickens subjected to different freezing and thawing methods. *International Food Research Journal*, 21(3), 1125-1129.
ii. Antoniewski, M. N., Barringer, S. A., Knipe, C. L., & Zerby, H. N. (2007). Effect of a gelatin coating on the shelf life of fresh meat. *Journal of Food Science*, 72(6), 382-387.
iii. AOAC, (2000). Official Methods of Analysis, 17th Edition. Washington: Association of Official Analytical Chemists.
iv. Battisti, R., Fronza, N., Júnior, Á. V., da Silveira, S. M., Damas, M. S.P., & Quadri, M. G. N. (2017). Gelatin-coated paper with antimicrobial and antioxidant effect for beef packaging. *Food Packaging and Shelf Life,* 11, 115-124.
v. Ee, K.Y., Rehman, A.,Agboola, S. and Zhao, J., (2009). Influence of heat processing on functional properties of Australian wattle seed (Acacia victoriae Bentham) extract. *Food Hydrocolloids*, 23, 116-124.
vi. Egan, A. F., Eustace, I. J., & Shay, B. J. (1988). Meat packaging-maintaining the quality and prolonging the storage life of chilled beef, pork and lamb. Meat 88: Proceedings of Industry Day, 68-75.
vii. González-Ferrero, C., Irache, J. M., & González-Navarro, C. J. (2018). Soybean protein-based microparticles for oral delivery of probiotics with improved stability during storage and gut resistance. *Food Chemistry*, 239, 879-888.
viii. Herring, J. L., Jonnalongadda, S. C., Narayanan, V. C., & Coleman, S. M. (2010). Oxidative 406 stability of gelatin coated pork at refrigerated storage. *Meat Science*, 85, 651-656.
ix. Jridi, M., Mora, L., Souissi, N., Aristoy, M. C., Nasri, M., & Toldrá, F. (2018). Effects of active gelatin coated with henna (L. inermis) extract on beef meat quality during chilled storage. *Food Control*, 84, 238-245.
x. Köhn, C. R., Fontoura, A. M., Kempka, A. P., Demiate, I. M., Kubota, E. H., & Prestes, R. C. (2015). Assessment of different methods for determining the capacity of water absorption of ingredients and additives used in the meat industry. *International Food Research Journal*, 22(1). 356-362.
xi. Normah, I., & Muhammad Fahmi, I. (2015). Physicochemical characteristics of gummy added with sutchi catfish (Pangasius hypophthalmus) gelatin. *International Food Research Journal*, 22(3). 1059-1066.
xii. Utami, R., Kawiji Khasanah, L. U., & Nasution, M. I. A. (2017). Preservative effects of kaffir lime (*Citrus hystrix DC*) leaves oleoresin incorporation on cassava starch-based edible coatings for refrigerated fresh beef. *International Food Research Journal*, 24(4). 1464-1472.

JUNIOR SCIENCE COMMUNICATION
https://jscfsg.uitm.edu.my/
Volume 2 (2019)
eISSN 2637-0689

Colloquium of Chemistry and Environment 2018
Faculty of Applied Sciences, Universiti Teknologi MARA, Shah Alam.

PHYSICOCHEMICAL PROPERTIES OF RAW AND AUTOCLAVED BILIMBI (*Averrhoa bilimbi* L.)

Normah Ismail*, Effah Haziqah Aminudin
Faculty of Applied Sciences, Universiti Teknologi MARA, 40450, Shah Alam, Selangor, Malaysia

norismel@salam.uitm.edu.my

Abstract: This study was carried out to evaluate the effect of autoclaving on the physicochemical properties of raw bilimbi fruit (*Averrhoa bilimbi* L.). Raw bilimbi fruit at the harvesting stage (yellowish green) was autoclaved for 3 hours at 121°C, 15psi and analysed for ash, vitamin C, titratable acidity, pH and colour. Autoclaved bilimbi fruit contains 0.65% ash which was significantly ($p<0.05$) higher than the raw bilimbi (0.50%). pH slightly increased (2.78) after autoclaving. Vitamin C content (12mg/100g) and titratable acidity which was reported as oxalic acid (0.34mg/100g) were lower in the autoclaved fruits and the fruits were darker based on the 'L' value (42.63). Thus, autoclaving affects some of the physicochemical properties of the bilimbi fruits.

***Keywords*:** autoclave, bilimbi, *Averrhoa bilimbi* L.

INTRODUCTION

Bilimbi are starchy fruit that grows on tree trunk. The fruit is generally regarded as too acid when eaten raw. In some countries, the fresh fruits are prepared as relish served with rice and beans. Half-ripe fruits are salted into pickles while the juice are popular as cooling beverages. The fruits have a short shelf-life around 2-3 days and undergo enzymatic browning due to oxidation process. Hence, the taste will be altered and undesired odour will be produced. The traditional method to increase shelf-life of bilimbi is boiling for more than 8 hours through the production of "Sambal hitam". This method is not practical as it needs a long time to produce the boiled bilimbi. Alternative method may be used such as autoclaving. Bilimbi fruit produced its own unique flavour after boiling for more than 8 hours. This kind of flavour produced by bilimbi fruit is used as the main ingredient in the "Sambal hitam" production that is popular in Pahang, Malaysia. Boiled bilimbi fruit can last long up to 3 months without altering its taste. However, autoclave can be used as a substitute to boiling method. Therefore, the shelf-life of the fruits may be extended and the taste can be enhanced. Furthermore, the fruit can be consumed without harming human body as the microorganisms are killed during the autoclaving process. The potency of bilimbi fruits as natural seasoning, especially its flavor, may increase the economic benefit of the fruits.

METHODOLOGY

Raw bilimbi fruit at the harvesting stage (yellowish green) was initially washed, cleaned, drained and then autoclaved for 3 hours at 121°C, 15psi. The samples were then cooled and stored at room temperature before analysis. Ash content and titratable acidity were determined according to AOAC [1]. Vitamin C was determined by titration method [2], pH using pH meter by homogenizing the samples in 50ml distilled water and color by using a chromameter.

RESULTS AND DISCUSSION

Autoclaving of bilimbi fruit affects the ash content which resulted in significantly ($p<0.05$) higher amount (0.65%) than the raw bilimbi (0.50%) (Table 1). The ash content of raw bilimbi was reported to fall within the range of 0.31-0.40% [3, 4]. High ash content revealed the presence of elevated mineral content [5].

Bilimbi variety has been determined as one of the factors contributed to the elevated amount [6]. Vitamin C content of raw bilimbi was 36.33mg/100g. 36.68mg/100g and 5.20mg/100ml have been reported for fresh bilimbi fruit and fruit juice, respectively [6,7]. However, vitamin C content of freeze-dried bilimbi was 182.98mg/100g [8]. Vitamin C is very sensitive to light, heat and air [8] while vitamin C content of fruit might be influenced by environmental factors such as soils, climate and light [9]. Raw bilimbi contained higher vitamin C than autoclaved bilimbi (12.00mg/100g). This might due to heating during the autoclaving process that degraded most of the vitamin C.

Titratable acidity content was reported as oxalic acid due to its dominance in bilimbi constituents [10]. Oxalic acid content of raw bilimbi fruit was 4.0mg/100g which was higher than those in autoclaved sample (0.34mg/100g). The oxalic acid content in the bilimbi was in the range of 8.57 to 10.32mg/g [6]. Previously, oxalic acid range lies between 8.45-9mg/g [11]. Different concentration of oxalic acid content might be due to varieties and agronomic conditions [8]. Different level of oxalic acid gave different intensity of sour taste in bilimbi [12]. The lower titratable acidity content in autoclaved bilimbi was due to degradation of oxalic acid over time when subjected to autoclaving process.

Table 1. Physicochemical properties of raw bilimbi (*Averrhoa bilimbi* L.) fruits autoclaved at 15psi for 3 hours at 121°C

Analysis	Raw bilimbi	Autoclaved bilimbi
Ash content (%)	0.50 ± 0.04^{b}	0.65 ± 0.05^{a}
Vitamin C (mg/100g)	36.33 ± 0.76^{a}	12.00 ± 0.50^{b}
Titratable acidity (oxalic acid) (mg/100g)	4.00 ± 0.04^{a}	0.34 ± 0.02^{b}
pH	2.60 ± 0.09^{b}	2.78 ± 0.08^{a}
Color		
L	54.28 ± 0.77^{a}	42.63 ± 0.66^{b}
a	-2.76 ± 0.08^{b}	5.47 ± 0.19^{a}
b	16.74 ± 0.25^{a}	8.21 ± 0.24^{b}
Means within rows followed by different superscripts are significantly different at $p<0.05$.		

The pH of raw bilimbi was 2.60. The reported pH of bilimbi was 2.83 [13]. Other findings reported lower range between 0.9-1.5 [6]. Usually unripe fruits showed lower pH [12]. However, as the fruit ripen, pH increases due to increase in total soluble solid [12]. pH of raw bilimbi was slightly lower than autoclaved bilimbi and this indicated that autoclaved bilimbi was less acidic then raw bilimbi. However, the results showed no significant ($p>0.05$) difference between the autoclaved and raw bilimbi.

Colour is essential in determining ripeness, defects and the freshness of the bilimbi. The bilimbi L*, a*, and b* values obtained were 54.28, -2.76, and 16.74, respectively. Previous study reported that the L*, a*, and b* values for bilimbi were 43.89, -16.76, and 30.26, respectively [14]. Slightly different values for colour might be due to bilimbi maturity stage. When the bilimbi is at maturity stage, there were maximum increase in bilimbi weight, dimensions and appearance; from green colour to light yellow [6]. The

autoclaved bilimbi was darker (42.63) than raw bilimbi (54.28) based on L* value. Luminosity measurement was denoted by L*, reddish colour by positive a* value, greenish colour by negative a* value, yellowish colour by positive b* value and bluish colour by negative b* value [15]. This means that colour of autoclaved bilimbi was slightly reddish and yellowish colour compared to raw bilimbi which is greenish and yellowish. The luminosity which denoted by L* represented a perfect reflecting diffuser that had maximum value of 100 and the minimum value which represented as black colour was zero [16]. It could be deduced that raw bilimbi had more luminous colour than autoclaved bilimbi.

CONCLUSIONS

Autoclaving of bilimbi fruits at 121°C for 3 hours resulted in higher ash content and pH value with lower vitamin C, titratable acidity and darker color.

REFERENCES

[1] AOAC, (2000).Official Methods of Analysis, 17th Edition. Washington: Association of Official Analytical Chemists.

[2] Tee, E. S., Rajam, K., Young, S. I., Khor, S. C., & Zakiyah, H. O. (1996). laboratory procedure in nutrient analysis of foods. Kuala Lumpur, Malaysia: Division of Human Nutrition. Institute for Medical Research.

[3] Kumar, G. V., Kumar K. A., Patel G.R. R. & Manjapp, S. (2013). Determination of vitamin C in some fruits and vegetables in Davanagere city, (Karanataka) – India. *Int. J. of Pharmacy & Life Sci.*, 4(3), 2489-2491.

[4] Bhaskar, B. & Shantaram, M. (2013). Morphological and biochemical characteristics of Averrhoa fruits. *Int. J.of Pharm., Chem.and Biol. Sci.*, 3(3), 924-928

[5] Felsner, M. L., Cano, C. B., Bruns, R. E. & Matos, J. R. (2004). Characterization of monofloral honeys by ash contents tough a hierarchical design. *J.of Fd. Composition and Analysis*. 17(6). 737-747.

[6] De Lima, V.L.A.G., Mélo, E.D.S. & Lima, L.D.S. (2001). Physicochemical characteristics of bilimbi (*Averrhoa bilimbi L.*). *Revista Brasileira de Fruiticultura*, 23(2):421-423.

[7] Benoy, N. S., Sailesh, S. K., Joseph, M. & Kurien, M. K. (2016). Estimation of vitamin C content and antibiotic effect of various citrus fruits on different strains of oral bacteria. BEMS Reports, 2(2): 44-50.

[8] Yan, S. W., Ramasamy, R., Alitheen, N. B. M. & Rahmat, A. (2012). A comparative assessment of nutritional composition, total phenolic, total flavonoid, antioxidant capacity, and antioxidant vitamins of two types of Malaysian underutilized fruits (*Averrhoa bilimbi* and *Averrhoa carambola*). *Int. J. of Food Properties*, 16(6), 1231-1244.

[9] Ruzainah, A.J., Ahmad, R.B.A.H., NorZaini, C.M. & Vasudevan, R. (2009). Proximate analysis of dragon fruit (*Hylecereus polyhizus*). *American J.of Applied Sci.*, 6 , 1341–1346.

[10] Saini, S. (2016). A review on phytochemistry and pharmacology of *Averrhoa bilimbi* Linn. Department of Botany, 2(1), 2454-9916.

[11] Joseph, J. & Mendonca, G. (1989). Oxalic acid content of carambola (*Averrhoa carambola* L.) and bilimbi (*Averrhoa bilimbi* L.). Proceedings of the Interamerican Society for Tropical Horticulture. Georgetown. v.33.117-120.

[12] Seri, I. M. & Nur, A. A. A. (2015). Changes ın physicochemical characteristics and organic acids during ripening of five tropical fruit species in Malaysia. Faculty of Agro Based Industry. Universiti Malaysia Kelantan, Jeli Campus.

[13] Virgolin, L. B., Seixas, F. R. F. & Janzantti, N. S. (2017). Composition, content of bioactive compounds, and antioxidant activity of fruit pulps from the Brazilian Amazon Biome. *Brasília,* 52(10). 933-941

[14] Xu, E., Wijaya, C. H. & Faridah, D. N. (2016). Characterization of aroma compounds in Indonesian traditional seasoning (Asam Sunti) made from *Averrhoa bilimbi* L. Faculty of Agricultural Engineering and Technology. Bogor Agricultural University. Campus IPB Dramaga. West Java, Indonesia.

[15]]Leahu, A., Damian, C., Carpiuc, N., Oroian, M., & Avramiuc, M. (2013). Change in colour and physicochemical quality of carrot juice mixed with other fruits. *J.of Agroalimentary Proc.and Tech.*, 19(2), 241-246.

[16] HunterLab (2007). CIE L*a*b* Color Scale. 8(7). Insight on Color. Applications Notes. Hunter Associates Laboratory, Inc. Reston, Virginia.

JUNIOR SCIENCE COMMUNICATION
https://jscfsg.uitm.edu.my/
Volume 2 (2019)
eISSN 2637-0689

Colloquium of Chemistry and Environment 2018
Faculty of Applied Sciences, Universiti Teknologi MARA, Shah Alam.

OXIDATIVE STABILITY OF FISH BALLS INCORPORATED WITH HYDROLYSATE FROM SUTCHI CATFISH (*Pangasius hyphophthalmus*)

Normah Ismail*, Najla Ahmad Kendong
Faculty of Applied Sciences, Universiti Teknologi MARA, 40450, Shah Alam, Selangor, Malaysia

*norismel@salam.uitm.edu.my

Abstract: Sutchi catfish hydrolysate was produced by hydrolysis of sutchi catfish using Alcalase 2.4L for a duration of 120 min at pH 8.5, 60°C and enzyme/substrate ratio 0.5%. The hydrolysates which were either boiled or non-boiled were then stored for 4 weeks at 4°C and analysed weekly for antioxidative activity. 2,2-diphenyl-1-(2,4,6-trinitrophenyl) hydrazyl (DPPH) radical scavenging activity and reducing power of the hydrolysate were compared with the commercial butylated hydroxyl anisole (BHA). The hydrolysate was also incorporated into fish balls where the oxidative stability of the fish balls during the twelve days storage at -20°C was evaluated. The fish balls were analysed for free fatty acid contents, peroxide value and thiobarbituric acid reactive substances (TBARS). Results showed that both BHA and sutchi catfish hydrolysate effectively prevented lipid oxidation of fish balls during storage. Therefore, protein hydrolysate derived from sutchi catfish may potentially serve as a natural food additive with antioxidative properties in food systems.

***Keywords*:** antioxidant, hydrolysate, sutchi catfish, fish ball, *Pangasius hyphophthalmus*

INTRODUCTION

Protein hydrolysate is a hydrolysed protein produced from protein rich resources such as fish, shellfish, whey and soybean by heating in acid, alkali or enzyme. Hydrolysates derived from fish have been shown to contain bioactive peptides with immuno modulatory, anti-microbial, anti-thrombotic, anti-hypertensive and anti-proliferative properties [1, 2]. According to Nesse *et al.*, [3] and Nesse *et al.*, [4], fish protein hydrolysates have promising potential for use as nutritional supplementation since it is easily absorbed and can be utilized in various metabolic activities.

The antioxidative potential and effectiveness of fish protein hydrolysate in preventing oxidation of different food products have also been reported previously. Papain-hydrolysed grass carp protein produced at 10% degree of hydrolysis exhibited high antioxidant activities besides showing high solubility and heat stability characteristics [5]. The antioxidant and biochemical properties of enzymatically hydrolyzed silver carp (*Hypophthalmichthys molitrix)* protein were studied by Dong *et al*., [6]. They found that the inhibition of linoleic acid peroxidation appeared to reach a maximum level at 1.5 and 2.0 hrs of hydrolysis and the hydrolysates antioxidant activity was close to that of α-tocopherol in a linoleic acid emulsion system. Hu *et al*., [7] used hydrolysate from the skin and muscle of silver carp (*Hypophthalmichthys molitrix*) as coatings to extend the shelf life of common carp (*Cyprinus carpio*). They found that the rate of increase in TVB-N, TVC, TBA and K values were lower. Dekkers *et al*., [8] investigated the oxidative stability of mahi mahi red muscle dipped in tilapia protein hydrolysates for 2 or 4 minutes and then stored at 4°C. Their results revealed that dip treatments decreased the formation of lipid hydroperoxides and TBARS over 90 hrs storage time. In Sakanaka *et al.*, [9] studies, egg yolk protein hydrolysates showed strong antioxidant activities on cookies containing linoleic acid. In this study, fish protein hydrolysate was produced from

sutchi catfish and antioxidant activity of the hydrolysate was evaluated. The oxidative stability of fish balls incorporated with the hydrolysate was also determined.

METHODOLOGY

Sutchi catfish (*Pangasius hyphophthalmus*) was purchased from a fish supplier at Sungai Buloh, Selangor. Alcalase 2.4L with a declared activity of 2.4 AU/g and density of 1.18 g/mL is a bacterial protease extracted from *Bacillus licheniformis*. Other chemicals used were purchased from Sigma Chemical Co. (St. Louis, MO). The fish was eviscerated, washed and filleted to collect the flesh. The flesh was mixed with deionized water and then homogenized until fine in a blender. The hydrolysis process was performed in a thermostatically controlled water bath at pH 8.5, 60°C, enzyme/substrate ratio 0.5% for 120 minutes as described by Normah *et al*., [10]. Five grams of hydrolysate and a commercial antioxidant (BHA) were packed separately in polyethylene bags and analysed weekly for 4 weeks for antioxidant activity during storage at 4°C. Another set of the hydrolysate was also prepared similarly, however, the sample was boiled for 10 minutes prior to storage and analysis. DPPH radical-scavenging activity and reducing power were determined as described by Wu *et al.,* [11]. Three types of fish balls containing either sutchi catfish hydrolysate, BHA or without any antioxidant (control) were prepared. Sutchi catfish hydrolysate or BHA was added into the minced flesh followed by the addition of corn flour sufficient to shape into balls. The fish balls were boiled for 10 minutes and then stored for twelve days at -20°C and analysed every three days. Prior to analyses, lipid from the fish balls was extracted [12]. The extracted lipid was analysed for free fatty acids, peroxide value (PV) and thiobarbituric acid (TBARS) value [13, 14].

RESULTS AND DISCUSSION

DPPH radical scavenging activities and reducing power of boiled sutchi catfish hydrolysate, non boiled sutchi catfish hydrolysate and BHA during storage are shown in Figure 1. DPPH radical scavenging activities and reducing power decreased in all samples. Higher DPPH and reducing power were exhibited by BHA and non boiled hydrolysate than those from boiled hydrolysate. Results suggested that sutchi catfish hydrolysate had antioxidant activities close to BHA.

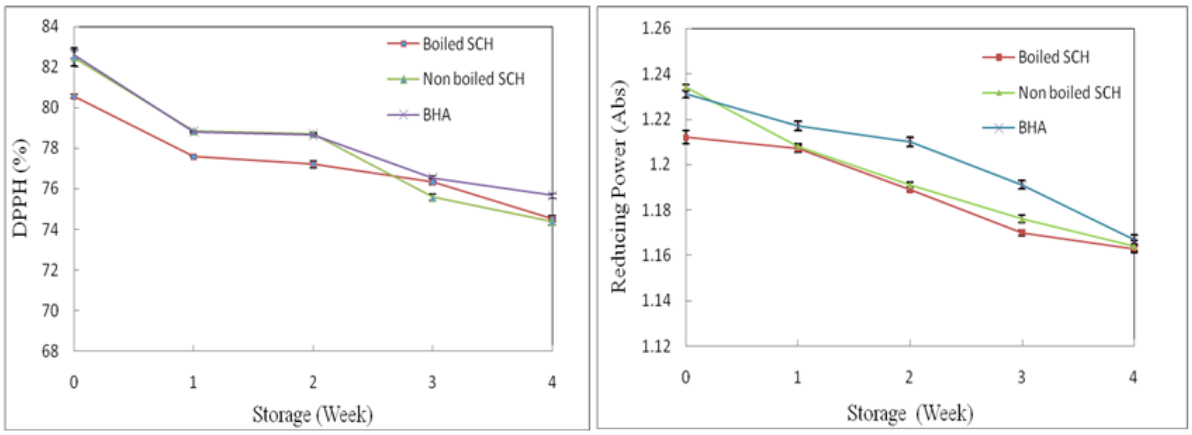

Figure 1. Reducing power and DPPH radical scavenging activities of boiled sutchi catfish hydrolysate (SCH), non boiled SCH and BHA during 4 weeks storage at 4°C**.**

FFA, peroxide value and TBARS increased slightly with storage for fish balls incorporated with sutchi catfish hydrolysate and BHA compared to control (Figure 2). Significantly higher ($p<0.05$) values were exhibited by controls, however, no significant difference ($p>0.05$) between fish balls containing sutchi catfish hydrolysate and BHA. These findings supported the fact that sutchi catfish hydrolysate can effectively prevent lipid oxidation comparable to BHA. Amino acids within the hydrolysate could be the contributing factor towards the antioxidant activity. Similar observation was reported for fish fillet containing silver carp protein hydrolysates [7].

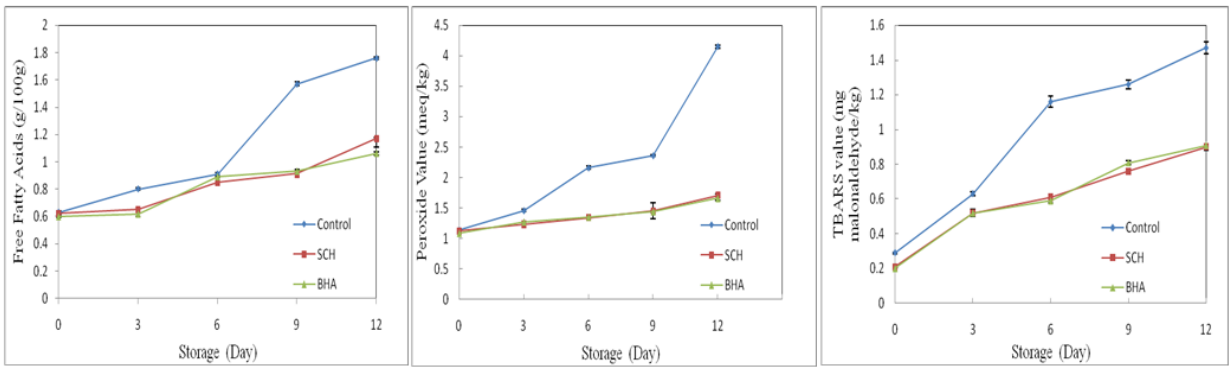

Figure 2. Free fatty acids, peroxide values and TBARS of fish balls without sutchi catfish hydrolysate (control), fish balls incorporated with sutchi catfish hydrolysate (SCH) and BHA during twelve days storage at -20°C.

CONCLUSIONS

DPPH radical scavenging activity and reducing power analysis indicated that sutchi catfish hydrolysate had antioxidant activities close to BHA. The incorporation of sutchi catfish hydrolysate also delays lipid oxidation of fish balls during storage. Therefore, sutchi catfish hydrolysate can be a novel source of natural antioxidant to be applied in food.

REFERENCES

[1] L. Picot, R. Ravallec, M. Fouchereau-peron, L. Vandanjon, P. Jaouen, M. Chaplain-Derouiniot, F. Guerard, A. Chabeaud, Y. LeGal, O.M. Alvarez, J. Berge, J. Piot, I. Batista, C. Pires, G. Thorkelsson, C. Delannoy, G. Jakobsen, I. Johansson, P. Bourseau. J. of the Sci. of Fd. and Agr. 2010; 90, 1819-1826.
[2] M. Chalamaiah, B. Dinesh Kumar, R. Hemalatha, T. Jyothirmayi. Fd. Chem. 2012; 135, 3020-3038.
[3] K.O. Nesse, A.P. Nagalakshmi, P. Marimuthu, M. Singh, P.J. Bhetariya, M. Ho, R.R. Simon, R.R., Regulatory Tox. and Pharm. 2014; 69, 1-6.
[4] K.O. Nesse, A.P. Nagalakshmi, P. Marimuthu, M. Singh. India J. Clin. Biochem. 2011; 26, 360-365.
[5] X. Li, Y. Luo, H. Shen, J. You. J. of the Sci. of Fd. and Agr. 2011; 92, 292-298.
[6] S. Dong, M. Zeng, D. Wang, Z. Liu, Y. Zhao, H. Yang. J. of Fd. Chem. 2008; 107, 1485-1493.
[7] S. Hu, Y. Luo, J. Cui, W. Lu, H. Wang, J. You, H. Shen. J. of Fd. Sci. and Tech. 2013; 48, 187-194.
[8] E. Dekkers, S. Raghavan, H.G. Kristinsson, M.R. Marshall. Fd. Chem. 2011; 124, 640-645.
[9] S. Sakanaka, Y. Tachibana, N. Ishihara, L.R. Juneja. Fd. Chem. 2004; 86(1), 99-103.

Volume 2 (2019)
eISSN 2637-0689

[10] I. Normah, B. Jamilah, N. Saari, B.C.M. Yaakob. J. of the Sci. of Fd. and Agr. 2004; 84, 1290-1298.
[11] H.C. Wu, H.M. Chen, C.Y. Shiau. Fd. Res. Int. 2003; 36, 949-957.
[12] E.G. Bligh, W.J. Dyer. Can. J. of Biochem. and Physiol. 1959; 37, 911-917.
[13] R.R. Lowry, L.J. Tinsley. J. of the Am. Oil. Chem. Soc. 1976; 53, 470-472.
[14] L. Zhang, J. Li, K. Zhou. Biores. Tech. 2006; 101: 2084-2089.

JUNIOR SCIENCE COMMUNICATION
https://jscfsg.uitm.edu.my/
Volume 2 (2019)
eISSN 2637-0689

Colloquium of Chemistry and Environment 2018
Faculty of Applied Sciences, Universiti Teknologi MARA, Shah Alam.

EFFECT OF BANANA *(Musa accuminata cv 'berangan')* MATURITY STAGES ON THE FORMATION OF ACRYLAMIDE IN FRIED BANANA BALLS

Normah Ismail*, Anis Nedya Ramli
Faculty of Applied Sciences, Universiti Teknologi MARA, 40450, Shah Alam, Selangor, Malaysia

*norismel@salam.uitm.edu.my

Abstract: The effect of maturity stages of banana (Musa accuminata cv 'berangan') on the formation of acrylamide in fried banana balls were studied. Stage 5 (yellow with a trace of green) and 7 (all yellow with brown speckles) banana were mashed and added with wheat flour to form a batter. A table spoon of the batter was then scooped into a ball and subsequently fried at 180 ºC for 2-4 minutes. The batter was analysed for total soluble solids and total reducing sugar. Fried banana balls were analysed for acrylamide content, colour and browning index. Acrylamide content of fried banana balls at stage 7 (3.29mg/ml) was significantly higher ($p<0.05$) than stage 5 (1.59mg/ml). The balls were darker as indicated by low 'L' value (42.77) and higher browning index which is 2.13 at 360nm and 1.08 at 420nm were recorded. Higher acrylamide content was in line with the total soluble solids and total reducing sugar of the batter. Thus, frying of banana balls at 180°C resulted in the formation of acrylamide and the amount is enhanced at higher maturity index of the fruit.

Keywords: banana balls, acrylamide, sugar

INTRODUCTION

Foods with high carbohydrate content when heated at high temperatures have been shown to produce various kinds of heat processing induced toxicants. One of the detected food toxicants produced by heat processing is acrylamide [1]. Acrylamide can be found in fried, deep fried, roasted or oven cooked foods which basically consist of starch and when these foods are heated above 120°C [2]. Reducing sugars and amino acid asparagine also largely contribute to acrylamide formation [3, 2]. However, the type of sugar may significantly affect the final concentration of acrylamide produced through the Maillard reaction [2].

Fried banana balls and baked traditional banana based-food is a popular snack in Malaysia. These foods may contain acrylamide at concentrations which may be of concern due to its toxicity. Hence, this study determined the effect of banana maturity stages on the formation of acrylamide in fried banana balls.

METHODOLOGY

Banana (*Musa accuminata cv 'pisang berangan'*) at maturity stages 5 (yellow with trace of green) and 7 (all yellow with brown speckles) were peeled and mashed. Wheat flour was added to form a batter. A table spoon of the batter was then scooped into a ball and subsequently fried at 180 ºC for 2-4 minutes. After frying, the balls were placed at room temperature to cool. The batter was analysed for total soluble solids and total reducing sugar [4]. Fried banana balls were analysed for acrylamide content [5], color and browning index [6].

Colloquium of Chemistry and Environment 2018
Faculty of Applied Sciences, Universiti Teknologi MARA, Shah Alam.

RESULTS AND DISCUSSION

Acrylamide was formed during the frying of banana balls (Table 1). The amount was significantly higher ($p<0.05$) while the balls were darker ($p<0.05$) which is supported by higher browning index for balls prepared using banana at maturity stage 7. The acrylamide content of banana balls from stage 7 were approximately two times higher than those from stage 5. This result was in line with the reducing sugar concentration and total soluble solids in the batter (Table 2). Acrylamide content was higher for stage 7 (3.29 mg/mL) fried banana balls as compared with stages 5 (1.59 mg/mL), which can be due to the high content of reducing sugar present in the former, rather than the later. Increase in acrylamide content in the fried banana balls corresponds with the increases in glucose and fructose concentration. Fructose leads to the formation of relatively higher levels of acrylamide [3, 7] whereas glucose leads to the formation of acrylamide at a relatively lower level. These findings were in agreement with [8] where the results showed that glucose and fructose concentrations in the potato tubers were positively correlated with acrylamide formation in the products, whereas tuber sucrose and asparagine concentrations did not have an effect on acrylamide levels. Study by Daniali *et al.* [4] showed the range from 74.0 to 7468.8 µg/ kg for banana fritter, 28.9 to 243.7 µg/kg for banana chips, 160.7 to 500.4 µg/kg for sweet banana chips, not detected to 154.4 µg/kg for banana cake and 31.7 to 609.1 µg/kg for banana balls. Moreover, a significant difference ($p< 0.05$) was found between acrylamide contents of stage 5 and stage 7, which supports the results found for the sugar concentration. L value for banana balls at stage 7 was lower, indicating that the balls were darker. The reducing sugars has an impressive part in Maillard browning during frying, causing the L value to decrease and a* value to increase. Baik and Mittal [9] studied the kinetics of colour changes of tofu during deep-fat frying at 147-172°C, and from the study conducted, there is a decrease in L value from 85.5 to 68.0 and an increase in redness or a value from 21.17 to 6.72 with the progress of frying time. The Hunter a* value measures the redness or greenness of the samples. The brightness of the fried banana balls decreased with increased sugar content which was expected since sugar is the main reacting compound in the Maillard reaction, resulting in brown pigments and a more colourful product, hence an increase in redness. For browning, absorbance values obtained at 360nm were higher than those obtained at 420nm. Browning was determined at 420 and 360nm since this parameter is associated with specific Maillard reaction products [6]. A higher browning index at 420 and 360nm (2.13 and 1.08) at stage 7 compared to stage 5, which might contain higher amount of melanoidin, indicating that it was much easier for the fructose to generate the Maillard reaction compared to glucose and sucrose.

Table 1. Acrylamide content, colour and browning index of fried banana balls prepared from batter containing banana at different maturity stages

	Maturity stages	
	5	7
Acrylamide (mg/ml)	1.59 ± 0.03^{b}	3.29 ± 0.19^{a}
Colour		
L	47.41 ± 4.12^{a}	42.77 ± 3.18^{b}
a	4.22 ± 1.71^{a}	5.62 ± 1.14^{a}
b	15.10 ± 2.55^{a}	8.97 ± 2.85^{b}
Browning index		

360nm	1.63 ± 0.58^{b}	2.13 ± 0.03^{a}
420nm	0.40 ± 0.14^{b}	1.08 ± 0.06^{a}

Values are expressed as mean ± standard deviation
Mean with different letters within rows are significantly different at ($p<0.05$)

Table 2. Total soluble solids and total reducing sugar of banana balls' batter containing banana at different maturity stages

	Maturity stages	
	5	7
Total soluble solids (°Brix)	24.11 ± 0.74^{b}	34.55 ± 1.73^{a}
Total reducing sugar (%)		
Glucose	2.77 ± 0.11^{b}	4.09 ± 0.34^{a}
Fructose	2.54 ± 0.03^{b}	8.09 ± 0.43^{a}
Sucrose	3.06 ± 0.41^{b}	4.28 ± 0.72^{a}

Values are expressed as mean ± standard deviation
Mean with different letters within rows are significantly different at ($p<0.05$)

CONCLUSIONS

The concentration of acrylamide in fried banana balls of '*berangan'* banana was enhanced by the increase in the concentration of the reducing sugars; glucose and fructose with the increase of the maturity stages of banana. This finding demonstrated that the acrylamide concentration is strongly dependent on the concentration of reducing sugars and the reducing sugars are the limiting factor for the formation of acrylamide in fried banana balls.

REFERENCES

[1] Jagerstad, M., & Skog, K. (2005). Genotoxicity of heat-processed foods. Review. *Mutation Research*, 574:156–172.
[2] Zyzak, D. V., Sanders, R. A., Stojanovic, M., Tallmadge, D. H., Eberhart, B. L., Ewald, D. K., Gruber, D.C., Morsch, T.R., Strothers, M.A., Rizzi, G.P., & Villagran, M. D. (2003). Acrylamide formation mechanism in heated foods. *Journal of Agricultural and Food Chemistry*, 51(16):4782-4787.
[3] Stadler, R. H., Blank, I., Varga, N., Robert, F., Hau, J., Guy, P. A., Robert, M-C., & Riediker, S. (2002). Food chemistry: acrylamide from Maillard reaction products. *Nature*, *419* (6906): 449.
[4] Daniali, G., Jinap, S., Hanifah, N. L., & Hajeb, P. (2013). The effect of maturity stages of banana on the formation of acrylamide in banana fritters. *Food Control*, 32(2): 386-391.
[5] Muchtaridi, M., Levita, J., Rahayu, D., & Rahmi, H. (2012) Influence of Using Coconut, Palm, and Corn Oils as Frying Medium on Concentration of Acrylamide in Fried Tempe. *Food and Public Health*, 2(2): 16-20.

[6] Kukurova, K., Morales, F.J., Bednarikova, A., & Ciesarova, Z. (2009). Effect of L-asparaginase on acrylamide mitigation in fried-dough pastry model. *Molecular Nutrition Food Research*, 53(12):1532-1539.

[7] Becalski, A., Lau, B. P. Y., Lewis, D., Seaman, S. W., Hayward, S., Sahagian, M., Ramesh, M., & Leclerc, Y. (2004). Acrylamide in French fries: influence of free amino acids and sugars. *Journal of Agricultural and Food Chemistry*, 52(12): 3801-3806.

[8] Silva, E. M., & Simon, P. W. (2005). Genetic, physiological, and environmental factors affecting- 386). Springer, Boston, MA.

[9] Baik, O.D., & Mittal, G.S. (2003). Kinetics of tofu color changes during deep-fat frying. *Lebensm.-Wiss. U.-Technol*., 36 :43-48.